MAILLARD INDUCED PEA PROTEIN-POLYSACCHARIDE CONJUGATES: A FUNCTIONALLY ENHANCED INGREDIENT FOR THE FOOD AND BEVERAGE INDUSTRY

A Thesis Submitted to the
College of Graduate and Postdoctoral Studies
in Partial Fulfillment of the Requirements for the
Degree of Doctor of Philosophy in the
Department of Food and Bioproduct Sciences
University of Saskatchewan
Saskatoon

By

ABHIROOP MOOKERJEE

Permission to use

In presenting this thesis in partial fulfillment of the requirements for a Postgraduate degree from the University of Saskatchewan, I agree that the Libraries of this University may make it freely available for inspection. I further agree that permission for copying this thesis/dissertation in any manner, in whole or in part, for scholarly purposes may be granted by the professor or professors who supervised my thesis work or, in their absence, by the Head of the Department or the Dean of the College in which my thesis work was done. It is understood that any copying, publication, or use of this thesis or parts thereof for financial gain shall not be allowed without my written permission. It is also understood that due recognition shall be given to me and the University of Saskatchewan in any scholarly use which may be made of any material in my thesis.

Requests for permission to copy or to make other uses of the materials in this thesis in whole or part should be addressed to:

Head of the Department,
Department of Food and Bioproduct Sciences
University of Saskatchewan
Room 3E08, Agriculture Building, 51 Campus Drive,
Saskatoon, Saskatchewan, S7N 5A8 Canada

OR

Dean
College of Graduate and Postdoctoral Studies
University of Saskatchewan
116 Thorvaldson Building, 110 Science Place
Saskatoon, Saskatchewan, S7N 5C9 Canada

Abstract

Pea proteins are increasingly recognized as a cost-effective, sustainable source of legume proteins with a well-balanced amino acid profile. The primary goal of this research was to enhance the functional properties of pea proteins by combining enzymatic hydrolysis with Maillard conjugation, using starch and other carbohydrate fractions from air-classified pea flours. The process was designed to be environmentally sustainable, relying on food-grade enzymes and heat-induced Maillard reactions, eliminating the need for enzyme inhibitors and supporting a "green label" approach. In the first study, pea protein-enriched flour (PPEF) was hydrolyzed using trypsin and papain to achieve low to medium degrees of hydrolysis (2% – 15%). These hydrolysates were then conjugated with residual starch and non-starch polysaccharides within the PPEF through heat conjugation by the Maillard reaction. The resulting conjugates showed improved functional properties compared to the raw samples, particularly foaming (~20% - 40%) and emulsifying capacities (~2% - 14%), with enhanced stability (3% - 28%) at acidic pH. Water-holding capacity was improved by ~42% - 100% and oil-holding capacity also increased by about 72% - 254%. The second study focused on obtaining conjugates having higher degrees of hydrolysis (above 15%) of the pea proteins, with additional carbohydrate hydrolysis using α-amylase. These hydrolysates were then heat-conjugated with intact starch and other carbohydrates in the flour, including non-starch carbohydrates. The trypsin-hydrolyzed conjugates outperformed papain-hydrolyzed ones across a range of pH levels (4, 7, and 10), demonstrating superior foaming (60% - 90%) and emulsifying (~ 6% - 210% improvement) properties whereas water-holding and oil-holding properties did not show any significant differences. Contrary to previous findings in the literature, the research showed that extensive hydrolysis, when combined with Maillard conjugation, did not impair functionality but enhanced it. In the third study, both fine and coarse fractions from air classification, *i.e.*, protein- and starch-rich flour, were hydrolyzed using trypsin and α-amylase, respectively, and conjugated using heat through the Maillard reaction. Molecular weight analysis indicated a shift towards higher molecular weights, while microstructural analysis revealed protein-protein aggregates and starch-protein conjugates. Functional evaluations showed significantly higher starch solubility (<200%), improved foaming capacity (~50 % - 75%) and emulsifying properties (~9% - 33%) of the conjugates as compared to the controls, particularly at acidic pH, with notable enhancements across all pH levels (4, 7, and 10). Overall, this research demonstrated the potential of conjugating residual carbohydrate and low-value starch fractions to

enhance the functional properties of pea proteins which can be used to improve the texture and stability of foams and emulsions or to improve sensory attributes in alternate meat products. The process not only adds value to starch fractions typically used for animal feed but also promotes eco-friendly, cost-effective solutions for food and beverage applications, such as alternative meats, acidic beverages, and emulsifiers.

Acknowledgements

I would like to extend my deepest gratitude to Dr. Takuji Tanaka for accepting me into his lab to pursue my PhD at a time when the world was gripped by the pandemic and job opportunities were scarce. I am also sincerely thankful to Dr. Nickerson for allowing me to work in his lab and for his invaluable feedback, expert insights, and guidance throughout my project.

I would like to express my appreciation to my other committee members, Dr. Ai, Dr. Warkentin, Dr. Ghosh, and Dr. Tulbek, for their ongoing feedback and comments during my PhD journey.

A special thank you goes to Ana, Shangyi, and Dellaney for taking extra time to teach me lab work during my early days. I am also deeply grateful to Donna, Ann, and Shahrima for their prompt responses to my administrative needs. I would like to thank Connie Briggs and Doug Medernach for their assistance with the LECO analysis, and I am particularly grateful to Guosheng Liu from the Department of Biology for his help with the SEM analysis. My sincere thanks also go to Jason Maley of the Structural Sciences Centre for his support in carrying out the FTIR analysis.

I want to thank my lab mates and colleagues from different labs for the meaningful scientific discussions, their assistance, and their motivation, all of which helped me to complete my PhD research. Finally, but certainly not least, I would like to thank my family. My heartfelt gratitude goes to my parents, Abhijit and Karabi Mookerjee, for believing in me, and to my wife, Parul, for her unwavering support, encouragement, and motivation, which helped me reach the finish line with ease.

Financial support was provided by the Agriculture Development Fund of the Ministry of Agriculture, the Natural Sciences and Engineering Research Council of Canada (NSERC) CREATE Capture grant, and the Departmental Devolved Scholarship.

Table of Contents

List of Tables

List of Figures

List of Symbols/Abbreviations

AA	Amino acids
AG	Acacia gum
AO	Alginate oligosaccharide
ARP	Amadori reaction product
ATR	Attenuated total reflection
CPS	Cycles per second
CD	Degree of conjugation
d.b.	Dry basis
DE	Dextrose equivalent
DH	Degree of hydrolysis
DNS	Dinitro salicylic acid
E/S	Ratio of enzyme to substrate
EAA	Essential amino acids
EAI	Emulsion activity index
EPS	Exopolysaccharides
ES	Emulsion stability
ESI	Emulsion stability index
f (κα)	Smoluchowski approximation
FC	Foam capacity
FS	Foam stability
GA	Gum Arabic
Glc	Glucose
h	Millimolar amino equivalent
HMF	Hydroxymethylfurfural
MD	Maltodextrin
MRP	Maillard Reaction products
n	Number of replicates
NSCS	N-succinyl-chitosan

OHC	Oil holding capacity
OPA	*o*-phthaldialdehyde
O/W	Oil in water
p	Significance level
PAGE	Polyacrylamide gel electrophoresis
PGWP	Partially glycosylated whey protein
PMSF	phenylmethylsulfonyl fluoride
PnPI	Peanut protein isolate
PPC	Pea protein concentrate
PPEF	Pea protein enriched fraction
PPI	Pea protein isolate
PSEF	Pea starch enriched fraction
R_C	Area under the curve at 280 nm/ Area under the curve at 304 nm
RDA	Recommended dietary allowance
RP	Rice protein
SPI	Soybean protein isolate
TNBS	Trinitrobenzene sulfonic acid
Tp	peak temperature
WGP	Wheat germ protein
WHC	Water holding capacity
WPI	Whey protein isolate
XOS	xylo-oligosaccharides
zP	Zeta potential
α	Particle radius
ε	permittivity
κ	Debye length
λ_{max}	maximum emission
η	Dispersion viscosity
%N	Percentage of nitrogen

CHAPTER I

1 Introduction, General Hypothesis, General Objectives

1.1 Introduction

The global population is expected to reach 9 billion by 2050, making it crucial to produce and distribute food effectively. Proteins play a particularly significant role among the essential macronutrients necessary for growth and metabolism. Proteins are vital for a variety of anabolic and catabolic reactions in the body like the formation of muscles, transport of materials, regulation of genetic materials, functioning as enzymes and hormones and many more (Carbone *et al.*, 2019; Chatterjee *et al.*, 2017; Robinson, 2015). According to the Recommended Dietary Allowance (RDA), a healthy adult male should consume about 0.8 g protein/kg body weight in order to maintain body musculature (Consultation, 2013).

Animal proteins have been the primary source of protein consumption production, but this method is now linked to significant greenhouse gas emissions and high-water consumption (Grossi *et al.,* 2019). Additionally, the consumption of animal products raises various social, religious, and ethical concerns. Over the past few decades, scientists have been exploring alternative sources of proteins, and extracted proteins from plants are considered as a practical alternative. The employment of plant proteins is driven by the lower cost of crop production, easier accessibility, and sustainability concerns (Sim *et al.,* 2021). Aside from their nutritional importance, plant proteins are also gaining increased attention as important techno-functional ingredients in the food industry for use in processed foods to enhance their organoleptic properties like taste, texture, aroma and mouthfeel (Nwachukwu *et al.,* 2021). In this regard, proteins from pea (*Pisum sativum* L.) are becoming increasingly popular in the plant protein industry because of their economic feasibility and associated health benefits (Boye *et al.*, 2010). Their essential amino acid profile is comparable to that of other commercially produced legumes, such as soybeans, and they are

particularly rich in lysine, an amino acid often limiting in cereals (Pownall *et al.*, 2010; Tömösközi *et al.*, 2001). Consequently, when paired with cereals that are high in sulfur-containing amino acids, pea proteins can serve as a complete protein source. Meanwhile, pea proteins have two major disadvantages: digestibility-bioavailability and functionality. Generally, these characteristics are influenced by the structure of protein fractions and amino acid composition. The inherent structure of the protein fractions is predominantly composed of globular proteins such as albumins and globulins (Sim *et al.*, 2021). This directly results in the poor functionality of pea proteins in their raw form. Their poor functionality often arises from the harsh commercial extraction conditions. Many food processing companies use extrusion in order to manipulate the structure of proteins and starches and develop new food products. Traditional steam-based industrial extrusion for product development operates at high temperatures (>130°C) and shear (>150 rpm screw speed) and have irreversible adverse effects on thermolabile biomolecules like protein. Although milder techniques like supercritical fluid extrusion (Paraman *et al.*, 2012; Sauceau *et al.*, 2011), ohmic heating (Varghese *et al.*, 2014), ultrasound extraction (Malik *et al.*, 2017) are used in the food processing industry, they are highly expensive when operated for industrial scale production.

Enzymes are biological catalysts which are gaining increased attention as an alternative to manipulating the structure of proteins and starches in the food industry. Enzyme treatment offers a cost-effective means in food processing as enzymes function under mild temperature and pH conditions and exhibit high specificity for substrates and end products (Ramos *et al.*, 2011). As a result, other constituents in the food system are not influenced. Enzyme treatment modifies the structure of the proteins leading to an enhancement in their techno-functional properties and bioavailability resulting in increased solubility, foaming, emulsification, water, and oil-holding properties (Achouri *et al.*, 1998; Avramenko *et al.*, 2013; Goertzen, *et al.*, 2021a; Konieczny *et al.*, 2020a; Mokni Ghribi *et al.*, 2015). Protease treatment can control the exposure of buried hydrophobic amino acids from the core and as a result, alter the surface hydrophobicity (Mookerjee *et al.*, 2023; Panyam *et al.*, 1996). Moreover, in combination with localized hydrophilic patches on the outside, the enzymatically modified proteins can show some amphiphilicity. It has been extensively reported that low to moderate degrees of proteolysis unraveled the protein structure and led to a balance of hydrophobic and hydrophilic patches on the protein surface thereby leading to an increase in the functional properties (Eckert *et al.*, 2019; Mookerjee *et al.*, 2023; Yin *et al.*,

2008). However, the increase could be insignificant since increased proteolysis resulted in the breakdown of the protein structure into short-chain soluble peptides and ultimately to constituent amino acids. Thus, extensive degrees of hydrolysis potentially worsen the functionality.

Heat-induced glycation has been considered as an alternative means to change the structure of proteins. Utilizing heat can result in the formation of covalent linkages between peptides and dextrins through a naturally occurring conjugation between them called the Maillard Reaction. In this reaction, the ε-NH_2 group of the proteins (mainly lysine residues) reacts with the terminal carbonyl group of reducing sugars in a series of chemical reactions and finally results in the formation of protein-starch conjugates (de Oliveira *et al.*, 2016; Kutzli *et al.*, 2021). Owing to the differences in molecular weights between proteins and polysaccharides as well as the variability in different functional groups, the food industry formulates various processed foods with better functional properties using a mixture of proteins and polysaccharides (Cassiani *et al.*, 2013). It is believed that the covalent bond formation between the two macromolecules upon Maillard Reaction are very stable against changes in pH, temperature and ionic strength, thus making the conjugates resistant to changes in processing conditions (Dickinson *et al.*, 1991).

Pea protein-enriched flour, arising from air classification fractionation, contains about 45% – 50% protein by weight, minute quantities of lipid and the rest carbohydrates. Konieczny *et al.* (2020a) studied the influence of protease treatment on the functional properties of pea protein-enriched flours, and reported that although protein functionality increased, it was limited to certain degrees of hydrolysis after which, the functionality decreased due to loss in protein structure upon extensive hydrolysis. It was believed that hydrolysis exposes the buried hydrophobic cores form the protein and as a result increases the amphiphilicity (Mookerjee *et al.,* 2023). Carbohydrates/polysaccharides are hydrophilic in nature and conjugating the polysaccharide fraction to the hydrolyzed proteins by heat induced Maillard Reaction would further increase the amphiphilic nature of the proteins. This led us to develop this thesis research idea of conjugating hydrolyzed pea proteins with intact starch/non-starch polysaccharides or hydrolyzed dextrins from pea, and the structural and functional characteristics of the conjugate mixtures formed were analyzed.

1.2 General hypotheses

- Hydrolyzing pea protein followed by carbohydrate conjugation will enhance the amphiphilicity of the proteins at low and medium hydrolysis levels, leading to improved functional properties.
- Conjugating extensively hydrolyzed pea proteins with hydrolyzed starch and intact non-starch polysaccharide fraction of pea flour will enhance their techno-functionality.
- Combining hydrolyzed pea proteins from the air-classified fine fraction with hydrolyzed pea starch from the air-classified coarse fraction will produce amphiphilic protein-starch conjugate mixtures with improved functionality, especially at acidic pH.
- Maillard Reaction-induced conjugation of hydrolyzed pea proteins from fine fraction and hydrolyzed pea starch from the coarse fraction will result in the formation of a diverse array of compounds.

1.3 General objectives

- To investigate the enzymatic hydrolysis of pea protein-enriched and pea starch-enriched fractions, followed by heat-induced Maillard conjugation, and to confirm the occurrence of conjugation.
- To analyze the effects of a variety of starch to protein ratios and degrees of hydrolysis in the conjugation products
- To analyze the functional properties of the resulting conjugates, including solubility, foaming capacity, emulsification, water-holding capacity, and oil-holding capacity, to identify potential application areas.
- To conduct molecular weight, structural, and functional group analyses of the conjugates to elucidate the complexity of the conjugate mixtures and their structure-function relationships.

CHAPTER II

2 Literature Review

2.1 Proteins and their importance

Proteins are organic compounds composed of linear polymers of amino acids linked in a single chain by peptide bonds (Arif *et al.,* 2018). They are physiologically active molecules that govern nearly all life activities in organisms. Proteins are essential for various crucial anabolic and catabolic reactions in the body, such as muscle formation and maintenance (Carbone *et al.,* 2019); material transport across cells; synthesis, repair, and modification of genetic materials including DNA and RNA (Chatterjee *et al.,* 2017); and functioning as enzymes (Robinson, 2015) and hormones, among other roles. According to the recommended dietary allowance (RDA), a healthy adult male should consume about 0.8 g of protein per kilogram of body weight (Consultation, 2013). Proteins are composed of 20 different amino acids and while plants can produce all these amino acids, higher organisms, especially humans, cannot synthesize 9 of them and must obtain them from external sources. These amino acids are referred to as essential amino acids (EAAs). A protein source suitable for human consumption must contain all the EAAs, which include isoleucine, leucine, methionine, lysine, phenylalanine, threonine, tryptophan, and valine. Although plant sources have lower concentrations of these essential amino acids, a proper combination of various plant-based proteins can provide the ideal nutritional balance (including all the essential amino acids) for human consumption (Hertzler *et al.,* 2020; Nikbakht Nasrabadi *et al.,* 2021; Panghal *et al.,* 2006).

Beyond their role as vital nutritional components, proteins are extensively employed in the food industry as key techno-functional ingredients to enhance the taste, texture, and mouthfeel of processed and ultra-processed foods (Mookerjee *et al.*, 2023). These functional properties arise from factors inherent to the protein molecule and the surrounding environment and can be classified as intrinsic, extrinsic, and processing factors (Abd El-Salam *et al.*, 2009).

Intrinsic factors are inherent to the protein molecule, including amino acid composition, three-dimensional conformation of the polypeptide chain, reactive sites on the protein surface, molecular flexibility of subunits, and the presence of other conjugated subunits like carbohydrates and phospholipids. Extrinsic factors involve the solution the proteins are in, such as pH, salt concentration, temperature, solvent nature, and minor ingredients like lipids, phenolics, metal ions, vitamins, and minerals. Processing factors are techniques applied to modify protein molecules, such as heating/cooling, pressure, mechanical shear, freezing, drying, and chemical and enzymatic modifications.

These factors directly or indirectly alter the exposure of hydrophobic and charged groups on the protein surface, affecting their interactions with water, other protein bodies, starch, non-starch polysaccharides, cell wall materials, lipids, vitamins, and minerals in the food matrix. It leads to the development of specific characteristics called functional properties. These functional properties, also known as techno-functionality, are utilized in the food industry to enhance the textural and sensory properties of processed and ultra-processed foods, making them more desirable for human consumption (Capozzi *et al.*, 2021).

2.2 Plant proteins- legumes as alternative protein source

In developed countries, the consumption of animal protein has historically been high. However, producing animal proteins is significantly more expensive in terms of energy and water consumption compared to plant-based proteins. With the global population rapidly increasing and growing concerns about environmental protection, the sustainability of animal production is becoming increasingly challenging. Therefore, it is crucial to focus on alternative protein sources to provide quality nutrition for the global population. Many leguminous crops, such as peas, lentils, faba beans, chickpeas, soybeans, kidney beans and black beans are being cultivated in larger quantities in Canada for use as food ingredients, as they are believed to contain the essential amino acids necessary for human nutrition (Alajaji *et al.*, 2006; Gorissen *et al.*, 2018). They are rotated with cereal and oilseed crops due to their ability to fix atmospheric nitrogen by symbiotic associations with rhizobacteria, leading to a reduction in the use of chemical fertilizers, which in turn, can also lead to economic and environmental benefits (Wang *et al.*, 2018).

While protein content of cereals ranges between 10% to 15% (on a dry basis; d.b.), legumes have a protein content ranging from 20% to 30% (d.b.). They are high on aspartic and glutamic

acid, leucine, arginine and lysine but low on tryptophan and the sulphur-containing amino acids cysteine and methionine, which are complemented by cereals if consumed together (Konieczny *et al*., 2020b; Nosworthy *et al*., 2018). Pulses are the dried edible seeds of leguminous crops excluding oilseeds and are an excellent source of various nutrients, including complex carbohydrates (*e.g.*, resistant starch and other dietary fibers), proteins, vitamins, minerals, and phytochemicals (*e.g.*, isoflavones, phytosterols, and alkaloids) (Rebello *et al.*, 2014).

2.3 Pea- production, distribution, morphology and fractionation

Among legume sources, field pea also known as *Pisum sativum* L. (garden pea; a Fabaceae family pulse) is attracting significant attention due to abundant availability, low production cost, environmentally friendly nature, and numerous health benefits (Boye *et al.*, 2010; Lam *et al.*, 2018; Lu *et al.*, 2019; Petruzzello, 2018). Canada has consistently been one of the largest producers (~25% of total world production) and exporters (40% of total world exports) of field pea in the world (Ratnayake *et al.*, 2002). Reports from Pulse Canada in 2019 indicated that 4.2 million metric tonnes of peas were produced in that year, making Canada one of the largest pea producers globally (Bekkering, 2014). Consequently, peas are of significant interest and value to scientists in the fields of food and agriculture in Canada. Numerous studies are being conducted to extract and modify proteins from peas, aiming to expand the use of pea products as nutritious and functional food ingredients. Peas, typically climbing plants reaching heights of around 1 meter in vine length, are spring planted crops that thrive mainly in temperate regions with moderate rainfall. Field pea and garden pea are among the oldest domesticated crops, serving as food for humans and feed for livestock. Garden peas are commonly consumed as green vegetables, while field peas dominate the global market as dry grains and are used in the production of commercial pea products (Lu *et al.*, 2019). Pea is a spherical seed with an outer skin called the testa or hull. The core of the seed is dicotyledonous containing two embryonic leaves. Within the cotyledons, protein bodies and starch granules are embedded in the storage tissues of pea cells (Möller *et al.*, 2021).

In the past two to three decades, some pulses are fractionated into protein and starch rich fragments for utilization in the food and feed industries. Fractionation of pulses can be achieved through both dry and wet methods. Dry method usually constitutes dehulling as a pretreatment to minimize the contamination of hull fibers in the starch and protein fractions (Saldanha do Carmo *et al.*, 2020). Thereafter, the seeds are milled using different milling technologies (pin, hammer,

roller, stone, disc and jet milling) to grind them into flour (Joshi *et al.*, 2013; Pelgrom *et al.*, 2013, 2015). The resultant pulse flours can be further separated into starch-rich and protein-rich fractions through different approaches, among which air-classification is most commonly used (Ren *et al.*, 2021). In the air classification process, dehulled pulses are finely ground into flour and then separated into fractions based on particle size and density differences using a centrifugal air classifier with an air stream. It separates the flour into two fractions. The heavier fraction is mostly composed of larger starch granules with lower protein content, whereas the fine fraction is comprised mostly of protein bodies and has lower starch, or other carbohydrates, content (Wood & Malcolmson, 2020).

2.4 Pea proteins

Pea flour contains about 15% - 20% protein whereas the fine fraction from air classification contains about 50% - 55% proteins (Konieczny *et al.*, 2020a; Mookerjee *et al.*, 2023; Stone *et al.*, 2015). The protein bodies obtained from peas are spherical organelles, having a diameter of around 1 – 3 μm (Ratnayake *et al.*, 2002). The concentration of proteins in peas varies between 22% and 23%, depending on growth conditions, cultivars, and environmental factors (Konieczny *et al.*, 2020; Rubio *et al.*, 2014). In terms of dry weight, peas contain approximately 200 g of protein per kilogram (Rubio *et al.*, 2014). Additionally, peas consist of 40% – 50% starch and 10% – 20% fiber (Ren *et al.*, 2021). Pea proteins can be classified into four major groups: albumin, globulin, glutelin, and prolamin, with globulin being the primary storage protein (55% – 65%) (Adebiyi *et al.*, 2011). Globulin is further divided into two main types based on sedimentation coefficient: 11*S* legumin and 7*S* vicilin. Vicilin and legumin are present in a 1:2 ratio, with legumin being rich in sulfur-containing amino acids (Lu *et al.*, 2019; Mertens *et al.*, 2012; O'Kane *et al.*, 2004). Legumin is a hexameric protein, approximately 320 – 400 kDa in size, composed of acidic (40 kDa) and basic (20 kDa) subunits connected by disulfide bonds (Barac *et al.*, 2010). The hydrophilic α-chains, mostly in the acidic subunit, are on the surface, while the hydrophobic β-sheets in the basic subunit are buried inside, linked by disulfide bridges (Reinkensmeier *et al.*, 2015). Vicilin, a trimeric protein of about 150 – 180 kDa, lacks disulfide bonds due to the absence of cysteine residues (Shewry *et al.*, 1995; Tzitzikas *et al.*, 2006). Albumin (2*S*) is a water-soluble protein, making up 18% – 25% of the total protein content in pea seeds. It includes two low molecular weight, cysteine-rich albumins (PA1a and PA1b) of 4 and 6 kDa, respectively (Eyraud *et al.*, 2013;

Higgins *et al.*, 1986; Lu *et al.*, 2019). Prolamins are glutamine- and proline-rich proteins utilized for storage in plants, comprising a small fraction of pea proteins. Similarly, glutelin is present in minor quantities in pea seeds and constitutes a significant portion of the protein mass as gluten (Guleria *et al.*, 2009; Reinkensmeier *et al.*, 2015). Prolamins are rich in hydrophobic amino acids such as valine, phenylalanine, proline, and tyrosine. The globulin fraction is abundant in arginine, phenylalanine, leucine, and isoleucine, while the albumin fraction primarily contains tryptophan, lysine, and threonine (Stone *et al.*, 2015). Overall, pea proteins consist of a well-balanced amino-acid profile, especially rich in lysine (Barac *et al.*, 2010; Reinkensmeier *et al.*, 2015; Schneider, 2002).

2.5 Pea starch and non-starch polysaccharides

Pea flour contains approximately 20% to 50% starch granules and 15% to 21% total dietary fiber, primarily composed of non-starch polysaccharides. These include resistant starches, maltodextrins, cellulose, hemicelluloses, and pectins all embedded within the protein matrix. (Pelgrom *et al.*, 2013; Rempel *et al.*, 2019). Starch serves as the primary carbohydrate reserve in the cotyledons, with its granules exhibiting oval, spherical, kidney, and irregular shapes. The average granule sizes range from 15 to 28 μm. (Ma *et al.*, 2017; Wang *et al.*, 2014). Pea starch is primarily obtained as a by-product of protein isolation, making it a more economical source of carbohydrates compared to corn, wheat, or potato starches (Ratnayake *et al.*, 2002). The air-classified coarse fraction contains about 60% to 70% starch. Starch granules are typically semi-crystalline, with amylopectin branch chains forming double helices that pack into crystalline lamellae. These double-helical crystallites alternate with amorphous regions, mainly composed of branch points (Ren *et al.*, 2021). The two primary components of starch are amylose and amylopectin. In starch granules, amylose is usually found in amorphous regions and interspersed among amylopectin molecules. Smooth pea starches have an amylose content ranging from approximately 31% to 49% (Li *et al.*, 2019; Raghunathan *et al.*, 2017) and certain varieties of wrinkled pea can have amylose content of around 78% (Liu *et al.*, 2019; Zhou *et al.*, 2004). Amylopectin branch chains typically form double helices that pack into lamellar crystallites. These crystallites alternate with amorphous regions, primarily consisting of branch points, to create the semi-crystalline structure of starch granules (Oates, 1997).

The major carbohydrate building blocks of pea constitute glucose (approx. 50% w/w) followed by galactose (3% w/w), arabinose (2.8% w/w), uronic acids (3.5% w/w) and xylose (1% w/w). Rhamnose is also present in minor quantities. Among various other legumes, pea carbohydrates have the highest ratio of insoluble: soluble fibers at 3.8:1 (Tosh *et al.*, 2013). Amylose is significantly characterized by α-(1→4) linked D-glucopyranosyl residues with diverse chain lengths ranging in length from 4 residues to over a 100 (Hizukuri *et al.*, 1981; Takeda *et al.*, 1987). The molecular weight of amylose generally varies between 105 – 106 kDa (Hizukuri *et al.*, 1989). A slight degree of branching in amylose has been reported in starch sources from various pea cultivars as well. Amylopectin has an average molecular weight between 107 – 109 kDa and is made up of linear chains of α-(1→4)-D-glucose residue connected by α-(1→6) linkages (Ratnayake *et al.*, 2002). They contain multiple distributions of chains, each differing in length (Kobayashi *et al.*, 1986). Approximately 20 – 25 residues consists of each linear chain (Hizukuri, 1985).

2.6 Protein modification techniques

Plant proteins are being extensively utilized in the food industry to improve the functional properties and add value to foods. They serve as thickening and gelling agents, stabilizers for emulsions and foams, and binding agents for fat and water among many more (Sedaghat Doost *et al.*, 2020a, 2020b). However, plant proteins face several limitations as techno-functional ingredients due to various factors. For instance, plant proteins, including those from peas, consist of a mixture of different protein fractions, each with its own isoelectric point (pI), rather than a single uniform pI (Adal *et al.*, 2017). Apart from that, techno-functionality is also limited by several other factors, including the presence of plant-specific residuals known as antinutritional factors, inherent protein structural features, the complexation of protein bodies with other components in the plant matrix, harsh commercial extraction conditions that denature protein structures, and poor aqueous solubility (Mookerjee *et al.*, 2023; Nikbakht Nasrabadi *et al.*, 2021). To overcome these limitations, it is crucial to modify the physicochemical properties of proteins to enhance their functionality as ingredients in food systems. "Protein modification" refers to the process of altering the molecular structure or specific chemical groups of a protein molecule through various techniques to improve its nutritional value, techno-functionality, and bioactivity

(Nikbakht Nasrabadi *et al.*, 2021). Generally, protein modification methods can be classified into physical, chemical and biological.

Physical modification methods include heat treatment, irradiation with gamma rays, electron beams, and UV light, pulsed electric fields, high-pressure treatment, sonication, extrusion, plasma processing, and ultrafiltration (Chao *et al.*, 2018; Hadidi *et al.*, 2020; Li *et al.*, 2020; Mir *et al.*, 2019, 2020). Chemical protein modification methods broadly encompass glycation, phosphorylation, acylation, deamidation, cationization, and pH shifting (Kumar *et al.*, 2021; Kutzli *et al.*, 2021; Nesterenko *et al.*, 2014; Sánchez-Reséndiz *et al.*, 2018; Sebii *et al.*, 2021; Shah *et al.*, 2019; Zhong *et al.*, 2019). Biological modification includes enzymatic treatments and fermentation using microbial cultures. Compared to other modification methods, biological modification methods are relatively mild and environmentally sustainable, producing non-toxic byproducts (Çabuk *et al.*, 2018; Goertzen, *et al.*, 2021b; Goertzen *et al.*, 2021a; Konieczny *et al.*, 2020a,2020b; Kryachko *et al.*, 2020; Mokni Ghribi *et al.*, 2015; Xing *et al.*, 2020).

Among these modification methods, enzymatic treatments are receiving growing attention in the food industry for enhancing the nutritional and functional properties of proteins. This is because they operate under mild conditions of temperature and pressure, are easier to control, exhibit high specificity towards the substrate, and produce minimal toxic byproducts (Aluko *et al.*, 2003; Mookerjee *et al.*, 2023; Tavano, 2013). Extensive protein hydrolysis can fully unravel the protein structure, leading to a deterioration in its functional properties and quality. Therefore, it is crucial to monitor the degree of hydrolysis to ensure it does not exceed a certain threshold (Mookerjee *et al.*, 2023). Although a strict method for determining the degree of hydrolysis is not universally established, it has been broadly categorized the DH as follows: 2% – 7% DH is considered low, 8% – 14% DH is medium, 15% – 20% DH is high, and anything beyond 20% DH is classified as extensive. Limited enzymatic hydrolysis results in a reduction in the molecular weight of the protein, an increase in the number of ionizable groups, and the exposure of previously concealed hydrophobic moieties that were hidden from the solvent (Panyam *et al.*, 1996). These changes in properties lead to modifications in functional characteristics, enabling treated proteins to be used in a broader range of applications compared to their raw counterparts.

The degree of protein hydrolysis can be defined as the proportion of the total number of peptide bonds that are cleaved during hydrolysis and can be analyzed using a variety of methods

(Rutherfurd, 2010). The pH-stat method developed by Jacobson *et al.* (1957) is one of the most common methods. However, its major drawbacks include dependency on the type of enzyme used, its typical application in alkaline reaction mixtures, and the complex relationship between base consumption and degree of hydrolysis (DH) (Rutherfurd, 2010). The Osmometric method is another technique which focusses on the relationship between the number of hydrolyzed peptide bonds and the osmolarity of the reaction mixture (Dzwolak *et al.*, 1999). The OPA (*o*-phthaldialdehyde) method, which uses 2-mercaptoethanol, is also commonly employed to determine the degree of protein hydrolysis by derivatizing amino groups. This method requires the presence of a thiol group (Roth *et al*., 1973). The main disadvantages of the OPA method are that it is inaccurate for proteins rich in cysteine and proline, is affected by interference from lysine side chains, and is most effective only for soluble proteins. (Rutherfurd, 2010). In recent years, the TNBS (trinitrobenzenesulfonic acid) method has become one of the more commonly used techniques for determining the degree of proteolysis. This method relies on the reaction of the TNBS reagent with N-terminal amino groups (Adler-Nissen, 1979, 1986). The degree of hydrolysis is calculated as the ratio of the total number of N-terminal amino groups after hydrolysis of the original protein source to the amino acid composition after hydrolysis in 6 M HCl at 110°C for 24 hours. Synthetic leucine or glycine is used as a standard amino acid to determine the quantity of trinitrophenyl-amino acid derivatives present (Avramenko *et al.*, 2013; Bandyopadhyay *et al.*, 2008; Cheison *et al.*, 2009; Goertzen *et al.*, 2021; Jamdar *et al.*, 2010).

2.7 Impact of enzymatic hydrolysis on plant proteins

Ghribi *et al.* (2015) studied the effects of enzymatic (alcalase) hydrolysis on the conformational and functional properties of chickpea protein isolate. The degree of protein hydrolysis was analyzed using the TNBS method (Adler-Nissen, 1986). His study revealed that chickpea protein hydrolysates contained a higher protein content (79.2% – 83.75%) compared to the isolate. It was also observed that, with an increase in the extent of hydrolysis, there was a significant rise in protein content, indicating a progressive reduction in the insoluble protein fraction due to the proteolytic cleavage of peptide bonds, which resulted in a higher yield of soluble protein. Similar results were obtained by Achouri *et al.* (1998) who used bacterial protease to study the enzymatic hydrolysis of soy protein. Their results demonstrated a significant increase in protein content, rising from 66.8% at DH 4 to 86.8% at DH 10, with the extent of proteolysis. This

indicated that the cleavage of peptide bonds led to a progressive reduction in the insoluble protein fraction. Additionally, the increase in the number of free amino groups was directly related to the degree of hydrolysis. Yin *et al.* (2008) investigated the effects of limited enzymatic hydrolysis using trypsin on hemp protein isolate, and they employed the TNBS method to measure the DH (Adler-Nissen, 1979). It was reported that the DH profile was comparable to other protease-induced hydrolysis during the initial phase (0 – 300 minutes). However, the hydrolysis rate increased significantly after 300 minutes of incubation. The authors attributed this increase to the conversion of insoluble components into soluble ones by trypsin. They also stated that pretreatment significantly influenced the DH in the later stages of hydrolysis, while the initial digestion remains largely unaffected. Periago *et al.* (1998) investigated the effects of protease treatment (obtained from *Aspergillus saitoi*) on pea flour derived from wrinkled pea seeds to understand its nutritional and functional properties. Their experiments revealed that the true protein content in the hydrolyzed fraction was lower after enzymatic treatment compared to the original pea flour. They concluded that this decrease was due to the hydrolysis of pea protein, which released free peptides and amino acids as a result of the enzymatic process. Kumitch *et al.* (2020) investigated the effects of fermentation by *Aspergillus niger* and *Aspergillus oryzae* on PPEF. It was documented that fungal growth increased the DH of the proteins from 0% to 10% over a 6-hour fermentation period, without causing significant changes in the pH of the media. The crude protein concentration also rose from approximately 46.8% to 49.2% (d.b.) with *Aspergillus oryzae* and from 46.5% to 53.3% (dry basis) with *Aspergillus niger*. Konieczny *et al.* (2020a) investigated the modification of pea protein-enriched flour (PPEF) using trypsin, Savinase, papain, and pepsin to achieve specific levels of hydrolysis (2% – 4% and 10% – 12%). They also assessed the surface and functional properties of the hydrolyzed products. The study reported that untreated PPEF contained a higher concentration of larger molecular weight peptides (~93 – 31 kDa) and fewer smaller peptides (~15 – 3.5 kDa) compared to the hydrolyzed samples. This difference was attributed to the enzymatic action that reduced larger peptides to smaller ones. Overall, enzyme hydrolysis increased the protein content from 49.3% to 53.8%, while decreasing the lipid and ash contents from 7.0% and 4.3% to 2.4% and 3.7%, respectively. Goertzen *et al.* (2021a) used trypsin, pepsin and papain to hydrolyze chickpea proteins for their functional and nutritional properties enhancement. Hydrolysis showed a significant decrease in the protein content from 87.4 % – 85.4 % to about

79.2 % – 83.5 % with the decrease being more pronounced at higher degrees of hydrolysis. The surface charge, surface hydrophobicity and the techno functional properties of the hydrolysates were compared against the raw chickpea proteins.

2.8 Starch hydrolysis

Starch in its native state has very limited industrial applications, but when chemically or physically modified, it plays a major role in textural properties of food and has significant applications in food, paper, textile as well as pharmaceutical and higher value nutraceutical industries (Ahmed & Auras, 2011). Enzymatic hydrolysis of starch takes place in three steps- gelatinization which increases the accessibility of the substrate and enhances the rate of hydrolysis; liquefaction, which reduces the viscosity of the reaction mixture and hydrolyzes the gelatinized starch to form a product having a dextrose equivalent (DE) between 15 and 30 and finally saccharification, which breaks down partially hydrolyzed starch chains into glucose, maltose, maltotriose and some higher oligomers depending upon the specificity of the used enzyme (Baks, Bruins, *et al.*, 2008).

Ahmed and Auras (2011) studied the hydrolysis of lentil starch using sulfuric acid. The increase in peak temperature (Tp) in the differential scanning calorimeter in his study proved that significant hydrolysis took place in the starch structures. Baks *et al.* (2008) investigated the effects of starch pretreatment, enzyme addition timing, hydrolysis conditions, and reaction rate on the composition of hydrolysates during wheat starch hydrolysis with α-amylase from *Bacillus licheniformis*. It was reported that the highest enzyme-to-substrate ratio (10% w/w) achieved the greatest dextrose equivalent (DE) and that the initial rate of DE increase over time was maximized at this highest enzyme-to-substrate (E/S) ratio. The study also found that adding the enzyme during gelatinization at 90°C resulted in a higher DE compared to adding the enzyme after gelatinization at the same temperature. While the weight fraction profiles of maltose, maltotetraose, maltohexaose, and maltoheptaose were similar in both scenarios, the presence of the enzyme during gelatinization led to higher weight fractions of glucose, maltotriose, and maltopentanose. Manelius *et al.* (1997) investigated the action of bacterial α-amylase on wheat starch, focusing on A and B granules. Findings showed that the smaller starch granules were hydrolyzed to about 15% by α-amylase, while the larger granules were hydrolyzed to approximately 8% within the same time frame. Although the initial hydrolysis rate was faster, it eventually became constant and linear

for both types of granules as the reaction progressed. Gel permeation chromatography indicated that 80% of the starch components were eluted at the void volume. The study also indicated that, although the distribution of components for A granules remained unchanged, the proportion of high molecular weight components decreased slightly to about 2%, while the relative amount of low molecular weight components modestly increased for B granules. Edwards and colleagues assessed the starch digestibility of two different pea varieties using porcine pancreatic α-amylase to compare the kinetics of starch digestion in vitro. Their results indicated that starch digestibility was influenced by particle size and cell wall encapsulation. They concluded that the rate of starch digestion by α-amylase was not affected by the pea variety used in the experiments (Edwards *et al.*, 2018).

Rocha *et al.* (2010) investigated the hydrolysis of sweet potato, cassava, Peruvian carrot, and potato starches using bacterial α-amylase at 37°C for 48 hours. Their findings showed a reduction in amylose content for all starches, with cassava decreasing from 19.9% to 16.2%, sweet potato from 20.7% to 19.2%, and Peruvian carrot from 18.7% to 17.3%. In contrast, potato starch retained its amylose content at 29%. This indicated that the reduction in amylose content was proportional to the starch's enzymatic susceptibility to α-amylase. However, it was unclear whether amylose or amylopectin was more affected. The study concluded that starch susceptibility to hydrolysis varied among different botanical sources due to their distinct structural characteristics.

Biliaderis *et al.* (1979) compared the enzymatic hydrolysis of smooth pea starch with that of corn and wheat starches. It was revealed that pea starch hydrolysis resulted in a significantly lower DE compared to corn or wheat starches. This lower DE was credited to the higher amylose content in pea starch, which may be advantageous for the production of high-viscosity, non-sweet conversion products. Additionally, the study concluded that a substantially higher enzyme concentration was necessary to achieve complete solubilization of pea starch compared to the other starch varieties.

2.9 Protein-polysaccharide complexes

The chemical diversity of proteins allows them to engage in various molecular interactions, such as hydrophobic, electrostatic, hydrogen bonding, van der Waals forces, steric repulsion, and disulfide bridges with different substances. These interactions facilitate the formation of micro- and nanoparticles with enhanced technical and functional stability. Consequently, the

complexation of plant-based proteins with other macromolecules, particularly other proteins and polysaccharides, is attracting significant interest (Nikbakht Nasrabadi *et al.*, 2021).

Proteins can interact with both starches and other non-starch carbohydrates by engaging in strong non-covalent interactions as well as by forming robust covalent linkages. Protein-polysaccharide complexes and coacervates are attracting considerable interest from researchers because of their potential to transform the contemporary food industry. Typically, electrostatic interactions between oppositely charged macromolecules lead to the formation of coacervate complexes. Proteins can form electrostatic interactions with polysaccharides of opposite charges, resulting in the assembly of insoluble or soluble aggregated complexes with novel surface, structural, and functional properties (Fan *et al.*, 2020). At thermodynamic equilibrium, a two-phase system is formed, consisting of a coacervate and a solvent-rich subphase. Complexes between two macromolecules form when the total free energy of the system is negative. The formation of protein-polysaccharide complexes or coacervates primarily depends on the reduction of the system's total electrostatic energy (Gibbs free energy, ΔG) due to the release of counterions through ion-exchange processes during complex formation (De Kruif *et al.*, 2004; Turgeon *et al.*, 2007). De Kruif *et al.* (2004) examined the conformational modifications of pea globulin and α-gliadin proteins during coacervate formation with gum Arabic at various pH levels using Raman spectroscopy. Initial Raman spectroscopic analysis revealed the presence of β-sheets and random coils in the pea globulin structure, while α-helices were predominant in gliadin. Amide I band analysis indicated that the globulin-gum Arabic complex favored α-helix and random coil conformations at pH 4.0-3.5. Additionally, the increase in random coils in globulin was suppressed in favor of β-sheets at pH 2.75. Zhu *et al.* (2007) studied the interactions between N-succinyl-chitosan (NSCS) and bovine serum albumin (BSA), reporting conformational changes in BSA when mixed with NSCS. Pure BSA was found to contain 30.6% α-helix and 14.9% β-sheet. In the presence of NSCS, the helix component increased to about 34.5%, likely due to BSA dissolving in the hydrophobic domain of NSCS, resulting in a higher percentage of α-helices. The β-sheet component remained unchanged, suggesting that the polypeptide backbone and side chain functional groups of BSA remained intact, and BSA retained its folded conformation within the NSCS matrix.

2.10 Maillard reaction

Among the chemical modification methods, glycation stands out as particularly promising and highly desirable for food applications. This method does not require the use of hazardous chemicals and produces no by-products, making it an excellent plant protein modification technique in terms of consumer preferences, clean labeling, and commercialization (Nikbakht Nasrabadi *et al.*, 2021). Unlike strong electrostatic interactions, glycation results in the formation of irreversible covalent bonds between protein and polysaccharide molecules (Kutzli *et al.*, 2021b). The Maillard reaction, a naturally occurring glycation process, is the most commonly used method to form protein-carbohydrate conjugates (Arena *et al.*, 2017; de Oliveira *et al.*, 2016).

The Maillard reaction, also known as non-enzymatic browning, involves a series of complex chemical reactions that result in the formation of covalent bonds between amine groups and carbonyl groups at elevated temperatures. According to Hodge (1953), Maillard reactions can be classified into three stages: early, advanced, and final. These stages are interconnected and occur simultaneously (Hodge, 1953). The early stage of the Maillard reaction is marked by the initial glycosylation process. This involves a condensation reaction between the carbonyl group of a reducing sugar and the deprotonated amine group of an amino acid or protein, forming an N-glycosylamine and releasing a water molecule, resulting in the formation of a Schiff base (Ames, 1992). The Schiff base, being thermodynamically unstable, undergoes an irreversible spontaneous rearrangement to produce the Amadori reaction product (ARP). The ε-amino group of lysine residues, imidazole groups from histidine residues, indole from tryptophan residues, and guanidyl groups from arginine residues primarily participate in this condensation reaction. If ketoses such as fructose are used instead of aldoses in the Maillard reaction, the products formed after rearrangement are known as Heyn's products.

The intermediate stage of the Maillard reaction begins with the degradation of Amadori/Heyns products and is characterized by dehydration and fission, primarily through dealdolization and Strecker degradation. This leads to interactions between amino acids and dicarbonyl compounds. Under neutral or acidic pH conditions, these products undergo 1,2-enolization, resulting in the formation of furfural or hydroxymethylfurfural (HMF). At alkaline pH, the Amadori/Heyns products degrade via 2,3-enolization into reductones and various fission

products, such as acetol, pyruvaldehyde, and diacetyl. These fission products are highly reactive and immediately participate in further reactions (Martins *et al.*, 2001).

The final stage of the Maillard reaction is highly dependent on the reaction conditions and involves the dehydration and decomposition of early reaction products through various pathways, with Strecker degradation being the most common (de Oliveira *et al.*, 2016). This stage encompasses a wide array of reactions including cyclizations, dehydrations, retro-aldolizations, enolizations, oxidations, fragmentations, rearrangements, isomerizations, and further condensations, leading to the formation of numerous compounds (Friedman, 1996; Hodge, 1953). Although some color is produced during the intermediate stage, most of the color development occurs in the final stage when melanoidins are formed. These are nitrogen-containing polymers and co-polymers responsible for the characteristic brown coloration. (H. Y. Wang *et al.*, 2011).

Researchers have extensively examined the potential of protein-starch conjugation and investigated the products generated through the Maillard reaction. Mulcahy *et al.* (2015) investigated the physicochemical properties of whey protein conjugated with starches of varied dextrose equivalents using the Maillard reaction. They reported a 4.8% reduction in the available amino groups in the whey protein isolate control solution after heating at 90°C for 24 hours. This decrease was attributed to the heat-induced reaction of whey protein with low lactose levels and structural changes in the protein, which blocked the available amino groups. The greatest reduction in available amino groups occurred within the first 8 hours of heating the protein-starch solution, with a significantly lower decrease observed during the subsequent 16 hours. It was concluded that 8 hours of heating was optimal for maximizing protein conjugation while minimizing the progression of the Maillard reaction into its later stages. Heat treatment at pH 4.5 led to a significant decrease in protein solubility (from 87% to 9%), attributed to increased lysinoalanine levels and thermal-induced protein unfolding. This unfolding exposed previously shielded reactive sites, resulting in greater interactions and aggregation among the protein residues. Conversely, solutions containing conjugated whey protein isolate and starch products exhibited very high protein solubility (>95%) at pH 2-3 after 8 hours of heat treatment, compared to protein solutions heated alone (80%). SDS-PAGE results revealed the formation of large aggregates (>250 kDa) of α-lactalbumin and β-lactoglobulin upon heat treatment at 90°C for 8 hours, in contrast to the monomers of α-lactalbumin (14.2 kDa) and β-lactoglobulin (18.4 kDa) found in unheated samples.

This indicated that covalent bonding, rather than disulfide bonds, was responsible for aggregate formation. It was concluded that 8 hours of heating the starch-protein conjugate yielded the highest level of conjugation and enhanced functional properties (Mulcahy *et al.*, 2016). Zhu *et al.* (2010) studied the production of conjugates between whey protein isolates (WPI) and dextran (DX) by incubating aqueous solutions containing 10% WPI and 30% DX at pH 6.5 and 65℃ for 48 h. The study reported an increase in solubility of the protein-starch conjugates which was attributed to the attachment of bulky hydrophilic polysaccharides with the proteins. It was also shown that owing to the production of strong covalent bonds between the protein and carbohydrate residues, the conjugated products were very stable against changes in pH and temperature. It was concluded that the WPI-DX conjugates produced in mild conditions (60℃ for 48 h) had an enhanced solubility over the pH range from 3.2 to 7.5, elevated ionic strengths from 0.05 to 0.2 M, improved emulsifying ability and stability of emulsions as well as high heat stability compared to native WPI (Zhu *et al.*, 2010). Maitena *et al.* (2004) investigated the conjugation of alginate oligosaccharide (AO) with carp myosin (CM) using the Maillard reaction under controlled relative humidity to examine the functional properties of the CM-AO conjugate products. The results showed a loss in the total available lysine when 3.7 mg/mg of AO was bound to the myosin. This indicated that AO was covalently attached to the heavy chain of myosin through the Maillard reaction between the ε-amino group of lysine and the reducing terminus of AO. The study concluded that the conjugation of protein with AO improved solubility at low ionic strengths as well as the thermal stability of the compound, thereby enhancing its functionalities. Chen *et al.* (2015) investigated how the structure of sugars, considering size, position of the carbonyl group, and charge state, affects the thermostability of β-lactoglobulin while maintaining a consistent level of glycation with reducing sugars. The study found that β-lactoglobulin was more stable at pH 5 than at pH 3 or 7. Sugars with larger molecular sizes were more effective in enhancing the thermostability of the conjugated product due to increased steric hindrance, which inhibited the formation of large aggregates during heating at elevated temperatures. Zhao *et al.* (2022) investigated the impact of grafting xylo-oligosaccharides (XOS) onto pea protein using the Maillard reaction, focusing on the functional properties of the modified proteins. Their study demonstrated that the polysaccharide-to-protein ratio played a crucial role in the grafting degree. Analysis via SDS-PAGE and grafting degree measurements confirmed successful conjugation, revealing significant

variations in molecular weight distribution. Structural examination using FTIR and CD spectroscopy showed alterations in the secondary structure, with a reduction in α-helix content and an increase in β-sheet content, indicating protein unfolding and interaction with XOS. Additionally, the heat-induced Maillard conjugation treatment notably decreased particle size and increased zeta potential, suggesting improved stability. Kutzli *et al.* (2021) examined the influence of various Maillard reaction conditions on the formation and solubility of pea protein isolate (PPI)-maltodextrin conjugates. Their findings revealed that the browning index increased with elevated temperatures and prolonged heating durations, signifying advanced Maillard reaction progression. This was accompanied by a reduction in free lysine groups, indicating successful glycation. SDS-PAGE and size exclusion chromatography analyses demonstrated an increase in molecular weight with heating. Additionally, the isoelectric point shifted from pH 4.05 to pH 3.02 after 24 hours at 70°C, suggesting structural alterations in the proteins. Solubility tests further showed that glycation generally enhanced the solubility of the fibers, with higher temperatures and extended heating times leading to significant improvements in solubility. Zhang *et al.* (2022) studied the impact of Maillard conjugation of maltodextrins to pea proteins for emulsion stabilization. There was a significant increase in the absorbance values at 304nm and 420nm indicating continuous conjugation between maltodextrin and pea proteins. There was a noticeable increase in the absorbance at higher pH values which translated to higher Maillard conjugate formation at high pH values. SDS-PAGE of the conjugates revealed new bands with higher molecular weight beyond 250 kDa after Maillard reaction for the conjugate samples.

2.11 Structural characteristics

Depending upon the nature of the protein and polysaccharide interacting, their concentration, reaction time and temperature, a large amount of highly reactive compounds are produced some of which react further to form the advanced stages of the Maillard reaction products (de Oliveira *et al.*, 2016; Kutzli *et al.*, 2021). In order to have a holistic understanding of the nature of compounds formed, it is very essential to dive deeper and understand the structure and nature of the Maillard reaction products produced. These Maillard products are composed of a variety of volatile and non-volatile compounds like aldehydes, esters, furans, ketones, pyrazines, organic acids and contribute to the aroma, colour and taste of a variety of food products (Cui *et al.*, 2019; Siewe *et al.,* 2020). In addition to flavour, the MRPs also produce various colour compounds

(Kutzli *et al.*, 2021). Analyzing the conjugates will provide insights into the compounds responsible for specific functional attributes and may indicate whether they can demonstrate enhanced techno-functionality when produced on a larger scale.

2.12 Scanning electron microscopy

Scanning electron microscopy (SEM) is a powerful analytical technique used to examine the particle size and surface morphology of materials at a high resolution. SEM operates by scanning a focused beam of electrons across a sample, which interacts with the atoms on the surface to produce various signals that are detected and translated into an image (Goldstein *et al.*, 2003). This technique provides detailed topographical information and can achieve magnifications of up to 500,000 times, making it invaluable in fields such as materials science, food engineering, and biotechnology. SEM can reveal surface features down to the nanometer scale, allowing for the analysis of complex microstructures (Koga *et al.*, 2021). SEM has become an invaluable tool in food science for its ability to provide high-resolution images and detailed information about the microstructure of food products (Aguilera, 2005). SEM allows researchers to examine the surface morphology, texture, and structural integrity of various food items, which is crucial for understanding their physical properties, quality, and stability (Zha *et al.*, 2019). For instance, SEM can be used to study the effects of processing techniques such as drying, freezing, and extrusion on food texture and to analyze the structural changes in ingredients like proteins, fats, and carbohydrates (Jia *et al.*, 2022; S. Liu *et al.*, 2019; Ren *et al.*, 2021). This technique also aids in the investigation of food contaminants, packaging materials, and the interactions between different components within a food matrix. By offering insights into the microstructural aspects of foods, SEM helps improve product formulation, enhance sensory attributes, and ensure food safety and quality (Sharma *et al.,* 2019).

The microstructures of protein-polysaccharide conjugates have been widely studied using Scanning electron microscopy. The microstructure of pea protein-gum Arabic conjugates obtained using a controlled Maillard reaction have been observed by using Scanning Electron microscopy (Zha *et al.,* 2019a). The SEM results showed distinct differences in the surface morphology of pea protein isolate (PPI) and gum Arabic (GA) before and after the Maillard reaction. Initially, PPI exhibited a smooth surface, while GA had an irregular, rough texture. After undergoing the Maillard reaction, the PPI-GA conjugates showed significant changes. The surface of PPI became

more aggregated and rougher, indicating the formation of new molecular structures due to the reaction. The conjugates displayed a more compact and irregular structure compared to the individual components, suggesting successful conjugation between PPI and GA.

Wang and team examined the microstructure of soybean protein isolate and its maltose complex using SEM to assess the impact of irradiation treatment on their physical properties (Wang *et al.*, 2020). It was reported that the untreated soybean protein isolate exhibited a smooth surface, while the maltose-added isolate showed significant changes post-Maillard reaction, characterized by a honeycomb-shaped network structure with numerous small voids. It was stated that the irradiation treatment caused protein unfolding, exposing more active groups that facilitated the formation of disulfide bonds and hydrophobic interactions, resulting in a uniform and dense network. These findings suggested that irradiation treatment effectively promoted the reaction between proteins and saccharides, enhancing their structural properties.

Microstructures of rice protein-*Arthrobacter* exopolysaccharide conjugates have also been studied by Zhao *et al.* (2021). SEM analysis revealed significant morphological differences between the native rice protein (RP), exopolysaccharides (EPS), and the Maillard Reaction Products (MRPs). The rice protein showed a rough surface and irregular shape, while the MRPs displayed a more homogeneous and fine particle structure. The Maillard reaction led to the dispersion of aggregates and formation of tiny particles due to the steric block effect of polysaccharides. The authors discussed that those specific structural modifications could potentially enhance the functional properties of rice protein.

2.13 Fourier transform infrared imaging- attenuated total reflection (FTIR-ATR)

Fourier Transform Infrared (FTIR) spectroscopy is an analytical technique used to obtain the infrared spectrum of absorption or emission of a solid, liquid, or gas. It works by measuring how infrared light is absorbed by a sample, providing a molecular fingerprint that can be used to identify and quantify various substances. FTIR is widely employed in food science and technology due to its non-destructive nature, rapid analysis, and minimal sample preparation requirements. In food science, FTIR is used to analyze the composition and quality of food products, detect adulteration, and monitor changes during processing and storage (Kopjar *et al.*, 2021). For instance, FTIR can identify different types of carbohydrates, proteins, and lipids, helping in the assessment of nutritional content and food authenticity (Diblan *et al.*, 2018; Nunes, 2014).

Additionally, it is used to study protein secondary structure, monitor lipid oxidation, and evaluate the effects of food additives. The technique's ability to provide detailed molecular information makes it a valuable tool for ensuring food safety, quality control, and product development in the food industry (Wang *et al.*, 2020; Zhao *et al.*, 2021).

The structural analysis can be further confirmed (quantitatively) using the Fourier Transform Infrared (FTIR) spectroscopy. Zhang *et al.* (2022) and Zha *et al.* (2019b) studied the secondary structures of pea protein concentrate conjugated with gum Arabic and pea protein isolate and maltodextrin respectively in separate studies using the FTIR. The FTIR results provided detailed insights into the chemical interactions between PPI and GA during the Maillard reaction. Zhang and his group discussed characteristic peaks for proteins, including amide I and II bands for the native protein isolate samples. While analyzing PPI-Maltodextrin (MD) mixture and conjugates it was revealed that the intensity of specific peaks increased with the reaction time, indicating covalent bonding between PPI and MD. The composition of secondary structural features changed, with an increase in α-helix and random coil content, and a decrease in β-sheet and β-turn content after conjugation. These changes indicate the alteration in spatial structure due to the Maillard reaction (Zhang *et al.*, 2022).

Zha *et al.* (2019a) revealed that PPI exhibited characteristic amide bands at 1633 cm^{-1} (C=O stretching), 1525 cm^{-1} (N-H deformation), and 1398 & 1240 cm^{-1} (C-N stretching and N-H bending vibrations). GA showed bands in the region of 1500–800 cm^{-1}, attributed to C-H deformation, C-O, and C-C stretching. Post Maillard reaction, new bands appeared at 1568 cm^{-1} (possibly carboxylate ion COO^- or pyridine derivatives), 1654 cm^{-1} (C=N stretching from Schiff's base), and 3305 cm^{-1} (O-H and N-H stretching). These new bands confirmed the formation of PPI-GA conjugates and the structural modifications due to the reaction.

FTIR analysis of rice protein Maillard conjugated with *Arthrobacter* exopolysaccharides showed distinct changes in the infrared spectra of rice protein, exopolysaccharides, and MRPs. The spectra of MRPs indicated new absorption bands and shifts in existing bands, reflecting the formation of new covalent bonds and structural modifications. Specifically, the increase in amide I and II bands suggested enhanced protein-polysaccharide interactions. These changes confirmed the successful conjugation and potential improvement in the functional properties of the rice protein due to the Maillard reaction (Zhao *et al.,* 2021).

FTIR profile of soybean meal hydrolysates conjugated with different reducing sugars have also been studied (Sun *et al.*, 2023). An intensity decrease for amide I (1147 cm^{-1}) and amide II (1450 – 1240 cm^{-1}) peaks was observed for the MRPs which was related to the consumption of amino group in the curse of the Maillard reaction and the creation of novel functional group containing Schiff base (C=N), Amadori compound (C=O) as well as pyrazines (C–N). In summary, the FTIR spectra revealed a similar appearance of bands for MRPs formed using xylose and ribose and in contrast showed significant differences in bands in the intensity and position for MRPs obtained glucose, galactose and fructose which translated to a difference in the reactivity of different reducing sugars.

2.14 Protein secondary structure analysis using fluorescence spectra

Intrinsic fluorescence spectroscopy is a powerful analytical technique that leverages the natural fluorescence emitted by certain amino acids, primarily tryptophan, tyrosine, and phenylalanine, within proteins (Parolia *et al.*, 2022). When these aromatic amino acids are excited by UV light, they emit fluorescence, providing valuable information about the protein's environment, structure, and dynamics (Radotić *et al.*, 2023). In food science and technology, intrinsic fluorescence is extensively used to study proteins and their modifications, such as those occurring during the Maillard reaction—a non-enzymatic browning process where reducing sugars react with amino acids (Kutzli *et al.*, 2021). This reaction leads to the formation of Maillard conjugated products, which significantly impact the flavor, color, and nutritional value of foods (Yuan *et al.*, 2024). By analyzing the intrinsic fluorescence spectra, researchers can monitor changes in protein conformation, stability, and interactions during food processing (Kharbach *et al.*, 2023). For instance, intrinsic fluorescence can help detect structural alterations in proteins due to thermal treatment, pH changes, or the presence of additives, thereby providing insights into the quality and functionality of food proteins. This technique is particularly useful for characterizing the extent of Maillard-induced modifications by understanding the secondary structure and changes in confirmation, thereby enabling the assessment of their effects on food properties and nutritional value (Wang *et al.*, 2018).

While studying rice protein-Arthrobacter exopolysaccharide conjugates, Zhao *et al.* (2021) scanned the excitation from 300 nm to 400 nm and the emission was scanned from 370 nm to 570 nm. The fluorescence spectra analysis indicated that the emission wavelength was at 420 nm, with

excitation scanned from 300 to 400 nm and emission scanned from 370 to 570 nm. The MRPs showed distinct fluorescence properties compared to the native rice protein, indicating changes in the molecular environment and the formation of new fluorophores during the Maillard reaction. This suggested successful conjugation between rice protein and exopolysaccharides, enhancing the protein's structural properties. Sun *et al.* (2023) utilized an excitation wavelength of 295 nm, and an emission range from 375 nm to 550 nm to analyze the intrinsic fluorescence spectra of soybean hydrolysate conjugated with glucose, fructose, or galactose. The fluorescence intensity spectrum analysis indicated the formation of fluorescent substances, with the strongest fluorescence detected at emission wavelengths between 420 nm and 427 nm when the excitation wavelength was set to 347 nm. Tryptophan exhibited a blue shift in the maximum emission (λ_{max}) from 426 nm to 420 nm, indicating a shift towards shorter wavelengths. These results demonstrated the formation of characteristic fluorescent small molecules during the Maillard reaction. The analysis further demonstrated that the rise in fluorescence intensity and the shift in emission maximum were distinctive markers of the conjugation reaction between soybean hydrolysate and reducing sugars. Consequently, the authors concluded that fluorescence intensity served as an effective indicator of the production of fluorescent substances during the advanced stages of the Maillard reaction. Fluorescence spectra of sweet potato protein hydrolysates Maillard conjugated (ultrasound assisted) with xylose has been studied in a different research (Habinshuti *et al.*, 2021). It was reported that there was a significant increase in fluorescence intensity of the MRPs, with one sample showing the highest intensity at 450 nm post-Maillard reaction. The study revealed that ultrasound-assisted Maillard conjugation significantly enhanced the formation of fluorescent compounds, potentially improving the functional properties of MRPs derived using sweet potato proteins.

The intrinsic fluorescence spectra of glycosylated soybean proteins have also been examined (Wang *et al.*, 2020). The authors reported that the fluorescence emission spectrum of soybean proteins reflected changes in protein conformation at the tertiary structure level. Excitation at 290 nm revealed a shift in the maximum absorption wavelength (λ_{max}), where a red shift indicated structural unfolding, and a blue shift showed structural tightening. Maillard induced soybean protein conjugates revealed various degrees of red shift and significant decreases in fluorescence intensity. These changes suggested that irradiation treatment caused protein

unfolding, exposing fluorescent chromophore groups to the solvent and resulted in fluorescence quenching.

2.15 Molecular weight analysis using sodium dodecyl sulfate polyacrylamide gel electrophoresis

Sodium dodecyl sulfate polyacrylamide gel electrophoresis (SDS-PAGE) is a widely used technique for separating proteins based on their molecular weight. In SDS-PAGE, proteins are denatured by the anionic detergent SDS, which binds uniformly to proteins and imparts a negative charge proportional to their length (Laemmli, 1970). This allows the proteins to be separated solely based on size when an electric field is applied across a polyacrylamide gel matrix. In food science, SDS-PAGE is instrumental for analyzing food proteins, helping to determine their purity, molecular weight, and the presence of protein subunits or modifications (Goertzen *et al.*, 2021a; Mokni Ghribi *et al.*, 2015). This method is particularly useful for examining changes in protein composition during food processing, identifying allergens, and ensuring product quality.

SDS-PAGE gels can be stained using various dyes to visualize the separated proteins, and one effective staining method for detecting protein-carbohydrate conjugates apart from Coomassie Briliant Blue (CBB) is fuchsin sulfite staining. Fuchsin sulfite specifically binds to glycoproteins, highlighting the carbohydrate moieties attached to proteins (Zacharius *et al.*, 1969). This staining technique is valuable for studying the structure and extent of glycosylation in protein-carbohydrate conjugates, including those formed during the Maillard reaction (Li *et al.*, 2013; Liu *et al.*, 2012; Zha *et al.*, 2020). By using SDS-PAGE followed by fuchsin sulfite staining, researchers can gain detailed insights into the molecular structure and functional properties of these conjugates, which are crucial for understanding their roles in food flavor, texture, and nutritional quality.

Fechner *et al.* (2007) and group used SDS-PAGE to analyze the electrophoretic patterns of caseinate-dextran conjugates. The results indicated successful covalent linkage of sodium caseinate (SC) to dextran (Dex), shown by a gradual disappearance of the characteristic casein bands. Notably, the peak area of α-casein decreased significantly, suggesting better accessibility for covalent linkage due to its higher lysine content, while the presence of residual protein bands indicated significant unreacted protein in the conjugate sample. In a separate study, SDS-PAGE showed that glycation of pea protein isolate (PPI) with saccharides eliminated lipoxygenase, as evidenced by the vanishing lipoxygenase band. The emergence of new bands near the gel's loading

boundary indicated the formation of glyco-PPI (>250 kDa), suggesting that glycation and potential protein cross-linking occurred during the Maillard reaction (Zha *et al.*, 2020). Zhao *et al.* (2022) reported that after the Maillard reaction, protein bands in an SDS-PAGE at ~75 and ~45 kDa moved upward, and the ~23 kDa band faded, indicating the formation of higher molecular weight conjugates. The combination of high-pressure homogenization and ultrasound-assisted Maillard reaction enhanced the binding of pea protein molecules to xylooligosaccharides (XOS), increasing the formation of XOS-PPI conjugates. Kutzli *et al.* (2020) employed SDS-PAGE under reducing conditions to confirm covalent coupling between PPI and maltodextrin. The SDS-PAGE patterns of unheated and heated electrospun PPI-maltodextrin fibers showed characteristic bands of pea protein subunits. They reported that upon heating, the bands blurred, and a new high molecular weight band appeared at the top of the gel, indicating promoted glycation with increased heat and reaction time. The broad molecular weight distribution (~20 – 250 kDa) was attributed to the reaction of pea protein with maltodextrins of various molecular weights. Zhang *et al.* (2022) studied the Maillard reaction between pea protein isolate and maltodextrin. SDS-PAGE demonstrated molecular weight changes in PPI during conjugation with maltodextrin. New high molecular weight bands (>250 kDa) appeared after the Maillard reaction, indicating successful conjugation. Some protein fractions (37 – 50 and 75 – 100 kDa) disappeared due to covalent bonding with maltodextrin, with increased high molecular weight conjugates forming after 5 hours of reaction compared to 2.5 hours. Pea protein isolate gum Arabic conjugates have also been studied by Zha *et al.*, 2019a. SDS-PAGE was used to monitor molecular weight changes in PPI and PPI-GA systems during incubation. Novel high molecular weight fractions near the loading end confirmed the formation of PPI-GA conjugates, with notable reductions in specific polypeptide bands (~15 kDa and ~28 kDa) indicating participation of 11*S* and 7*S* globulins in the conjugation reaction.

2.16 Molecular weight distribution using HPLC

High-performance liquid chromatography (HPLC) is a highly efficient analytical technique used to separate, identify, and quantify components in a mixture. By passing a liquid sample through a column packed with a solid adsorbent material, HPLC leverages differences in the interactions between the sample components and the adsorbent to achieve separation (Rahimi *et al.*, 2020). In food science and technology, HPLC is extensively utilized for its precision, accuracy,

and ability to handle complex mixtures (Núñez *et al*., 2020). It plays a critical role in the analysis of high molecular weight MRPs, formed during food processing. Understanding these conjugated MRPs is essential because they contribute significantly to the flavor, color, and potential health effects of foods. HPLC helps in identifying and quantifying these compounds, thereby aiding in the assessment of food quality and safety (Martins *et al.*, 2001). For instance, HPLC can be used to monitor the formation of MRPs in processed foods, study their antioxidant activities, and investigate their implications on human health. This detailed molecular insight is invaluable for improving food processing techniques and developing healthier food products. The conjugates produced will be of different molecular sizes because of the polydispersity of the hydrolysates obtained by enzymatic hydrolysis (Zhao *et al.*, 2021). Hence a MW distribution analysis of the conjugates is necessary.

The MW distribution of sweet potato proteins conjugated with xylose was analyzed using the HPLC method (Habinshuti *et al.,* 2021). The rise in higher molecular weight fractions of 1,000 – 3,000 Da and 500 – 1,000 Da was attributed to the cross-linking of lower molecular weight proteins (200 – 500 Da and <200 Da) with xylose during the Maillard reaction. The HPLC profile for soybean meal hydrolysates conjugated with reducing sugars like D-glucose, D-fructose and D-galactose has been studied in detail by Sun and group (Sun *et al.*, 2023). Molecular weight analysis of Maillard reaction products (MRPs) revealed significant changes in molecular distribution due to complex chemical interactions, including peptide cross-linking and degradation. Post Maillard reaction, the distribution of MRPs showed a marked decrease in low molecular weight fractions (<128 kDa, 31.44%; 128 – 500 kDa, 37.24%; and 500 – 1000 kDa, 25.56%), particularly in those below 128 kDa compared to the starting sample. In contrast, the proportion of higher molecular weight MRPs (>1000 kDa) increased, suggesting that low molecular weight peptides were more susceptible to degradation while simultaneously forming larger compounds through cross-linking. Specifically, MRPs in the 1000 – 5000 kDa range were significantly enhanced, indicating that different sugar types influence MRP formation. Overall, the molecular weight results underscored the dynamic balance of degradation and polymerization processes during the Maillard reaction, impacting the functional properties of food products. In a different study, molecular weight distributions of rice proteins Maillard conjugated with *Arthrobacter* exopolysaccharides have also been studied using the HPLC method (Zhao *et al.*, 2021). HPLC analysis revealed that MRPs had

a broader molecular weight distribution compared to the native rice protein. New peaks corresponding to higher molecular weight compounds were observed, indicating the formation of macromolecular conjugates. The presence of these high molecular weight compounds confirmed successful conjugation through the Maillard reaction.

2.17 Surface properties analysis: surface charge & surface hydrophobicity

The surface properties of proteins, particularly surface charge and surface hydrophobicity, play a crucial role in their functionality, stability, and interactions in food science. Surface charge, determined by the ionization of amino acid side chains, influences protein solubility, aggregation, and interaction with other molecules (Avramenko *et al.*, 2013). A protein surface hydrophobicity, which refers to the tendency of its nonpolar amino acids to repel water, significantly affects its ability to interact with lipids and other hydrophobic substances, impacting emulsification and texture in food products (Konieczny *et al.,* 2020a). The correlation between surface charge and hydrophobicity is vital; for instance, proteins with a balanced charge and moderate hydrophobicity tend to exhibit better solubility and functional properties, such as foaming and emulsifying capacities (Mookerjee *et al.,* 2023). Understanding these surface properties is essential for designing and improving food products, enhancing flavor release, and optimizing texture, thereby contributing to consumer acceptance and overall quality.

A high zeta potential, defined as -30 mV or lower or +30 mV or higher, indicates the stability of proteins in solutions due to strong electrostatic repulsive forces between protein molecules (Stone, *et al.*, 2015). Conversely, a low zeta potential, ranging from -30 to +30 mV, suggests weaker repulsive forces, which can lead to protein-protein aggregation (Stone *et al*., 2015). Lam *et al.* (2017) investigated the surface properties of pea proteins and reported zeta potential values between -23.0 and -24.3 mV at pH 7, with no significant differences observed among the various cultivars studied. These low zeta potential values indicate that the proteins are unstable in solution and are prone to aggregation at a pH of 7. Konieczny *et al.* (2020a) studied the surface charge of pea protein enriched flour hydrolyzed using three different proteases. It was revealed that all samples exhibited a net-negative charge at pH 7.0, with untreated PPEF showing a significantly lower zeta potential (-12.6 mV) compared to enzyme-treated PPEF (-16.3 mV). This increase in charge from hydrolysis was attributed to the exposure of buried hydrophilic amino acids and peptide liberation. Among enzyme treatments, trypsin, Savinase, and papain resulted in

a lower charge (-15.4 mV) than pepsin (-18.9 mV), likely due to pepsin's cleavage at glutamic acid residues. Surface charge increased moderately from -15.7 to -16.6 mV as the DH rose from 2% – 4% to 10% – 12%. Untreated PPEF had a lower surface charge than pea protein hydrolysate (-24 mV), suggesting that carbohydrates and minerals in PPEF may shield protein charges and influence starch–protein interactions in solution. Wang *et al.* (2018) investigated the zeta potential of soybean proteins conjugated with xylose and fructose through the Maillard reaction. Their findings revealed that the Maillard reaction altered the charge density of soybean protein isolate (SPI), with the effects depending on the sugar type and reaction time. Initially, the zeta potential of SPI-MRPs increased, indicating the participation of $–NH_2$ groups. However, the authors noted that as the reaction progressed, the overall charge decreased, suggesting the formation of positively charged products. The results demonstrated that SPI's charge properties can be effectively modified through the Maillard reaction, enabling the customization of charge density according to the selected saccharide and reaction conditions, thus enhancing its potential as a polyelectrolyte wall material.

Konieczny *et al.* (2020a) also investigated the surface hydrophobicity of hydrolyzed pea proteins. Their results showed that untreated PPEF had significantly lower surface hydrophobicity compared to hydrolyzed PPEF, regardless of the enzyme or degree of hydrolysis (DH). This increase in hydrophobicity during hydrolysis was attributed to the unfolding of the protein structure, which exposed buried hydrophobic groups. Overall, surface hydrophobicity tended to rise with higher DH for all enzymes except pepsin, which exhibited consistent hydrophobicity across different DH levels. Conversely, treatments with trypsin, Savinase, and papain led to significant increases in surface hydrophobicity as DH increased. These results indicated that distinct surface properties can be achieved depending on the specific enzyme utilized in the hydrolysis process.

Wang *et al.* (2012) investigated the surface properties of glycosylated whey proteins, finding that the surface hydrophobicity index of partially glycosylated whey proteins (PGWP) was initially lower than that of whey protein isolate (WPI), indicating reduced overall surface hydrophobicity. However, at elevated temperatures, WPI exhibited a significant increase in surface hydrophobicity, which peaked after a certain heating time due to the exposure of buried hydrophobic regions. Prolonged heating resulted in a gradual decrease in hydrophobicity, likely due to intermolecular hydrophobic interactions. In contrast, PGWP showed a smaller increase in

surface hydrophobicity upon heating. The number of surface –SH groups in WPI increased with heating, while for PGWP, this increase was delayed. These findings suggested that PGWP had greater resistance to heat-induced unfolding compared to WPI. Ultimately, it was concluded that WPI-polysaccharide conjugates could help prevent protein aggregation and enhance the thermal stability of whey proteins across various concentrations and pH levels.

2.18 Functional properties analysis

2.18.1 Solubility

Protein solubility can be described as the balance between protein-protein (hydrophobic) and protein-solvent (hydrophilic) interactions, represented by the equation: Protein-Solvent ↔ Protein-Protein + Solvent-Solvent (Hall, 1996). It is sometimes referred to as "nitrogen solubility" because nitrogen from protein and nonprotein sources (such as nucleic acids, free amino acids, peptides, and phospholipids) is measured in solubility tests. Key factors affecting protein solubility include solvent pH, ionic strength, temperature, and the presence of organic solvents (Damodaran, 2008). The surface properties of proteins, particularly the quantity and distribution of hydrophilic and hydrophobic amino acid residues, significantly influence how a protein behaves in solution (Lam *et al.*, 2018).

Zhao *et al.* (2022) explored the pH-dependent solubility of pea protein isolate (PPI) and its conjugates, observing that solubility was relatively high at alkaline pH (10-8), dropped significantly at pH 8-5 (with the lowest solubility at pH 5, near its isoelectric point), and then increased slightly at lower pH levels. The authors suggested that the conjugation process did not fully prevent protein aggregation near the isoelectric point due to the presence of carbohydrate moieties on the protein surfaces, which could interfere with solubility. They cited earlier studies that showed that similar modifications, such as high-intensity ultrasound and high-pressure homogenization, had successfully improved the solubility of other proteins (*e.g.*, rapeseed and cod proteins). The authors concluded that combining high-pressure homogenization with an ultrasound-assisted Maillard reaction could further enhance the solubility and functionality of pea proteins, making them more suitable for food applications. Zha *et al.* (2019) measured the solubility of pea protein hydrolysate (PPH) and glyco-PPH with varying conjugation times. The solubility of the PPH-GA mixture was similar to that of PPH alone at neutral pH, indicating no

significant interaction. However, solubility increased from 19.4% to 26.2% after 1 day of conjugation with GA. Notably, extending the conjugation time beyond 3 days led to a sharp decline in solubility, attributed to overreaction and excessive cross-linking during the Maillard reaction. The authors emphasized the necessity of carefully modulating conjugation time to achieve desirable solubility and functional properties in glyco-PPH, thereby enhancing its potential for food applications. Kutzli *et al.* (2020) studied the solubility of PPI-MD conjugates before and after conjugation. The authors found that unheated fibers exhibited lower solubility, with a range of 23.5% at pH 4 (the isoelectric point) to 32.5% at pH 7. In contrast, heated fibers showed a marked increase in solubility across all pH levels studied, particularly at pH 2-4, where maximum solubility (44.5%) was observed at 65°C for 12 hours. Above pH 4, fibers heated at 70°C for 24 hours showed slightly higher solubility (34.2% – 35.3%). The authors concluded that glycation through the Maillard reaction, which occurs during the heating process, increased hydrogen bonding and improved interactions between protein and water, thereby enhancing solubility. In a separate study, Zhang and subordinates investigated the solubility profiles of PPI-MD conjugates in the pH range of 3.0 – 8.0 (Zhang *et al.*, 2022). The authors found that PPI exhibited the lowest solubility (2.8% at pH 4.4), aligning with its isoelectric point. In contrast, the solubility of PPI-MD conjugates increased significantly, particularly by 2-3 times between pH 4.0 and 5.0. They attributed this enhancement to the formation of covalent bonds between PPI and MD, which improved the protein's affinity for water. Additionally, they noted that increasing the reaction time from 2.5 to 5 hours led to further solubility increases, as higher conjugation levels reduced the availability of hydrophobic amino acids (cysteine and isoleucine) that typically hindered solubility. This study highlighted the potential for improving protein solubility and functionality through controlled Maillard reaction processes. Maillard induced pea protein gum Arabic conjugates have also been studied for their solubility by Zha *et al.* (2019b). The authors addressed the low solubility of pea protein concentrate (PPC), which poses challenges for its use in functional food applications. They reported that the solubility of PPC improved significantly when conjugated with gum Arabic (GA), with solubility increasing from 29.2% to 36.4% after 1 day and reaching 40.9% after 3 days of incubation. However, a decline in solubility was noted after 5 days, attributed to excessive conjugation leading to the formation of a dense network that hindered interactions with water. The authors emphasized the importance of controlling incubation time to optimize the

functional properties of PPC-GA conjugates and maximize their potential in food applications. Liu and group also studied the solubility of peanut protein isolate conjugated with dextran by the Maillard reaction (Liu *et al.*, 2012). The solubility of peanut protein isolate (PnPI) was monitored before and after conjugation with dextran. It was reported that the solubility of the peanut protein isolate-dextran mixture was higher than that of PnPI alone across a wide pH range, particularly at pH levels 2 – 4 and 7 – 10. The improved solubility was attributed to reduced protein denaturation and enhanced hydrophilicity due to dextran's influence. It was noted that the conjugates exhibited significant solubility improvements at pH 4.5 – 6.0 after 1 day heating, suggesting that the interaction of hydrophilic polysaccharides with PPI improved its affinity for water. However, only minor improvements were observed near the isoelectric point, indicating that the degree of glycosylation had a slower progression in this pH range.

2.18.2 Foaming properties: foam capacity (FC) and foam stability (FS)

Foams are dispersions of gas bubbles within a liquid (typically water) or a solid continuous phase, created through methods like sparging, whipping, shaking, or pouring (Hall, 1996). Because of the high free energy at the gas–liquid interface, foams are thermodynamically unstable and undergo coalescence and disproportionation to minimize the interfacial area. Solubilized proteins diffuse and adsorb to the gas–liquid interface, which reduces surface tension (Phillips *et al.*, 1990). They then unfold and orient hydrophobic regions to the gas phase and hydrophilic regions to the liquid phase to assume train and loop formations (Mookerjee *et al.,* 2023). This results in the formation of a cohesive, continuous film around gas bubbles due to interactions between polypeptides (Kinsella, 1981; Wierenga *et al.,* 2010). The foaming properties of food macromolecules can be determined by measuring the foam capacity (FC) and the foam stability (FS). Foam capacity (FC) refers to a protein's ability to trap air within a continuous liquid or semi-solid phase. Protein molecules diffuse to the air-water interface, where they unfold, orient themselves, and concentrate to form a thick, viscoelastic film around gas bubbles. This process results in a reduction of interfacial tension (Goertzen, *et al.*, 2021a). Conversely, foam stability (FS) measures how effectively a protein can maintain the volume and thickness of the continuous viscoelastic film over time. It prevents atmospheric air bubbles from infiltrating and breaking the film into its individual components (Konieczny *et al.*, 2020aShen *et al.,* 2021).

Konieczny *et al.* (2020a) assessed the foaming properties of untreated and hydrolyzed pea protein-enriched flour (PPEF) across different pH levels. It was reported that the foaming capacity (FC) of hydrolyzed PPEF decreased significantly compared to untreated PPEF, with reductions observed at pH 4.0 (from 133% to 97%), pH 7.0 (from 221% to 166%), and pH 10.0 (from 231% to 170%). The authors hypothesized that lower solubility in hydrolyzed samples inhibited their ability to migrate to the air-water interface and unfold, which are crucial for foam formation. It was discussed that although higher pH levels generally improved FC due to increased protein charge, specific enzyme treatments yielded different results. For example, trypsin-treated PPEF showed a decrease in FC with increasing hydrolysis levels at pH 4.0, while at pH 10.0, FC improved despite similar solubility levels. Overall, hydrolysis generally enhanced foam stability (FS) at pH 7.0 and 10.0, but FS remained low (<20%) at pH 4.0. The authors noted that factors such as peptide chain length and the hydrophilic/hydrophobic ratio of amino acids played significant roles in foaming properties, referencing other studies that reported similar findings in hydrolyzed proteins (Konieczny *et al.*, 2020a). Zhao *et al.* (2022) and associates investigated the effects of high-pressure homogenization combined with an ultrasound-assisted Maillard reaction on the functional properties of PPI. Results indicated that the conjugation of PPI through these treatments significantly improved both foaming capacity and stability compared to individual treatment groups. The study suggested that synergistic effects of these techniques could enhance the foaming properties of plant proteins, thus offering potential applications in food formulations that require improved functional performance. Zhao *et al.* (2021) explored the foaming properties of rice protein (RP) conjugates formed with *Arthrobacter* exopolysaccharides through the Maillard reaction. The foaming capacity of RP was found to surpass that of the conjugates, particularly at pH levels below 5.5 and above 10.0, with RP's foaming properties doubling at pH 6.5. Conversely, the conjugates displayed improved foaming stability, indicating their potential for application in foamy food products. The findings emphasized the importance of pH in determining the foaming behavior of RP and its conjugates, suggesting that the conjugates could still be beneficial in specific formulations requiring enhanced stability. Liu *et al*. (2021) investigated the foaming properties of PnPI-dextran conjugates. The FC and FS of dextran-conjugated PnPI showed significant improvements compared to untreated PnPI. It was reported that the FS increased by about 115% after 7 days of reaction time relative to PnPI. The authors attributed this enhancement

to the higher solubility of dextran-conjugated proteins, which allowed for faster transfer to the air-water interface, thereby improving FC. The research suggested that further improvements in functional properties could be achieved by optimizing glycosylation conditions involving different peanut protein fractions, highlighting the role of arachin and conarachin in this context.

2.18.3 Emulsification properties: emulsion activity and emulsion stability

An emulsion is a dispersion or suspension of two immiscible liquids formed through mechanical agitation, resulting in a dispersed phase of submicron droplets suspended within a continuous phase (Hall, 1996). Emulsions are thermodynamically unstable because of increases in the interfacial area, thereby raising the free energy of the system (McClements, 2015). Over time, oil-in-water (O/W) emulsions are susceptible to phenomena such as creaming, flocculation, and coalescence as the system strives to regain stability (Lam *et al.*, 2018). Proteins migrate to the interface to reduce interfacial tension between the two phases and orient themselves at the interface based on their amphiphilic properties, adopting train, loop, and tail configurations to create a viscoelastic interfacial film (Mookerjee *et al.*, 2023). The net charge of a protein and its capacity for rapid reorientation at the interface influences its molecular flexibility, a key characteristic of effective emulsifiers. Increased emulsion stability is demonstrated at a pH away from its pI and at low ionic strength, where electrostatic repulsive forces are stronger. Conversely, emulsions are least stable near the protein's pI and at high ionic strength, as the electrostatic repulsion is weaker compared to the attractive forces between droplets (Avramenko *et al.*, 2013). The emulsification properties of food macromolecules can be estimated by measuring the following properties. The emulsion activity index (EAI) provides a measure of the interfacial area between the oil droplets and water that can be coated by one gram of an emulsifier, during the formation of an emulsion and has been used as a good predictor for understanding the surface activity of proteins (Konieczny *et al.*, 2020a; Pearce *et al.*, 1978). The emulsion stability index (ESI) measures the emulsion's ability to resist changes over time (Boye *et al.*, 2010; Konieczny *et al.*, 2020a). Emulsion stability (ES %) provides a visual indication of the separation between the cream and serum layers, reflecting the percentage of the emulsion that remains intact and has not undergone separation over a designated time period (McClements, 2015).

Zha *et al.*, 2019b investigated the emulsification properties of pea protein concentrate-gum Arabic (PPC-GA) conjugates. It was reported that the conjugates significantly improved the

physical stability of corn oil-in-water emulsions under varying pH conditions. Specifically, emulsions stabilized by PPC-GA conjugates formed much smaller droplets (as low as 0.75 μm) and showed consistent stability across a pH range of 2 to 8, unlike emulsions stabilized by PPC alone, which experienced severe phase separation at pH 4 to 6 due to aggregation near the protein's isoelectric point. The study suggested that covalent bonding of GA to PPC enhanced the emulsification properties through improved steric repulsion and reduced aggregation, attributed to structural changes in glycoproteins that enhanced their interfacial activity.

Kasran *et al.* (2013) and group studied the emulsification properties of fenugreek gum-soy whey protein isolate conjugates. It was reported that emulsions stabilized by unhydrolyzed fenugreek gum conjugates produced significantly smaller droplet sizes and maintained stability over a 28-day storage period compared to those stabilized by partially hydrolyzed fenugreek gum. The study showed that the unhydrolyzed conjugate resulted in a monomodal droplet size distribution, indicating a stable emulsion. In contrast, emulsions with hydrolyzed gum exhibited a bimodal distribution, indicating instability as the average droplet size increased over time. Emphasis was laid on the importance of the structure of stabilizers used in emulsions, since unhydrolyzed fenugreek gum provided better emulsifying properties by preventing coalescence and maintaining small droplet sizes.

In a separate study, Li *et al.* (2013) and colleagues investigated the influence of saccharide structures on the emulsification activity and stability of rice protein hydrolysates. It was reported that the degree of glycation of rice peptides significantly impacted emulsifying activity, with an optimal range of glycation enhancing emulsification properties before a decline at higher glycation levels. The study highlighted the necessity of achieving an optimal hydrophilic-lipophilic balance for effective interfacial adsorption. The results emphasized the importance of saccharide structure in modifying the functional properties of rice protein, paving the way for potential applications in food formulations that required effective emulsifiers.

Zhao and colleagues reported that rice protein-*Arthrobacter* exopolysaccharide conjugates displayed improved emulsifying ability across various pH levels, with the emulsifying activity and stability significantly higher than untreated rice protein, particularly at pH levels between 4.0 and 10. The increased emulsification properties were linked to changes in solubility, surface hydrophobicity, and charge distribution. Additionally, the authors reported that the modified

proteins exhibited better interfacial activity due to the exposure of hydrophobic groups, which enhanced their ability to stabilize oil-water interfaces. Overall, the findings highlighted the potential of using Maillard reaction products as effective natural emulsifiers in food formulations (Zhao *et al.*, 2021).

2.18.4 Texture properties: water holding capacity (WHC) and oil holding capacity (OHC)

Water/oil-holding capacity determines the amount of water or oil retained by the conjugate solution (per gram basis) and is an important aspect of the textural and sensory properties of food products (Konieczny *et al.*, 2020a).

Water-holding capacity (WHC) ca be defined as the amount of water a sample can absorb per gram of material, reflecting its ability to retain water against gravity (Boye *et al.*, 2010). Water binding in proteins occurs through various forces, including ion-dipole, dipole-dipole, dipole-induced dipole, and hydrophobic interactions. The amino acid composition of a protein also plays a crucial role in determining its WHC. Water molecules bind to charged groups, backbone peptide groups, amide groups, hydroxyl groups, and nonpolar residues of amino acids, with each group having a different capacity to bind water (Damodaran, 2008). Highly charged proteins exhibit greater coulombic attraction toward water (Stone *et al.*, 2015). Likewise, WHC is lowest at the protein's isoelectric point due to maximum protein-protein interactions. Additionally, WHC increases at low salt concentrations because salt ions help bind water to proteins (Damodaran, 2008).

Shen *et al.* (2021) investigated the effect of guar gum conjugation and acylation on the WHC of PPI. The physical mixture of guar gum and pea protein showed significantly higher WHC compared to conjugated and unmodified proteins, due to guar gum's strong water-binding ability. Acylation further enhanced WHC by unfolding proteins and altering charge distribution. Sequential acylation and conjugation, especially with succinylated agents, had a synergistic effect, achieving the highest WHC of 10.91 g water/g protein among all modified proteins. Yang *et al.* (2022) examined the WHC of gliadin–amylopectin conjugates. They found that the WHC of these conjugates was generally lower than that of gliadin alone due to amylopectin's interference with protein aggregation and gel network formation. However, certain ratios of gliadin to amylopectin (1:1, 1:2) showed improved WHC due to increased solubility and free SH content. Higher ratios (1:4, 1:8) resulted in reduced WHC, likely due to protein conformation changes that hinder water

absorption. Konieczny *et al.* (2020a) explored the impact of enzyme treatment on the WHC of PPEF. Their study found that enzyme treatment more than doubled the WHC, with untreated PPEF showing a WHC of 0.60 g/g and hydrolyzed samples averaging 1.69 g/g. Pepsin- and papain-treated samples had higher WHC due to increased exposure of ionizable groups and capillaries from protein unfolding. The study also noted that a higher DH (10%-12%) improved WHC regardless of the enzyme used. Goertzen *et al.* (2021a) examined the WHC of chickpea protein isolate (CPI) after hydrolysis with different proteases. Hydrolysis significantly increased the WHC of CPI, with hydrolysates ranging from 3.6 to 5.1 g/g, compared to untreated CPI (2.8 g/g). The increase was attributed to higher zeta potential and protein affinity for water post-hydrolysis. Pepsin and papain hydrolysis, particularly at higher degrees (15% DH), yielded the highest WHC, in line with findings for pea protein flour.

Oil-holding capacity (OHC), also known as oil absorption capacity, is the measure of oil that can be absorbed per gram of protein (Konieczny *et al.*, 2020a). The interaction between lipids and proteins occurs through the binding of lipid aliphatic chains to the nonpolar side chains of amino acids (Lam *et al.*, 2018). Consequently, proteins with higher hydrophobicity generally exhibit a greater capacity to hold oils. OHC values can be affected by the protein's matrix structure, its amino acid composition, the type of lipid present, as well as the distribution and stability of the lipids (Damodaran, 2008).

Shen *et al.* (2021) demonstrated that all modified proteins had significantly higher OHC compared to unmodified pea protein. Conjugation modification notably increased OHC by altering and unfolding protein structure to expose more hydrophobic residues. Succinylated pea proteins exhibited higher OHC than acetylated ones, with the highest OHC observed in sequentially acylated and conjugated proteins. It was concluded that factors such as protein surface area, hydrophilicity/hydrophobicity ratio, and net charge affected the OHC. In a different study, Yang *et al.* (2022) explored the oil holding ability of wheat gliadin-maize glycoprotein conjugates. It was reported that the OHC of gliadin was 198.5 g/100 g, and conjugation significantly improved OHC. Conjugates at ratios of 1:2, 1:4, and 1:8 showed observable increases in OHC, with the 1:4 ratio reaching a maximum of 260.5 g/100 g, a 31.2% increase compared to gliadin alone. The improvement was attributed to interactions between exposed hydrophobic residues in gliadin and lipophilic substances, enhancing the lipophilicity and OHC of the conjugates. Konieczny *et al.*

(2020a) studied the OHC of hydrolyzed pea proteins and reported that the OHC of PPEF increased from 0.74 g/g to an average of 1.08 g/g with enzyme treatment. Hydrolysis increased OHC from 0.97 g/g at 2% – 4% DH to 1.20 g/g for 10% – 12% DH samples, likely due to increased surface hydrophobicity. Papain treatment resulted in the highest OHC increase, attributed to its nonspecific proteolytic action that opens up protein structure. In a separate research study, Goertzen *et al.* (2021a) reported that the native CPI had an OHC of 3.6 g/g. It was discussed that heat treatment mildly increased OHC to 4.0 g/g, while subsequent hydrolysis led to slight decreases (2.9 – 3.7 g/g). Pepsin treatment progressively decreased OHC, while trypsin and papain hydrolysates showed minimum OHC following ~10% DH. The authors declared that the decrease in OHC was unexpected despite high hydrophobicity of hydrolysates, likely due to conformational or size changes in the protein molecules.

CHAPTER III

3 Improving Techno-Functionality Of Air-Classified Pea Flour Fine Fraction By Enzymatic Proteolysis Followed By Maillard-Induced Conjugation With Available Carbohydrates In The Flour

3.1 Abstract

Background and objectives: Air-classified pea protein-enriched flour (PPEF) was hydrolyzed with trypsin and papain and heat conjugated with the carbohydrate fraction of the flour via Maillard reaction to form protein-carbohydrate conjugates. The surface and functional properties of the conjugates were assessed thereafter. **Findings:** The surface charge of the trypsin and papain conjugates were higher than that of PPEF at pH 7 and 10. Low degrees of trypsin hydrolysis followed by conjugation resulted in enhanced foam capacity (109.2% ± 2.0%) compared to the other conjugates and heated trypsin controls had the highest foam stability (76.9%) at pH 4. The emulsion activity index of the hydrolyzed-protein carbohydrate conjugates was higher at pH 4 (15.9 - 22.2 min) as compared to pH 7 (16.5 - 21.3 min). Trypsin conjugates showed the highest emulsion stability (ES) at pH 4 (96.4% - 98%). ES at pH 7 and 10 were similar. Both oil holding (OHC; 1.9 – 3.9 g/g) and water holding capacities (WHC; 1.7 – 2.4 g/g) were significantly improved. **Conclusions:** Maillard conjugated proteins have enhanced functional properties at pH 4, 7, and 10 as compared to PPEF. Most of the conjugates show high functionality at pH 4. Also, it was observed that only heating the low-cost, raw materials produced conjugates with enhanced functional properties. **Significance and novelty:** Enhanced functional properties at acidic pH are indicative of their use in beverage emulsions like fruit juices and processed drinks. High WHC and OHC show their potential use in food industry as an alternative to animal proteins.

Mookerjee, A., Nickerson, M., & Tanaka, T. (2024). Improving the techno-functionality of air-classified pea flour fine fraction by enzymatic proteolysis, followed by Maillard-induced conjugation with available carbohydrates in the flour. Cereal Chemistry, 101(1), 99–119. https://doi.org/10.1002/cche.10727

3.2 Introduction

Proteins are one of the major organic compounds and are involved in various important functions in the body. Nutritionally, proteins are one of the major macromolecules, which we need to consume in adequate quantities to maintain the daily calorie requirements by the body (Kumanyika *et al.*, 2020). According to the Dietary Guidelines for Americans, an adult between the age group of 19 – 59 eating a 2000-calorie diet a day must consume about 5.5 oz (155.9 g) of protein (Dietary Guidelines for Americans, 2020). Apart from their nutritional importance, proteins are gaining increased attention as important techno-functional ingredients in the food industry for use in processed foods to enhance their organoleptic properties like taste, texture, aroma, and mouthfeel (Nwachukwu *et al.*, 2021). The structure and amino acid composition are believed to influence such functional properties of proteins. For example, proteins derived from milk and egg play a crucial role as surfactants to stabilize edible foams and emulsions (Lafarga *et al.*, 2020). While the majority of functional proteins for such purposes are historically animal proteins, animal rearing is associated with high amounts of water consumption and greenhouse gas emissions, posing concerns in sustainability (Grossi *et al.*, 2019; Herrero *et al.*, 2011). Moreover, with the population projected to reach 9.7 billion by 2050, it is important to find alternate, sustainable, low-impact sources of proteins to supply adequate food to mankind (Sim *et al.*, 2021). Thus, a significant shift towards the use of plant-based protein sources in recent years has been noticed. Plant proteins have high availability, higher sustainability, and lower production costs (Sim *et al.*, 2021). Among plant proteins, pulse proteins are becoming increasingly popular because of their economic feasibility and numerous health benefits (Boye *et al.*, 2010). Meanwhile, pulse proteins are generally lysine-rich while sulphur-amino acids are present in sub-optimal amounts. This essential amino acid profile complements that of cereal proteins (lysine sub-optimal and sufficient sulphur amino acids) in diet (Pownall *et al.*, 2010; Tömösközi *et al.*, 2001). Besides these, pulses enjoy the status of non-genetic engineered. A major drawback of pulse protein is its inferior digestibility and bioavailability owing to harsh commercial protein extraction/isolation conditions like traditional steam-based extrusion which leads to denaturation and aggregation of proteins (Sim *et al.*, 2021).

Enzyme treatment is gaining increased attention owing to “clean” label, specificity, and mild operating conditions (Ramos *et al.*, 2011). Protease treatment can control the exposure of

buried hydrophobic amino acids from the protein internal structure (or core) and as a result alter the surface hydrophobicity (Mookerjee *et al.*, 2023; Panyam *et al.*, 1996). Moreover, in combination with dominating hydrophilic surface of protein molecules, the enzymatically modified proteins can result in an increase in their amphiphilicity. Trypsin and papain are two of the most widely used proteases in the food industry for protein structure manipulation (Nadzri *et al.*, 2021). It has been extensively reported that low to moderate degrees of proteolysis unravels the protein structure and leads to a balance of hydrophobic and hydrophilic patches (amphiphilicity) on the protein surface thereby enhancing the functional properties like foaming, emulsification, solubility, water holding (WHC) and oil holding capacities (OHC). (Eckert *et al.*, 2019; Konieczny *et al.*, 2020a; Mookerjee *et al.*, 2023; Yin *et al.*, 2008). However, the functional properties are significantly reduced with extensive hydrolysis beyond a certain degree of hydrolysis (DH) due to complete unravelling of the protein structure.

As mentioned, amphiphilic natures of unraveled proteins are important for their functionality. Further modification of amphiphilic nature may lead to additional and/or enhanced functionality of proteins. Heat-induced glycation is a possible technique to modify amphiphilic nature of partially unraveled proteins. In glycation reactions, the ε-NH2 group of proteins (mainly lysine residues) react with the terminal carbonyl group of the reducing sugar by a naturally occurring phenomenon called the Maillard reaction (de Oliveira *et al.*, 2016; Liu *et al.*, 2012). It is believed that the covalent bond formation between the two macromolecules upon Maillard reaction are very stable against changes in pH, temperature, and ionic strength, thus making the conjugates resistant to changes in processing conditions (Dickinson *et al.*, 1991). The resulting proteins are conjugated with more hydrophilic substances, and it would alter their conformation and surface chemistry leading to enhanced functional attributes like solubility, foaming, emulsification, and thermal stability (Qu *et al.*, 2018; Zhao *et al.*, 2022a). Zhao *et al.* (2022a) reported a significant increase in the solubility, foaming and emulsifying properties of pea protein isolate (PPI) conjugated with xylo-oligosaccharides (XOS) as compared to PPI. Similarly, Mu *et al.* (2011) reported a significant increase in the solubility and emulsifying properties of soy protein isolates (SPI) conjugated with acacia gum (AG) as compared to native SPI at the same pH values. Similarly, Niu *et al.* (2011) reported an improvement in the solubility and emulsifying properties of wheat germ protein (WGP) glycated with different saccharides. Another study by Yadav *et al.*

(2012) demonstrated the capability of forming fine emulsions with enhanced stability by corn fiber gum-milk protein conjugates. It was also reported that WPI-Dex conjugates enhanced heat stability, and significantly improved solubility and emulsifying ability as compared to the native WPI (Zhu *et al.*, 2010).

Much of the literature reported enhanced functional properties of Maillard conjugates between proteins and carbohydrates obtained from different sources which, when operated on an industrial scale, is not always economically feasible. In order to extend the realm of research concerning Maillard conjugates, in this study, a starting material (PPEF) was set without the addition of external carbohydrates keeping economic concerns in mind. The major objectives of this study are as follows: (1) obtaining protein hydrolysates with low to medium DH using two different proteases (trypsin, and papain) (2) development of heat-induced Maillard conjugated products (hydrolyzed pea protein- pea carbohydrate) (3) functional properties analysis of the conjugates. This would lead to the formation of pea protein-carbohydrate conjugates having various combinations of hydrolyzed protein and carbohydrate fractions giving a wide range of functional properties. It will also eliminate the use of harsh reaction conditions like high shear and temperature as well as other non-food-grade additives like lysine or phenylmethylsulfonyl fluoride (PMSF) thus giving it a clean label.

3.3 Materials and methods

3.3.1 Materials

Pea protein enriched flour (PPEF), which is the fine fraction obtained after air classification of milled pea flours was kindly donated by AGT Foods (Saskatoon, SK, Canada). Petroleum ether was purchased from Fisher Scientific (Ottawa, ON, Canada). Trinitrobenzenesulfonic acid (TNBS), porcine trypsin (10,600 units/mg), papain (1.5-10 units/mg solid) from papaya latex, were purchased from Sigma-Aldrich Canada (Oakville, ON, Canada). All other chemicals used in this study were ACS-grade or better. The water used in this research was produced from a Millipore Milli-Q™ water purification system (Millipore Corp., Milford, MA, USA).

3.3.2 Proximate composition analysis

Proximate analysis of the samples was measured according to AOAC Official Methods 925.10 (moisture), 923.03 (ash), 920.85 (lipid), 997.09 (crude protein by using %N×6.25) and

AACC Method 76-13.01. The amounts of protein, lipid, moisture, ash, and total starch were subtracted from the total amount, and this remaining amount was considered as other carbohydrates.

Moisture

The moisture content of both untreated and processed PPEF samples was determined gravimetrically using a gravity-flow convection oven (Fisher Scientific Isotemp Standard Lab Oven, Thermo Fisher Scientific Inc., Waltham, MA, USA) set at 105°C, in accordance with the Official Method 925.10 of AOAC International (AOAC, 2005). Aluminum dishes (57 mm) were pre-dried in the oven for 1 hour, then allowed to cool to room temperature in a desiccator. Approximately 0.5 g of each sample was weighed into the pre-dried dishes and dried for 20 hours. The following day, the samples were removed from the oven and cooled for one hour in a desiccator before being weighed on an analytical balance. The moisture content (%MC) was calculated using the following formula:

$$Moisture\ (\%) = \frac{Weight\ of\ sample - Weight\ of\ dried\ sample}{Weight\ of\ sample} \times 100 \quad \text{.....(3.1)}$$

Ash

The ash content of both untreated and treated PPEF samples was determined gravimetrically using a muffle furnace (Fisher Scientific Isotemp Basic Muffle Furnace, Thermo Fisher Scientific Inc., Waltham, MA, USA), following a modification of AOAC International's Official Method 923.03 (AOAC, 2005). Porcelain crucibles were pre-dried for 1 hour at 525°C, then left to cool for 2 hours before being placed in a desiccator to reach room temperature. Approximately 0.5 g of sample was added to the pre-dried crucibles, followed by pre-ashing on a hot plate at high heat inside a fume hood until the samples were completely blackened. Afterward, the samples were placed in the muffle furnace and heated overnight at 525°C until white ash was obtained. The crucibles were then cooled for 2 hours before being transferred to a desiccator to cool down to room temperature. The ash content was calculated using the following formula:

$$Ash\ (\%) = \frac{Weight\ of\ sample - weight\ of\ driend\ sample}{Weight\ of\ sample} \times 100\%$$

……(3.2)

Lipid

The crude lipid content of PPEF samples was determined using a Goldfisch apparatus, following a modified version of AOAC International's Official Method 920.85 (AOAC, 2005). Prior to the extraction, glass beakers were pre-dried in a forced air oven at 105°C for 1 hour, then transferred to a glass desiccator to cool to room temperature for 1 hour. Approximately 0.6 g of each sample was weighed, placed into cellulose extraction thimbles, and inserted into the extraction sleeve. The pre-weighed glass beakers were filled with approximately 40 mL of petroleum ether and positioned on the Goldfisch apparatus to begin the extraction process. The samples were extracted for 6 hours to ensure thorough removal of lipid components. After extraction, the petroleum ether was allowed to evaporate, and the beakers were placed on a heating plate at 250°C for 30 minutes, followed by overnight drying in a forced air oven. Once cooled in a glass desiccator, the beakers were re-weighed, and the lipid percentage was calculated using the following equation:

$$Lipid\ (\%) = \frac{Weight\ of\ beaker\ after - weight\ of\ beaker\ before}{sample\ weight} \times 100\ \%$$

……(3.3)

Protein

The protein content of both untreated and treated PPEF samples was measured using the LECO method, in accordance with AOAC International Official Method 997.09 (AOAC, 2005), utilizing a FP628 LECO analyzer (3000 Lakeview Avenue, Saint Joseph, MI). Approximately 0.250 g of sample was placed into a sample chamber, where it was combusted at 1000°C in the presence of oxygen. During this process, the carbon and nitrogen in the sample were converted into CO2 and NOx, respectively. These gases were then separated by chromatography and analyzed using a thermal conductivity detector. The protein content was calculated by applying a conversion factor of 6.25.

Total starch

Total starch content was determined using the Megazyme Total Starch Assay Kit (Ireland Ltd., Bray, Ireland) (AACC Method 76-13.01). In brief, a pre-treatment to the flours with dimethyl sulfoxide was performed at 100°C to solubilize resistant starch. The sample was then heated in the presence of α-amylase, followed by hydrolysis into glucose by amyloglucosidase.

3.3.3 Protein solution preparation

Protein solutions (1.5% and 2% w/v based on protein amount in PPEF) were prepared in 2 L of 50 mM sodium phosphate buffer solution (pH 7.0), and 1 L of 50 mM sodium phosphate buffer solution (pH 6.5), respectively, based on the results obtained from a series of small-scale experiments (data not show). The solutions were left to stir overnight at 4°C, and the pH was readjusted using 0.5 M NaOH or HCl.

3.3.4 Production of hydrolyzed protein-carbohydrate and hydrolyzed protein-hydrolyzed starch Conjugates

PPEF solutions were initially heated at 80°C for 60 min for starch gelatinization. Once cooled, the temperature and pH were adjusted to 37°C and pH 7 for trypsin reaction, and to 60°C and pH 6.5 for papain reaction (Konieczny *et al.*, 2020). Following 60 min of incubation, the solutions were heated to 90°C for 30 minutes to terminate enzymatic reaction and induce Maillard reaction. The Maillard reactions were quenched through prompt freezing of the solutions. Later they were freeze-dried for functional properties analysis.

Heated controls (37°C for trypsin reaction and 60°C for papain) were also run parallelly where no enzymes were added but followed all the heat treatment procedures for the enzymatic reactions. Throughout the article, samples designated as PPEF are raw materials without any Maillard treatment. Tryp0 and Pap0 are heat controls (raw PPEF) without any enzymatic hydrolysis heated for Maillard conjugation to mimic the enzymatic reactions. Tryp2.5, Tryp9.9, Tryp10.8, Pap3.3, Pap5.2, Pap8.1, Pap9.1 and Pap10.2 are proteolyzed PPEF conjugated (Maillard) with carbohydrates/starch. For simplicity, the naming and different reaction parameters are summarized in Table 3.1.

3.3.5 Determination of the degree of hydrolysis (DH)

The DH was analyzed using the Adler-Nissen method (Adler-Nissen, 1979) with slight modifications as reported by Avramenko, Low & Nickerson, (2013) (Figure 3.1). In brief, a 0.25-mL aliquot of the sample solution was removed at 60 min of proteolysis described in section 2.4, and it was added to 2 mL of 1% (w/v) SDS (prepared in Milli-Q water). The mixture was then

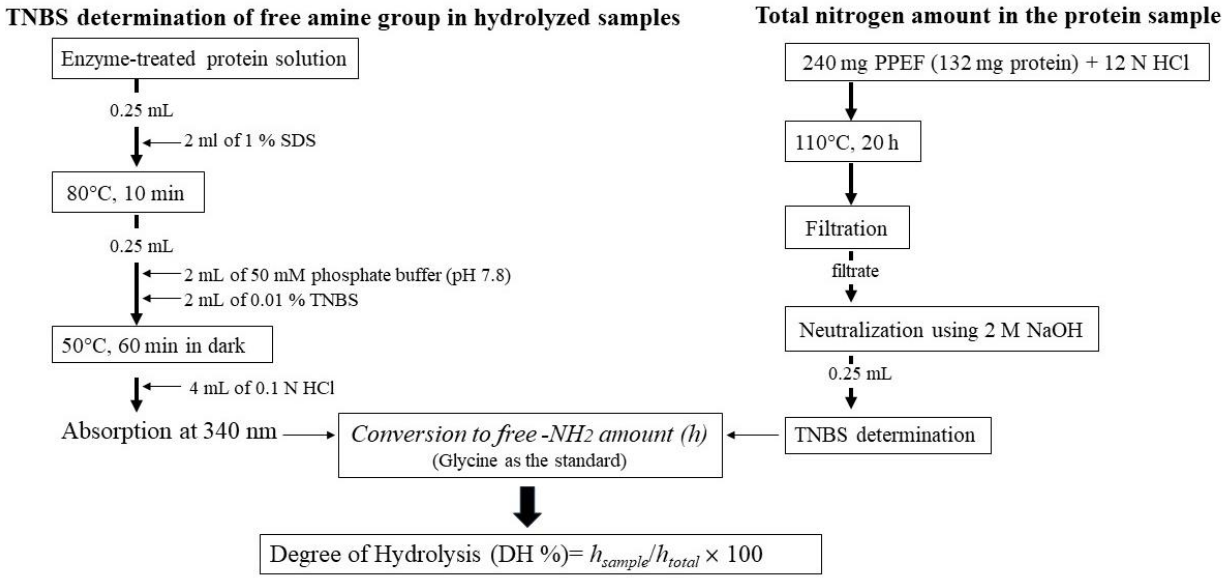

Figure 3.1. Flow chart of degree of hydrolysis (DH) determination

For enzyme-treated protein solutions: 0.25 mL of enzyme-treated solutions were added to 2 mL of 1% SDS from which 0.25 mL was withdrawn and mixed with 2 mL 50 mM of sodium phosphate buffer at pH 7.8. Two milliliters of 0.01 % TNBS was added to this solution, and the mixture was incubated at 50°C for 60 min. The reactions were terminated using 4 mL of 0.1 N HCl. The absorption was read at 340 nm, and the absorbance values were converted in terms of molarity of glycine equivalents (h_{sample}) using a glycine standard plot. For the determination of total nitrogen in the protein sample: 240 mg PPEF (132 mg protein) was added to 7.5 ml of 12 N HCl and 7.5 ml of ddH_2O in a capped test tube. The mixtures were stirred for 1 hr before heating them in a forced air oven at 110°C for 20 hr for complete hydrolysis of proteins. Thereafter, the solutions were filtered using Whatman #3 filter paper, and the filtrates were neutralized using about 20 milliliters of 2 N NaOH. Following this 0.25 mL of the solutions were dispensed and the TNBS reaction was performed as described above to determine the total nitrogen amount (h_{total}).

heated at 85°C in a water bath for 10 min to quench the hydrolysis reaction. A 0.25-mL aliquot was taken from this SDS mixture and diluted with 2 mL of 50 mM sodium phosphate buffer (pH

7.8). The diluted solutions were mixed with 2 mL of 0.01%(w/v) TNBS solution (freshly prepared), and the mixtures were incubated in a covered (protected from light) shaking (90 rpm) water bath at 50°C for 1 h. To this TNBS reaction mixture, 4 mL of 0.1 N HCl was added to terminate the derivatization reaction. The samples were cooled to room temperature (30 min), and their absorbance was read at 340 nm using a Genesys 10S UV vis spectrophotometer (Thermo Scientific, OR USA). A standard curve was prepared with Gly. The glycine equivalents of each experiment were determined based on the following formulae:

$$h_{sample} = h_t - h_c \quad \text{.....} \quad (3.4)$$

where, h_{sample} is the yield of hydrolysis equivalents (of α-amino groups formed during the hydrolysis reaction), h_t is the concentration (mM) of α-NH_2-Gly equivalent at the time point under consideration (obtained using the Gly standard curve), and h_c is the millimolar concentration of α-NH2-Gly equivalent from the initial solution before the addition of enzymes (control).

To determine the total acid hydrolysis of PPEF, 240 mg of PPEF (132 mg protein) was digested using 12 N HCl in a forced-air oven (Yamoto Mechanical Convection DKN600, Yamoto Scientific America, Inc., CA, USA) at 110°C for 20 h. Samples were cooled and filtered through Whatman filter paper #3 (Whatman International Ltd., Maidstone, UK), and the filtrates were neutralized with 1 M NaOH. The amount of liberated amine group was analyzed using the TNBS reaction. The determined α-NH_2-Gly equivalent was represented as h_{total}.

The DH was determined as a ratio of the concentration of α-NH_2-Gly equivalent obtained from enzymatic hydrolysis (h_{sample}) to the total concentration of α-NH_2-Gly equivalent obtained from the total acid hydrolysis (h_{total}).

$$DH\ (\%) = \frac{h_{sample}}{h_{total}} \times 100 \quad \text{.....} \quad (3.5)$$

3.3.6 Sodium dodecyl sulfide polyacrylamide gel electrophoresis (SDS-PAGE)

The polypeptide profiles of the hydrolyzed PPEF, and confirmation of the size shift of the conjugates before and after conjugation were determined by sodium dodecyl sulfide

polyacrylamide gel electrophoresis (SDS-PAGE) using the Laemmli method (1970). In short, proteins were prepared by heating them in a sample buffer containing SDS. The buffer also includes a reducing agent, such as β-mercaptoethanol or DTT, which breaks disulfide bonds to further denature the proteins. Samples were then loaded onto a polyacrylamide gel composed of a stacking gel at the top, with lower acrylamide concentration and pH, and a resolving gel below, with higher acrylamide concentration and pH to separate proteins by size as they migrate. An electric field was applied, for proteins to move toward the positive electrode, with smaller proteins migrating faster than larger ones. After electrophoresis, proteins were stained with Coomassie Brilliant Blue dye to visualize the separated bands, where each band corresponds to proteins of similar molecular weight.

For confirmation of the size shift of the conjugates prior to and after reaction, as well as determination of glycosylated proteins, the gels were stained using a Fuchsine-sulfite staining method as demonstrated by Zacharius, Zell, Morrison & Lockwood (1969). The conjugated protein bands were quantified using ImageJ® (National Institutes of Health, Bethesda, USA) using the digitized image of the gel.

3.3.7 Monitoring of amadori compounds formation and browning

The conjugated samples were dissolved in 10 ml of 0.1% SDS to prepare a 0.025% w/v protein solution. The absorption of the solutions was measured at 304 nm. The difference in UV absorption between the control sample (PPEF) and the conjugates at 304 nm indicates the formation of Amadori compounds (Wang & Ismail, 2012; Zhu, Damodaran and Lucey, 2008). The browning index was analyzed at 420 nm (Jiménez-Castaño, Villamiel, & López-Fandiño, 2007; Wang & Ismail, 2012).

3.3.8 Degree of conjugation

The amount of unreacted amine groups in the conjugates was measured based on the number of free amino groups available after conjugation using the TNBS assay method as described above. (Adler-Nissen, 1979; Y. Li *et al.*, 2013; Niu *et al.*, 2011; Sedaghat Doost *et al.*, 2020; Jiménez-Castaño *et al.*, 2007). The absorbance values recorded at 340 nm were converted in terms of Gly equivalents obtained from a standard curve and the degree of the substitution was expressed as follows:

$$\text{CD (\%)} = \frac{Gly_0 - Gly_{con}}{Gly_0} \times 100 \quad \text{.....(3.6)}$$

where Gly_0 is glycine equivalent of protein at the onset of Maillard Reaction, and Gly_{Con} is glycine equivalent of conjugated proteins.

3.3.9 Surface and functional properties analysis

3.3.9.1 Surface charge

The zeta potential (zP) of the conjugates was determined at pH 4, 7, and 10 based on the changes in electrophoretic mobility as a function of pH using a Nano-ZS90 Zetasizer (Malvern Instruments, Westborough, MA, USA) (Avramenko *et al.*, 2013). In brief, a 0.05% (w/w) protein solution of each conjugate was dispersed in water and the pH adjusted to 4, 7, and 10 using 0.5 M HCl or NaOH. The solutions were left to stir for an hour with readjustment of the pH every 15 min to maintain uniformity of pH throughout the duration of the analysis. Thereafter, an aliquot of the solution was transferred to a zeta cuvette which was then inserted in the Zetasizer for measurement. The surface charge, *i.e.,* zeta potential, was computed by application of the Henry Equation (Avramenko *et al.*, 2013).

3.3.9.2 Foaming properties- foaming Capacity (FC) and foam stability (FS)

The foaming capacity and foam stability of samples were measured at three different pH (4, 7, 10) based on the method of Avramenko *et al.* (2013). Briefly, a 1% (w/w) protein solution was prepared, and the pH adjusted to 4.0, 7.0, and 10.0 using dilutants such as 0.5 N NaOH or HCl. The solutions were then left to stir for an hour with the pH readjustment every 15 minutes. To prepare the foam, 15 mL of the adjusted solution was transferred into 400-mL beakers and homogenized using a benchtop homogenizer (IKA, Wilmington, NC, USA) with a saw tooth probe at speed 2 (~11,000 rpm) for 3 min. The wedges of the probe were immersed in the protein solution just below the surface for maximizing the foam generation. Following 3 min of foam preparation, the sample was transferred to a 50-mL graduated cylinder and the volume of the foam immediately after transfer was recorded as V_1. The foam was left standing still on the counter for 30 min, and the volume of the foam was measured and recorded as V_2. When recording the foam volume (V_1

and V_2), the upper and lower levels of the foam were carefully recorded in the cylinder. The FC and FS were measured as follows:

$$\text{FC (\%)} = \frac{\text{initial volume of foam after homogenization } (V_1)}{\text{Volume of protein solution before homogenization } (15\ mL)} \times 100$$

……(3.7)

$$\text{FS (\%)} = \frac{\text{initial foam volume } (V_1) - \text{final foam volume } (V_2)}{\text{initial foam volume}} \times 100$$

……(3.8)

3.3.9.3 Emulsifying properties - emulsion stability (ES), emulsion activity index (ESI) and emulsion stability index (ESI)

For emulsion stability measurements, a 1% (w/v) protein solution was prepared in Milli-Q water, and the pH adjusted to 4.0, 7.0 and 10.0 using 0.5 N NaOH or HCl. The solutions were then left to stir for an hour while pH was adjusted every 15 minutes. Oil-in-water emulsions between 5 g of sample solution and 5 g of canola oil were prepared in a 50-mL conical centrifuge tube using a benchtop homogenizer (IKA, Wilmington, NC, USA) with a 20-mm saw tooth probe at speed 2 (~11,000 rpm) for 3 min. The prepared emulsions were then poured into 10-mL graduated glass cylinders and were left standing still for 30 min at room temperature. The stability was monitored through visual observation of the separation of solution into two layers: an optically opaque darker cream layer (top) and a turbid aqueous layer (bottom). The volume of the aqueous layer was immediately recorded.

Emulsion stability was calculated using the following formula:

$$\text{ES (\%)} = \frac{V_b - V_a}{V_b} \times 100$$ …...……(3.9)

where, V_b is 5 ml (the volume of the aqueous layer at the bottom right before homogenization), and V_a is the volume of the aqueous layer at the bottom after the time period of static rest (30 min or 60 min).

The emulsion activity (EAI) and stability indices (ESI) for untreated and enzyme-treated PPEF conjugates were conducted based on the method of Pearce and Kinsella (1978), and as described in detail by Avramenko *et al.* (2013). Briefly, a 0.25% (w/v) protein solution was prepared in Milli-Q water, and the pH was adjusted to 4.0, 7.0 and 10.0. Emulsions was then prepared with 5 g of 0.25% protein (w/w) solution and 4.0 g canola oil with a 20-mm saw tooth probe at ~11,000 rpm for 3 minutes using a benchtop homogenizer (IKA, Wilmington, NC, USA). The absorption of emulsion was measured at 500 nm. The EAI were calculated using the following equation:

$$\text{EAI } (m^2) = 2T \times \left(A_0 \times \frac{dilution\ factor}{C} \times \Phi \times 10000\right) \quad \text{..... (3.10)}$$

where T is 2.303, A_0 is the absorbance immediately after emulsion formation, dilution factor is 151, C is the weight of the protein per unit volume of aqueous phase before emulsion formation (g/ml), and Φ is the oil volume fraction of the emulsion.

The ESI were calculated using the following equation:

$$\text{ESI (min)} = A_0 \times \Delta t / \Delta A \quad \text{.....(3.11)}$$

where A_0 is the absorbance immediately after emulsion formation, Δt is the change in time between 0 and 10 min, and ΔA is the change in absorbance of the emulsion (A_0–A_{10}).

Although both ES and ESI are aimed at achieving similar objectives, the former gives us a visual representation of the emulsion separation into its respective phases and its numeric interpretation while the latter is a more quantitative determination of the time required for the separation to take place.

3.3.9.4 Water and oil holding capacities (WHC/OHC)

For WHC and OHC measurements, 0.5 g of sample was weighed into a 50-mL conical centrifuge tube, to which 5 g of Milli-Q water was added and the dispersion was vigorously vortexed for 10 s every 5 min for 30 min using an Analog Vortex Mixer (VWR International, Mississauga, ON, Canada) and then centrifuged at 1,000 × g for 15 min using a Sorvall ST8 Centrifuge (Thermo Fisher Scientific Inc., Waltman, MA, USA). Thereafter, the supernatant was carefully pipetted out, and the mass of the resulting pellet was weighed. The amount of water absorbed was determined based on differences in mass prior to and after analysis and reported as g water /g sample. A similar method was used for OHC, except the water was replaced with canola oil. The supernatant was decanted, and the mass of the resulting pellet was measured and reported as g oil/ g sample. All measurements were performed in triplicate.

$$\text{WHC or OHC} = \frac{\text{Weight of wet pellet} - \text{Weight of dry pellet}}{\text{Weight of dry pellet}} \quad \ldots\ldots\ldots\ldots\ldots\ldots\ldots\ldots(3.12)$$

3.3.10 Statistical analysis

Data for the proximate composition of the PPEF are reported in mean ± standard deviation of triplicates. All enzymatic hydrolysis + conjugation reactions were performed in duplicates (biological duplicates). Data for proximate composition, DH, surface, and functional properties of each biological duplicate were measured in triplicates. All data for DH, surface and functional properties are reported as mean ± standard deviation six values (values of duplicates, each calculated in triplicates i.e. n=6). Mean comparisons between the different enzymatic reactions were performed using the One-way ANOVA followed by Tukey mean comparison post-hoc test. The difference is reported to be significant at $p < 0.05$.

3.4 Results

3.4.1 Proximate composition

The composition of protein, lipid, moisture content (MC), ash, total starch, and other carbohydrates of the PPEF are 55.0% ± 0.0%, 1.0% ± 0.3%, 1.2% ± 0.0%, 5.4% ± 0.1%, 3.1% ± 0.2% and 37.3 ± 1.0%, respectively. Similar proximate composition for the protein-enriched

fraction of pea was also obtained by Konieczny *et al.* (2020a). The protein and moisture content of the conjugates were also determined and summarized in Table 3.2. The protein percentage of the heated controls and hydrolyzed-protein carbohydrate conjugates are significantly reduced (46% - 52%). The formation of covalent bonds (resulting in new compound generation) involving the nitrogen of the α-amino group with the hydroxyl group of the reducing sugar can also be speculated for the lower protein ratio of the conjugates (Kutzli , Weiss & Gibis 2021) (Table 3.2).

3.4.2 Effect of E/S ratio on the degree of hydrolysis of protein (DH)

The degree of hydrolysis (DH) is defined as the percentage of peptide bonds cleaved as a ratio of the total number of peptide bonds present (Adler-Nissen, 1979b). Hydrolysis leads to an increase in the exposure of buried hydrophobic amino acids as a result of protein structure unfolding (Mookerjee *et al.*, 2023). Moreover, since the enzyme cleaves the protein at different amino acids along the chain, neither the resulting peptides are uniform in size or are the hydrophobic patches exposed consistent. Although a strict scheme for defining the DH has not been defined (Avramenko *et al.*, 2013) it can be hypothesized roughly that 2% – 7% DH is low, 8% – 14% is medium, 15% - 20% is high and beyond that (>20%) is extensive. The optimum E/S ratios were determined through preliminary tests to achieve aimed DH (data not shown). The E/S ratios used for trypsin hydrolysis of the PPEF were 1:20,000 and 1:30,000 which was lower than the ratios previously used for legume protein hydrolysis (García Arteaga *et al.*, 2020; Konieczny *et al.*, 2020a; Mokni Ghribi *et al.*, 2015).

One-way ANOVA followed by Tukey mean comparison test showed that trypsin E/S did not significantly impact ($p<0.05$) the DH at 60 min with E/S of 1:20,000 and 1:30,000 producing DH 10.8% ± 0.8% and 9.9% ± 2.3%, respectively. However, E/S of 1:20,000 for 8 min resulted in a low DH (2.5% ± 0.3%) which was reported to be significantly different than the other two (Table 3.1).

For papain treatment, E/S, had a significant impact on the DH observed for some of the conjugates (Table 3.1). An E/S of 1:2,000 resulted in a DH of 3.3% ± 0.7% (Pap3.3) which was significantly different as compared to the other conjugates (Pap8.1, Pap 9.1, Pap10.2) ($p<0.05$). (Andlinger *et al.*, 2022; Leite *et al.*, 2021)

The introduction of a heat treatment step (1 hour; 80°C) prior to the hydrolysis reaction allowed the use of a lower trypsin E/S. Heat treatment leads to a partial denaturation of the protein

structure by breakdown of hydrogen bonds and disruption of electrostatic forces holding the three-dimensional structure of the proteins (Andlinger *et al.*, 2022). This unravels the protein structure and exposes more susceptive sites to proteolysis (Leite *et al.*, 2021). A similar relationship between time and DH has been reported elsewhere where the author's showed an increase in the DH of *Bunium persicum Bioss* (Shahi *et al.*, 2020) and Persian strutgeon viscera proteins (Ovissipour *et al.*, 2009) with time. Increased cleavage of the peptide bonds leading to the formation of soluble peptides could be a possible explanation for the direct correlation between DH and time for trypsin (Haslaniza *et al.*, 2010).

Table 3.1. Sample representation and influence of E/S ratio on the DH of PPEF; SDS-PAGE ImageJ quantification of % intensity of lanes in gels stained by Coomassie Brilliant Blue (CBB) R-250 (<100 kDa) and basic fuchsine

Sample	Name	DH	Trypsin E/S	Time (min)	% Intensity	
					CBB	Fuchsine
Raw sample	PPEF	-	-	-	8.3	7.9
Trypsin control	Tryp0	-	-	60	11.4	9.5
Trypsin conjugates (Tryp-conjugates)	Tryp2.5	2.5 ± 0.3^{a}	1:30,000	8	9.1	9.4
	Tryp 9.9	9.9 ± 2.3^{b}	1:30,000	60	8.4	9.1
	Tryp 10.8	10.8 ± 0.8^{b}	1:20,000	60	10.0	9.0
Papain control	Pap 0	-	0	60	10.2	8.9
Papain conjugates (Pap-conjugates)	Pap3.3	3.3 ± 0.7^{a}	1:2000	60	7.7	9.0
	Pap5.2	5.2 ± 1.0^{ab}	1:5000	60	8.2	9.2
	Pap8.1	8.1 ± 0.9^{b}	1:2500	60	8.4	9.3
	Pap9.1	9.1 ± 0.5^{b}	1:2500	60	8.6	9.3
	Pap10.2	10.2 ± 0.3^{b}	1:1000	60	9.6	9.5

DH values are reported as mean ± standard deviation of two biological duplicate samples, DH of each calculated in triplicates (n=6). Different superscript letters (a,b) represent significantly different values at (p<0.05). Abbreviations: DH (degree of protein hydrolysis); E/S (Ratio of enzyme: substrate *i.e.,* amount of enzyme per unit quantity of substrate)

3.4.3 Formation of Amadori compounds

Covalent cross-linking between protein and carbohydrates plays a pivotal role in the determination of conjugate functional properties. The Maillard reaction involves a complex series of chemical reactions initiated by reactions between the free amino groups of proteins and carbonyl groups of carbohydrates. N-glycosylamine is formed initially which condenses into Schiff base. The Schiff base further undergoes rearrangement to form Amadori compounds (aldoses) or Heyns products (ketoses) (Kutzli *et al.*, 2021). The initial stages of the Maillard reaction results in the formation of mild coloured/colourless Heyn's/Amadori products (absorption at 304 nm) whereas brown coloured nitrogen-containing pigments called melanoidins (absorption at 420 nm) are generated at the later stages (de Oliveira *et al.*, 2016; Kutzli *et al.*, 2021). Major factors influencing the extent of the Maillard reaction are temperature, reaction time, pH, and moisture content of the solution (Kutzli *et al.*, 2021).

The formation of Amadori compounds and extent of browning upon heat-induced conjugation of the raw samples, controls and hydrolyzed-protein carbohydrate conjugates were investigated by measuring the absorbance at 304 nm and 420 nm, respectively (Figure 3.2A). These absorbance results have been widely employed as indicators for the conjugation degree as they reflect early intermediate (Amadori compounds) as well as final stages (melanoidins) of the Maillard reaction (Wang *et al.*, 2012; Zha *et al.*, 2019b). All conjugates under analysis reported higher absorbance as compared to PPEF at 304 nm and 420 nm, indicating the formation of Amadori compounds and melanoidins (Zha *et al.*, 2019; Zhu *et al.*, 2008). These results corelate with the studies of Zhang *et al.* (2022) and Zha *et al.* (2019) in which both the groups reported an increase in absorbance at 304 nm and 420 nm for Maillard-induced PPI-maltodextrin and PPI-gum Arabic conjugates, respectively. Both Tryp0 and Pap0 showed higher absorbances as compared to most of the hydrolyzed-protein polysaccharide conjugates (except Pap9.1) indicating increased levels of Schiff base formation (Zhu *et al.*, 2008). These results correspond to both the SDS-PAGE (Figure 3.3) as well as the % intensity results (Table 3.1) which showed higher values for the Tryp0

and Pap0 as compared to the other conjugates. Moreover, the absorbance at 304 nm was significantly higher than that at 420 nm indicating the dominance of early Maillard reaction intermediate formation as compared to the later stages (Zha *et al.*, 2019). The fact that the Maillard reaction was limited to its early stages can be justified by the short reaction time (30 min) used for the experiments (de Oliveira *et al.*, 2016). The absorbance of the conjugates at 420 nm was significantly higher as compared to both the PPEF and control samples. This can be attributed to the formation of brownish melanoidin colorants which increased considerably upon crosslinking with protein hydrolysates (Zha *et al.*, 2019). Hydrolysis cleaves the peptide bonds and results in an increase in the availability of the α-NH_2 group responsible for Maillard conjugation with the reducing sugar which then undergoes a series of complex reactions to form melanoidins (de Oliveira *et al.*, 2016; Kutzli *et al.*, 2021). Among the two conjugates, the Pap-conjugates showed higher absorbance at 304 nm indicating a higher index of conjugate formation as compared to the Tryp-conjugates. The non-specificity of papain might have led to the cleavage of the protein chains at different sites leading to the exposure of a variety of amino acids which were able to take part in the condensation reaction with the ketone group of the reducing sugar. Moreover, most of the Pap-conjugates had higher absorbance at 420 nm indicating an increased degree of browning as compared to the Tryp-conjugates.

3.4.4 Degree of conjugation

The residual amount of free amino groups after conjugation can be monitored in order to determine the conjugation degree (CD) and development of the Maillard conjugates (Niu *et al.*, 2011; Sedaghat Doost *et al.*, 2020). TNBS was used to determine the free amino group content in the protein-polysaccharide conjugates after heat treatment. The reaction between the TNBS reagent and free amino groups leads to a yellow color detected at 340 nm, which was used to quantify glycine equivalents using a standard curve. Then the Gly equivalent was used to calculate the degree of conjugation. As evident from the results (Figure 3.2B), the CD of both Tryp0 and Pap0 were higher than the hydrolyzed-protein carbohydrate conjugates. Between the heated controls (Pap0 and Tryp0), the CD of Pap0 was higher than Tryp0. These results matched the determination of Amadori compounds resulting from the conjugation reaction. The Abs_{304nm} values also indicated a higher formation of Amadori compounds for Tryp0 and Pap0 as compared to the hydrolyzed-protein starch conjugates (Figure 3.2A). Additionally, both the Abs_{304nm} and Abs_{420nm}

were greater for Pap0 as compared to Tryp0, indicating an increased covalent carbohydrate-protein crosslinking during the heating process. Among the conjugates, Pap-conjugates had higher CD as compared to the Tryp-conjugates which also correlate with the Abs_{304nm} and Abs_{420nm} data reported in Figure 3.2A indicating an increased formation of both initial and final stages of Maillard conjugates. Among all the conjugates, Pap5.2 reported the highest CD (48.2%) which also correlated to the highest Abs_{420nm} value (0.43) reflecting increased browning as compared to the other conjugates (Figure 3.2A). The current results correlate with Li *et al.* (2013) in which an inverse relationship was also established between the degree of protein hydrolysis and DC. It can be argued that hydrolysis resulted in the formation of short-chain polypeptides with greater mobility which resulted in the movement of lysine (primarily responsible for Maillard reaction) to an increased hydrophobic environment that made it difficult for the reactive $-NH_2$ to covalently react with reducing sugar resulting in a lower Maillard reaction activity (Li *et al.*, 2013).

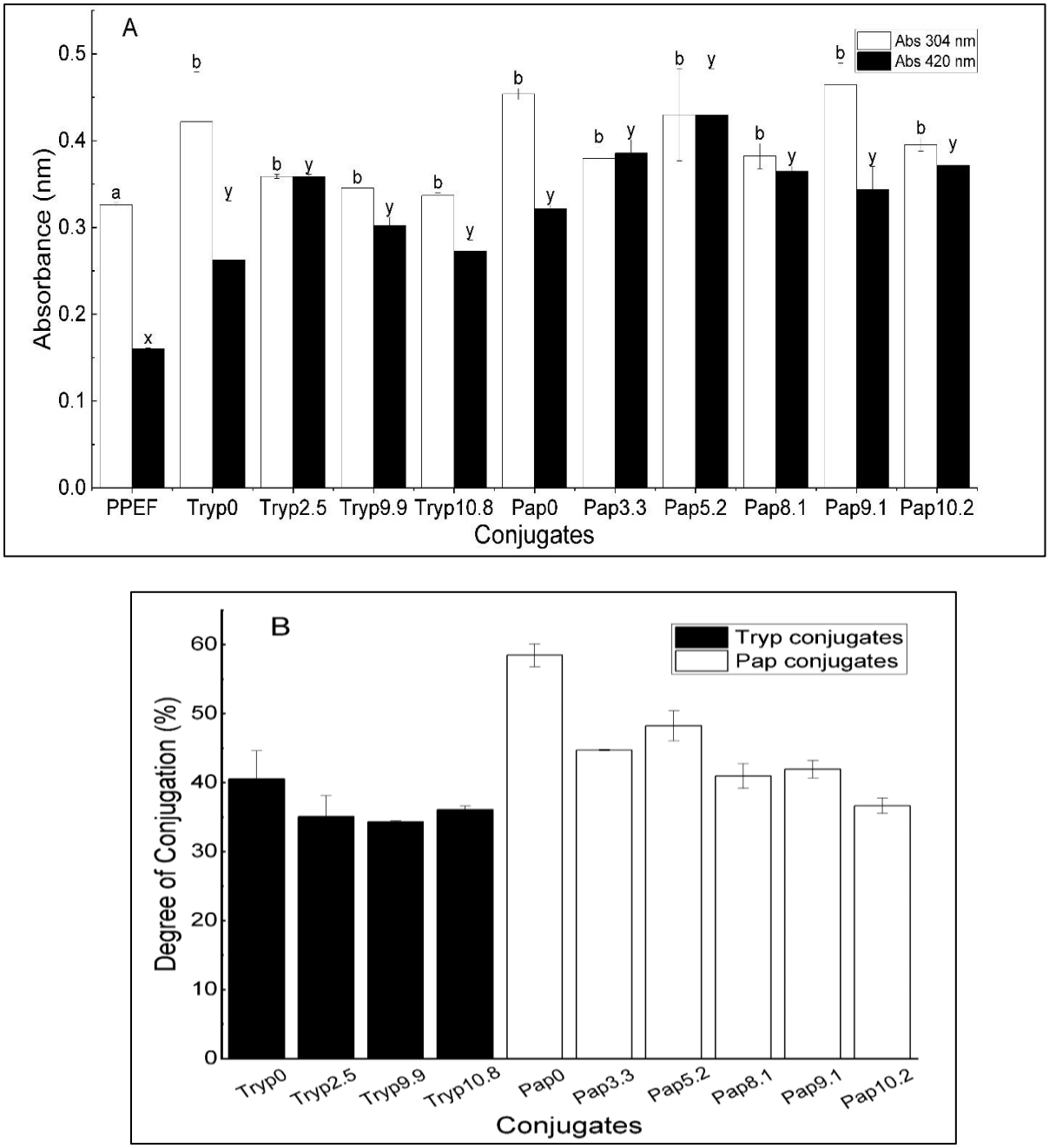

Figure 3.2. A. Absorbance values of PPEF, control and hydrolyzed-protein carbohydrate starch conjugates at 304 nm and 420 nm B. Degree of conjugation of the conjugates

A. A 1% (protein basis) solution of the raw, control and hydrolyzed-protein carbohydrate were prepared, and the absorbance values noted at 304 nm and 420 nm respectively. Data represents the mean ± standard deviation of triplicates (n=3). Different superscript letters (a,b,) and (x,y) among the same-coloured bars represent significantly different values at (p<0.05).

B. A 1.5 % (protein basis) solution for the Trypsin conjugates and 2 % (protein basis) solution for the Papain conjugates were prepared. A quarter milliliter of the sample solution was added

to 2 ml SDS from which 0.25 ml was pipetted and mixed in 2 ml of sodium phosphate buffer (pH 7.8). Thereafter, the solutions were incubated at 50 °C with 2 ml trinitrobenezenesulfonic acid solution (0.01% v/v). After 1 hour of incubation, the reactions were terminated by the addition of 4 ml HCl solution (0.1 N). The degree of conjugation was calculated using the formula shown in Section 2.9. Data represent the mean ± standard deviation of triplicates (n=3).

Abbreviation: PPEF (pea protein enriched flour fraction); Tryp0 (Trypsin control); Tryp2.5 (Trypsin conjugate having a DH of 2.5%); Tryp9.9 (Trypsin conjugate having a DH of 9.9%); Tryp10.8 (Trypsin conjugate having a DH of 10.8%); Pap0 (Papain control); Pap3.3 (Papain conjugate having a DH of 3.3%); Pap5.2 (Papain conjugate having a DH of 5.2%); Pap8.1 (Papain conjugate having a DH of 8.1%); Pap9.1 (Papain conjugate having a DH of 9.1%); Pap10.2 (Papain conjugate having a DH of 10.2%).

3.4.5 Molecular weight analysis

3.4.5.1 Molecular weight distribution analysis of the hydrolysates

The DH of the pea protein fraction was determined qualitatively by analyzing the molecular weight distribution profiles of the untreated and conjugated PPEF on an SDS-PAGE gel followed by staining using Coomassie Brilliant Blue R-250 (Figure 3A). Pea proteins contain about 10% - 20% albumins (5 – 25 kDa) and 70% – 80% globulins which can be further divided into convicilin (~70 kDa), legumin (acidic subunit ~40 kDa; basic subunit ~20 kDa) and vicilin (~50 kDa) (Lam *et al.*, 2018). The SDS-PAGE gels (Figure 3A) reveal that PPEF and unhydrolyzed controls (Tryp0 and Pap0) have higher concentrations of convicilin subunits in the range of ~70 – 75 kDa. They decrease as the proteins are hydrolyzed, and all hydrolyzed-protein conjugates showed less intensities of convicilin bands. Similarly, concentrations of vicilin and acidic subunit of legumin for PPEF, Tryp0 and Pap0, respectively, are higher as compared to the other conjugates. On the other hand, concentrations of albumins (~25kDa) and smaller protein subunits (~11 – ~25 kDa) are higher (5.6% – 16.7%) for the hydrolyzed-protein starch conjugates (Tryp2.5, Tryp9.9, Tryp10.8, Pap3.3, Pap5.2, Pap8.1, Pap9.1 and Pap10.2) as compared to the control samples PPEF, Tryp0 and Pap0 (4.8% - 12.1 %). This suggests the majority of hydrolysis occurs on larger proteins with these ranges of papain and trypsin hydrolysis. A comparison between Tryp- and Pap-conjugates showed that the thickness and intensity of the higher molecular weight bands/smears (~30 – ~95 kDa) on the SDS-PAGE were much lower for the Pap-conjugates as compared to the Tryp-conjugates (Figure 3A). On the other hand, the intensities of low molecular weight range

(~11 kDa, ~12kDa, ~15kDa, ~17 kDa,) showed a thicker smear for the Pap-conjugates as compared to the Tryp-conjugates. The SDS-PAGE also reveals a higher breakdown of the convicilin, vicilin and acidic subunit of legumin of the Pap-conjugates as compared to the Tryp-conjugates.

The decrease in high molecular weight peptides and increase in low molecular weight peptides can be attributed to the cleavage of the peptide bonds by enzymes trypsin and papain resulting in the generation of smaller peptides which pass rapidly through the pores to the bottom half of the gel (Elgendy, 2016; Konieczny *et al.*, 2020). The difference in enzymatic action can be attributed to the nature and specificity of the enzyme used (Robinson, 2015). Trypsin, a serine protease is highly specific in nature which hydrolyzes the C-terminal side (carboxyl side) of lysine or arginine (Elgendy, 2016). On the other hand, papain has a broad specificity for peptide bonds thus leading to enhanced protein cleavage resulting in the formation of low molecular weight polypeptides (Amri & Mamboya, 2012).

3.4.5.2 Molecular weight distribution analysis of the Maillard-induced conjugates

SDS-PAGE stained using Coomassie Brilliant Blue R-250 not only showed the effects of enzymatic hydrolysis but also supports the presence of starch-conjugated proteins. The appearance of a thick longitudinal blue smear at the top of the gel near the loading end (~100 kDa to ~245 kDa) can be attributed to the increase in molecular weight of convicilin/convicilin fragments through conjugation of starch (Figure 3A). Densitometry analysis (%) of the blue smear using ImageJ has shown that the density of the smear at the top is greater for most of the conjugated samples (except Pap3.3 and Pap5.2) as compared to PPEF (Table 3.1). Apart from that, a faint blue smear was also recorded throughout the lanes for the conjugated samples (Figure 3A).

In order to further prove the formation of conjugates by analyzing banding patterns, the samples were run on a separate SDS-PAGE gel and stained using a special fuchsin-sulfite staining method (Zacharius *et al.*, 1969). Tryp-conjugates showed heavy bands at the top of the lane (at the boundary between stacking and separating gels) followed by a smear throughout the lane (Figure 3B). Similar, but slender bands were observed for the Pap-conjugates. Size comparison with an available marker showed that the topmost bands were >245 kDa in size. Densitometry analysis using ImageJ showed that the density of PPEF bands was the least (7.9%) as compared to the other conjugates (8.9% – 9.5%). The smear also denotes a trail of the fuchsin dye which was left along

the gel as short-chain polypeptides conjugated with dextrins of different chain lengths traveled through the lanes of the gel. The presence of N-glycosylated legumin fraction of the protein can be a possible reason for the faint smear in the PPEF lane for both gels (Lam *et al.*, 2018). The presence of a blue longitudinal smear along the lanes of the gel stained with CBB was due to the presence of conjugates which were unable to show regular protein banding patterns due to the attachment of carbohydrate fragments with various lengths (Figure 3A). Similar presence of a blue smear in the SDS-PAGE data has been reported by Zha and his group in two separate studies where they studied the conjugation of pea-protein isolate-gum Arabic conjugates (Zha *et al.*, 2019a, 2019b). Peanut protein isolates conjugated with dextran also showed a similar smear above 66.2 kDa with a gradual disappearance in the characteristic banding pattern of peanut proteins (Liu *et al.*, 2012)

The presence of bands at the junction between the loading and separating gels was likely due to the formation of large molecular weight protein-carbohydrate conjugates (>250 kDa) which were not able to pass through the pores of the polyacrylamide gel and have remained at the top (Mu *et al.*, 2011; Zha, *et al.*, 2019b). The percentage intensity of the PPEF lane was the lowest because of the absence of protein-conjugated starch/other carbohydrates. The varying intensity of the smear for the different conjugates stained using fuchsin-sulfite can be attributed to the extent of conjugation as well as the polydispersity of the conjugates formed (Zhu *et al.*, 2010). Fuchsin staining of peanut protein-maltodextrin Maillard-induced conjugates also showed purple bands near the top of the running gels and a faint purple smear throughout the lanes indicating protein-carbohydrate conjugation (Liu *et al.*, 2012). Similar observations using fuchsin-stained SDS-PAGE gel have been made by Zhu *et al.* (2010) and Mu *et al.* (2011) in separate research where a dense broad heavy band was formed at the top of the gel indicating the formation of Maillard-induced whey protein isolate-dextran conjugates and soy protein isolate-acacia gum conjugates respectively.

The formation of strong covalent linkages (C=N) between the free amine groups of lysine/terminal amino acids and reducing sugars of starch/long chain polysaccharides leading to the formation of Schiff base (conjugates) can be confirmed by the blue smear since most of the non-covalent linkages are disrupted in an SDS-PAGE (presence of β-mercaptoethanol which acts as a reducing agent) (Wang *et al.*, 2012; Zhu *et al.*, 2010). Similar results showing the heterogeneity

of protein-polysaccharide complexes have also been reported by other researchers (Zhu *et al.*, 2010; Zhu *et al.*, 2008).

Based on the above results, six molecular species can be argued to be present in the conjugate mixtures: intact proteins conjugated with intact bulky starch molecules; intact proteins linked with short polysaccharides; unraveled, truncated proteins conjugated with long carbohydrate molecules; unraveled, truncated proteins with short chain dextrins; hydrolyzed and intact protein aggregates and non-conjugated hydrolyzed proteins.

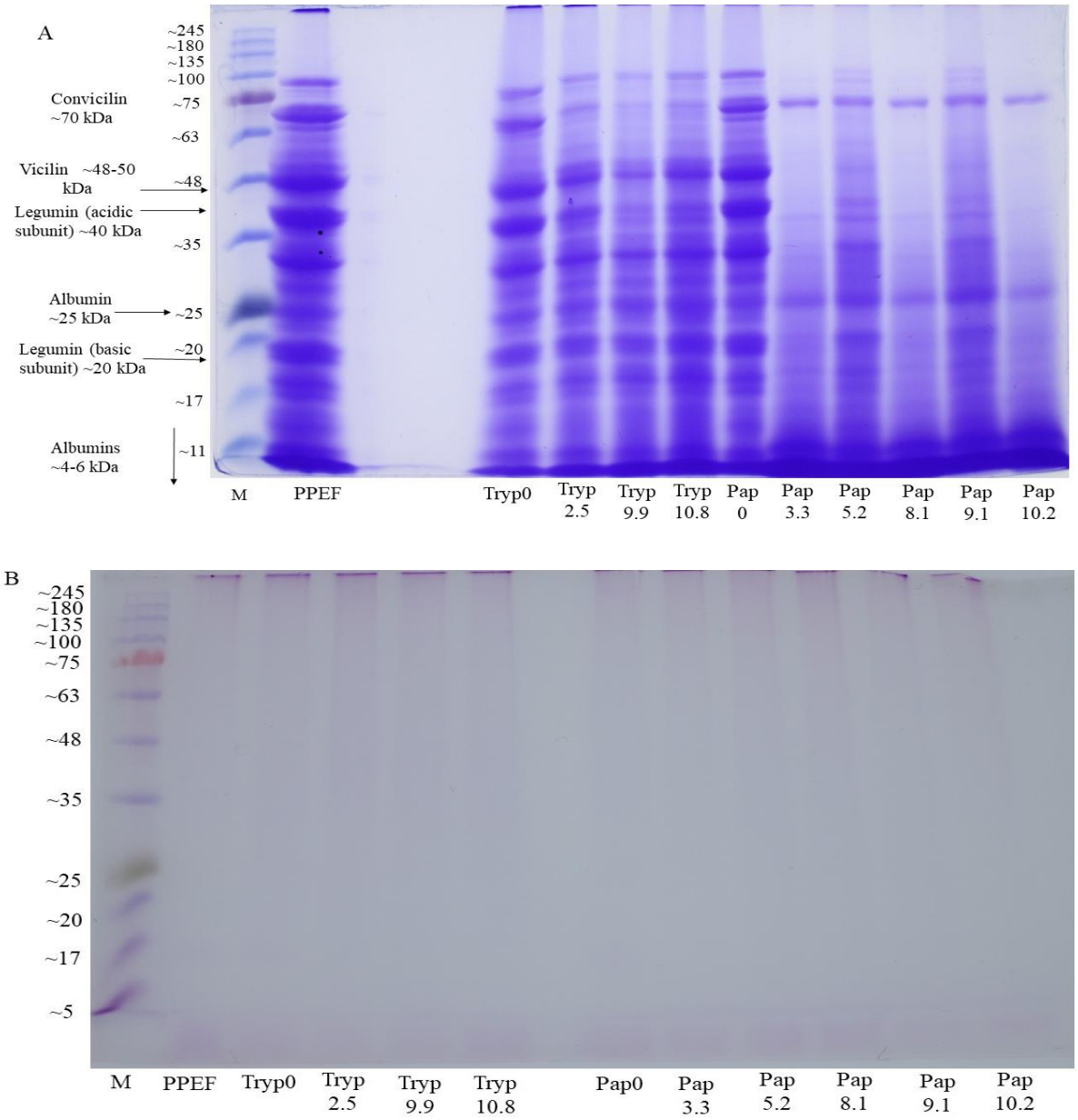

Figure 3.3. SDS-PAGE gel for PPEF, heated controls and hydrolyzed-protein carbohydrate starch conjugates stained with (A) Coomassie Brilliant Blue R-250 and (B) Fuchsin sulfite. From left to right: (M) Molecular weight marker, Tryp0 (Trypsin control), Tryp2.5 (Trypsin conjugate having a DH of 2.5%), Tryp9.9 (Trypsin conjugate having a DH of 9.9%), Tryp10.8 (Trypsin conjugate having a DH of 10.8%), Pap0 (Papain control), Pap3.3 (Papain conjugate having a DH of 3.3%), Pap5.2 (Papain conjugate having a DH of 5.2%), Pap8.1 (Papain conjugate having a DH of 8.1%), Pap9.1 (Papain conjugate having a DH of 9.1%), Pap10.2 (Papain conjugate having a DH of 10.2%).

3.4.6 Surface charge

The surface charge is an important parameter for understanding the functional properties of conjugates and has been represented in terms of the Zeta potential (zP). The surface charge of the unheated, heated controls and enzymatically-hydrolyzed protein-polysachharide conjugates were analyzed at pH 4, 7 and 10 (Table 3.2). At pH 4, the zP of PPEF (8.2 ± 0.4 mV), Tryp0 (8.3 ± 0.2 mV) and Pap0 (8.4 ± 0.2 mV) were higher as compared to the hydrolyzed-protein carbohydrate conjugates. Overall, the surface charge of the hydrolyzed Tryp-conjugates (2.4 – 3.4 mV) was observed to be higher than the hydrolyzed Pap-conjugates (-2.3 – 1.2 mV) at pH 4. The zP of both control and hydrolyzed-protein carbohydrate conjugates were higher than that of PPEF (-24.2 ± 0.5 mV and -27.3 ± 1.1 mV) at pH 7 and 10 (Table 3.2) indicating better solubility of the conjugates due to enhanced electrostatic repulsion (Yan *et al.*, 2022). Pap10.2 conjugates had the most negative value of -32.2 ± 0.1 mV and -38.9 ± 0.4 mV at pH 7 and 10, respectively.

Generally speaking, proteins carry a positive charge below their isoelectric point (pI) and a negative charge above their pI (Mokni Ghribi *et al.*, 2015). The pI of pea proteins lies within 4 and 5 (Lam *et al.*, 2018). The steric effect of the bulky starch group in shielding charges must be a major cause for the differences in zP of the conjugates studied (Yan *et al.*, 2022). The negative pI of the Pap-conjugates at pH 4 could be a result of the electrostatic screening effect by the bulky carbohydrate molecules thus retarding the ionization of NH_2 group to NH_3^+ (Kutzli *et al.*, 2021). This is further strengthened by both the Abs_{304nm}, Abs_{420nm}, and DC data which revealed enhanced Amadori product formation indicating higher conjugation for the Pap-conjugates (Figure 3.2).

3.4.7 Functional properties

3.4.7.1 Foaming- foam capacity (FC), foam stability (FS)

Foams are believed to consist of two immiscible layers (water and gas) which need to be stabilized to prevent their separation. While studying the formation and stability of foams, two important aspects come into play which are foam capacity and foam stability. The FC and FS of the raw flours, heated control and hydrolyzed protein-polysaccharide/starch conjugates were analyzed at three different pH values 4, 7 and 10 to understand the effect of H^+ ions on the formation and stability of the foams.

Table 3.2. Protein composition (%) and moisture content (MC) Water holding Capacity (WHC), Oil holding capacity (OHC), and surface charge (Zeta Potential) of PPEF, controls and hydrolyzed-protein carbohydrate conjugates.

Sample	M.C. (%)	Protein (db%)	WHC (g/g)	OHC (g/g)	Zeta Potential (mV)		
					pH 4	pH 7	pH 10
PPEF	1.2 ± 0.0^{a}	55.0 ± 0.0^{d}	1.2 ± 0.1^{a}	1.1 ± 0.0^{a}	8.19±0.4^{f}	-24.2±0.5^{e}	-27.3±1.1^{d}
Tryp0	18.4 ± 2.1^{d}	51.6 ± 1.2^{c}	2.4 ± 0.1^{d}	3.9 ± 0.5^{c}	8.3 ± 0.2^{g}	-28.6 ± 0.4^{bcd}	-35.2 ± 2.4^{abc}
Tryp2.5	9.4 ± 0.3^{ab}	46.2 ± 0.3^{a}	2.0 ± 0.1^{bcd}	2.3 ± 0.1^{b}	3.4 ± 0.2^{e}	-28.2 ± 0.5^{cd}	-35.9 ± 1.2^{ab}
Tryp9.9	9.7 ± 0.5^{ab}	46.8 ± 0.0^{ab}	2.3 ± 0.1^{cd}	2.3 ± 0.1^{b}	2.7 ± 0.3^{de}	-28.4 ± 0.5^{bcd}	-36.6 ± 0.5^{ab}
Tryp10.8	9.8 ± 0.5^{ab}	46.4 ± 0.2^{a}	2.0 ± 0.2^{cd}	2.2 ± 0.1^{b}	2.4 ± 0.3^{cde}	-27.5 ± 0.3^{d}	-34.9 ± 0.4^{abc}
Pap0	12.3±0.2^{bc}	48.5 ± 0.1^{ab}	2.1 ± 0.0^{bcd}	2.8 ± 0.0^{b}	8.4±0.2^{h}	-28.5 ± 1.4^{bcd}	-30.6±1.2^{cd}
Pap3.3	16.8 ± 1.^{2cd}	47.1 ± 0.1^{ab}	1.7 ± 0.0^{ab}	2.0 ± 0.1^{ab}	-0.7 ± 0.4^{abc}	-30.4 ± 0.4^{abc}	-37.5 ± 0.3^{ab}
Pap5.2	8.6 ± 0.^{1ab}	49.0 ± 0.1^{b}	2.3 ± 0.1^{bcd}	2.2 ± 0.1^{b}	1.2±0.1^{bcde}	-30.5 ± 1.3^{abc}	-34.7 ± 0.6^{abc}
Pap8.1	7.2 ± 0.3^{a}	47.6 ± 0.0^{ab}	2.0 ± 0.0^{bcd}	1.9 ± 0.0^{ab}	-1.3±0.0^{ab}	-31.1±0.0^{ab}	-34.8 ± 1.0^{abc}
Pap9.1	14.5 ± 0.8^{cd}	47.9 ± 0.4^{ab}	1.9 ± 0.2^{bc}	2.2 ± 0.1^{b}	-0.6±0.0^{abcd}	-31.9 ± 0.2^{a}	-33.1 ± 0.5^{bcd}
Pap10.2	7.9 ± 0.6^{ab}	47.8 ± 0.7^{ab}	2.0 ± 0.2^{bcd}	2.0 ± 0.0^{b}	-2.3 ± 1.9^{a}	-32.2 ± 0.1^{a}	-38.9 ± 0.4^{a}

Data represents the mean ± standard deviation of triplicates (n=3). Different superscript letters (a,b,c,d) within the same column represent significantly different values at (p<0.05). *Abbreviations*: db (dry basis); g/g (gram water/oil per gram protein); mV (millivolts); PPEF (pea protein enriched flour fraction); Tryp0 (Trypsin control); Tryp2.5 (Trypsin conjugate having a DH of 2.5%); Tryp9.9 (Trypsin conjugate having a DH of 9.9%); Tryp10.8 (Trypsin conjugate having a DH of 10.8%); Pap0 (Papain control); Pap3.3 (Papain conjugate having a DH of 3.3%); Pap5.2 (Papain conjugate having a DH of 5.2%); Pap8.1 (Papain conjugate having a DH of 8.1%); Pap9.1 (Papain conjugate having a DH of 9.1%); Pap10.2 (Papain conjugate having a DH of 10.2%).

Foam capacity (FC) can be defined as the ability of a protein to trap air in a continuous liquid or semi-solid phase. The protein molecules diffuse to the air/water interface, unfold, orient, concentrate and form a thick visco-elastic film around the gas bubbles leading to a decrease in the interfacial tension (Akharume *et al.*, 2020). The FC of all conjugates were higher than the raw PPEF at pH 7 and 10 (Figure 3.4A). The FC of most of the hydrolyzed Pap-conjugates (Pap5.2, Pap8.1 and Pap10.2) were lower than the PPEF at pH 4 (Figure 3.4B). Tryp2.5 showed better FC at pH 4 (109.2% ± 2.0%) whereas Tryp10.8 showed enhanced FC at pH 7 (103.3% ± 20%). On the other hand, Tryp0 showed the best FC (106.4% ± 0.3%) at pH 10 (Figure 3.4A). Among the Pap-conjugates, Pap 9.1 showed the highest FC at pH 7 (111.7% ± 5.0%) and Pap3.3 showed the highest FC at pH 4 (87% ± 15.2%). Similar to the Tryp-conjugates, the Pap0 showed the highest FC at pH 10 (110% ± 8.8%).

Foam stability (FS) is an indication of the efficiency of a particular protein to retain the volume and thickness of the continuous viscoelastic film over a specified period of time by inhibiting atmospheric air bubbles to permeate inside and separating the film into its constituent parts. Alternatively, it can also be defined as the ability of the conjugates to maintain the structure of the bubble in suspension and slow down the coalescence rate (Shen *et al.*, 2022). Among all the conjugates studied, the Tryp controls had the highest FS at pH 4 (76.9%) and 7 (77.5%), whereas the Pap controls had the highest FS at pH 10 (77.3%) (Figure 3.4B). The FS of the Tryp-conjugates were significantly higher than those of the Pap-conjugates ($p< 0.05$) at pH 4 (Tryp conjugates: 57.6% ±1.4% – 76.9% ± 0.9%; Pap conjugates: 19% ±1.0% – 68% ± 2.7%), 7 (Tryp: 43.9% ± 6.8% – 70.3% ± 3.8%; Pap: 13.8% ± 8.6% – 61.6% ± 4.1%) and 10 (Tryp: 35.2% ± 1.4% – 69% ± 1.2%; Pap: 16.1% ± 0.8% – 45.7% ± 11%) (Figure 3.4B).

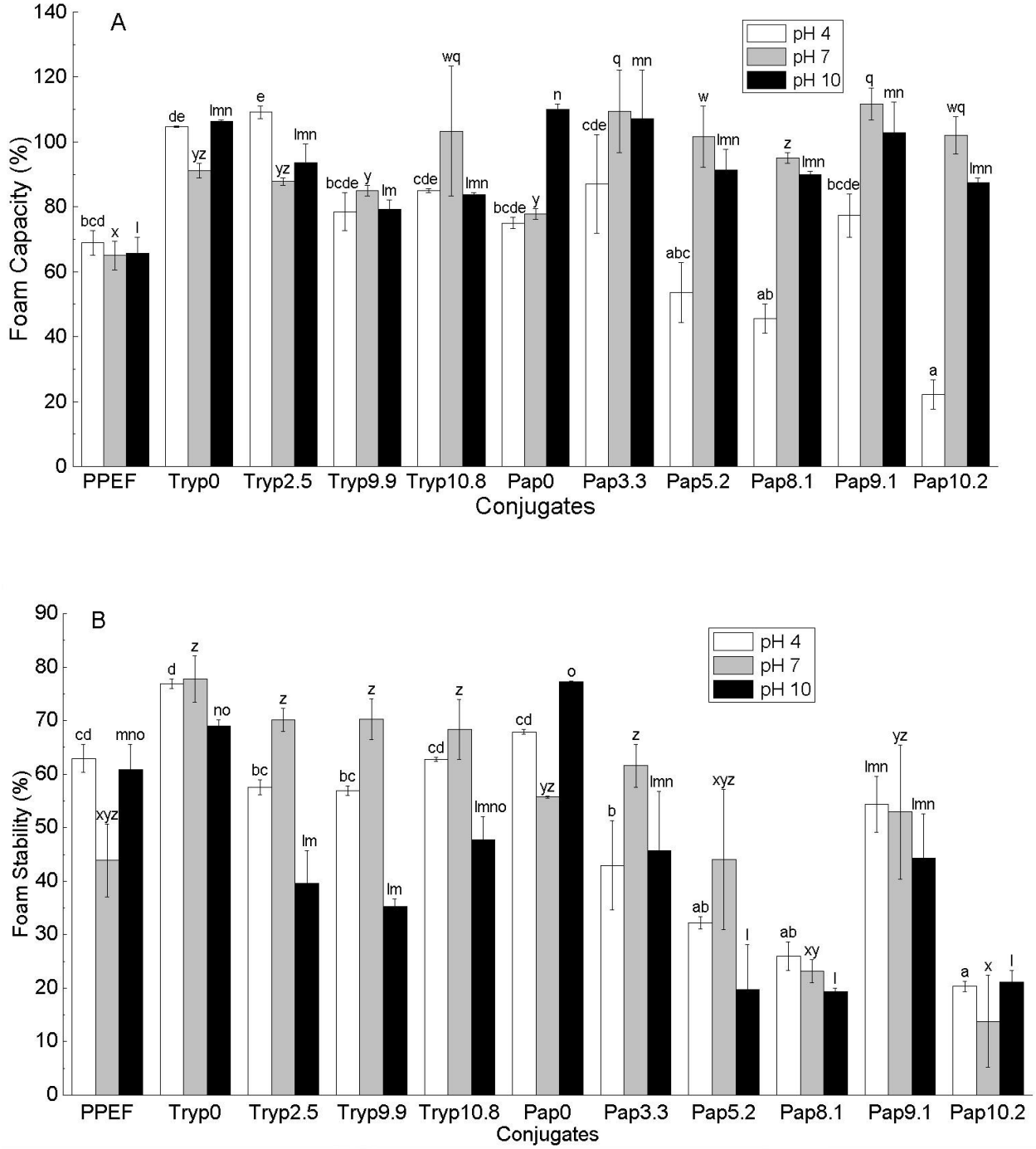

Figure 3.4. Comparative analysis of the foaming properties (A: foam capacity; B: foam stability) at pH 4, 7 and 10.

A 1% (w/w) protein solution was prepared, and the pH was adjusted to 4.0, 7.0, and 10.0. To prepare the foam, 15 mL of the adjusted solution was transferred into 400 mL beakers and homogenized using a benchtop homogenizer at about 11,000 rpm for 3 min following which the samples were transferred to a 50-mL graduated cylinder and the foaming properties calculated.

Abbreviation: PPEF (pea protein enriched flour fraction); Tryp0 (Trypsin control); Tryp2.5 (Trypsin conjugate having a DH of 2.5%); Tryp9.9 (Trypsin conjugate having a DH of 9.9%); Tryp10.8 (Trypsin conjugate having a DH of 10.8%); Pap0 (Papain control); Pap3.3 (Papain conjugate having a DH of 3.3%); Pap5.2 (Papain conjugate having a DH of 5.2%); Pap8.1 (Papain conjugate having a DH of 8.1%); Pap9.1 (Papain conjugate having a DH of 9.1%); Pap10.2 (Papain conjugate having a DH of 10.2%).

3.4.7.2 Emulsifying properties- emulsion activity index (EAI), emulsion stability (ES) and Emulsion Stability index (ESI)

The emulsion activity index (EAI) gives a measure of the interfacial area between the oil droplets and water that can be coated by one gram of an emulsifier, such as protein, during the formation of an emulsion. It has been used as a good predictor for protein surface activity (Pearce *et al.*, 1978; Konieczny *et al*., 2020a; Stone *et al.*, 2015). One-way ANOVA followed by Tukey mean comparison test showed that the EAI of the conjugates were significantly different at pH 4, but there were no significant differences at pH 7 and 10 ($p < 0.05$) (Table 3.3). EAI of all conjugates under observation were higher than the EAI of PPEF at the three different pH values tested. Medium hydrolyzed Tryp-conjugates (Tryp10.8 and Tryp9.9) had higher EAI at pH 4 and 10 (EAI of Tryp10.8: 22.2 m^2/g and 23.9 m^2/g at pH 4 and 10 respectively; EAI of Tryp9.9: 22.1 m^2/g and 23.6 m^2/g at pH 4 and 10 respectively) as compared to Tryp conjugate (Tryp2.5) having low degrees of proteolysis (EAI of Tryp2.5: 21.5 m^2/g and 22.9 m^2/g at pH 4 and 10 respectively). On the other hand, Tryp0 had the highest EAI at pH 7 (21.3 m^2/g) as compared to the other Tryp-conjugates. Among the Pap-conjugates, Pap0 reported the highest EAI at pH 7 (~23.2 m^2/g) and pH 10 (~24.6 m^2/g) whereas Pap3.3 reported the highest EAI at pH 4 (~20.7 m^2/g). On the other hand, Tryp0 had the highest EAI at pH 7 (21.3 m^2/g) as compared to the other Tryp-conjugates.

The emulsion stability Index (ESI) is a measure of the change in EAI over the course of 10 min indicating how well a certain sample can keep the two immiscible layers intact (Wani *et al.*, 2015). The ESI for both the Tryp (12.2 min - 12.3 min) and Pap (12.3 min - 13.3 min) conjugates were significantly higher at pH 4 as compared to the raw PPEF (11.8 min). Increased ESI of the conjugates is also correlated to the increased ES values indicating that carbohydrate conjugation plays an important role in providing stability to the structure of the conjugates at low pH. On the other hand, the ESI of the Tryp-conjugates were similar to (Tryp10.8) or lesser than the ESI values reported by PPEF at pH 7 and 10 (Table 3.3). Pap-conjugates on the other hand showed higher ESI values as compared to PPEF (pH 7: 14.4 min; pH 10:14.5 min) at pH 7 (Pap-conjugates: 12.5 - 16.6 min) and 10 (Pap-conjugates: 13.4 – 16.6 min). The ESI of all the hydrolyzed-protein polysaccharide conjugates at pH 7 (13.5 – 16.6 min) and 10 (14 – 16.6 min) were also reported to be higher than those at pH 4 (12.2 – 13.3 min) for all degrees of hydrolysis. Emulsion stability (ES) refers to the ability of the emulsion to resist changes in its property over

Table 3.3. Properties of protein-starch conjugates as an emulsifier

Sample	DH	Emulsion Activity Index (m^2/g)			Emulsion Stability Index (min)			Emulsion Stability (%)		
		pH 4	pH 7	pH 10	pH 4	pH 7	pH 10	pH 4	pH 7	pH 10
PPEF	-	8.1 ± 1.6^{a}	17.7 ± 0.6^{a}	20.6 ± 1.5^{a}	11.8 ± 3.8^{a}	14.4 ± 0.4^{a}	14.5 ± 0.5^{a}	68.0 ± 3.0^{b}	82.5 ± 2.2^{a}	81.6 ± 0.8^{a}
Tryp0	-	18.2 ± 0.7^{cd}	21.3 ± 0.6^{a}	22.9 ± 0^{a}	12.2 ± 0.1^{b}	12.7 ± 0.2^{a}	13.6 ± 0.2^{a}	96.4 ± 0.3^{cde}	93.3 ± 2.0^{b}	91.3 ± 0.4^{b}
Tryp2.5	2.5 ± 0.3	$21.5 \pm 0.^{7cd}$	21.1 ± 1.5^{a}	22.9 ± 0.9^{a}	12.3 ± 0^{b}	13.5 ± 0.5^{a}	14.2 ± 0.1^{a}	97 ± 1.1^{de}	93.3 ± 1.0^{b}	91.8 ± 0.6^{b}
Tryp9.9	9.9 ± 2.3	22.1 ± 1.4^{cd}	20.3 ± 2.8^{a}	23.6 ± 1.8^{a}	12.2 ± 0.2^{b}	14.1 ± 0.8^{a}	14.1 ± 0.4^{a}	96.9 ± 0.6^{cde}	94.2 ± 0.3^{b}	92.1 ± 1.0^{bc}
Tryp10.8	10.8 ± 0.8	22.2 ± 1.7^{d}	18.1 ± 0.1^{a}	23.9 ± 0.5^{a}	12.3 ± 0.1^{b}	14.6 ± 0.5^{a}	14.0 ± 0.2^{a}	98 ± 0.3^{e}	94.9 ± 0.1^{b}	92.5 ± 0.2^{bcd}
Pap0	-	10.1 ± 2.1^{ab}	23.2 ± 1^{a}	24.6 ± 1^{a}	14.6 ± 1.4^{b}	12.5 ± 0.3^{a}	13.4 ± 0.3^{a}	92.1 ± 0.1^{cde}	93.5 ± 0.5^{b}	90.5 ± 0.1^{b}
Pap3.3	3.3 ± 0.7	20.7 ± 1.2^{cd}	19.5 ± 3.5^{a}	21.3 ± 0.4^{a}	12.3 ± 0.2^{b}	15.2 ± 1.5^{a}	15.2 ± 0.4^{a}	75.1 ± 2.6^{bc}	91.4 ± 0.3^{b}	95.0 ± 0.2^{e}
Pap5.2	5.2 ± 1.0	17.5 ± 1.5^{bcd}	16.5 ± 1.1^{a}	19.3 ± 2.8^{a}	13.1 ± 0.5^{b}	16.6 ± 0.5^{a}	16.6 ± 1.2^{a}	94.8 ± 1.1^{cde}	92.3 ± 0.3^{b}	94.2 ± 0.2^{cde}
Pap8.1	8.1 ± 0.9	19.9 ± 0.4^{cd}	18.2 ± 1.4^{a}	20.6 ± 1^{a}	12.5 ± 0.1^{b}	15.6 ± 0.6^{a}	15.6 ± 0.7^{a}	71.2 ± 0.8^{bc}	91.0 ± 0.2^{b}	95.6 ± 0.3^{e}
Pap9.1	9.1 ± 0.5	20.3 ± 1.0^{cd}	17.9 ± 3.1^{a}	21.3 ± 1.9^{a}	12.5 ± 0.2^{b}	16.2 ± 2^{a}	15.3 ± 1.3^{a}	83.5 ± 7.2^{cd}	92.6 ± 0.9^{b}	94.5 ± 0.3^{de}
Pap10.2	10.2 ± 0.3	15.9 ± 0.4^{bc}	19.6 ± 0.2^{a}	21 ± 1.6^{a}	13.3 ± 0^{b}	14.4 ± 0.3^{a}	15 ± 1^{a}	50.0 ± 2^{a}	90.4 ± 0.7^{b}	92.6 ± 0.1^{bcd}

Data represents the mean ± standard deviation of triplicates (n=3). Different superscript letters (a,b,c,d,e) within the same column represent significantly different values at (p<0.05). *Abbreviations*: PPEF (pea protein enriched flour fraction); Tryp0 (Trypsin control); Tryp2.5 (Trypsin conjugate having a DH of 2.5%); Tryp9.9 (Trypsin conjugate having a DH of 9.9%); Tryp10.8 (Trypsin conjugate having a DH of 10.8%); Pap0 (Papain control); Pap3.3 (Papain conjugate having a DH of 3.3%); Pap5.2 (Papain conjugate having a DH of 5.2%); Pap8.1 (Papain conjugate having a DH of 8.1%); Pap9.1 (Papain conjugate having a DH of 9.1%); Pap10.2 (Papain conjugate having a DH of 10.2%).

time *i.e.*, separate into its constituent phases owing to various phenomenon like creaming, flocculation, coalescence, and so on (Pearce *et al.*, 1978). Unlike ESI, it gives us a visual representation of the emulsion being formed and its resistance to separate into two separate phases. The ES of PPEF, heated controls and conjugates were evaluated at pH 4, 7 and 10 by measuring its change over a period of 30 min (Table 3.3). Statistically significant differences (ANOVA) were observed between the ES of the conjugates at pH 4 and 10 but not at pH 7 ($p < 0.05$).

The ES of all conjugates at pH 7 and 10 were higher than raw PPEF. Tryp10.8 conjugates had the highest ES at pH 4 (~98%), whereas Pap10.2 conjugates had the least ES at 4 (~50%) (Table 3.3). Among the Tryp and Pap-conjugates, the Tryp-conjugates had higher ES (96.4% - 98%) at pH 4 as compared to Pap-conjugates (50% – 94.8%). The ES at pH 7 and 10 were almost comparable. As evident from the results, the ES of the Tryp-conjugates are the highest at pH 4 (96.4% – 98%) as compared to pH 7 (93.3% – 94.9%) and pH 10 (91.3% – 92.5%). Pap9.1 conjugates also showed comparable ES at pH 4 (83.5%) compared to pH 7 (92.6%) and pH 10 (94.5%).

3.4.7.3 Water holding capacity (WHC) and oil holding capacity (OHC)

Water/oil holding capacity determines the amount of water or oil retained by the conjugate solution (per gram basis) and is an important aspect of the structural and sensory properties of food products. Both WHC and OHC were analyzed at neutral pH (7). The WHC of all the conjugates were significantly higher ($p < 0.05$) than the PPEF samples (Table 3.2). Among the Tryp-conjugates, Tryp0 showed the highest WHC (2.4 g/g) as compared to the other conjugates (2.0 g/g – 2.3 g/g). However, one-way ANOVA showed that the differences were not very significant ($p < 0.05$). The DH of the protein did not have any correlation with the WHC. Among the Pap-conjugates, Pap5.2 (DH= ~5.2%) showed the maximum WHC (2.3 g/g), whereas Pap3.3 showed the least WHC (1.7 g/g) (Table 3.2).

Similar to the WHC, a significant increase in the OHC was observed for the conjugates as compared to the raw PPEF samples (Table 3.2). Similar to the WHC, a significant increase in the OHC was observed for the conjugates as compared to the raw PPEF samples (Table 3.2). The DH did not significantly impact the OHC for both the Tryp and Pap-conjugates. The effect of enzyme used for proteolysis also had a minor effect on the OHC. The OHC of the hydrolyzed Tryp-conjugates was in the range of 2.2 to 2.3 g/g whereas the OHC of the enzyme-modified Pap-conjugates lie within the range of 1.9 to 2.2 g/g.

3.5 Discussion

Plant proteins have drawn major attention as functional food ingredients. Improvement in legume protein techno-functionality through partial enzymatic hydrolysis of protein has been extensively reported in the literature. The major objective of this study was to further improve pea protein functionality using Maillard Reaction-induced covalent crosslinking of partially hydrolyzed proteins with starch or other non-starch carbohydrates in pea flour.

Potential influences of conjugated carbohydrates have been argued to modify the physicochemical properties of proteins. Firstly, steric repulsion and shielding of the electrostatic double layer on the proteins are significantly influenced by the bulky starch/high MW dextrin layers, especially at low pH ranges (Zha *et al.*, 2019a; Kato, 2000; McClements, 2015). The increased steric repulsion counteracts the van der Waals attraction between emulsion/foam droplets thereby preventing flocculation. Optimal distribution of hydrophobic amino acids of the protein and -OH groups of hydrophilic carbohydrate moieties on the surface of the conjugates increases its amphiphilic nature and can lead to favorable interactions with the solvents (Kasran *et al.*, 2013a; Kasran *et al.*, 2013b). Introduction of conjugated starch can add hydrophilic moiety, thus changing the distribution of hydrophilic and hydrophobic moieties in the starch-conjugated protein species. Thus, it influences amphiphilic properties, especially when proteins are partially hydrolyzed to expose their hydrophobic core prior to the conjugation reactions. Moreover, variability in size, structure and orientation of the conjugates also play a key role in their mobility, flexibility and steric interactions with other molecular species (Che *et al.*, 2017). Owing to these factors, the conjugates can rapidly diffuse to the solvent-water interface, orient themselves with the polysaccharide group towards water and protein towards the non-polar phase and restrict the thermodynamically unfavorable contact area, thereby reducing the interfacial/surface tension and improving the foaming and emulsification properties (Mookerjee *et al.*, 2023; Shen *et al.*, 2021; McClements, 2015).

The influences from these property changes owing to starch-protein conjugation results in a significant impact on the solubility and stability of the conjugates (Kasran *et al.*, 2013a). From Figure 3.3A, it is evident that various protein species were formed by enzymatic hydrolysis having different chain lengths and exposure of hydrophobic amino acids from the protein core. These hydrolyzed proteins coupled with intact proteins have formed different molecular species of conjugates with carbohydrates (Figure 3.3B), resulting in various sizes and differential surface

properties (Table 3.2). In addition, Table 3.2 shows highly negative surface charge values (zP) for the conjugates indicating better solubility. Increased negative charges imply enhanced electrostatic repulsion between the protein component of the conjugates resulting in reduced aggregation (Avramenko *et al.*, 2013; Goertzen *et al.*, 2021). Optimum conjugate size and surface properties can therefore be considered another major cause for improved FC, FS (Figure 3.4) EAI and ESI (Table 3) of the conjugates at various pH values. In these conjugation experiments, the increased FC (Tryp-conjugates: Tryp0, Tryp2.5; Pap-conjugates: Pap0, Pap9.1), EAI (Tryp-conjugates: Tryp2.5, Tryp9.9, Tryp10.8; Pap-conjugates: Pap3.3, Pap5.2, Pap8.1, Pap9.1, Pap10.2) and ES (Tryp-conjugates: Tryp0, Tryp2.5, Tryp9.9, Tryp10.8) of the conjugates at acidic pH can be attributed to the steric repulsion caused by the conjugates which counteracted the charge on the proteins. Similar observation was made by Wang and Ismail (2012) and Mulcahy *et al.* (2016) and they also attributed the increased conjugate functional properties to enhanced steric repulsion caused by the bulky carbohydrate molecules. Similar increases have been reported for increases in foam capacity of various polysaccharides conjugated with soy, whey, and soybean proteins (Zhao *et al.*, 2022; Chiu *et al.*, 2009; Garcia-Amezquita *et al.*, 2014; Wang *et al.*, 2020). Significant increases in ES, EAI and ESI of pea, peanut and soy proteins conjugated (Maillard reaction) with different polysaccharides like sodium alginate and gum Arabic has been reported extensively in literature (Liu *et al.*, 2012; Wang *et al.*, 2021; Zha *et al.*, 2019a). Pea proteins are also insoluble at acidic pH (close to its pI) which could reflect the minimized functional properties for some of the conjugates at lower pH (Konieczny *et al.*, 2020a). These results can be verified from the zP data which shows a surface charge close to 0 for the conjugates (1.9 – 3.9 mV) at pH 4 (Table 3.2) indicating a high possibility of aggregation. This could be a possible explanation for the decreased EAI (Tryp0, Pap0), ES (Pap3.3, Pap8.1, Pap9.1, Pap10.2) and ESI (except Pap0) which caused the protein terminal of the conjugates to aggregate resulting in droplet rupture. However, owing to the presence of starch/polysaccharide conjugated proteins, the difference in the ESI between pH 4 and pH 7, pH 10 was only about 2% – 5%.

Modification in water- and oil-holding properties was attributed to the combined effects of protein structure changes and addition of hydrophilic properties through conjugated starch. The water-binding property of starch/dextrins by virtue of hydrogen bonds coupled with the high molecular weight of the starch molecule must be a possible explanation for the increased WHC of the conjugates as compared to the PPEF (Shen & Li, 2021). Heating coupled with enzymatic

hydrolysis during conjugate preparation denatures the protein structure and exposes the buried hydrophobic groups which are better able to orient towards the oil phase and bind it via hydrophobic interactions (Shen *et al.*, 2021). The reduced WHC of the hydrolyzed-protein carbohydrate conjugates as compared to the heated controls could be the exposure of buried nonpolar, aromatic and sulfhydryl groups on the protein surface owing to enzymatic cleavage. As a result, hydrophobic interactions were favoured over conjugate-water (polar) interactions resulting in lower WHC. The zP (Table 3.2) values corelate with the data which shows that at neutral pH, Tryp0 had higher zP (-28.6 mV) as compared to the other Tryp-conjugates (-27.5 mV to -28.4 mV) indicating higher polarity. Similar increases in WHC of chickpea protein hydrolysates and Maillard conjugated pea protein isolates have been reported previously (Goertzen *et al*., 2021; Shen *et al.*, 2022; Shen *et al.*, 2021). Moreover, the WHC reported in this study is higher than the WHC of enzymatically hydrolyzed PPEF (1.49 – 1.94 g/g) that has been reported previously by Konieczny *et al.* (2020a) indicating that hydrolysis followed by conjugation increased the WHC as compared to only enzymatic hydrolysis.

Exposure of buried hydrophobic moieties could explain the enhanced OHC of the conjugates. Goertzen *et al.* (2021a) attributed lower OHC to smaller size of the polypeptide chain produced due to enzymatic cleavage which were unable to entrap the oil. This could explain the low OHC values obtained for the hydrolyzed Tryp and Pap-conjugates. The OHC of the PPEF conjugates reported in this study are significantly higher (1.9 g/g – 3.9 g/g) than the OHC data of hydrolyzed PPEF conjugates (0.74 – 1.46 g/g) previously reported by Konieczny *et al.* (2020) indicating better oil binding of the conjugates. Enhanced OHC can be attributed to higher exposure of hydrophobic amino acids which were better able to interact and bind oil. Increased OHC of Maillard conjugated pea protein with different polysaccharides has been also reported elsewhere (Shen *et al.*, 2022).

3.6 Conclusion

In this study, hydrolyzed pea protein-carbohydrate conjugates showed increases in surface charge at pH 7 and 10 indicating higher solubility. All conjugates showed a significantly higher FC at pH 7 and 10 as compared to the PPEF. The FS values showed a slightly different trend with Tryp conjugates having the maximum stability at pH 4 and 7, whereas the Pap conjugates showing improved stability at pH 10. EAI and ES of the Tryp conjugates at pH 4 were greater than that at

pH 7. On the other hand, the EAI of the Pap conjugates at pH 4 were comparable to that at pH 7. Both WHC and OHC of the conjugates showed significant improvements as compared to PPEF. Interestingly, some of the functional properties (WHC, OHC, FC, FS, ES) of the heated controls (Tryp0 and Pap0) at certain pH were higher than the hydrolyzed-protein starch conjugates. Overall, an increase in the functionality of the conjugates was observed. Enhanced functional properties (foaming and emulsification) at pH 4 can indicate their possible uses in beverage emulsions like fruit juices and instant coffee. Improved oil and water holding capacities can be of immense importance to enhance the taste, texture, and mouthfeel of plant-based processed meat alternatives. The combination of partial proteolysis with starch conjugation showed good improvements in the techno-functional properties of pea proteins. As this approach does not require exogenous material inputs, and no special chemical substances, but only enzymes and heat treatment, the process is a cost-effective and promising approach to create functionally enriched products using pulse proteins. In this study, the DH of the protein fraction was limited to moderate levels and the use of any external starch as raw material was avoided. The subsequent future studies will separately examine the effects of extensive proteolysis coupled with carbohydrate conjugation and the addition of an external starch source on the functional properties of the conjugates. Moreover, it was aimed to reproduce subsequent hydrolysis followed by heat treatment conditions on an industrial scale for the production of value-added functional food prototypes like salad dressings or mayonnaise that can be sold to consumers.

3.7 Connection to next study

The initial phase of the study (Chapter III) examined the effects of low and medium degrees of hydrolysis, followed by conjugation with starch and other non-starch polysaccharides, on the functional properties of pea proteins. The findings in this study indicated moderate improvements in functional attributes such as foaming and emulsification at pH 7 and pH 10, with significant enhancement observed at pH 4. Literature suggests that extensive proteolysis leads to complete unfolding of protein structures, resulting in short polypeptide chains. The addition of carbohydrates provides stability to the conjugates, a finding corroborated by the study of this chapter and widely supported by existing literature. Therefore, the subsequent phase of the research aimed to determine whether a high degree of proteolysis, paired with carbohydrate conjugation, could produce stable conjugates with optimal size and amphiphilicity, enhancing

functional properties at pH 4, pH 7, and pH 10, and challenging the widely accepted notion of poor functionality at high levels of hydrolysis. We hypothesized that increased hydrolysis will translate to increased hydrophobicity and due to carbohydrate conjugation the extensively unraveled proteins can still maintain their shape and display improved flexibility and orient at the solvent/air interface and could exhibit better functionality than the conjugates studied in this chapter.

CHAPTER IV

4 Enhancing Functional Properties Of Extensively Hydrolyzed Pea Proteins Using Trypsin And Papain Through Maillard Conjugation With Pea Starch And Other Non-Starch Polysaccharides

4.1 Abstract

Enzymatic hydrolysis of pea proteins using trypsin and papain to high degrees was followed by heat-induced Maillard conjugation with starch and non-starch polysaccharides present in the flour. The resulting protein-starch conjugates were investigated for their structure, surface, and functional properties which were compared against PPEF. SDS-polyacrylamide gel electrophoresis and scanning electron microscopy analyses showed the presence of different molecular species and altered macrostructure in the conjugate preparations. The zeta potentials at pH 7 (-20.6 to -32.3 mV) and pH 10 (-29.2 to -36.6 mV) were more negative compared to pH 4 (0.2 to 8.6 mV). All trypsin-hydrolyzed protein-starch conjugates exhibited better foaming and emulsification properties at pH 4, 7, and 10 compared to the papain-hydrolyzed protein-starch conjugates. Trypsin-hydrolyzed conjugates with a degree of hydrolysis at 24% showed the highest foam capacity (126.6%) at pH 7 and emulsion activity of 24.0 m^2/g at pH 10. In contrast, trypsin hydrolysates (21.7% degree of hydrolysis) exhibited increased emulsion stability (99.4%) at pH 7. The non-hydrolyzed conjugates also showed improved functional properties compared to the pea protein enriched flour fraction, displaying enhanced water hydration (2.4 g/g) and oil holding (3.9 g/g) abilities. It is commonly considered that high degrees of hydrolysis results in unraveling proteins too much, resulting in lower functionality. The results of this study showed that conjugation between proteins and polysaccharides can counterbalance the negative effects of unravelling and can further enhance functional properties.

4.2 Introduction

Proteins are essential macromolecules vital for numerous metabolic functions and human nutrition, particularly due to the need for essential amino acids that we are unable to synthesize. Beyond their nutritional value, proteins are also extensively used in the processed food industry to enhance techno-functional properties of the final products (Mookerjee *et al.,* 2023). The functionality of proteins depend on intrinsic properties, like its molecular weight and structure, as well as extrinsic properties like pH, salt concentration, and temperature and these external conditions alter protein surface charge and hydrophobicity, influencing interactions with other food components and affect their functional properties. Historically, the food industry has utilized animal proteins, such as whey, casein, and ovalbumin, as functional ingredients. However, in the past decade, there has been a gradual shift towards plant-based ingredients. This trend is driven by changing consumer preferences influenced by health, environmental, economic, and ethical considerations (Avramenko *et al.*, 2013; Nikbakht Nasrabadi *et al.*, 2021). Among plant proteins, pea proteins have gained significant attention due to their low potential for causing allergies, high nutritional quality, improved bioavailability, and affordability (Barac *et al.*, 2010; Lam *et al.*, 2018). Stone *et al.* (2015) investigated the functional properties of pea protein isolates derived from different cultivars and reported that the water holding capacity (WHC) and oil holding capacity (OHC) of these pea protein isolates were comparable to the values observed with commercially extracted pea protein. However, the use of peas as functional ingredients is limited due to two main reasons: solubility difference due to the extraction methods and the presence of antinutritional factors. It has been reported that commercial extraction of pea proteins using alkali leads to a decline in solubility, which in turn affects other solubility-related functional properties such as foam formation, emulsification, and gelling abilities. This deterioration restricts their application as food ingredients. (Lam *et al.*, 2018; Zha *et al.*, 2019b). Antinutrients in peas, like phenolic compounds and tannins, interact with proteins, forming stable complexes or precipitating them, which reduces protein functionality and solubility (Goertzen *et al.*, 2021a; Konieczny, *et al.*, 2020a; Nikbakht Nasrabadi *et al.*, 2021).

To enhance the functional properties of pea proteins, various modification techniques have been employed to alter the structure of their molecules or specific functional groups. (Nikbakht Nasrabadi *et al.*, 2021). Among the various approaches, enzymatic hydrolysis has garnered

increasing attention due to the specificity of enzyme activity, milder processing conditions, and its sustainable nature (Mookerjee *et al.*, 2023; Ramos *et al.*, 2011; Robinson, 2015). Konieczny *et al.* (2020a) investigated the functionality of hydrolyzed pea protein concentrates. The study reported low solubility, but improvements in water holding capacity (WHC) and oil holding capacity (OHC). While controlled enzyme treatment can lead to the exposure of hydrophobic moieties from the protein core leading to a hydrophilic-lipophilic balance on the surface, high degrees of hydrolysis can result in complete unraveling of the proteins. This results in the formation of short-chain soluble peptides, causing a significant reduction in functional properties. (Leni *et al.*, 2020; Chapter III; Zhang *et al.*, 2019).

Heat-induced Maillard conjugation between the protein and carbohydrates, documented as an effective approach can be another path to improve techno-functionality of proteins (de Oliveira *et al.*, 2016; Hiller *et al.*, 2010; Jiménez-Castaño *et al.*, 2007; Y. Liu *et al.*, 2012; Chapter III; Zha *et al.*, 2020; Z. Zhang *et al.*, 2022). Maillard reaction comprises a series of complex reactions categorized into early, intermediate and advanced stages (de Oliveira *et al.*, 2016; Liu *et al.*, 2012). This reaction involves a condensation reaction where a reducing sugar reacts with the free amino group of a compound, such as a protein, to form a Schiff base. This intermediate then undergoes an irreversible rearrangement, leading to the formation of the Amadori Rearrangement Product (ARP) (Liu *et al.*, 2012). These protein-carbohydrate conjugates remain extremely stable against variations in temperature and pH leading to enhanced resistance to alterations in processing conditions (Dickinson *et al.*, 1991; Chapter III). In Chapter III, an increase in the foaming and emulsifying properties of pea proteins conjugated with carbohydrates at pH 4 in comparison to pH 7 was reported. Additionally, the conjugates also exhibited an increase in the water holding capacity (WHC) and oil holding capacity (OHC). Zhang *et al.* (2022) studied the functional properties of Maillard-induced pea protein isolate-maltodextrin (PPI-MD) conjugates. An increase in the solubility and emulsion stability index (ESI) were reported for the conjugates compared to the native PPI. In a separate study, increased solubility at pH 3, improved emulsification and foaming properties were reported for Maillard-induced pea protein isolates conjugated with xylo-oligosaccharides (Zhao *et al.*, 2022). Similar improvements in the emulsifying properties of pea protein concentrate- gum Arabic conjugates with resistance to pH changes were observed by Zha *et al.* (2019b). The impact of carbohydrate/polysaccharide conjugation with intact pea proteins and moderately hydrolyzed pea proteins have been previously studied.

As mentioned earlier, high degrees of proteolysis generally degrade the functionality of proteins while low degrees can enhance the functions. Additionally, carbohydrate conjugation has been demonstrated to improve the functional properties of proteins. Thus, this study hypothesized that the carbohydrates/dextrin conjugated can enhance the functional properties of highly hydrolyzed pea proteins. Pea proteins were conjugated with the existing carbohydrate in pea protein enriched flour (PPEF) hydrolyzed with combinations of proteinase and amylase hydrolysis. The structure, physicochemical characteristics and their functionality were examined in this study.

4.3 Materials and methods

4.3.1 Materials

Pea flours were milled to produce a protein enriched fine fraction also known as the pea protein-enriched flour (PPEF), which was generously donated by AGT Foods. Petroleum ether, trinitrobenzenesulfonic acid (TNBS), porcine trypsin (10,600 units/mg), and crude papain (1.5-10 units/mg solid) from papaya latex were purchased from Fisher Scientific and Sigma-Aldrich Canada respectively. The water was produced using a Millipore Milli-Q™ water purification system (MilliporeSigma, MA).

4.3.2 Proximate composition analysis

The AOAC Official Methods 925.10, 923.03, 920.85, 997.09, and AACC Method 76-13.01 were employed to determine the moisture, ash, lipid, crude protein (calculated as %N × 6.25), and total starch content. The percentages of protein, lipid, moisture, ash, and total starch were subtracted from 100% to represent the overall composition of the flour, with the remaining portion being expressed as other carbohydrates present in the PPEF. The details were described in Section 3.3.2.

4.3.3 Protein solution preparation

Protein solutions were prepared at concentrations of 1.5% and 2% w/v, (protein content basis) in 2 L, 50mM sodium phosphate buffer solution at pH 7.0 and 1 L 50mM sodium phosphate buffer solution at pH 6.5, respectively. These concentrations and pH values were determined through preliminary small-scale experiments (data not included). The solutions were stirred at 4°C overnight, and the pH was adjusted using 0.5 M dilutants (NaOH/HCl) as appropriate.

4.3.4 Conjugate preparation

Conjugates were prepared according to the procedure discussed in Chapter III. Initially, PPEF solutions were subjected to heating at 80°C for a period of 60 min to facilitate gelatinization of starch. Upon cooling, the temperature and pH were adjusted to 37°C, pH 7 for the trypsin and *Aspergillus* α-amylase reaction, and to 60°C, pH 6.5 for the papain and *Bacillus* α-amylase reaction. Both protease and amylase were simultaneously incorporated into the reaction mixture, creating a "one-pot" reaction. Typically, enzymes are added sequentially; however, in this experiment, they were added simultaneously to simplify the modification process for further scale-up reactions. The optimal temperature and pH for hydrolysis were pre-determined through a series of small-scale reactions. After a 60-minute incubation period, the solutions were heated at 90°C for 30 min to terminate the enzymes and initiate Maillard reactions. After that, the Maillard reactions were promptly stopped by freezing the solutions. Subsequently, the solutions were freeze-dried and stored for functional properties investigation.

For comparison, heated controls were prepared parallelly without enzymes (37°C for the trypsin reaction; 60°C for the papain reaction) but using all heat treatment procedures employed for protease-treated PPEF experiments above.

Throughout the study, the following designations are used: PPEF represents intact raw materials. Trypsin and papain treated samples are represented by T and P, respectively. T0 and P0 serve as untreated controls (raw PPEF not subjected to enzymatic hydrolysis) subjected to heat for Maillard conjugation to simulate the enzymatic reactions. T-numerical figure-A (T19.4A *etc.*) and P-numerical figure-A are hydrolyzed PPEF using trypsin or papain and conjugated (Maillard) with α-amylase hydrolyzed starch/non-starch polysaccharides. T-numerical figure and P-numerical figure are trypsin or papain hydrolyzed PPEF Maillard conjugated with unhydrolyzed starch/carbohydrates present in the flour. The naming and conditions are summarized in Table 4.1.

4.3.5 Determination of the degree of protein hydrolysis (DH)

The degree of proteolysis was assessed using the method outlined by Adler Nissen with minor modifications as detailed by Goertzen *et al.* (2021a). The details were described in Chapter III.

4.3.6 Determination of the degree of starch hydrolysis/dextrose equivalent (DE)

The DE was determined using the 3,5-dinitrosalicylic acid (DNS) method (Miller, 1959). A 1-mL aliquot of both the blank and hydrolyzed samples was transferred to 0.5 mL of Milli-Q water, followed by the addition of 1.5 mL of DNS reagent. For acid-hydrolyzed samples, 0.25 mL of the reaction mixture was diluted with 2 mL of water, to which 0.15 mL of DNS was added. The solutions were vortexed for 10 seconds and immediately transferred to a hot water bath at 100°C for 5 minutes. Subsequently, the test tubes were placed into an ice bath for 10 min – 15 min to facilitate color development. After allowing the tubes to reach room temperature, the absorbance was measured at 540 nm using a spectrophotometer (Genesys 10UV Scanning Thermo Scientific, USA). A standard curve was prepared using glucose, and a series of glucose solutions with concentrations ranging from 0.03 mM to 0.5 mM were utilized to determine the glucose equivalents of the hydrolyzed starch fraction. The DE was calculated as the ratio of the number of reducing ends measured following enzymatic hydrolysis (h_{sample}) to the number of reducing ends obtained after total acid hydrolysis (h_{total}), multiplied by the appropriate dilution factors and glucose equivalents.

$$\text{DE} = \frac{h_{sample}}{h_{total}} \times 100 \quad \text{.....(4.1)}$$

4.3.7 Sodium dodecyl sulfide polyacrylamide gel electrophoresis (SDS-PAGE)

The molecular weight distribution profile of the hydrolyzed PPEF were established, and verification of the size alteration of the conjugates pre- and post-conjugation was conducted via sodium dodecyl sulfate polyacrylamide gel electrophoresis (SDS-PAGE) following the method outlined by Laemmli (1970).

The Fuchsine-sulfite staining technique was employed to verify the molecular size changes of the conjugates pre- and post-reaction, as well as to identify glycosylated proteins within the gels (Zacharius *et al.*, 1969). The quantification of the conjugated protein bands was performed using ImageJ® (National Institutes of Health) with the digitized image of the gel.

4.3.8 Microstructure using Scanning Electron Microscope (SEM)

The sample powder was evenly applied to the observation platform using conductive double-sided tape and subsequently coated with gold using an Edwards S150B sputter coater (BOC Edwards, UK). A Phenom^{TM} field emission scanning electron microscope (FEI Company, USA)

was used for observation under the condition that the acceleration voltage was 5 kV. Samples were observed under magnifications of ×3000, ×5,000 and ×10,000.

4.3.9 Monitoring of Amadori compounds formation and browning

To prepare a 0.025% (w/v) protein solution, the conjugated samples were dissolved in 10 ml of 0.1% SDS. Absorbance readings were taken at 304 nm, where the difference in UV absorption between the control (PPEF) and the conjugated samples at this wavelength indicated the formation of Amadori compounds (Wang *et al*., 2012; Zhu *et al.*, 2008). Additionally, the browning index was measured at 420 nm (Jiménez-Castaño *et al.*, 2007; Wang *et al*., 2012).

4.3.10 Analysis of Surface, functional and texture properties

4.3.10.1 Surface charge

The zeta potential (zP) of the conjugates was evaluated at pH levels of 4, 7, and 10 by assessing their electrophoretic mobility, utilizing a Nano-ZS90 Zetasizer (Malvern Instruments, Westborough, MA, USA) following the method described in Chapter III. A detailed description of the methodology has been provided in Chapter III.

4.3.10.2 Foaming properties- foaming capacity (FC) and foam stability (FS)

The foaming capacity and foam stability of the samples were evaluated at pH levels of 4, 7, and 10 following the procedure described by Avramenko *et al.* (2013). A detailed description of the methodology has been provided in Chapter III.

4.3.10.3 Emulsifying properties - emulsion activity index (EAI) and emulsion stability (ES)

The emulsion activity index (EAI) of both untreated and enzyme-modified PPEF conjugates was assessed according to the method of Pearce *et al.* (1978), as further described in Chapter III. A detailed description of the methodology has been provided in Chapter III.

4.3.10.4 Water and oil holding capacities (WHC/OHC)

The water and oil holding capacities were analyzed based on the method of further described in Chapter III and has been described in detail in Chapter III.

4.3.11 Statistical analysis

The proximate composition data for the PPEF are presented as the mean ± standard deviation from triplicate measurements. Enzymatic hydrolysis and conjugation reactions were

carried out in biological duplicates. Proximate composition, degree of hydrolysis (DH), surface properties, and functional properties of each biological duplicate were assessed in triplicate, and the results are reported as the mean ± standard deviation of six values (derived from duplicates, each measured in triplicate, thus n=6). Statistical analysis was conducted using One-way ANOVA, followed by the Tukey post-hoc test for mean comparisons among different enzymatic reactions. Statistical significance is denoted at $p < 0.05$.

Table 4.1. Sample representation and influence of protease and amylase E/S ratio and time on the DH and DE of samples; Maillard reaction conditions (temperature and time) to achieve different conjugates

Sample	Name	Enzymatic reaction conditions					Maillard reaction conditions	
		DH(%)	Protease E/S	DE	α-Amylase E/S	Time (min)	Temperature (°C)	Time (min)
Raw sample	PPEF	-	-	-	-	-	-	-
Trypsin control	T0	-	-	-	-	60	90	30
Trypsin treated conjugates	T17.7A	17.7 ± 1.25^{cde}	1:5,000	< 1%	1:83.4	60	90	30
	T19.4A	19.4 ± 4.7^{ce}	1:7,500	< 1%	1:50	60	90	30
	T21.7A	21.7 ± 4.2^{de}	1:5,000	< 1%	1:50	60	90	30
	T24A	24.1 ± 0.9^{e}	1:2,500	< 1%	1:50	60	90	30
	T25.9	25.9 ± 2.9^{e}	1:5,000	-	-	60	90	30
Papain control	P0	-	0	-	-	60	90	30
Papain treated conjugates	P14.8A	14.8 ± 1.9^{cde}	1:1000	< 1%	1:50	60	90	30
	P15.6	15.6 ± 1.9^{cde}	1:500	-	-	60	90	30
	P18.7A	18.7 ± 1.0^{cde}	1:500	< 1%	1:50	60	90	30

E/S: Ratio of enzyme to substrate; DH: Degree of protein hydrolysis; DE: Degree of starch hydrolysis

4.4 Results

4.4.1 Proximate composition

The different proximate analysis percentages were as follows: protein, 55.0% ± 0.0%; lipid, 1.0% ± 0.3%; moisture content (MC), 1.2% ± 0.0%; ash, 5.4% ± 0.1%; total starch, 3.1% ± 0.2%; and other carbohydrates, 37.3 ± 1.0%. Similar proximate composition for the protein-enriched fraction of pea was also obtained in Chapter III and Konieczny *et al.* (2020a). The protein and moisture content of the conjugates are also presented in Table 4.2. The protein ratio of the heated conjugates is found to be significantly higher than the hydrolyzed conjugates. High degrees of enzyme hydrolysis led to the formation of short-chain polypeptides with increased exposure of α-amino terminals which were better able to conjugate with the available carbohydrates resulting in new compound formation, thus showing a decrease in the protein content (Chapter III).

Table 4.2. Proximate composition and ImageJ densitometry analysis of the raw, untreated and hydrolyzed conjugates; zeta potential of the raw, untreated and hydrolyzed conjugates at pH 4, 7 and 10

			zeta potential (mV)			Intensity (%)	
	Protein (db%)	M.C. (%)	pH 4	pH 7	pH 10	Fuchsin sulfite	CBB
PPEF	55.0 ± 0.0^{a}	5.4 ± 0.0^{b}	8.2 ± 0.2^{x}	-24.2 ± 0.4^{abc}	-27.3 ± 0.2^{l}	3.52	4.10
T0	51.6 ± 1.2^{ab}	18.4 ± 2.1^{a}	8.3 ± 0.2^{x}	-28.6 ± 0.4^{abc}	-35.2 ± 2.4^{lm}	4.93	6.78
T17.7A	46.5 ± 1.3^{bc}	10.9 ± 1.3^{ab}	-1.3 ± 1.5^{yz}	-20.9 ± 0.2^{ab}	-29.8 ± 0.9^{lm}	5.02	5.21
T19.4A	44.3 ± 0.8^{c}	10.3 ± 0.2^{ab}	0.9 ± 1.0^{yz}	-20.6 ± 0.8^{a}	-29.3 ± 0^{lm}	5.04	4.42
T21.7A	46.8 ± 2.8^{bc}	13.3 ± 4.7^{ab}	1.8 ± 0.2^{y}	-21.1 ± 0.1^{ab}	-29.4 ± 0.8^{lm}	5.06	4.40
T24A	43.9 ± 0.5^{c}	11.3 ± 0.6^{ab}	0.2 ± 1.1^{yz}	-20.7 ± 0.1^{a}	-28.7 ± 0.7^{lm}	5.13	5.32
T25.9	45.7 ± 1.3^{bc}	10.4 ± 2.5^{ab}	0.8 ± 0.7^{yz}	-30 ± 0.5^{bc}	-33.2 ± 0.1^{lm}	5.13	5.08
P0	48.6 ± 0.0^{bc}	12.3 ± 0.0^{ab}	8.6 ± 0.1^{x}	-28.5 ± 0.1^{abc}	-30.6 ± 1.2^{lm}	5.05	5.47
P14.8A	46.5 ± 0.6^{bc}	7.9 ± 1.2^{ab}	-0.4 ± 0.4^{yz}	-26.2 ± 5.0^{abc}	-31.3 ± 4.0^{lm}	5.02	4.76
P15.6	47.2 ± 0.0^{bc}	17.5 ± 2.6^{a}	-3.3 ± 0.3^{z}	-32.3 ± 0.3^{c}	-36.6 ± 0.2^{m}	5.2	5.1
P18.7A	45.7 ± 0.2^{bc}	8.4 ± 0.6^{ab}	-3.2 ± 1.0^{z}	-21.2 ± 0.7^{ab}	-29.2 ± 0.1^{lm}	4.97	4.98

Note: Data represents the mean ± standard deviation of six samples (n = 6). Different superscript letters (a,b,c,d, x,y,z,l,m,n) within the same column represent significant differences between groups ($p < 0.05$).

Abbreviations: M.C., moisture content; db, dry basis; PPEF, pea protein-enriched flour fraction; T0, trypsin control; T17.7A, conjugate samples hydrolyzed using trypsin to 17.7%DH and using amylase; T19.4A, conjugate samples hydrolyzed using trypsin to 19.4%DH and using amylase; T21.7A, conjugate samples hydrolyzed using trypsin to 21.7%DH and using amylase; T24A, conjugate samples hydrolyzed using trypsin to 24%DH and using amylase; T25.9, conjugate samples hydrolyzed using trypsin to 25.9%DH; P0, papain control; P14.8A, conjugate samples hydrolyzed using papain to 14.8%DH and using amylase; P15.6, conjugate samples hydrolyzed using papain to 15.6%DH; P18.7A, conjugate samples hydrolyzed using papain having to 18.7%DH and using amylase.

4.4.2 Preparation of PPEF hydrolysate

The degree of protein hydrolysis (DH) is quantified as the proportion of peptide bonds that have been hydrolyzed relative to the total number of peptide bonds in the protein (Adler-Nissen, 1979). The enzymatic reactions achieved different degree of hydrolysis, resulting in the alteration of protein and starch structures to certain extents prior to heat induced Maillard conjugation. The combinations are summarized in Table 4.1. It is generally considered that around 15 % – 20 % DH are high degrees of hydrolysis and more than 20 % indicates extensive hydrolysis (Chapter III). The Maillard conjugates were prepared with a series of combinations of proteolysis and amylolysis in "one-pot" reactions, followed by heating conjugation reactions. For hydrolysis of the protein fraction in the “one-pot” mixture, an enzyme to substrate ratio of 1:2,500, 1:5,000 and 1:7,500 were utilized for trypsin and an E/S of 1:500 and 1:1000 were used for papain; while amylase E/S was set at 1:83.4 and 1:50. The E/S ratios used were similar to those used for PPEF hydrolysis by Konieczny *et al.* (2020a) but higher than what was utilized in Chapter III. A low DH was observed for the "one-pot" trypsin-amylase hydrolysis compared to the reaction solution containing only trypsin. Conversely, the "one-pot" papain-amylase hydrolysis exhibited higher degrees of protein hydrolysis when amylase was included in the reaction, as opposed to using only papain. When compared between the two enzymes utilized, it was observed that a higher E/S concentration of papain (1:500 to 1:1000) resulted in a lower DH (14.8% to 18.7%) as compared to trypsin (E/S used: 1:2500 – 1:7500; Degree of hydrolysis obtained: 17.7% to 25.9%). The purity of the enzyme utilized can be a governing factor for the slight discrepancy. While trypsin utilized was a lyophilized powder of high purity, the papain utilized for the reaction was crude powder obtained from papaya latex and had added impurities. Results were in contrary to the findings of Konieczny *et al.* (2020a) where a higher reaction time was utilized for trypsin to achieve similar DH as papain, keeping the E/S constant. Heat-induced unfolding of the proteins coupled with the mode of trypsin action can be hypothesized to be a governing factor for the observed results. Trypsin is a serine protease that mainly acts on lysine and arginine residues (Elgendy, 2016). It is likely that these amino acid residues were inaccessible for enzymes before thermal treatment. The introduction of heat treatment prior to the one-pot reaction facilitated the unravelling of protein structure by disruption of electrostatic forces and hydrogen bonds and exposed them for cleavage (Andlinger *et al.*, 2022; Leite *et al.*, 2021; Mookerjee *et al.*, 2023).

Similar to proteolysis, the degree of starch hydrolysis (dextrin equivalent; DE) can be represented as a ratio of the total number of α-1,4 glycosidic bonds cleaved to the total number of α-1,4 bonds available in the carbohydrates present. α-amylase catalyzes the hydrolysis of α-1,4 bonds present in starches or other related polysaccharides and liberates sugars and limit dextrins (Sivaramkrishnan *et al.*, 2007). Literature has revealed that pea flour fine fractions contain about 30 % - 40 % total dietary fiber which is mostly comprised of non-starch polysaccharides, like cellulose, hemicelluloses and pectins embedded within the protein matrix (Pelgrom *et al.*, 2013; Rempel *et al.*, 2019). These non-starch carbohydrates cannot be hydrolyzed by α-amylase owing to the nature of different linkages present in them (Mudgil *et al.*, 2013; Sivaramkrishnan *et al.*, 2007). The PPEF samples utilized in this study consisted of 3.1% starch and approximately 35% non-starch carbohydrates. Given the initial low starch content, the degree of starch hydrolysis for all amylase treatments ranged between 0.4% and 0.8%. Therefore, for clarity, the absolute values have not been included in the article. Instead, samples treated with amylases are denoted by the letter A. A detailed nomenclature scheme used in the study is provided in Table 4.1.

4.4.3 Amadori compound formation

The formation of Amadori compounds is affected by the reaction temperature, moisture content, and treatment duration (Liu *et al.*, 2012). The degree of protein-carbohydrate conjugation has been demonstrated to impact the functional properties of the conjugates. Measuring absorbance at 304 nm and 420 nm can indirectly indicate the formation of early-intermediate stages and later stages of Maillard reaction products (MRPs), specifically melanoidins (Mookerjee *et al.*, 2023; Wang *et al.*, 2012). The Abs_{304} and Abs_{420} of the conjugates were significantly higher ($p < 0.05$) than those of the raw PPEF samples, indicating the formation of MRPs with increasing time and heat treatment (Figure 4.1). A comparison between Abs_{304} and Abs_{420} of both trypsin and papain hydrolyzed Maillard conjugates revealed higher absorbance values at 304 nm (0.40 to 0.47) compared to 420nm (0.26 to 0.37). The results are significant as it portrays an idea about the extent of Maillard reaction. The solutions were heated for a brief period of 30 minutes, primarily resulting in the early/intermediate stages of the Maillard reaction (de Oliveira *et al.*, 2016; Chapter III). Consequently, the formation of early stage Amadori compounds was more pronounced compared to the later-stage MRPs or melanoidins. ARPs are

generally unstable, and it is likely that the compounds formed further degraded into later stages of ARPs by 1,2 enolization and hydrolysis resulting in slight colouration (de Oliveira *et al.*, 2016). At 304 nm, trypsin hydrolyzed conjugates exhibited higher absorbance indices compared to those hydrolyzed by papain. In contrast, at 420 nm, conjugates hydrolyzed by papain displayed greater absorbance values. Papain, being a non-specific protease, generated peptides with exposed α-amino terminals at various amino acids during hydrolysis. These terminals readily conjugated with the -OH groups of carbohydrates in the flour, facilitating the formation of Amadori Reaction Products through condensation. (Kutzli *et al.*, 2021; Lowe, 1970). Trypsin is a more specific enzyme that hydrolyzes proteins at the carboxyl side of amino acids such as lysine or arginine. Consequently, the conjugates produced were fewer in number compared to those hydrolyzed by papain and were predominantly in their early and intermediate stages. Similar findings were discussed in Chapter III. Among all the conjugates studied, trypsin hydrolyzed conjugates at 25.9% DH gave the highest Abs_{304nm} at 0.47 indicating the maximum quantity of Amadori product formation. Abs_{420nm} of P14.8A conjugates at 0.37 revealed an increased index which translates to a higher quantity of later stages of ARP production (melanoidins). P0 samples also showed a higher Abs_{304} as compared to the papain hydrolyzed conjugates indicating that enzyme treatment did cause an increased exposure of the amino terminals readily available for conjugation thus prompting further degradation into melanoidins (Figure 4.1).

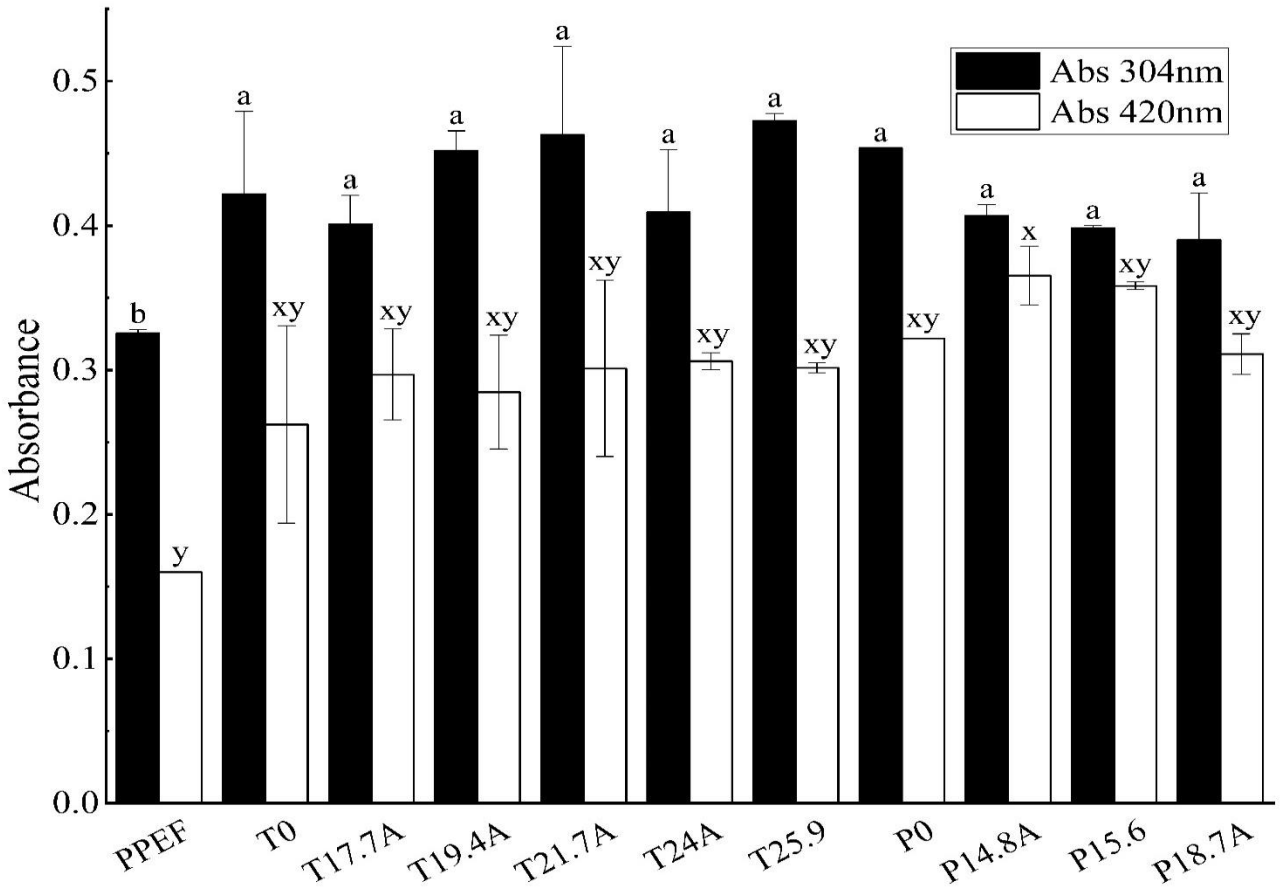

Figure 4.1. Quantification of Amadori Rearrangement Products

Absorbance values of PPEF, untreated, and hydrolyzed protein–starch/ protein-carbohydrate conjugates at 304 nm and 420 nm. Data represents the mean ± standard deviation of triplicates (n = 3). Each value is the mean of triplicate measurements, the error bars represent the standard deviation and different superscript letters (a,b) and (x,y) among the same ‑ colored bars represent significant differences between the groups ($p < 0.05$).

4.4.4 Molecular weight distribution and structural properties analysis

4.4.4.1 Molecular weight distribution and banding pattern of conjugates

The molecular weight distribution pattern on an SDS-PAGE gel stained using Coomassie Brilliant Blue (CBB) R-250 can be considered an indirect indication of the degree of protein hydrolysis and conjugation. Visual observation of the banding pattern showed a similar trend for all the trypsin conjugates indicating that at very high degrees of hydrolysis, most of the intact convicilins (70 kDa) and vicilins (40 kDa and 50 kDa) are broken down into smaller proteins Figure 4.2. Similar banding patterns have been observed in Chapter III. Enzyme hydrolysis cleaves the protein structures resulting in the formation of low molecular weight polypeptides which travel a longer distance in the lane when an electric field is applied (Elgendy, 2016).

Coomassie Brilliant Blue stained SDS-PAGE gels also revealed characteristic smearing patterns of the protein-carbohydrate conjugates. A blue band like pattern has appeared at the top of the separating gels which is not observed in the lane containing the raw PPEF samples. Similar high molecular weight bands were also observed for pea protein isolate conjugated with maltodextrins using the Maillard reaction (Zhang *et al.*, 2022). The presence of a thick band at the top of gel should be attributed to the formation of high M.W. protein-polysaccharide conjugates which were unable to pass through the pores of the gel (Zhang *et al.*, 2022; Zhao *et al.*, 2021). Apart from that, the presence of a thick blue smear was observed in the lane containing the heated conjugates (T0 and P0). The characteristic blue smear in the background is an indication that some of the proteins lost their characteristic banding pattern due to conjugation with the available starch or other non-starch carbohydrate components present in the flours. Densitometry analysis of the lanes using Image J revealed a higher CBB intensity (%) value for T0 (6.8%) and P0 (5.5%) as compared to the data for hydrolyzed conjugates which ranged between 4.4 % and 5.3% (Table 4.2). The CBB-stain intensity (%) in (Table 4.2) also corelates with the banding pattern obtained using SDS-PAGE (Figure 4.2A), where a thicker smear was observed for the T0 and P0 lanes, *i.e.*, higher intensities of non-banding proteins. Presence of a similar smear along the length of the lanes were observed for fenugreek gum conjugated with soy and whey proteins thorough Maillard reaction (Kasran *et al.*, 2013). Zhao *et al.* (2022) also revealed the upward movement of the original ~75 kDa and ~45 kDa bands present in pea proteins and fading of the ~23 kDa bands thereby indicating the formation of pea protein-xylo oligosaccharide conjugates by the Maillard reaction. The enzymatic hydrolysis process has

partially unfolded the protein structures and also led to the formation of polypeptides thereby increasing the number of reactive functional groups exposed to the carbohydrates for conjugation which is also reflected in the Abs_{304} data in Figure 4.1 (Mookerjee *et al.*, 2023; Mu *et al.*, 2010).

In order to further investigate the formation of conjugates, the gels were stained using a special fuchsine sulfite staining procedure using pararosaniline dye (Zacharius *et al.*, 1969). The pararosaniline dye stains the carbohydrate fraction of glycosylated proteins in an SDS-PAGE gel (Liu *et al.*, 2012). The banding pattern on the gel stained using fuchsin sulfite was analyzed using Image J software and the intensity has been represented as percentages in Table 4.2. Percentages have been expressed as a ratio of the density of the characteristic smear of the particular sample to all the smears (present in the gel) and has been employed as a means to quantitatively compare the amount of conjugates produced. All conjugates had higher fuchsin sulfite % intensity as compared to the PPEF (Table 4.2). This can be attributed to the formation of protein-carbohydrate conjugates upon thermal treatment that were actively stained using the dye. A similar observation was made by Liu *et al.* (2012) who reported an increased retention of purple stain when peanut protein isolates were conjugated with dextran. Rice proteins conjugated with *Arthrobacter* exopolysaccharides also showed a red smear along the length of the gel when stained using a carbohydrate specific stain (Zhao *et al.*, 2021). The first section of the study (Chapter III) also showed an increased intensity of Image J analyzed fuchsin sulfite-stained bands of pea protein-pea carbohydrate conjugates when compared with raw protein enriched flour. No significant differences were observed between the intensity of the different conjugates. Since the staining cannot distinguish between the different stages or nature of compounds produced, there were not much differences in the intensity data in between the lanes and hence a detailed characterization of the compounds produced cannot be performed from these SDS-PAGE data. However, the presence of faint pink bands and smearing was a direct indication of protein-starch and protein-non starch polysaccharide conjugation.

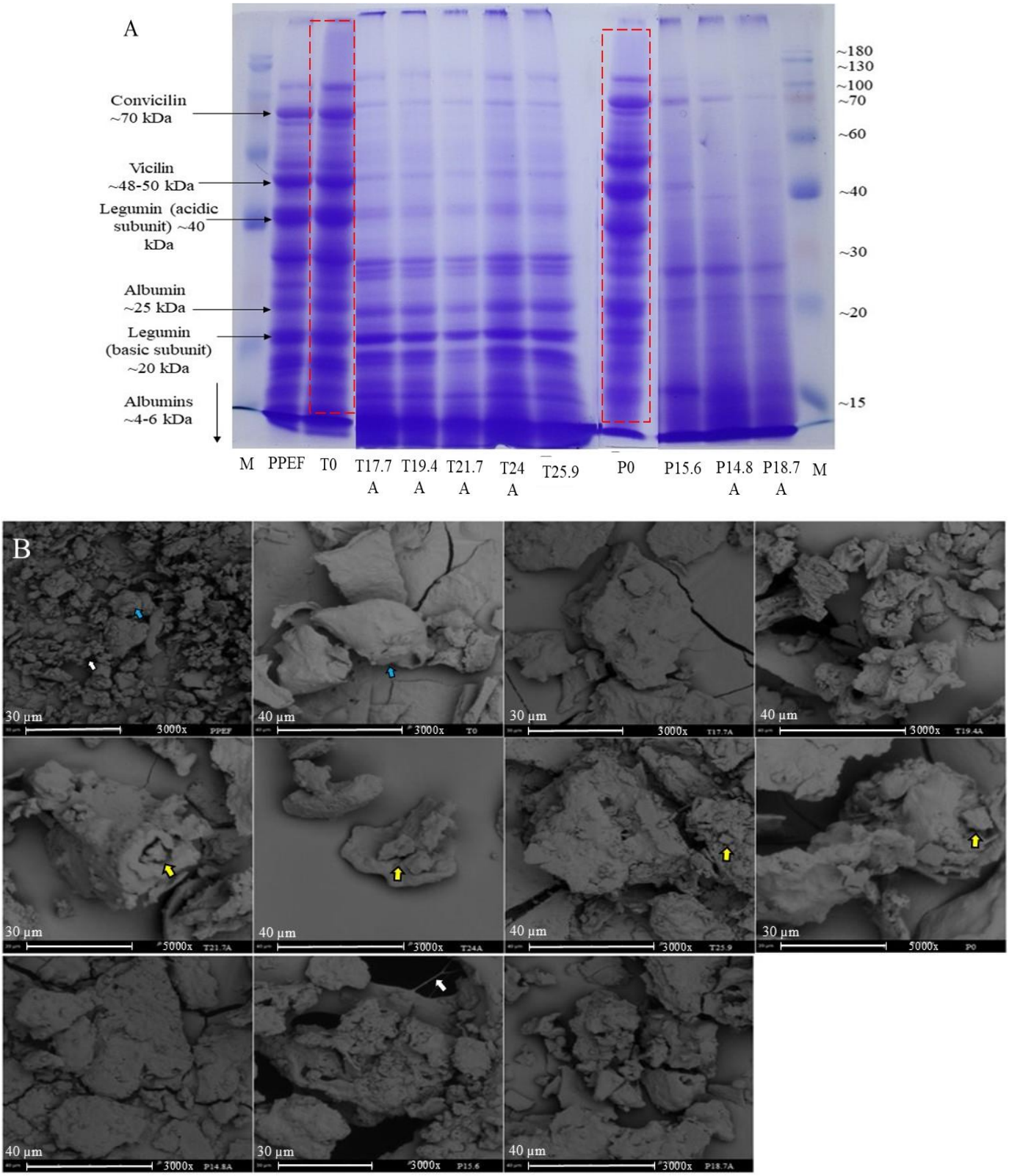
A
Convicilin
~70 kDa
Vicilin
~48-50 kDa
Legumin (acidic subunit) ~40 kDa
Albumin
~25 kDa
Legumin (basic subunit) ~20 kDa
Albumins
~4-6 kDa
~180
~130
~100
~70
~60
~40
~30
~20
~15
M
PPEF
T0
T17.7 A
T19.4 A
T21.7 A
T24 A
T25.9
P0
P15.6
P14.8 A
P18.7 A
M
B
30 µm
40 µm
30 µm
40 µm
30 µm
40 µm
40 µm
30 µm
40 µm
30 µm
40 µm

Figure 4.2. SDS-PAGE (A) and SEM (B) analyses of PPEF Maillard conjugates

(A) SDS-PAGE of PPEF, untreated conjugates, and hydrolyzed protein‑starch/non-starch polysaccharide conjugates stained using Coomassie Brilliant Blue R ‑ 250. From left to right: M, Molecular weight marker; PPEF, pea protein ‑ enriched flour fraction; T0, trypsin control; T17.7A, conjugate samples hydrolyzed using trypsin to 17.7%DH and using amylase; T19.4A, conjugate samples hydrolyzed using trypsin to 19.4%DH and using amylase; T21.7A, conjugate samples hydrolyzed using trypsin to 21.7%DH and using amylase; T24A, conjugate samples hydrolyzed using trypsin to 24%DH and using amylase; T25.9, conjugate samples hydrolyzed using trypsin to 25.9%DH; P0, papain control; P14.8A, conjugate samples hydrolyzed using papain to 14.8%DH and using amylase; P15.6, conjugate samples hydrolyzed using papain to 15.6%DH; P18.7A, conjugate samples hydrolyzed using papain having to 18.7%DH and using amylase. Red squares indicate thick background smear for T0 and P0.

(B) Microstructure analysis of raw, untreated and hydrolyzed conjugates using scanning electron microscopy (SEM). Magnification ×3,000 and ×5,000; Scale bar denoted by white horizontal lines correspond to 30μm and 40 μm; Green arrows indicate protein bodies, blue arrows indicate starch granules, yellow arrows indicate deformations in protein and starch structures and possibly the formation of protein-protein aggregates and protein- polysaccharide conjugation, and white arrow indicates linkages between heterogenous starch matrices. PPEF, pea protein ‑ enriched flour fraction; T0, trypsin control; T17.7A, conjugate samples hydrolyzed using trypsin to 17.7%DH and using amylase; T19.4A, conjugate samples hydrolyzed using trypsin to 19.4%DH and using amylase; T21.7A, conjugate samples hydrolyzed using trypsin to 21.7%DH and using amylase; T24A, conjugate samples hydrolyzed using trypsin to 24%DH and using amylase; T25.9, conjugate samples hydrolyzed using trypsin to 25.9%DH; P0, papain control; P14.8A, conjugate samples hydrolyzed using papain to 14.8%DH and using amylase; P15.6, conjugate samples hydrolyzed using papain to 15.6%DH; P18.7A, conjugate samples hydrolyzed using papain having to 18.7%DH and using amylase.

4.4.4.2 Macrostructure analysis of conjugates

In order to further validate the nature of the compounds formed, and demonstrate the formation of conjugates, the morphological characteristics of the freeze-dried mixtures were analyzed by scanning electron microscopy (SEM). Figure 4.2B reveals the scanning electron micrographs of PPEF, untreated conjugates and enzymatically modified conjugates at ×3,000 and ×5,000 magnifications. The pea protein enriched flour fraction showed a wide range of particles with different shapes and sizes. Individual protein bodies were observed in the protein enriched flour fraction along with protein bodies associated with the cell wall/fiber matrices. Apart from that, spherical and polygonal shaped intact starch granules were also present in the raw flour. Similar structural components in PPEF was also reported by Moller and his team who studied the microstructures of the fine fraction obtained after air classification of pea flours (Möller *et al.*, 2021). Heat treatment without any enzymes led to the formation of wedges on the surface of the starch granules for T0 conjugates. Some associations between the starch granules and protein bodies were also seen which could be a result of covalent bonding formed due to heat. P0 conjugates also revealed a loss of initial microstructures present in the flour and formation of a homogenous network. Loss in structural components present in the initial flours due to formation of covalent linkages have been reported for pea protein concentrate gum Arabic conjugates (Zha *et al.*, 2019b). Not many differences were observed between the microstructures of trypsin treated and papain treated conjugates. However, it was noticed that there was a considerable decrease in the size of the protein bodies as papain and trypsin were utilized for protein hydrolysis. These results are also consistent with the SDS-PAGE gels where a decrease in the molecular weight of the proteins with increased E/S ratios was also observed (Figure 4.2A). α-amylase treatment resulted in the formation of pores on the surface of the non-starch polysaccharide components which could be attributed to the presence of some reducing ends favorable for amylase to cleave the terminal glucose units resulting in increased porosity on the surface (Ren *et al.*, 2021). P15.6A samples also showed the formation of linkages between two continuous homogenous matrices. T17.7A, T19.4A and T21.7A showed some protein bodies being embedded on the surface of the starch granule which was attributed to the formation of covalent linkages between the α-amino terminal of the protein and the OH group present in the starch molecule. Such intimate associations between whey protein isolate and corn fiber gum conjugates were also observed by Yadav *et al.* (2012). Formation of protein-protein aggregates and protein-polysaccharide

conjugates were also noticed for P14.8A and T25.9 conjugates. In most of the conjugate mixtures, the molecules spread out as a result of thermal treatment thus reducing overall molecular aggregation and changing the spatial structure of the pea proteins. Similar homogenous structures were also reported for Maillard-induced rice protein-*Arthrobacter* exopolysaccharide conjugates (Zhao *et al.*, 2021).

4.4.5 Surface and functional properties analysis

4.4.5.1 Surface properties: zeta potential

The zeta potential (zP) of the raw, heated and hydrolyzed conjugates were analyzed at pH 4, 7 and 10. The zP at pH 4 was close to 0 for all the hydrolyzed conjugates studied. It was observed that the majority of the papain treated conjugates at pH 4 like P15.6, P18.7A, P14.8A had a net negative charge on the proteins (Table 4.2). On the other hand, only T17.7A had a net negative charge of -1.3 mV at pH 4. Moreover, at pH 4, PPEF, T0 and P0 had higher zP 8.2 mV, 8.3 mV and 8.6 mV than the conjugates. The zeta potential at pH 7 varied between -21.2 mV to -32.3 mV with the highest zeta potential recorded for P15.6 conjugates. Contrary to a previous report by Konieczny *et al.* (2020a), there were no significant differences between the zP of PPEF and the conjugate samples at pH 7. However, an increased negative charge was recorded for the protein enriched flour fraction. The zP at pH 10 was recorded between -28.7 mV and -36.6 mV with P15.6 conjugates showing the maximum zP -36.6 mV. There were no significant differences between the zP of the trypsin and papain treated conjugates at pH 10. However, at pH 10, the negative charge on the conjugates (-29.2 mV to -35.2 mV) was more pronounced as compared to the PPEF (-27.3 mV). Such decrease in the zeta potential of conjugates at higher pH values have been previously reported for pea protein-pea carbohydrate, canola protein-gum Arabic, whey protein-maltodextrin and oat protein-dextran conjugates in different research studies (Garcia-Amezquita *et al.*, 2014; Mookerjee *et al.*, 2023; Pirestani *et al.*, 2017; Zhang *et al.*, 2015).

The isoelectric point (pI) for proteins is the pH at which the net charge on a protein is 0 mV (Cleaves, 2022). Above the pI, the proteins carry a net negative charge and below it, they are associated with a positive charge (Mokni Ghribi *et al.*, 2015). Pea protein isoelectric point lies between pH 4 and pH 5 where there is no net charge on the protein surface (Lam *et al.*, 2018). Slight negative surface charges for some of the papain treated conjugates at pH 4 can be attributed to the exposure of negatively charged amino acids on the protein surface resulting from enzymatic

hydrolysis which can be a contributing factor to the overall negative zP values. Papain is less specific than trypsin and it is likely that papain activity resulted in unravelling of the protein core exposing an increased number of negatively charged amino acids leading to an increased negative charge (Amri *et al.*, 2012). Electrostatic shielding effect by starch/non-starch polysaccharide conjugated with the proteins also plays a major role in determining the overall protein surface charge (Yan *et al.*, 2022). A slight negative surface charge of T17.7A could be attributed to lesser interaction between the protein and polysaccharide chains resulting in decreased charge screening and an increased exposure of negative amino acids as compared to the other trypsin treated conjugates (Li *et al.*, 2016). Increased negative charges at pH 7 and 10 result from an inversion of surface charge from positive below the pI to negative at pH above pI (Novák *et al.*, 2016). On the other hand, the higher zP values recorded for trypsin and papain treated conjugates at pH 10 can be a result of the covalent attachment of the non-starch polysaccharides which might have lowered the overall electrophoretic mobility of the protein subunits (Zhang *et al.*, 2015).

4.4.5.2 Functional properties

4.4.5.2.1 Foaming properties: foam capacity & foam stability

Foam consists of gas bubbles dispersed within a liquid (usually water) or a solid matrix. These systems are thermodynamically unstable because of the elevated free energy at the gas-liquid interface, leading to processes such as coalescence and disproportionation that reduce the interfacial area and thereby stabilize the foam (Dickinson, 2010; Hall, 1996). The conjugates diffuse through the solution and adsorb to the gas-liquid interface, reducing surface tension. The protein-polysaccharide conjugates eventually undergo unfolding, with their hydrophobic segments aligning towards the gas phase and their hydrophilic portions facing the liquid phase. This reorientation leads to the formation of a cohesive, continuous film surrounding the gas bubbles, driven by interactions between the proteins and carbohydrates (Kinsella, 1981). Both foam capacity (FC) and foam stability (FS) of the raw PPEF, heated and hydrolyzed conjugates were analyzed at pH 4, 7 and 10.

Foaming capacity (FC) measures the extent to which proteins can generate interfacial area. It depends on the rate at which the conjugates or proteins migrate to the air-water interface, unfold, orient themselves, and develop a robust viscoelastic layer around the air bubbles (Akharume *et al.*, 2020). Overall, the foam capacity of both the untreated and hydrolyzed conjugates were significantly greater ($p < 0.05$) than that of the PPEF at pH 4, 7 and 10. However, some papain

treated conjugates like P14.8A (pH 4: 8.4%), P18.7A (pH 4: 6.7%; pH 7: 52.2%) showed lower foaming capacities than the PPEF (Figure 4.3). Overall, the trypsin hydrolyzed conjugates demonstrated a higher FC than the papain hydrolyzed conjugates at all the three pH values studied. The highest FC of 126.6% and 115% were recorded for T24A at pH 7 and P0 at pH 10 respectively. One interesting observation was that at pH 4 and 10, the untreated conjugates (T0: 104.7% at pH 4 & 106.4% at pH 10; P0: 75% at pH 4 & 115%) displayed higher FC as compared to the hydrolyzed ones. Zhao *et al.* (2021) demonstrated a two-fold increment in the foam capacity of rice protein-*Arthrobacter* exopolysaccharide conjugates as compared to untreated rice proteins at neutral pH, consistent with the findings observed in this study. Improvements in foam capacity have been discussed in Chapter III where pea proteins with moderate to low degrees of hydrolysis were conjugated with the carbohydrate fraction. Additionally, some conjugates with high degrees of protein hydrolysis, such as T24A (126.6%), T19.4A (116.7%), and T17.7A (113.3%) at pH 7, exhibited higher foam capacity compared to pea protein conjugates with low hydrolysis, as discussed in Chapter III.

Foam stability (FS) refers to the ability of a macromolecule to maintain the volume and thickness of a foam when subjected to external factors such as diffusion, drainage of lamella fluid, and mechanical disturbances (Lam *et al.*, 2018; Chapter III). Stable foams typically consist of cohesive interfacial films formed through hydrogen bonding and electrostatic interactions. These interactions result in the formation of intermolecular associations, creating a network structure that is both strong and exhibits high surface elasticity, allowing for some deformation (Wierenga *et al*., 2010). The FS of all the conjugates were significantly higher than the FS of PPEF at pH 7 (except P18.7A). However, the FS at pH 4 and 10 were not significantly different ($p < 0.05$). A different study has also reported an increase in foam stability for rice protein-Arthrobacter exopolysaccharide conjugates (Zhao *et al.*, 2021). Milk proteins Maillard conjugated with dextran and glucose have also been documented to form more stable foams as opposed to untreated milk proteins (Hiller *et al*., 2010). The untreated trypsin conjugates (T0) exhibited higher FS than all the trypsin hydrolyzed conjugates (Figure 4.3), whereas the P0 conjugates had higher FS at pH 7 and 10 as compared to the hydrolyzed papain treated conjugates. Amylase hydrolysis of the starch/non-starch polysaccharide fraction did not appear to affect the foam stability of the conjugates. Additionally, no significant differences in foam stability among the various conjugates were observed across the three pH values analyzed. In this research study, foam

stability (FS) at pH 4 was significantly improved compared to the use of only hydrolyzed pea proteins (Konieczny *et al.*, 2020).

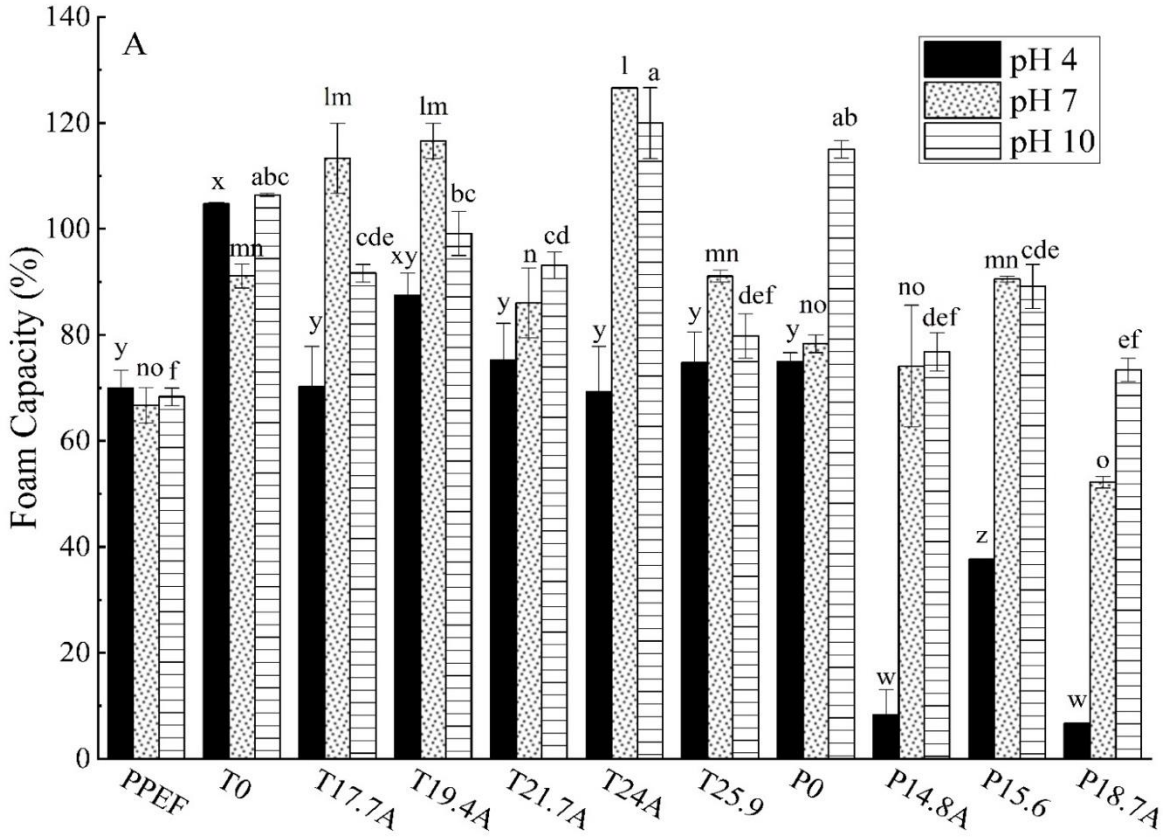
A
Foam Capacity (%)
pH 4
pH 7
pH 10
PPEF
T0
T17.7A
T19.4A
T21.7A
T24A
T25.9
P0
P14.8A
P15.6
P18.7A

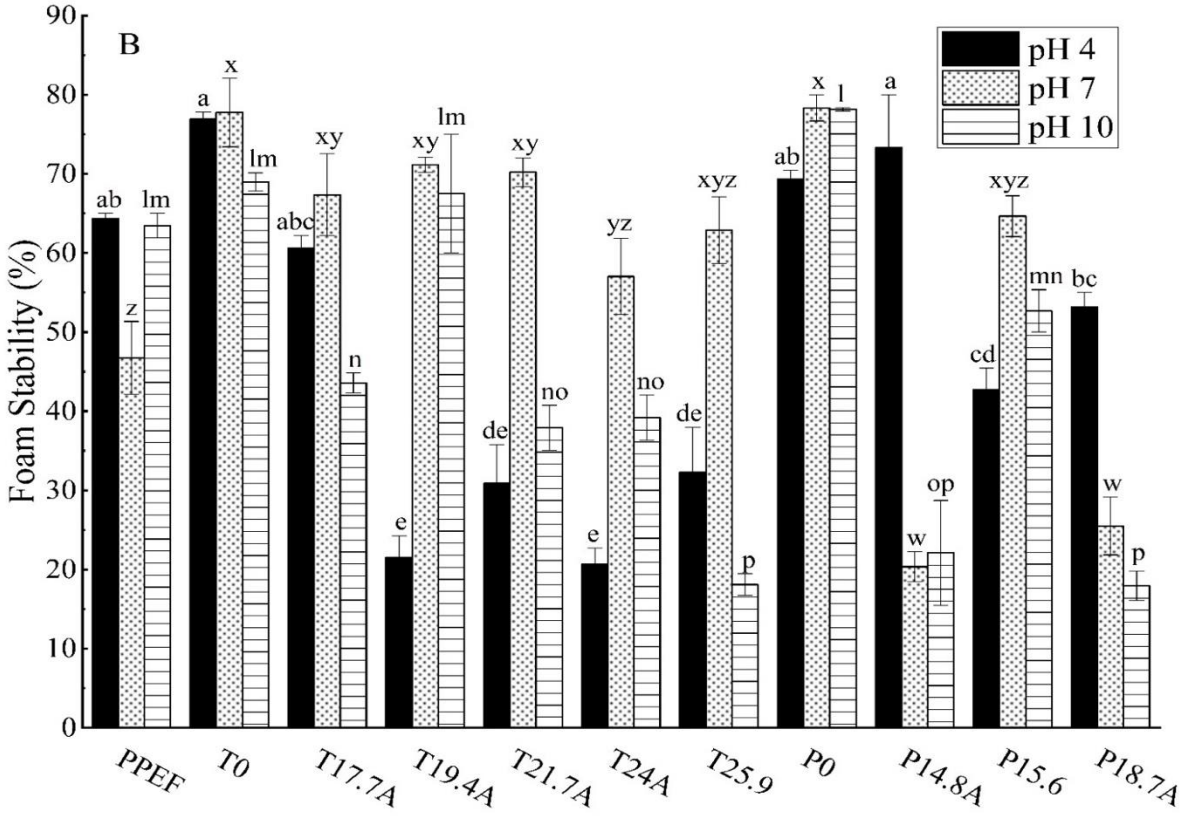
B
Foam Stability (%)
pH 4
pH 7
pH 10
PPEF
T0
T17.7A
T19.4A
T21.7A
T24A
T25.9
P0
P14.8A
P15.6
P18.7A

Figure 4.3. Comparative analysis of the foaming characteristics of conjugated proteins

Panel A and B show foam capacity (%) and foam stability (%), respectively, of raw, untreated, and hydrolyzed protein‑carbohydrate conjugates at pH 4, 7 and 10. A 1% (w/w) protein solution was prepared, and the pH was adjusted to 4.0, 7.0, and 10.0. Abbreviations: PPEF, pea protein ‑ enriched flour fraction; T0, trypsin control; T17.7A, conjugate samples hydrolyzed using trypsin to 17.7%DH and using amylase; T19.4A, conjugate samples hydrolyzed using trypsin to 19.4%DH and using amylase; T21.7A, conjugate samples hydrolyzed using trypsin to 21.7%DH and using amylase; T24A, conjugate samples hydrolyzed using trypsin to 24%DH and using amylase; T25.9, conjugate samples hydrolyzed using trypsin to 25.9%DH; P0, papain control; P14.8A, conjugate samples hydrolyzed using papain to 14.8%DH and using amylase; P15.6, conjugate samples hydrolyzed using papain to 15.6%DH; P18.7A, conjugate samples hydrolyzed using papain having to 18.7%DH and using amylase. Each value is the mean of triplicate measurements, the error bars represent the standard deviation and different superscript letters (a,b,c,d,e), (l,m,n,o,p) and (x,y,z) among the same ‑ colored bars represent significant differences between the groups ($p < 0.05$).

4.4.5.2.2 Emulsification properties: emulsion activity index & emulsion stability

An emulsion is created by mechanically mixing two immiscible liquids, leading to the formation of submicron droplets dispersed within a continuous phase (Hall, 1996). This system is thermodynamically unstable because the increased interfacial area between the two phases raises the system's free energy (McClements, 2015). Protein-starch conjugates are thought to migrate to the oil/water interface, where their amphiphilic properties drive them to adopt train, loop, and tail structures, forming a viscoelastic film that reduces interfacial tension (Alzagtat *et al.*, 2002). The properties of emulsions have been assessed using two techniques: the emulsion activity index (EAI) and emulsion stability (ES %) at pH values of 4, 7, and 10.

The emulsion activity index is a measure of the interfacial area that can be stabilized per unit weight of protein and has been established to be an important indicator of protein surface activity (Lam *et al.*, 2018; Pearce *et al.*, 1978). The EAI of the trypsin treated conjugates were found to be significantly higher than the PPEF at pH 4 ($p < 0.05$). For the papain treated conjugates however, except P14.8A, there were no significant differences in EAI ($p < 0.05$) between the conjugates. Between the two enzyme treatments, the trypsin treated conjugates showed an improved emulsion activity as compared to the papain treated conjugates (Table 4.3). T19.4A exhibited the highest EAI (24.0 m^2/g) at pH 10 among the trypsin treated conjugates, whereas the untreated papain control displayed the highest EAI (23.9 m^2/g) at pH 10. Similar improvement in the EAI of pea protein conjugated with xylo-oligosaccharides have been reported by Zhao *et al.* (2022). Zha *et al.* (2019) reported smaller droplet sizes for emulsions formed using pea protein-gum Arabic covalently linked Maillard induced conjugates thus demonstrating its enhanced emulsification properties. Improvements in EAI of low/medium hydrolyzed (using trypsin and papain) PPEF conjugated with pea carbohydrates hydrolyzed have also shown similar emulsifying activities (Chapter III).

Emulsion stability is a measure of the percentage of an emulsion that has not succumbed to separation into a separate cream and serum layer owing to various phenomenon like creaming, flocculation and coalescence (Lam *et al.*, 2018; Pearce *et al.*, 1978). The ES of all the trypsin treated conjugates were recorded to be significantly higher ($p < 0.05$) than the raw PPEF samples at pH 4, 7 and 10. Pea proteins hydrolyzed by papain showed significantly lower emulsion stability (15.5% to 65.5%) at pH 4 ($p < 0.05$) as compared to PPEF (66.5%). No significant differences in emulsion stability (ES) were observed between pH levels 4, 7, and 10. The highest emulsion

stability (ES) was observed for T21.7A at pH 7 (99.4%) among the trypsin-hydrolyzed conjugates, and for P14.8A (95.2%) among the papain-treated conjugates at pH 10 (Table 4.3). Unlike observations made in Chapter III, which did not show significant differences in emulsion stability (ES) between trypsin-treated and papain-hydrolyzed conjugates, this study found that proteins with high degrees of hydrolysis using trypsin exhibited significantly higher ES at pH 4 and 7 compared to pH 10, as opposed to the papain-treated conjugates (Chapter III). Significant improvements in the emulsion stability of pea protein isolate-maltodextrin conjugates and pea protein concentrate-gum Arabic conjugates have been reported in various studies (Zha *et al.*, 2019b; Zhang *et al.*, 2022). A substantial enhancement in the emulsion stability index of soybean protein isolates Maillard conjugated to sodium alginate has also been reported (Wang *et al.*, 2021).

Table 4.3. Emulsion activity index (m^2/g) and emulsion stability (%) of raw, untreated and hydrolyzed conjugates at pH 4, 7 and 10

Samples	Emulsion Activity Index (m^2/g)			Emulsion Stability (%)		
	pH 4	pH 7	pH 10	pH 4	pH 7	pH 10
PPEF	8.8 ± 1.6^{y}	18.1 ± 0.2^{lm}	21.5 ± 0.9^{a}	66.5 ± 1.5^{m}	81.3 ± 0.3^{d}	81.2 ± 0.4^{w}
T0	18.1 ± 0.6^{x}	21.3 ± 0.6^{l}	22.9 ± 0.0^{a}	96.4 ± 0.3^{l}	93.3 ± 2^{abc}	91.3 ± 0.4^{z}
T17.7A	21.1 ± 0.1^{x}	19.3 ± 1.8^{l}	21.9 ± 1.8^{lm}	93.1 ± 2.0^{l}	99.2 ± 0.8^{a}	91.5 ± 0.0^{yz}
T19.4A	21.3 ± 0.6^{x}	23.0 ± 1.2^{l}	23.2 ± 1.1^{a}	87.3 ± 7.2^{l}	99.0 ± 0.3^{a}	94.4 ± 0.8^{xy}
T21.7A	20.5 ± 0.4^{x}	21.7 ± 0.8^{l}	22.8 ± 3.1^{a}	92.0 ± 1.0^{l}	99.4 ± 0.7^{a}	94.8 ± 0.3^{x}
T24A	19.6 ± 0.5^{x}	20.8 ± 0.4^{l}	24.0 ± 0.9^{a}	79.9 ± 6.5^{lm}	98.9 ± 0.2^{ab}	93.4 ± 1.1^{xyz}
T25.9	21.4 ± 1.0^{x}	21.2 ± 0.2^{l}	22.6 ± 1.1^{a}	89.3 ± 1.2^{l}	97.3 ± 0.3^{ab}	92.8 ± 0.5^{xyz}
P0	8.9 ± 1.6^{y}	22.6 ± 0.6^{l}	23.9 ± 0.2^{a}	91.7 ± 0.7^{l}	93.5 ± 0.5^{abc}	90.5 ± 0.1^{z}
P14.8A	18.5 ± 2.4^{x}	14.0 ± 0.7^{mn}	17.8 ± 0.8^{a}	65.5 ± 1.5^{m}	85.8 ± 4.7^{cd}	95.2 ± 0.4^{x}
P15.6	10.5 ± 1.5^{y}	11.4 ± 1.5^{n}	21.1 ± 2.5^{a}	23.2 ± 0.2^{n}	89.8 ± 0.2^{bcd}	91.3 ± 0.7^{yz}
P18.7A	6.9 ± 1.4^{y}	9.3 ± 0.1^{n}	21.3 ± 0.7^{a}	15.5 ± 2.0^{n}	35.3 ± 1.3^{e}	85.5 ± 0.5^{v}

Note: Data represents the mean ± standard deviation of six samples (n = 6). Different superscript letters (a,b,c,d, x,y,z,l,m,n) within the same column represent significant differences between the groups ($p < 0.05$).

Abbreviations: PPEF, pea protein-enriched flour fraction; T0, trypsin control; T17.7A, conjugate samples hydrolyzed using trypsin to 17.7%DH and using amylase; T19.4A, conjugate samples hydrolyzed using trypsin to 19.4%DH and using amylase; T21.7A, conjugate samples hydrolyzed using trypsin to 21.7%DH and using amylase; T24A, conjugate samples hydrolyzed using trypsin to 24%DH and using amylase; T25.9, conjugate samples hydrolyzed using trypsin to 25.9%DH; P0, papain control; P14.8A, conjugate samples hydrolyzed using papain to 14.8%DH and using amylase; P15.6, conjugate samples hydrolyzed using papain to 15.6%DH; P18.7A, conjugate samples hydrolyzed using papain having to 18.7%DH and using amylase.

4.4.5.2.3 Water holding capacity and oil holding capacity

Water and oil holding properties is a measure of the amounts of oil and water retained in a food matrix, directly affecting the taste and mouthfeel of processed foods, and thereby significantly influencing its texture. Water/oil-holding capacity determines the amount of water or oil retained by one gram of the conjugate solution.

The WHC of all the conjugates were higher than the PPEF. Untreated conjugates exhibited higher WHC (T0: 2.4 g/g; P0: 2.1 g/g) than all the enzyme hydrolyzed conjugates (Figure 4.4). Among the two different enzyme treatments trypsin treated conjugates demonstrated an increased WHC (1.8 to 2.4 g/g) compared to the papain treated conjugates (1.5 to 2.1 g/g).

Improvements in the oil holding capacity were also observed for the conjugates compared to the raw protein enriched flour samples (Figure 4.4). Similar to the trend in WHC, the trypsin treated conjugates showed improved OHC (2.1 to 3.9 g/g) as compared to the papain treated conjugates (1.6 to 2.8 g/g). The highest OHC were also obtained for the untreated conjugates (T0: 3.9 g/g, P0: 2.8 g/g). Increased water and oil holding properties of pea proteins conjugated with guar gum and pea carbohydrates have been reported in separate research articles (Mookerjee *et al.*, 2023; Shen *et al.*, 2022). Significant improvement in the water and oil holding properties of wheat gliadin-amylopectin conjugates have also been reported by Yang *et al.* (2022).

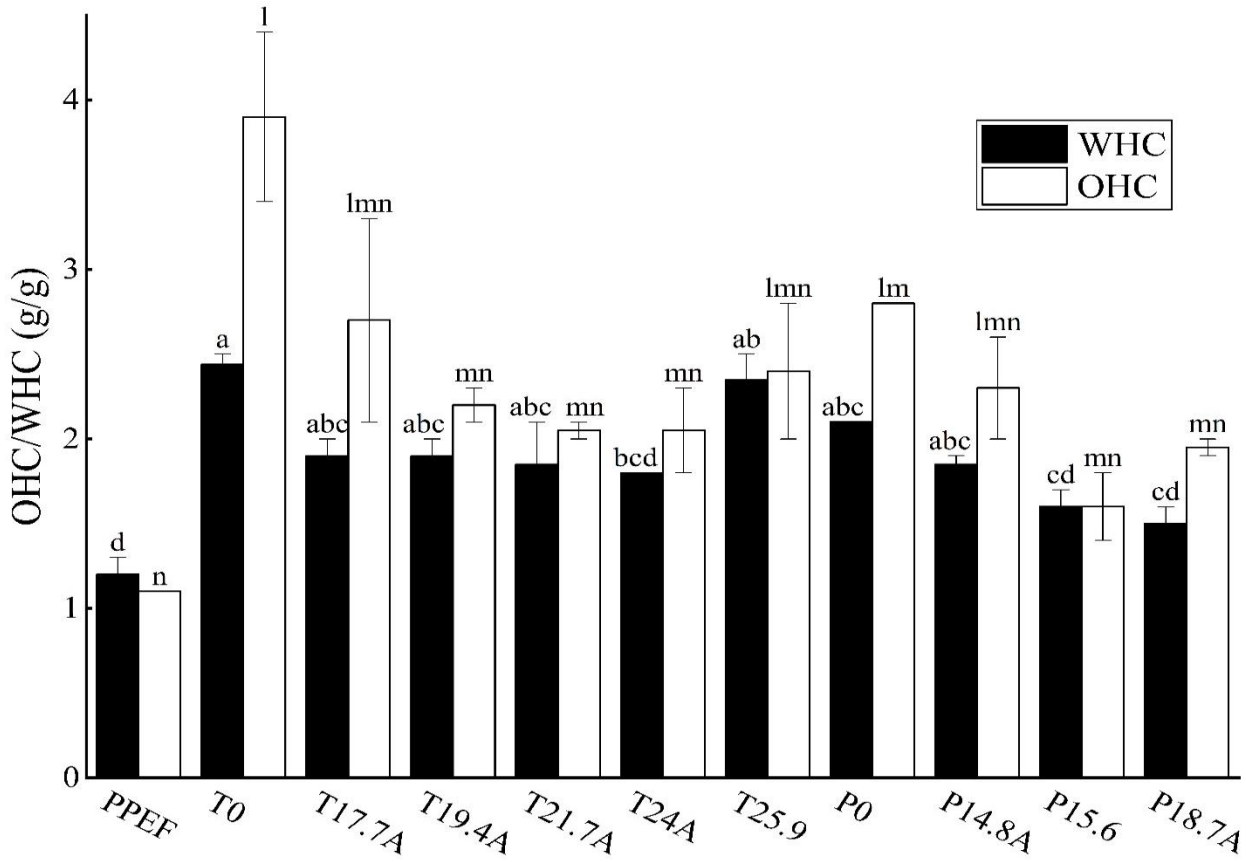

Figure 4.4. Comparative analysis of the water holding capacity (WHC) and oil holding capacity (OHC) of raw, untreated, and hydrolyzed protein–carbohydrate conjugates.

Abbreviations: PPEF, pea protein‐enriched flour fraction; T0, trypsin control; T17.7A, conjugate samples hydrolyzed using trypsin to 17.7%DH and using amylase; T19.4A, conjugate samples hydrolyzed using trypsin to 19.4%DH and using amylase; T21.7A, conjugate samples hydrolyzed using trypsin to 21.7%DH and using amylase; T24A, conjugate samples hydrolyzed using trypsin to 24%DH and using amylase; T25.9, conjugate samples hydrolyzed using trypsin to 25.9%DH; P0, papain control; P14.8A, conjugate samples hydrolyzed using papain to 14.8%DH and using amylase; P15.6, conjugate samples hydrolyzed using papain to 15.6%DH; P18.7A, conjugate samples hydrolyzed using papain having to 18.7%DH and using amylase. Each value is the mean of triplicate measurements, the error bars represent the standard deviation and different superscript letters (a,b,c,d) and (l,m,n) among the same‐colored bars represent significant differences between the groups ($p < 0.05$).

4.5 Discussion

This study primarily aimed to determine whether highly hydrolyzed pea proteins conjugated with starch or non-starch polysaccharides can achieve functional properties comparable to or better than those of raw PPEF samples or pea proteins with low to medium degrees of hydrolysis.

Close inspection of the SDS-PAGE gel and SEM images (Figure 4.2) revealed the presence of various complex compounds, including protein-protein aggregates, starch matrices, protein-starch conjugates, intact protein, intact starch, and other cell wall fragments. It is believed that the combined effect of these compounds plays a pivotal role in determining the functional properties of the conjugate mixtures. The surface charge, which directly affects the electrostatic double layer on the protein surface, is significantly shielded by the cell wall materials and bulky non-starch polysaccharide fragments covalently bound to the protein bodies at acidic pH ranges (McClements, 2015; Zha *et al.*, 2019a). A fine balance between steric repulsion and hydrophobic/van der Waals attraction is crucial for the formation of a viscoelastic film around air bubbles (in foams) and oil droplets (in emulsions), thereby preventing flocculation/coalescence and maintaining the integrity of the foam/emulsion system (Mookerjee *et al.*, 2023). Additionally, the bulky starch/cell wall matrix causes steric hindrance, preventing the protein bodies linked to the carbohydrate fractions from coming together (Mulcahy *et al.*, 2016; Wang *et al.*, 2012). This results in high emulsification properties of all the trypsin-treated conjugates and some of the papain-treated conjugates (P14.8A, P15.6) at pH 4, as well as improved foaming properties (T19.4A, T21.7A, T25.9, and P14.8A) at acidic pH. Reduced functional properties at acidic pH may still result from pea protein precipitation near its isoelectric point, as evidenced by the low zeta potential values listed in Table 4.2 (Mookerjee *et al.*, 2023; Zhao *et al.*, 2022).

The conjugation of starch or other non-starch carbohydrates introduces -OH groups into the protein system. The high degree of protein hydrolysis results in the extensive unraveling of the protein structure, thereby exposing many of the hydrophobic groups on the surface. Combined with the covalent attachment to highly hydrophilic starch, the conjugates exhibit increased amphiphilicity due to an improved balance between hydrophobic and hydrophilic groups on the protein. This enhances the interaction of the conjugates with water molecules and other macromolecules, such as polysaccharides and protein bodies, present in the food matrix. Additionally, extensive enzymatic hydrolysis shortens the polypeptide chain length, resulting in

increased molecular flexibility and dynamics. Due to the optimal hydrophilic-lipophilic balance, molecular size, and flexibility, the protein-polysaccharide conjugates and protein bodies can rapidly diffuse to the interface between the solvent and water. They arrange with the hydrophilic carbohydrate groups oriented towards the solvent phase and the hydrophobic amino acids directed towards the oil/air phase, thereby lowering surface tension and markedly enhancing foaming and emulsification properties (Kutzli *et al.*, 2021; McClements, 2015.; Mookerjee *et al.*, 2023). Table 4.2 reveals highly negative zP values, indicating improved solubility resulting from increased electrostatic repulsion. This improved solubility, coupled with optimal surface amphiphilicity and molecular conformation, likely contributes to the enhanced emulsification activity of the conjugates at pH 7 (except for P14.8A, P15.6, and P18.7A) and pH 10 (except for P14.8A, P15.6, and P18.7A), as well as improved foaming properties at pH 7 (except for P14.8A and P18.7A) (Cheetangdee *et al.*, 2014; Hiller *et al.*, 2010; Jiménez-Castaño *et al.*, 2007; Li *et al.*, 2016; Liu *et al.*, 2012).

The reduced foam capacities observed for the papain-treated conjugates can be attributed to the complete unraveling of the proteins, resulting in the formation of short-chain polypeptides conjugated with carbohydrates as discussed in Chapter III. These polypeptides could diffuse more effectively through the solution to the interface and align there, but their smaller size prevented them from stabilizing the interface for an extended period (Avramenko *et al.*, 2013; Konieczny *et al.*, 2020a). Therefore, high foam capacity was observed for the papain-treated conjugates at pH 7 and 10, but low foam stability (Figure 4.3). Papain is less specific in its action, leading to two primary effects (Lowe, 1970). Firstly, using high E/S ratios of papain (Table 4.1) extensively cleaved the proteins, producing a significant number of short-chain polypeptides, as evidenced by the SDS-PAGE gel stained with CBB (Figure 4.2A). Additionally, the available amino acid terminals were likely unable to form conjugates, resulting in shorter polypeptides or protein-protein aggregates. SEM images also indicated the presence of clustered protein bodies, which, due to their reduced molecular flexibility and mobility, did not exhibit improved functionality.

Both the untreated PPEF conjugates demonstrated improved functional properties across all tested pH values. Since no enzymes were used, the proteins remained mostly intact (Figure 4.2A). The conjugation with starch or non-starch polysaccharides produced conjugates of optimal size and flexibility. Consequently, they were better able to diffuse through the solution to the

interface, minimizing the thermodynamically unfavorable contact area and form a stable viscoelastic layer (Stone *et al.*, 2015).

Improvements in the water-holding capacity (WHC) of the conjugates can also be attributed to their conjugation with hydrophilic starch and non-starch polysaccharides, as well as the presence of cell wall fragments, which increased the number of -OH groups in the system. The water-binding properties of carbohydrates and dextrins through hydrogen bonding likely play a significant role in the increased WHC of the conjugates compared to the control PPEF samples as found in the study in Chapter III.

Significant improvements in oil-holding capacity (OHC) can be directly attributed to extensive protein hydrolysis, which exposed hydrophobic AA from the protein interior. These amino acids exhibited an enhanced capacity to interact with and bind oil molecules due to their hydrophobic interactions (Konieczny *et al.*, 2020a). The higher OHC observed in the untreated conjugates may be due to the short polypeptides' inability to entrap oil, as discussed by Goertzen and his team (Goertzen *et al.*, 2021a).

4.6 Conclusion

Pea protein-enriched flour was enzymatically hydrolyzed using trypsin and papain, then conjugated with the available starch and non-starch polysaccharides in the flour through heat treatment at 90 ℃. SDS-PAGE and scanning electron microscopy revealed a variety of compounds, including protein-protein aggregates, protein-starch conjugates, heterogeneous starch gels, non-starch carbohydrates, and smaller protein bodies. An increase in surface charge was recorded at pH 7 and 10, indicating higher solubility. Most trypsin-treated conjugates showed improved foaming capacity at pH 4, 7, and 10, and foam stability at pH 10 compared to the raw PPEF samples. These conjugates also exhibited improved emulsification properties across all three pH values tested. Conversely, papain-treated conjugates demonstrated improved emulsion stability at pH 7 and 10. Among them, P14.8A exhibited enhanced foaming capacity at pH 4 and stability at pH 7 and 10, while P15.6 showed increased foam stability at pH 7 and 10. Both heat treated unhydrolyzed (no enzymes) conjugates displayed improved foaming and emulsification properties, with trypsin-untreated samples showing the highest water and oil holding capacities. Enhanced foaming at acidic pH suggests potential applications in sports drinks and carbonated beverages for muscle recovery and nutritional benefits. Improved emulsification properties can be

useful in plant-based mayonnaise, salad dressings, or dairy-based beverages to enhance creamy texture and prevent ingredient separation. Enhanced water and oil holding capacities can benefit the processed meat industry by improving the juiciness, sponginess, and overall mouthfeel of alternative burger patties or sausages.

Various studies have highlighted the improvement in the techno-functional properties of both intact and low-degree hydrolyzed pea proteins. The study in Chapter III demonstrated that low to moderate degrees of protein hydrolysis followed by carbohydrate conjugation improve pea protein techno-functionality. This study successfully established that even extensive degrees of proteolysis positively impacted techno-functionality when proteolysis is coupled with conjugation with the available starch, non-starch carbohydrates, and cell wall materials present in the flour. Thus, it is evident that even after the complete unraveling of the protein structure and the formation of smaller peptides, conjugation with carbohydrates improved functional properties, likely due to optimal size and surface amphiphilicity. Since this method does not involve the use of external materials or specialized chemicals, but simply enzymes and heat treatment it offers a cost-efficient and advantageous strategy for developing functionally enhanced products utilizing legume proteins. The subsequent study will explore the possibility of pea protein conjugation to externally added pea starch. It was hypothesized that adding the starch fraction from air classified pea flours and enzymatically hydrolyzing them would lead to the formation of more dextrin units which would have increased number of available carbonyl (-OH) groups to facilitate the Maillard reaction. These protein-dextrin/starch conjugates would have improved functionality which can be utilized in different food applications like beverages, emulsions and chocolate bars. Future studies could also explore creating prototype foods using the best conjugates obtained in this research. If successful, this approach could be scaled up for industrial production of functional ingredients, which can be added to processed foods to enhance their sensory and textural attributes.

4.7 Connection to next study

In the first and second studies, the extent of conjugation between the residual starch and other non-starch polysaccharides present in the fine fraction of pea flour was investigated. Significant improvements in functionality were observed at pH 4, with slight enhancements at pH 7 and 10. However, given the low starch content of the pea protein-enriched fraction (PPEF), the impact of starch hydrolysis on the functional properties could not be fully evaluated. It was

hypothesized that the addition of hydrolyzed starch (coarse fraction) followed by heat treatment would further promote conjugation due to the availability of a greater number of hydroxyl (-OH) groups. Enhanced Maillard conjugation was expected to improve amphiphilicity, thereby further enhancing the functional properties of the resulting conjugates. Consequently, in the subsequent study, a starch-enriched fraction was utilized to examine the impact of starch hydrolysis followed by Maillard conjugation on the functional properties of the proteins, with the aim of determining whether this approach could further enhance the functionality of pea proteins.

Additionally, insights from the first two studies suggested that heating a mixture of pea protein and starch would result not only in the formation of protein-starch conjugates but also in the creation of various molecular species within the conjugate mixtures. These species included intact or hydrolyzed protein-protein aggregates, starch gels, polypeptides, and dextrins of diverse molecular weights, as well as protein bodies exhibiting a range of molecular weights and structural conformations. Therefore, the subsequent study also focused on analyzing the molecular weight distribution and structural characteristics of the compounds produced in these conjugates.

CHAPTER V

5 Improvement In Functional Properties Of Enzyme-Modified Air Classified Pea Proteins By Maillard Conjugation With Hydrolyzed Pea Starch Obtained As By Products

5.1 Abstract

The present study investigated the impact of protein-starch conjugation on different protein techno-functional and structural properties. Protein in the pea air-classified protein-rich flour and starch in starch-rich flour were enzymatically hydrolyzed at various degrees using protease and amylase, and the protein-starch blend was prepared by simply stirring them. The blended samples were then heat-treated to form conjugates through Maillard Reactions. The solubility of hydrolyzed conjugates was slightly lower than control (solution of the fine and coarse fraction mixed without any heat treatment), yet it maintained moderately high (31.6% – 46.8%) solubility. Surface charge analysis showed highly negative zeta potential (zP) values across all conjugates at pH 7 and 10; whereas zP at pH 4 was positive. The foam capacity (FC) and emulsion stability (EAI) also showed notable enhancements compared to the controls. FC of the conjugates at pH 4 reached 241.1 %, while the EAI at pH 7 achieved 35.1 m^2/g. The water holding capacity of the heated conjugates was notably high (2.1 g/g), attributed to the presence of hydrophilic starch granules, which increased the number of hydroxy groups, enhancing water-binding properties. Additionally, the oil holding capacity of conjugates between highly hydrolyzed protein and medium-degree hydrolyzed starch, was significantly improved (1.8 g/g). The structural analyses using SDS-PAGE, size exclusion chromatography, scanning electron microscope imaging, Fourier transform IR spectroscopy, and fluorescence spectroscopy, showed that the bulkiness of the starch molecules in the conjugates lowered the degrees of protein aggregation, and the structural change in proteins altered the overall structure and surface properties, leading to the enhancement in functionality.

5.2 Introduction

Proteins are one of the essential macronutrients, playing a crucial role in numerous bodily functions such as the development and maintenance of muscle tissue (Carbone *et al.*, 2019), transportation of substances across cell membranes, synthesis, repair, and modification of genetic materials like DNA and RNA (Chatterjee *et al.*, 2017), and functioning as enzymes (Robinson, 2015) and hormones, among other roles. For omnivorous human being, proteins have been mainly supplied from animal sources. Animal proteins are also very important as techno-functional ingredients in foods, such as emulsifier. Recently, due to the anticipated growth in global population, more sustainable plant proteins, particularly those derived from legumes, have gained significant popularity as a nutritious alternative to animal proteins. Globally legume proteins are increasingly being utilized in the food industry to enhance functional properties and add nutritional value to food products. However, plant proteins encounter several limitations as techno-functional ingredients due to various factors. For example, plant proteins, including those from peas, consist of a mixture of different protein fractions, each with its own isoelectric point (pI), rather than a single, uniform pI (Adal *et al.*, 2017). Additionally, their techno-functionality is constrained by other factors, such as the presence of plant-specific residuals known as antinutritional factors, intrinsic protein structural characteristics, the complex association of protein bodies with other components within the plant matrix, the harsh commercial extraction processes that can denature protein structures, and poor solubility in water (Mookerjee *et al.*, 2023; Nikbakht Nasrabadi *et al.*, 2021).

To mitigate these limitations, it is essential to modify the physicochemical properties of proteins to improve their functionality as ingredients in food systems. "Protein modification" involves altering the molecular structure or specific chemical groups of proteins through various techniques to enhance their nutritional values, techno-functionalities, and bioactivities (Nikbakht Nasrabadi *et al.*, 2021). Protein modification methods can generally be categorized into physical, chemical, and biological approaches. Among the biological methods, enzymatic modification is particularly important due to its ability to operate under mild temperature and pressure conditions. These methods are easier to control, demonstrate high substrate specificity, and generate minimal toxic byproducts, ensuring that other components in the food system remain unaffected (Aluko *et al.*, 2003; Mookerjee *et al.*, 2023; Tavano, 2013). Plant proteins are typically hydrophobic in nature

and protease treatments can modulate the exposure of buried hydrophobic amino acids from the protein core, thereby altering surface hydrophobicity (Panyam *et al.*, 1996). Additionally, when combined with localized hydrophilic regions on the exterior, enzymatically modified proteins can exhibit some degree of amphiphilicity. This structural modification leads to improvements in their techno-functional properties, including enhanced solubility, foaming, emulsification, and water and oil-holding capacities (Achouri *et al.*, 1998; Avramenko *et al.*, 2013; Goertzen *et al.*, 2021a; Konieczny *et al.*, 2020a; Mokni Ghribi *et al.*, 2015).

On the other hand, starch granules are generally hydrophilic. Starch is a main component of legume, and naturally preparations of legume, such as flour, protein-concentrate, and protein-isolates, contain varied amounts of starch. Therefore, conjugating hydrophilic starch with hydrophobic protein molecules is expected to further enhance amphiphilicity. There are several methods available to conjugate starch and proteins: such as chemical conjugation, linker addition, strong electrostatic interaction, and glycation (Nikbakht Nasrabadi *et al.*, 2021; Schmitt *et al.*, 2011; Warnakulasuriya *et al.*, 2018; Zhang *et al.*, 2015). For food purposes, utilization of external chemical agents can be undesirable. Electrostatic interaction is reversible and may not stably maintain the conjugates. Glycation leads to the formation of irreversible covalent bonds between protein and polysaccharide molecules (Kutzli *et al.*, 2021a). Thus, glycation is particularly promising and highly favorable for food applications. This approach does not require the use of harmful chemicals and generates no by-products, making it an excellent choice for plant protein modification in terms of consumer preferences, clean labeling, and commercialization (Nikbakht Nasrabadi *et al.*, 2021).

The Maillard reaction, a naturally occurring glycation process, is the most commonly employed method for attaching hydrophilic polysaccharides or dextrins to proteins, resulting in the creation of highly amphiphilic protein-carbohydrate conjugates (Arena *et al.*, 2017; de Oliveira *et al.*, 2016). When a mixture of proteins and carbohydrates are heated, a condensation reaction occurs between the -OH groups of reducing sugars and the amine moiety of terminal α-amino acids and of ε-group of lysine resulting in the formation of a Schiff base, a thermodynamically unstable compound which spontaneously rearranges into a more stable aminoketoses commonly known as the Amadori products (Kutzli *et al.*, 2021b). These Amadori compounds are further degraded by dealdolization and Strecker degradation to melanoidins. Depending upon the nature of the protein and polysaccharide interacting, their concentration, reaction time and temperature,

a large amount of highly reactive compounds are produced some of which react further to form the advanced stages of the Maillard reaction products (de Oliveira *et al.*, 2016; Kutzli *et al.*, 2021b).

It is believed that the covalent bonds formed between these two macromolecules during the Maillard reaction are highly stable against fluctuations in pH, temperature, and ionic strength, making the conjugates resilient to changes in processing conditions (Dickinson *et al.*, 1991). Mu *et al.* (2011) reported a significant increase in the solubility of soy protein isolates (SPI) conjugated with acacia gum (AG) as compared to native SPI at the same pH values. A significant increase was also reported in the emulsifying properties like emulsifying activity index (EAI) and emulsion stability index (ESI). Similarly, Niu *et al.* (2011) reported an improvement in the solubility and emulsifying properties of wheat germ protein (WGP) glycated with different saccharides like xylose, glucose, lactose, dextran and maltodextrin. A study by Yadav *et al.* (2012) demonstrated the capability of forming fine emulsions with enhanced stability by corn fiber gum-milk protein conjugates. In a separate study, it was reported that WPI-dextran conjugates had enhanced heat stability, significantly improved solubility over a wide pH range and emulsifying ability as compared to the native WPI (Zhu *et al.*, 2010). This study investigated the influence of conjugation between proteins and starch using pea proteins and starch. Air classification is a widely used as a dry processing technique for extracting protein-rich fractions from milled pea flours, and the by-product of this process is a starch-rich fraction, which is of lower value and primarily used in the feed industry. The first and second studies conjugated protein with starch in the air-classified protein-rich flour (PPEF). PPEF contains less than 2% starch, making the conjugation under the conditions with high protein to starch ratios. It showed improvements in the techno-functionality of protein-rich fraction. The main objective of this research was to complement the proteolyzed protein-enriched fraction in PPEF with the amylolyzed air-classified starch-rich fraction (*i.e.*, additional starch), followed by heat-induced Maillard conjugation to improve the techno-functional properties of the resulting conjugates. This facilitated conjugation under conditions with high starch content. This study further conducted a detailed study of the different molecular species present in the hydrolyzed pea protein fine fraction and coarse fraction conjugate mixtures like protein-starch conjugates, intact/hydrolyzed protein-protein aggregates, starch gels, polypeptides and dextrins of various molecular weights and structural confirmations.

5.3 Materials and methods

5.3.1 Materials

Pea protein enriched flour (PPEF) and pea starch enriched flour (PSEF) were kindly donated by AGT Foods (Saskatoon, SK, Canada). Trinitrobenzenesulfonic acid (TNBS), trypsin (10,600 units/mg), papain (1.5 – 10 units/mg solid), pepsin (≥250 units/mg solid), Savinase (≥16 U/g), α-amylase from *Aspergillus oryzae* (~30 U/mg) and α-amylase from *Bacillus licheniformis* (>500 units/mg) were purchased from Sigma-Aldrich Canada (Oakville, ON, Canada). Fuchsine sulfite staining solution was purchased from Fisher Scientific (Ottawa, ON, Canada). All chemicals used in this study were purchased from Fisher Scientific and VWR (Edmonton, AB, Canada), and of ACS grade or above. The water used in this research was purified using a Millipore Milli-Q™ water purification system (Millipore Corp., Milford, MA, USA).

5.3.2 Protein-starch mixture preparation for conjugation reactions

Protein and starch solutions (2% w/v based on protein/starch amounts in the PPEF/PSEF) were dispersed in 1 L of 50 mM sodium phosphate buffer solution (pH 7 for PPEF solutions and pH 6.5 for PSEF solutions). Starch solutions were heated at 80°C for 30 min to gelatinize the starch fraction. Thereafter, the solution was cooled, and the pH was readjusted to the appropriate pH of enzymatic activity. PPEF proteolysis and PSEF amylolysis were conducted using trypsin from porcine and α-amylase from *Bacillus licheniformis*, respectively, in separate reactions. The reaction mixtures were incubated at 37°C and 60°C for a specified period to obtain certain degrees of protein/starch hydrolysis in each reaction. Three different degrees of hydrolysis for the protein (DH) and starch (DE) fractions were employed for this study. Degrees of protein hydrolysis (DH) between 2% and 6% were classified as low protein (LwP), 8% to 15% as medium protein (MdP), and above 20% as high protein (HiP) as discussed in Chapter III. For starch hydrolysis, a DE of less than 5% was designated as low starch (LwS), 20% to 30% as medium starch (MdS), and above 40% as high starch (HiS). The methods to determine the degrees of hydrolysis are summarized later in the following sections. Immediately after incubation, the enzymatic reactions were terminated by a heat shock by plunging the vessels in an already boiling (<100°C) water bath for 15 min. The PPEF and PSEF hydrolysates were mixed at ratio of 1:1 (protein:starch), and the mixture was heated at 90°C for 30 min to induce Maillard reaction. After 30 min of heat treatment, the solution was immediately cooled to 4°C to stop Maillard Reactions. The mixture was then

spray-dried. Controls were also run in parallel where no enzymes were added but followed all the procedures for enzymatic hydrolysis.

Prepared samples are abbreviated as follows: Hconj, heated raw PPEF and PSEF without any enzyme treatment. The combinations of degree of hydrolyzed protein/starch are abbreviated with Hi, Md, Lw for high, medium, and low, respectively, and PPEF and PSEF were represented with P and S, respectively: *i.e.*, HiP-MdS, MdP-MdS, LwP-MdS, HiP-LwS, MdP-LwS, LwP-LwS, HiP-HiS, MdP-HiS and LwP-HiS. This naming and degree of hydrolysis of each preparation are summarized in Table 5.1.

5.3.3 Proximate composition analysis

Proximate analysis of the samples was measured according to AOAC Official Methods 925.10 (moisture), 923.03 (ash), 920.85 (lipid), 997.09 (crude protein by using %N×6.25) and AACC Method 76-13.01. The amounts of protein, lipid, moisture, ash, and total starch were subtracted from the total amount, and this remaining amount was considered as other carbohydrates. The details were described in detail in Section 3.3.2.

5.3.4 Determination of the degree of hydrolysis (DH) of the protein fraction

The degree of protein hydrolysis (DH) was analyzed using the Adler-Nissen (Adler-Nissen, 1986) method with slight modifications as reported by Avramenko *et al.* (2013). A detailed description of the procedure has been provided in Section 3.3.5.

5.3.5 Determination of the degree of hydrolysis (DE) of the starch fraction

The DE was determined using the 3,5-Dinitrosalicylic acid method (Miller, 1959). 1 mL aliquot of the blank and hydrolyzed samples were transferred to 0.5 ml Milli-Q water and 1.5 ml DNS reagent was added. For acid hydrolyzed samples, 0.25 mL of the reaction mixture was diluted with 2 ml water to which 0.15 ml DNS was added. The solutions were vortexed for 10 sec and immediately transferred to a hot water bath at 100°C for 5 min. Immediately after that, the test tubes were taken out and plunged into an ice bath for 10-15 min for colour development. The tubes were then left to reach room temperature after which the absorbance was read at 540 nm using a spectrophotometer (Genesys 10UV Scanning Thermo Scientific, USA). A standard curve was also prepared using glucose. A series of concentrations (0.03, 0.04, 0.06, 0.08, 0.10, 0.30 and 0.5 mM) of glucose solutions were also prepared to determine the glucose equivalents of the hydrolyzed

starch fraction. The S was determined as the ratio of the number of reducing ends measured upon enzymatic hydrolysis divided by the number of reducing ends obtained after total acid hydrolysis multiplied by appropriate dilution factors and glucose equivalents.

5.3.6 Structural, molecular weight and functional groups characterization

5.3.6.1 Microstructure using SEM

The sample powder was uniformly adhered to the observation table with a conductive double-sided tape, and then gold-plated with a Hitachi E-1010 ion sputtering coater. A field emission scanning electron microscope Hitachi SU8010 SEM was used for observation under the condition that the acceleration voltage was 5 kV. Samples were observed under magnifications of 3,000x, and 10,000x.

5.3.6.2 Molecular weight distribution using high-performance size exclusion chromatography (HP-SEC)

Molecular weight distribution was carried out as previously described (Habinshuti *et al.*, 2021). Each conjugate was dissolved in 0.05M NaOH, centrifuged at 14,000 RPM for 10 minutes, vacuum filtered at 45°C for 60 min to concentrate the samples. Thereafter, the solution was further filtered through 0.22 μm filters to remove any insoluble materials and fractionated by an AKTA pure HPLC (GE Healthcare, Toronto, ON) on a Superdex^{TM} 200 10/300 GL columns (GE Healthcare, Toronto, ON) at a concentration of 0.5 mg/mL, respectively. The elution solution was 0.05 M NaOH at a flow rate of 0.5 mL/min. The absorbance of the effluent was monitored at 280 nm, 304 nm and 420 nm. The area under the curve of the peaks in the chromatogram was further evaluated using the UNICORN^{TM} software (GE Healthcare, Toronto, ON). The retention time of the following standards- bovine thyroglobulin (670,000 Da), γ-globulin (158,000 Da), ovalbumin (44,000 Da), myoglobin (17,000 Da) and vitamin B12 (1350 Da) were utilized to prepare a molecular weight calibration to roughly determine the molecular weight of conjugates/aggregates. The area under the curve of the peaks at different retention times and at wavelengths 304 nm and 280 nm were expressed as a ratio (R_C).

5.3.6.3 Sodium dodecyl sulfide polyacrylamide gel electrophoresis (SDS-PAGE)

The polypeptide profiles of the hydrolyzed PPEF, and confirmation of the size shift of the conjugates before and after conjugation were determined by sodium dodecyl sulfide polyacrylamide gel electrophoresis (SDS-PAGE) using the Laemmli method (Laemmli, 1970).

For confirmation of the size shift of the conjugates before and after the reaction, as well as determination of glycosylated proteins, the gels were stained using a Fuchsine-sulfite staining method as demonstrated by Zacharius *et al.* (1969). The conjugated protein bands were quantified using ImageJ® (National Institutes of Health, Bethesda, USA) using the digitized image of the gel.

5.3.6.4 Functional group analysis using Fourier transform infrared- total attenuated reflection spectroscopy (FTIR-ATR) analysis

The Renishaw inVia™ Reflex Raman Microscope (Renishaw, Gloucestershire, UK) was used to record the infrared spectra of each sample using an IlluminatIR II Fourier transform infrared spectroscopy (FTIR) microscope accessory (Smith's Detection, USA) having a 36 × diamond ATR objective lens. Measurements were performed within the wavelength range of 4000 – 800 cm^{-1} with 4 cm^{-1} resolution. The data analysis was performed using Origin software (OriginLab, Northampton, MA, USA).

5.3.6.5 Quenching of aromatic amino acids using fluorescence intensity spectra

The intrinsic fluorescence spectra of the Maillard Reaction Products (MRPs) were investigated by a FluoroMax-4 spectrophotometer (Horiba Jobin Yvon Inc., USA) at room temperature by using the method of Sun *et al.* (2023). Solutions of MRPs were made at a concentration of 0.2 mg/mL by dispersing samples in MilliQ water, the pH was adjusted and maintained at 7.0 using dilutants such as HCl and NaOH. The spectra were collected with an excitation of 295 nm and emission ranged from 375 to 550 nm to determine the quenching of tryptophan. Additionally, the excitation wavelength was also set at 347 nm, and the emission spectra were recorded from 360 to 600 nm at a constant slit of 5 nm to determine the extent of fluorescent compounds produced.

5.3.7 Monitoring of amadori compound formation and browning

The Amadori compound formation was monitored according to the method outlined in Chapter III. The procedure has been elaborately described in Section 3.3.7.

5.3.8 Surface and Functional properties analysis

5.3.8.1 Surface charge

The zeta potential (zP) of the conjugates was determined at pH 4, 7, and 10 according to the procedure in Chapter III which has been elaborately described in section 3.3.9.1.

5.3.8.2 Protein solubility

Protein solubility was measured by dispersing 50 mg of protein in 25 ml MilliQ water, adjusting the solution to pH 7 and letting it stir overnight at 4°C. The solution was then centrifuged at 4200 × *g* for 10 min at room temperature. The protein content of the solution and the supernatant after centrifugation were determined using the modified Lowry method. The protein solubility was expressed as follows:

$$\text{Protein solubility (\%)} = \frac{\text{Protein content of supernatant (g)} \times 100}{\text{Protein content in the solution (g)}}$$

……(5.1)

5.3.8.3 Starch solubility

Starch solubility was measured using the Phenol-Sulfuric acid method using glucose as standard. In brief, about100 mg of the sample was dispersed in 10 mL MilliQ water in a 15-mL centrifuge tube, boiled at 95°C for 30 min and centrifuged at 6200 × g for 15 min. The supernatant was analyzed for the presence of -CHO groups spectrophotometrically at 490 nm using a spectrophotometer (Genesys 10UV Scanning Thermo Scientific, USA). Percentages of solubilized starch was expressed as follows:

$$\text{Starch solubility (\%)} = \frac{\text{Weight of supernatant (g)} \times \text{concentration} \times \frac{162}{180} \times 100}{\text{Sample weight (Dry basis)}}$$

……(5.2)

5.3.8.4 Foaming properties- foaming capacity (FC) and foam stability (FS)

The foaming capacity and foam stability of samples were measured at three different pH (4, 7, 10) based on the method reported in Chapter III. An elaborate description of the method has been provided in section 3.3.9.2.

5.3.8.5 Emulsifying properties - emulsion activity index (EAI) and emulsion stability index (ESI)

The emulsion activity (EAI) and stability indices (ESI) for untreated and enzyme-treated PPEF conjugates were conducted based on the method of Pearce and Kinsella (1978), and as described in detail in Chapter III. A detailed description of the method has been provided in section 3.3.9.3.

5.3.8.6 Water and oil holding capacities (WHC/OHC)

The water and oil holding capacities for untreated and enzyme-treated PPEF conjugates were conducted based on the method in Chapter III. The method has been described in detail in section 3.3.9.4.

5.3.9 Statistical analysis

The proximate composition data of the PPEF are presented as the mean ± standard deviation of triplicate measurements. All enzymatic hydrolysis and conjugation reactions were conducted in biological duplicates. Proximate composition, degree of hydrolysis (DH), surface properties, and functional properties of each biological duplicate were measured in triplicate, and the data are reported as the mean ± standard deviation of six values (calculated from duplicates, each measured in triplicate, n=6). Statistical analysis for surface charge, foaming and emulsification properties were performed using the Two-way ANOVA with pH and sample as the fixed variables followed by Tukey mean comparison as the post-hoc test. Significance is indicated at $p < 0.05$. All other statistical analysis were performed using the One-way ANOVA followed by Tukey means comparison post-hoc test for mean comparisons between different enzymatic reactions. Significance is indicated at $p < 0.05$.

5.4 Results

5.4.1 Proximate composition

The composition of proteins, lipid, moisture, ash total starch and other carbohydrates of the PPEF are 55.0% ± 0.0%, 1.0% ± 0.3%, 1.2% ± 0.0%, 5.4% ± 0.1%, 3.1% ± 0.2%, and 37.3% ± 1.0%, respectively. The total protein, moisture, ash, lipid and starch composition of the PSEF were 13.0%±0.0%, 8.0%±0.1%, 1.4%±0.1%, 0.2%±0.1% and 70.0%±1.6% respectively. The

protein composition of the conjugates was lower than the PPEF. It is speculated that the formation of conjugates led to a new molecular species after rearrangement reactions along with mechanical loss during the spray drying process.

5.4.2 Influence of enzyme/substrate ratio on the degree of protein and starch hydrolysis

Three different combinations of trypsin and amylase enzyme-to-substrate (E/S) ratios were employed to achieve various degrees of hydrolysis for the protein (DH) and starch (DE) fractions. A protein degree of hydrolysis (DH) between 2% and 6% was classified as low protein (LwP), 8% to 15% as medium protein (MdP), and above 20% as high protein (HiP). For starch hydrolysis, a DE of less than 5% was designated as low starch (LwS), 20% to 30% as medium starch (MdS), and above 40% as high starch (HiS). The enzyme-to-substrate ratio and reaction time significantly influenced the degrees of protein and starch hydrolysis in the conjugates. It was observed that using a low E/S ratio (1:5000) for a short duration (30 minutes) resulted in a lower degree of protein hydrolysis (less than 5%) compared to a higher E/S ratio. Additionally, for the same E/S ratio, extending the enzymatic reaction time to 60 minutes led to a higher degree of protein hydrolysis (greater than 20%) compared to a shorter duration (30 minutes). A similar increase in DH over time was found for pea proteins hydrolyzed with trypsin (Chapter III). Furthermore, increases in DH with higher E/S ratios and longer reaction times have also been observed for lentil protein hydrolysates (Avramenko *et al.*, 2013). The increased cleavage of peptide bonds resulting in the formation of short-chain polypeptides is thought to contribute to the higher DH observed with prolonged reaction times (Haslaniza *et al.*, 2010). Similarly, for amylase treatment, both the E/S ratio and reaction time affected the rate of starch hydrolysis. A combination of a low E/S ratio (1:1000) and a short duration (15 minutes) resulted in a low degree of starch hydrolysis (less than 5%), similar to the findings for protein hydrolysis (Table 5.1). Moreover, for the same reaction time, a higher amylase E/S ratio (1:250) produced a greater degree of starch hydrolysis (greater than 40%) compared to a lower E/S ratio (1:1000).

Table 5.1: Enzyme: substrate (E/S) ratio and time of enzymatic (trypsin, α-amylase) activity to achieve various degree of hydrolysis of the protein fraction (DH %) and starch fraction (DE %); surface charge of the raw, untreated and hydrolyzed conjugates at pH 4, 7 and 10; Densitometry analysis of controls, heated and hydrolyzed conjugates stained using fuchsin sulfite computed using ImageJ software reported as % intensity.

	Trypsin		α-amylase					Surface charge (zP)			Fuchsin stain (% Intensity)
Samples	E/S	Time (min)	E/S	Time (min)	DH (%)	DE (%)	Protein (d.b. %)	pH 4	pH 7	pH 10	
Controls					-	-	36.8±0.1	$4.0±1.5^{ab}$	$-26.6±0.9^{efgh}$	$-30.6±2.6^{h}$	8.5
Hconj					-	-	35.3±0.0	$8.4±0.3^{a}$	$-19.5±0.6^{c}$	$-30.9±0.4^{h}$	8.64
HiP-MdS	1:1000	60	1:1000	60	22.3±0.3	25.9±1.0	29.8±0.0	$1.6±0.5^{b}$	$-21.2±0.1^{cdef}$	$-30.7±1.5^{h}$	8.61
MdP-MdS	1:2500	60	1:1000	60	12.7±2.7	29.9±0.6	30.0±0.3	$3.8±0.5^{ab}$	$-25.2±2.9^{cdefgh}$	$-31.4±2.7^{h}$	8.61
LwP-MdS	1:5000	30	1:1000	60	4.5±0.4	24.7±2.1	29.6±0.0	$5.7±0.2^{ab}$	$-21.0±0.3^{cde}$	$-26.2±0.6^{defgh}$	8.63
HiP-LwS	1:1000	60	1:1000	15	19.4±1.7	3.5±0.3	29.2±0.8	$0.8±0.3^{b}$	$-21.6±0.7^{cdefg}$	$-27.4±1.3^{gh}$	8.66
MdP-LwS	1:2500	60	1:1000	15	14.6±0.2	3.6±0.1	29.0±0.7	$2.7±0.4^{ab}$	$-20.4±0.5^{cd}$	$-26.8±0.5^{efgh}$	8.67
LwP-LwS	1:5000	30	1:1000	15	4.3±0.7	3.4±0.2	29.7±0.0	$3.2±0.0^{ab}$	$-20.4±0.1^{cd}$	$-26.4±0.2^{defgh}$	8.75
HiP-HiS	1:1000	60	1:250	60	21.1±1.0	51.2±2.7	29.8±0.1	$2.7±0.2^{ab}$	$-22.7±0.7^{cdefg}$	$-30.0±0.1^{h}$	8.67
MdP-HiS	1:2500	60	1:250	60	12±0.7	51.2±2.1	29.8±0.1	$4.6±1.1^{ab}$	$-22.9±0.8^{cdefg}$	$-27.7±0.9^{gh}$	8.58
LwP-HiS	1:5000	30	1:250	60	5.4±0.9	50.2±5.9	29.4±0.1	$4.2±0.9^{ab}$	$-22.7±0.5^{cdefg}$	$-27.3±0.4^{fgh}$	8.45

Control: No heat or enzyme treatment. Hconj: Heated raw PPEF and PSEF mixtures without any enzyme treatment. HiP-MdS: Conjugates formed using a mixture of high degree of protein hydrolysis and medium degree of starch hydrolysis, MdP-MdS: Conjugates formed using a mixture of medium degree of protein hydrolysis and medium degree of starch hydrolysis, LwP-MdS: Conjugates formed using a mixture of low degree of protein hydrolysis and medium degree of starch hydrolysis, HiP-LwS: Conjugates formed using a

mixture of high degree of protein hydrolysis and low degree of starch hydrolysis, MdP-LwS: Conjugates formed using a mixture of medium degree of protein hydrolysis and low degree of starch hydrolysis, LwP-LwS: Conjugates formed using a mixture of low degree of protein hydrolysis and low degree of starch hydrolysis, HiP-HiS: Conjugates formed using a mixture of high degree of protein hydrolysis and high degree of starch hydrolysis, MdP-HiS: Conjugates formed using a mixture of medium degree of protein hydrolysis and high degree of starch hydrolysis and LwP-HiS: Conjugates formed using a mixture of low degree of protein hydrolysis and high degree of starch hydrolysis.

5.4.3 Formation of amadori compounds

Maillard Reaction is a multi-stage reaction: the initial products are aminoketones, and they further react into melanoidins. They have different light absorption spectrum where aminoketoses absorb 304 nm while melanoidins absorb 420 nm light. It was observed that the absorbance of protein-starch conjugates at 420 nm was significantly lower than at 304 nm, indicating that the reaction predominantly remained in the early stages, *i.e.*, Amadori reaction product, of the Maillard reaction. Similar findings were shown in Chapter III where the absorbance of pea protein-carbohydrate conjugates was higher at 304 nm compared to 420 nm. The heat treatment in the experiments of this study was limited to 30 minutes, suggesting that the conjugates did not have sufficient time to advance to later stages of the Maillard reaction, which supports the data obtained (Figure 5.1). All conjugates studied exhibited significantly higher absorbance at 304 nm (Abs_{304nm}) and 420 nm (Abs_{420nm}) compared to the protein-enriched fraction (PPEF). Additionally, the Abs_{304nm} and Abs_{420nm} of the conjugates were significantly higher than those of the control samples. However, the control samples showed higher absorbance than the PPEF. Despite the lack of heat treatment during control preparation, the slightly elevated absorbance values could be attributed to the formation of small amounts of Amadori compounds during the spray drying process. Although the differences in Abs_{304nm} among the conjugates were minimal, HiP-MdS conjugates exhibited significantly higher Heyns compound formation compared to the other conjugates (Figure 5.1). The high degree of hydrolysis likely led to extensive protein unfolding, exposing buried amino acids such as lysine or tryptophan, which then conjugated with the -OH terminal of polysaccharides, increasing Amadori compound formation (Kutzli *et al.*, 2021). The LwP-MdS conjugate showed the lowest Abs_{304nm} (0.48), indicating lower production of Heyns compounds compared to the other conjugates. Among all the conjugates studied, those with HiP-HiS and HiP-MdS showed the highest coloration at 420 nm (0.22), significantly higher ($p < 0.05$) than the other conjugates. The higher degree of hydrolysis may have resulted in an increased number of protein-dextrin conjugates, some of which could have undergone dehydration and fission through de-aldolization or Strecker degradation, leading to the formation of intermediate reaction products responsible for coloration. It is also possible that some intermediate compounds, such as reductone, underwent cyclization, dehydration, oxidation, rearrangement, and

condensation, resulting in the formation of later-stage Amadori products (Kutzli *et al.*, 2021). However, due to the short heat treatment period, the formation of advanced stages of these Maillard Reaction Products (MRPs) was very limited, as shown in Figure 5.1.

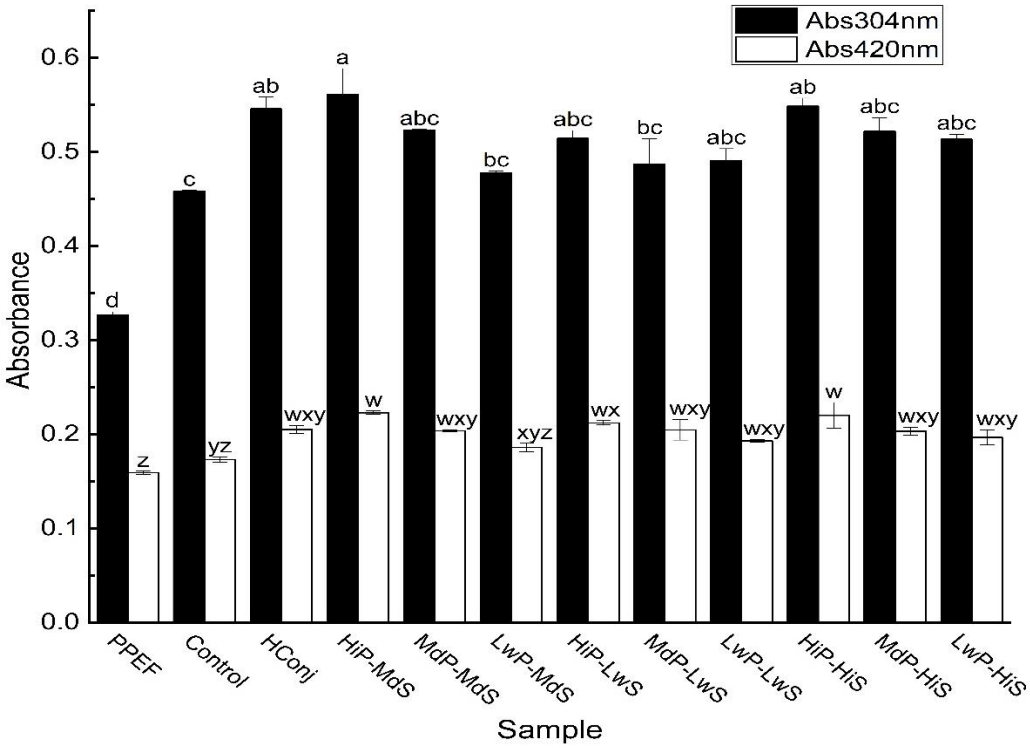

Figure 5.1. Comparative analysis of Amadori reaction product and melanoidin formation by measuring the absorbance of the conjugate mixtures at 304nm and 420nm of control and Maillard conjugates having different combinations of DH and DE measured at an excitation of 347 nm.

Control: No heat or enzyme treatment. Hconj: Heated raw PPEF and PSEF mixtures without any enzyme treatment. HiP-MdS: Conjugates formed using a mixture of high degree of protein hydrolysis and medium degree of starch hydrolysis, MdP-MdS: Conjugates formed using a mixture of medium degree of protein hydrolysis and medium degree of starch hydrolysis, LwP-MdS: Conjugates formed using a mixture of low degree of protein hydrolysis and medium degree of starch hydrolysis, HiP-LwS: Conjugates formed using a mixture of high degree of protein hydrolysis and low degree of starch hydrolysis, MdP-LwS: Conjugates formed using a mixture of medium degree of protein hydrolysis and low degree of starch hydrolysis, LwP-LwS: Conjugates formed using a mixture of low degree of protein hydrolysis and low degree of starch hydrolysis, HiP-HiS: Conjugates formed using a mixture of high degree of protein hydrolysis and high degree of starch hydrolysis, MdP-HiS: Conjugates formed using a mixture of medium degree of protein hydrolysis and high degree of starch hydrolysis and LwP-HiS: Conjugates formed using a mixture of low degree of protein hydrolysis and high degree of starch hydrolysis.

5.4.4 Molecular weight distribution analysis of conjugates

5.4.4.1 High pressure-size exclusion chromatography (HP-SEC)

HP-SEC can be an important technique to determine molecular size changes of the proteins bound to carbohydrates with UV detection. The ratio of the area under the curves at 280 nm and 304 nm was calculated (R_C) to provide insight into the extent of conversion of certain proteins into protein-polysaccharide conjugates. A high R_C indicates an increase in the production of MRPs, whereas a low R_C signifies lesser conjugation between proteins and dextrins resulting in conjugate production. The peaks obtained at 280 nm are due to the presence of proteins and that at 304 nm is primarily of the early stages of the protein-dextrin conjugates, the Amadori Reaction Products (ARP). Similar analysis for proteins at 289 nm and for polysaccharides at 470 nm has been performed previously for ovalbumin-dextran conjugates (Choi *et al.*, 2005). The area under the peaks at 420 nm (peaks indicating the final products of Maillard reaction) were also calculated, but the values were very low, indicating that the MRPs did not proceed to later stages.

Analysis of the chromatogram revealed four major peaks corresponding to approximately >670 kDa, 474 kDa, 57 kDa, and 4.9 kDa, as determined by the standard molecular weight curve. Molecular weight distribution of rice protein-*Arthrobacter* exopolysaccharide conjugates also revealed a variety of different molecular products when run on a high-pressure liquid Chromatography system equipped with a Ultrahydrogel™ 1,000 column (Zhao *et al.*, 2021). It was observed that the R_C of the ~474 kDa peak was the highest compared to other molecular weight ranges (474 kDa, 57 kDa and 4.9 kDa) for all the hydrolyzed conjugates. Among the conjugates, the highest level of conjugation was observed for the MdP-MdS conjugates (R_C = 1.15) in the 474 kDa peak. The higher area assessed in the chromatogram at 304 nm than at 280 nm for the proteins at 474 kDa indicated a greater involvement of proteins in that range in conjugation with dextrins/starches. This also suggested a higher formation of early stages of the Maillard reaction products near the molecular weight range of 474 kDa. LwP-MdS conjugates also showed a high R_C at 474 kDa.

In contrast, the R_C of the heated conjugates was highest at about 670 kDa, indicating the involvement of intact proteins in conjugation with intact starches, resulting in an overall increase in the molecular weight of the produced conjugates. HP-SEC data in Table 5.2 revealed higher molecular weights, for the hydrolyzed conjugates as evidenced by higher R_C values for the 474 kDa and 670 kDa peaks (ranging from 0.6 to 1.15), whereas lower values were observed for the

57 kDa and 4.9 kDa peaks (ranging from 0.18 to 0.85). A similar shift in the molecular weight peaks was observed from lower to higher molecular weights in a separate research with increasing covalent attachment of ovalbumin to dextran to form ovalbumin-dextran conjugates (Choi *et al.*, 2005). Zhao *et al.* (2021) also reported an increase in high molecular weight compounds with a corresponding decrease in small molecular weight compounds (Zhao *et al.*, 2021). In a separate study concerning Maillard reaction of rice proteins with mono, oligo and polysaccharides, Li and colleagues also reported an increase in the number of high molecular weight groups and decrease in low molecular weight compounds as Maillard reaction proceeded (Li *et al.*, 2013). The molecular weight distribution of sweet potato proteins conjugated with xylose was also analyzed using the HPLC method (Habinshuti *et al.*, 2021).

Furthermore, the R_C of the control samples was recorded at 1.18. This phenomenon can be attributed to the heat applied in the cyclone during the spray drying process, which likely facilitated the conjugation of smaller proteins with starches.

Table 5.2: Molecular weight (M.W.) of selected conjugates obtained and the ratio of area under the curve R_C of each peak obtained at 304 nm and 280 nm.

M.W. (kDa)	R_C = Ratio of area under the curve at 304nm/ Ratio of area under the curve at 280nm										
	Control	Hconj	HiP-MdS	MdP-MdS	LwP-MdS	HiP-LwS	MdP-LwS	LwP-LwS	HiP-HiS	MdP-HiS	LwP-HiS
>670	0.58	0.57	0.66	0.67	0.61	0.6	0.58	0.62	0.64	0.67	0.63
~474	0.69	0.38	0.79	1.15	0.89	0.69	0.70	0.60	0.68	0.73	0.67
~57	0.07	0.38	0.54	0.35	0.18	0.68	0.70	0.49	0.85	0.39	0.36
~4.9	1.18	0.34	0.31	0.34	0.33	0.3	0.41	0.35	0.33	0.34	0.38

Control: No heat or enzyme treatment. Hconj: Heated raw PPEF and PSEF mixtures without any enzyme treatment. HiP-MdS: Conjugates formed using a mixture of high degree of protein hydrolysis and medium degree of starch hydrolysis, MdP-MdS: Conjugates formed using a mixture of medium degree of protein hydrolysis and medium degree of starch hydrolysis, LwP-MdS: Conjugates formed using a mixture of low degree of protein hydrolysis and medium degree of starch hydrolysis, HiP-LwS: Conjugates formed using a mixture of high degree of protein hydrolysis and low degree of starch hydrolysis, MdP-LwS: Conjugates formed using a mixture of medium degree of protein hydrolysis and low degree of starch hydrolysis, LwP-LwS: Conjugates formed using a mixture of low degree of protein hydrolysis and low degree of starch hydrolysis, HiP-HiS: Conjugates formed using a mixture of high degree of protein hydrolysis and high degree of starch hydrolysis, MdP-HiS: Conjugates formed using a mixture of medium degree of protein hydrolysis and high degree of starch hydrolysis and LwP-HiS: Conjugates formed using a mixture of low degree of protein hydrolysis and high degree of starch hydrolysis.

5.4.4.2 SDS-PAGE and Image J densitometry analysis of the control and conjugates

The conjugates were run on an SDS-PAGE gel and stained using Coomassie Brilliant Blue R-250 (CBB) dye (Figure 5.2A). It was observed that the degree of hydrolysis (DH) had a direct relation with the intensity of protein bands. As the DH decreased, it was visually observed that the bands above ~35 kDa increased in intensity (Figure 5.2A). This can be attributed to enzymatic cleavage as a result of which the higher molecular weight proteins like convicilin (~70 kDa), vicilin (~50 kDa) and the acidic subunit of legumin (~40 kDa) were hydrolyzed into smaller protein fragments resulting in a lower intensity of those protein bands for the high DH conjugates as compared to med DH and low DH conjugates. Similar observations were made Chapter III.

The formation of conjugates were qualitatively analyzed on the SDS-PAGE gels using the fuchsin sulfite staining method which has been described in Section 2 above. Fuchsin binds to starch/dextrins and hence stains the polysaccharides conjugated with proteins when run on an SDS-PAGE gel (Chapter III). The conjugates stained using fuchsin sulfite showed heavy bands at the top of the lane separating gels followed by a smear throughout the lane. On size comparison with the molecular weight marker, it was seen that the band at the top were above 245 kDa in size. The same conjugates stained using CBB (Figure 5.2A) also showed a band at the top of the gel indicating large molecular weight structures. This was likely due to the formation of protein-starch conjugates which were not able to pass through the pores of the polyacrylamide gel (10 %) and have settled at the top (Mu *et al.*, 2011). HP-SEC data also solidifies the above argument since a higher R_C for conjugates having a molecular weight of 474 kDa and higher was observed (Table 5.2). A faint smear on the CBB-stained gel was also observed between the 100 – 245 kDa range as well as on the background throughout the lanes which could be due to short proteins conjugated with the starch that passed into the gel (Figure 5.2A). These proteins lost their regular banding patterns, *i.e.*, not in specific molecular weight, and hence left the smear throughout the lane of each conjugate sample. Similar observations using SDS-PAGE gel has been made by Zhu *et al.* (2010) and Mu *et al.* (2011) where a dense broad heavy band was formed at the top of the gel indicating the formation of whey protein isolate-dextran conjugates and soy protein isolate-acacia gum conjugates. Conjugation was quantitatively determined by analyzing the density (%) of the smear formed in the fuchsine-stained SDS-PAGE gels using ImageJ. It was observed that all the conjugates had a higher density as compared to the raw PPEF (data not shown). Although the difference in intensity values was not very different among the conjugated samples (Table 5.1),

LwP-LwS conjugates displayed the highest intensity (8.74 %) as compared to the other conjugates indicating increased polysaccharide conjugation to the proteins. Results were similar to those observed in Chapter III, who showed that protein-polysaccharide conjugates having a lower DH% showed a higher intensity when analyzed using ImageJ as compared to protein-bound carbohydrates having a lower degree of hydrolysis. The LwP-HiS conjugate showed the lowest intensity (8.45%). Although the HiP-MdS conjugates showed more Amadori compound formation (Figure 5.1), the intensity values were not the highest. A possible reason could be that starch was bound to small molecular weight proteins as a result of which they passed through the gels to the bottom of the gels and were not analyzed by the software.

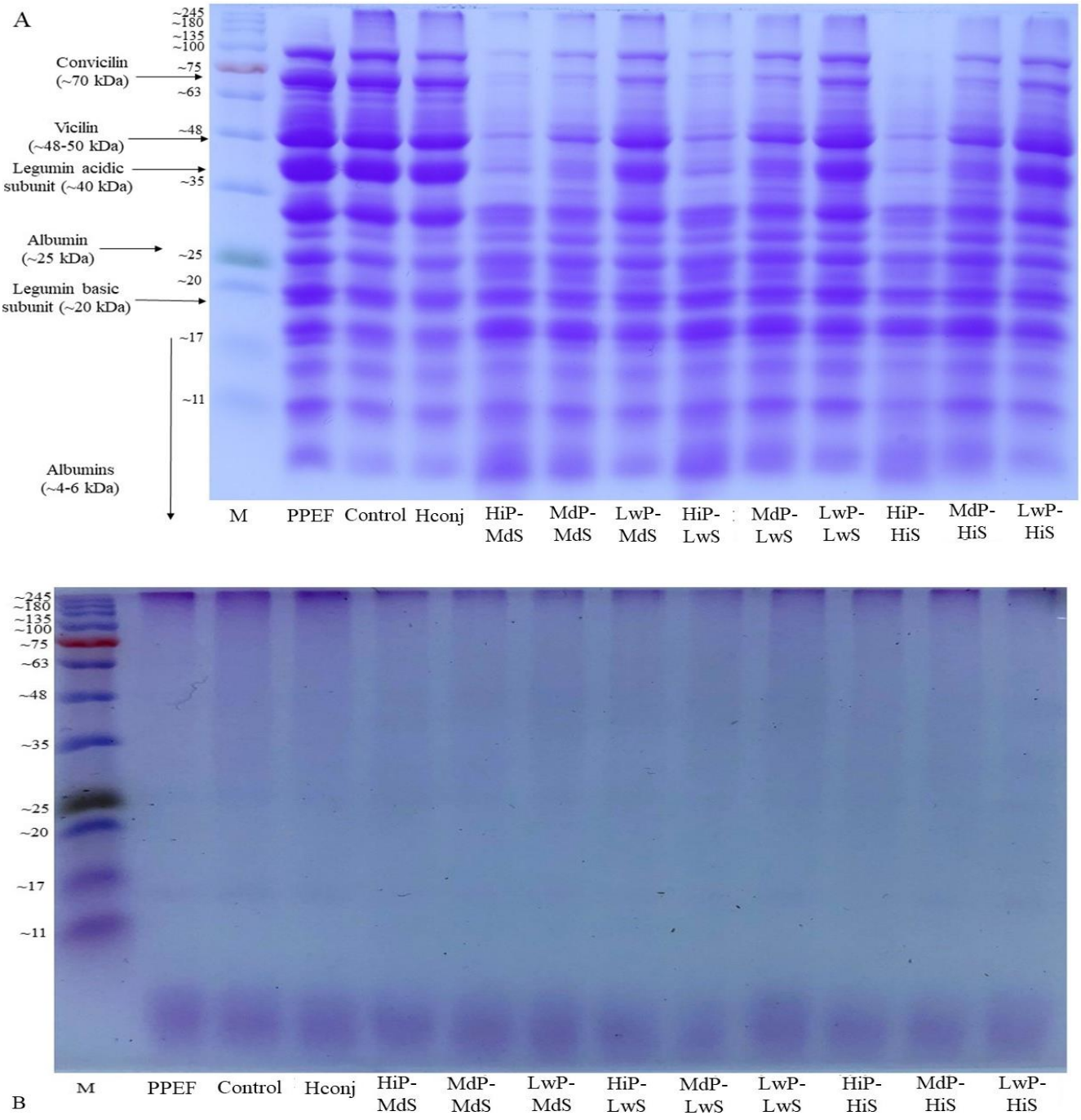

Figure 5.2. SDS PAGE of conjugates having various combinations of DH-DE stained using Coomassie Brilliant Blue R-250 (A) and Fuchsin sulfite (B)

PPEF: Pea protein-enriched flour fraction. Control: No heat or enzyme treatment. Hconj: Heated raw PPEF and PSEF mixtures without any enzyme treatment. HiP-MdS: Conjugates formed using a mixture of high degree of protein hydrolysis and medium degree of starch hydrolysis, MdP-MdS: Conjugates formed using a mixture of medium degree of protein hydrolysis and medium degree of starch hydrolysis, LwP-MdS: Conjugates formed using a mixture of low degree of protein hydrolysis and medium degree of starch hydrolysis, HiP-LwS: Conjugates formed using a mixture

of high degree of protein hydrolysis and low degree of starch hydrolysis, MdP-LwS: Conjugates formed using a mixture of medium degree of protein hydrolysis and low degree of starch hydrolysis, LwP-LwS: Conjugates formed using a mixture of low degree of protein hydrolysis and low degree of starch hydrolysis, HiP-HiS: Conjugates formed using a mixture of high degree of protein hydrolysis and high degree of starch hydrolysis, MdP-HiS: Conjugates formed using a mixture of medium degree of protein hydrolysis and high degree of starch hydrolysis and LwP-HiS: Conjugates formed using a mixture of low degree of protein hydrolysis and high degree of starch hydrolysis.

5.4.5 Microstructure analysis using SEM

Image A in Figure 5.3 depicts the SEM of PPEF, illustrating the presence of protein bodies alongside protein clusters associated with cell wall materials. Some starch granules are also discernible, although smaller in size compared to those found in the starch-enriched fraction. The high shear during air classification is presumed to have fragmented the starch structure, resulting in smaller, broken granule structures present in the fine fraction. The majority of carbohydrates appear in the form of fibers associated with protein bodies (Skylas *et al.*, 2023). Conversely, starch-rich PSEF predominantly exhibits spherical starch granules, with some cell wall proteins or other minor impurities present on its surface (Möller *et al.*, 2021). Irregular polygonal bodies present in PSEF are likely cell wall materials and protein bodies adhered to fibers that were not adequately separated during milling and air classification.

The image C (Figure 5.3) serves as the control sample, prepared with a mixture of similar concentrations of PPEF and PSEF as other reaction mixtures but without any heat or enzymatic treatments. This image reveals a blend of protein bodies and starch granules, with some evidence of bruising and deformation on the starch surface attributable to the spray drying process. The alternating pattern between irregular polygonal and irregular forms suggests physical mixing of the two biopolymers, with minimal chemical bonding apparent. Similar observations were made by Zha *et al.* (2019) in their study of microstructures of pea proteins conjugated with gum Arabic.

The image D (Figure 5.3) represents heated conjugates where protein and starch-enriched fractions were combined and subjected to Maillard conjugation. In the image D1, noticeable surface roughness and structural deformations are evident in the starch, while protein bodies have clustered. The images D1 and D2 illustrate the association of protein bodies with starch granules, indicative of heat-induced Maillard conjugation. This phenomenon distinguishes itself from mere association, as such complex microstructures are absent in untreated PPEF and PSEF micrographs (A and B) (Zha *et al.*, 2019). However, The image C does exhibit slight evidence of conjugation, likely due to the elevated temperature during the spray drying process.

Upon enzyme-mediated hydrolysis of protein and starch molecules, a reduction in protein body size was observed, along with surface perforations, crests, and troughs on starch granules, indicating amylase activity. Some inhomogeneities in the starch-protein matrix were noted, although protein bodies and starch granules retained their integrity, unlike the observations of Zha *et al.* (2019). This discrepancy may be attributed to the shorter, rapid heat treatment employed in

this thesis research compared to their prolonged heating durations. In Figure 5.3 (images F1 and F2), the starch granule surface appears scooped, potentially exposing hydroxy groups that may covalently link with amine groups of protein bodies to form conjugates. Figure 5.3 (image G1) reveals pores in the fiber matrix, directly linked to α-amylase activity. At lower degrees of protein and starch hydrolysis, the image J1 in Figure 5.3 displays some evidence of unbound protein body conjugation with the fiber matrix. The images J2 and K2 depict protein-protein conjugation, likely resulting from protein structure deformation due to heat-induced Maillard reactions, followed by disulfide bond formation leading to protein-protein aggregation. Overall, the conjugate structures exhibit increased lumpiness, consistent with observations by Yan *et al.* (2022), who studied the microstructures of dextran conjugated with *Cinnamomum camphora* proteins. The microstructure of pea protein-gum Arabic conjugates and compound gels formed with pea, soy and peanut proteins conjugated with konjac glucomannan have been reported by Zha *et al.* (2019a) and Yao *et al.* (2023) respectively using SEM who observed similar structural features.

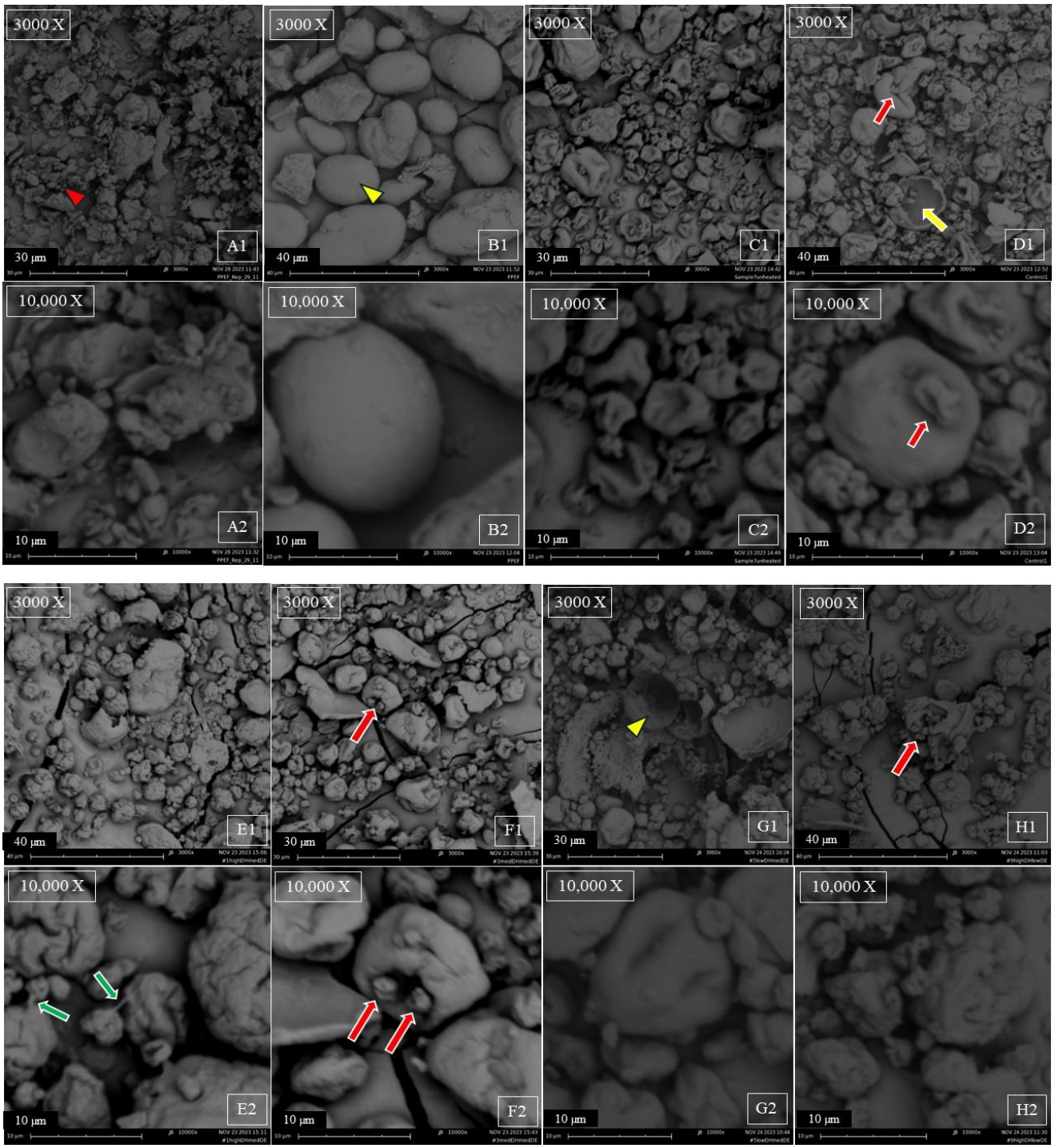
3000 X
A1
30 µm
3000 X
B1
40 µm
3000 X
C1
30 µm
3000 X
D1
40 µm
10,000 X
A2
10 µm
10,000 X
B2
10 µm
10,000 X
C2
10 µm
10,000 X
D2
10 µm
3000 X
E1
40 µm
3000 X
F1
30 µm
3000 X
G1
30 µm
3000 X
H1
40 µm
10,000 X
E2
10 µm
10,000 X
F2
10 µm
10,000 X
G2
10 µm
10,000 X
H2
10 µm

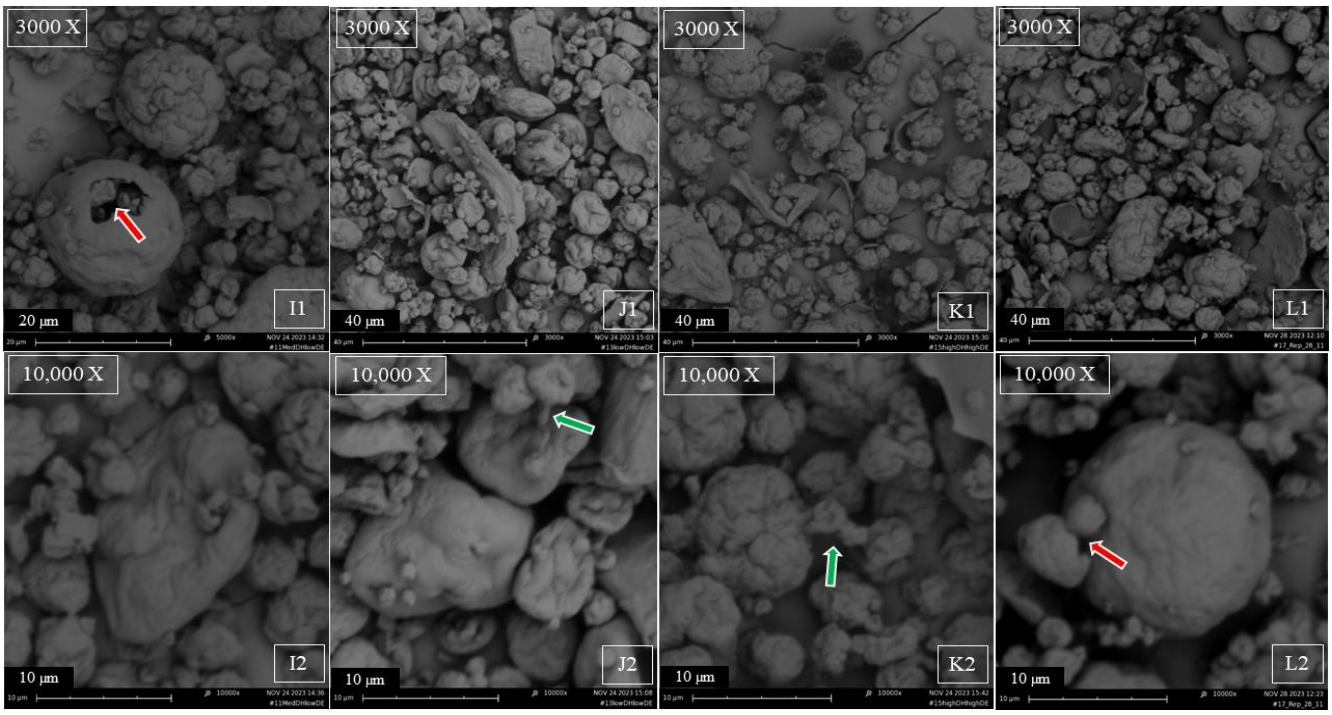

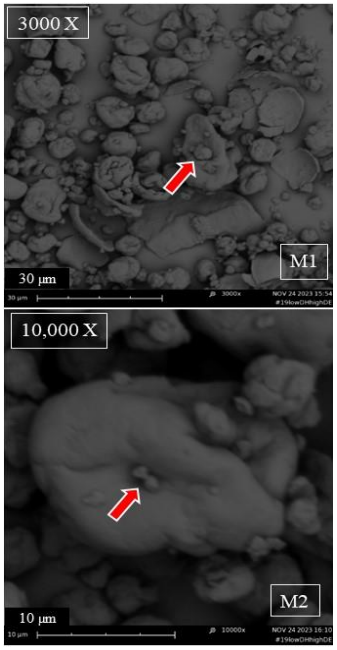

Figure 5.3. Scanning Electron Micrograph of pea protein-enriched fraction (PPEF), pea starch enriched fraction (PSEF), control, heated conjugates and hydrolyzed conjugates.

The different letters correspond to the following images: A, PPEF; B, PSEF; C, Controls; D: Heated conjugates; E: HiP-MdS; F: MdP-MdS; G: LwP-MdS; H: HiP-LwS; I: MdP-LwS; J: LwP-LwS; K: HiP-HiS; L: MdP-HiS; M: LwP-HiS

Numbers followed by the letter indicate the magnification that was used. 1: Magnification at ×3,000; 2: Magnification at ×10,000. Scale bar denoted by white horizontal lines correspond to 10 µm, 20 µm, 30 µm and 40 µm; The following shapes were used to highlight different molecular species and interactions. Red triangle: protein bodies; Yellow triangles: starch granules; Red arrows: Protein-starch conjugates; Green arrows: linkages between protein and starch granules and Yellow arrows: Damage on starch granules.

5.4.6 Secondary structure analysis of conjugates

5.4.6.1 Fourier transform infrared imaging- attenuated total reflection spectroscopy (FTIR-ATR)

The chemical structure of protein conjugated with starch was examined using the FTIR-ATR spectrography. Each distinct intensity corresponds to a specific functional group within the protein and starch structures (Habinshuti *et al.*, 2020). Distinguishing characteristic bands such as amides I, II, and III were identified in the PPEF spectrum at 1,641 cm^{-1} (C=O stretching), 1,528 cm^{-1} (N-H deformation), 1394 cm^{-1} (C-N stretching), and 1,235 cm^{-1} (N-H bending vibrations), respectively (Zha *et al.*, 2019; Zhang *et al.*, 2022). Carbohydrate-specific absorption bands, ranging from 1,180 cm^{-1} to 953 cm^{-1}, typically represent "saccharide" absorption bands resulting from the stretching vibration of C-C and C-O, and the bending of C-H groups (Zhang *et al.*, 2022). The overlapping peaks located in the wavelength range of 900 cm^{-1} to 1,150 cm^{-1} and the sharp peak at 1,002 cm^{-1} of PSEF can be attributed to the functional groups of starch, while overtones of saccharide absorption bands are also evident at 2,344 and 2,102 cm^{-1} (Yan *et al.*, 2022). The saccharide peak is also present for the PPEF which is due to the presence of starch granules and other cell wall materials as evident from the SEM micrograph (Figure 5.3: Image B). Additionally, the absorption band at 2,934 cm^{-1} was attributed to the antisymmetric stretching of C-H in CH2 and CH3 groups in Amide B (Habinshuti *et al.*, 2020; Zha *et al.*, 2019). The region from 3,301 to 3,237 cm^{-1} represents the N-H vibrations of Amide A, indicated by the peak at 3,281 cm^{-1} in the figure (Habinshuti *et al.*, 2020).

Observations from Figure 5.4 reveal that the peaks of Amide (I, II, III, A, and B) were notably sharp for PPEF and controls, but the peak intensity decreased as PPEF and PSEF were subjected to hydrolysis and heating to form conjugates. This suggests that degrees of hydrolysis and conjugation significantly impacted the structure of the conjugates as these treatments lead to the formation of covalent bonds between amino acid residues and hydroxyl groups of dextrins (Chen *et al.*, 2019). A substantial increase in transmittance intensity was noted from 1600 to 1700 cm^{-1} of C–O stretching assigned to amide I for the conjugates. These changes could be attributed to the formation of new groups of MRPs, including early stages of Amadori compounds (C–O), N-containing compounds (C–N), and some Schiff bases (C–N) (Liu *et al.*, 2020). There was a gradual shift in the amide A (from 3,281 to 3,272 cm^{-1}) and amide B peaks in the FTIR-ATR spectrum for the HiP-HiS, MdP-HiS, and LwP-HiS conjugates, akin to observations in sweet

potato protein hydrolysates conjugated with xylose by Habinshuti *et al.* (2020). The saccharide peak observed at 1,002 cm^{-1} for PSEF shifted to the left for both heated and hydrolyzed conjugates. Furthermore, the overtones of the saccharide peak at 2,344 cm^{-1} completely disappeared for Hconj, HiP-MdS, MdP-MdS, LwP-MdS, HiP-LwS, and MdP-LwS conjugates. This disappearance can be attributed to the formation of new covalent linkages between the C=O and NH_2 groups, leading to the formation of Schiff bases and the subsequent disappearance of its characteristic pattern. Zhang *et al.* (2022) and Zha *et al.* (2019) studied the secondary structures of pea protein concentrate conjugated with gum Arabic and pea protein isolate and maltodextrin respectively in two separate studies using the FTIR and revealed the formation of newer compounds.

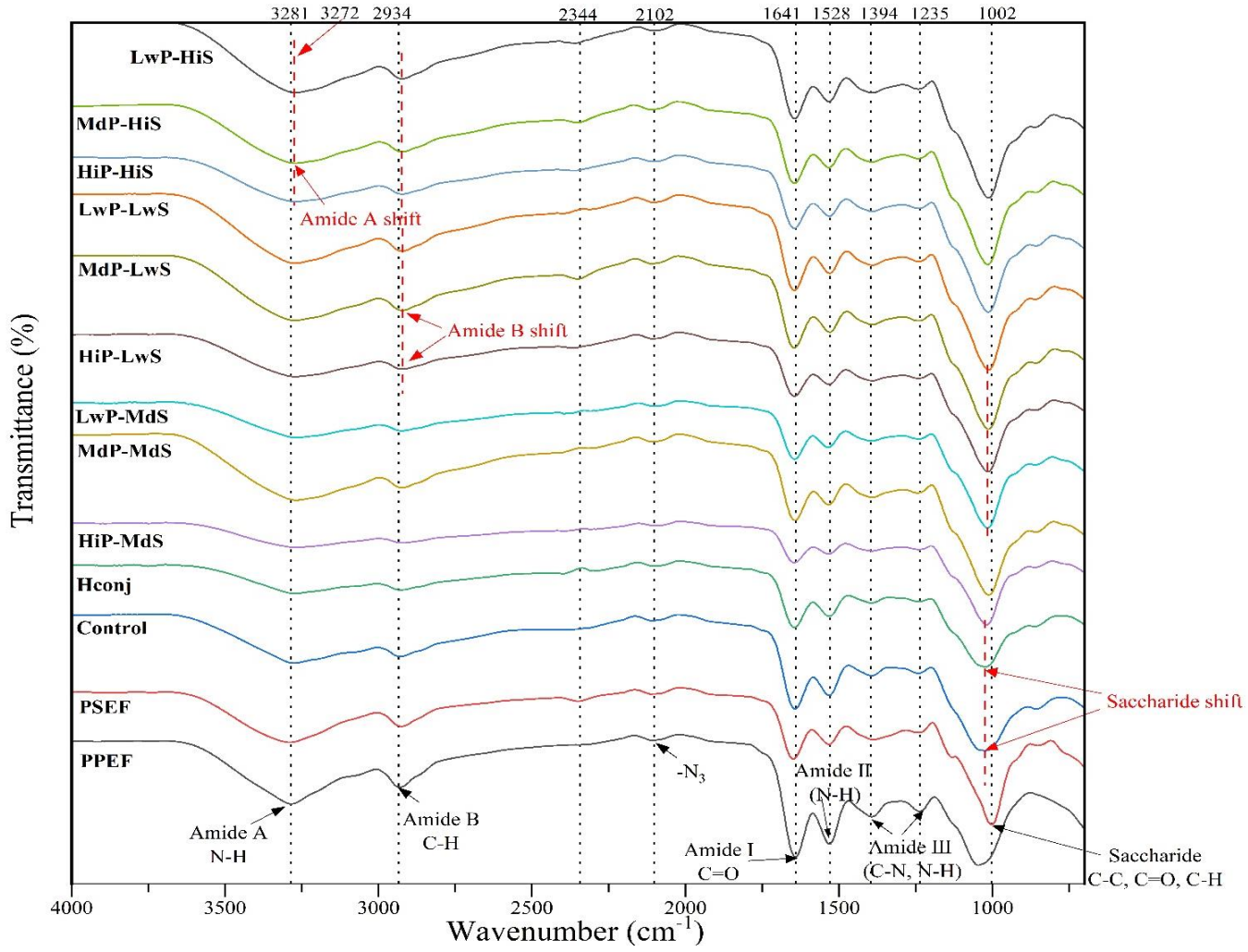

Figure 5.4: Characteristic structure of pea protein enriched flour (PPEF), pea starch enriched flour (PSEF), control, heated conjugates (Hconj) and hydrolyzed conjugates by Fourier transform infrared spectroscopy-attenuated total reflection (FTIR-ATR).

Control: No heat or enzyme treatment. Hconj: Heated raw PPEF and PSEF mixtures without any enzyme treatment. HiP-MdS: Conjugates formed using a mixture of high degree of protein hydrolysis and medium degree of starch hydrolysis, MdP-MdS: Conjugates formed using a mixture of medium degree of protein hydrolysis and medium degree of starch hydrolysis, LwP-MdS: Conjugates formed using a mixture of low degree of protein hydrolysis and medium degree of starch hydrolysis, HiP-LwS: Conjugates formed using a mixture of high degree of protein hydrolysis and low degree of starch hydrolysis, MdP-LwS: Conjugates formed using a mixture of medium degree of protein hydrolysis and low degree of starch hydrolysis, LwP-LwS: Conjugates formed using a mixture of low degree of protein hydrolysis and low degree of starch hydrolysis, HiP-HiS: Conjugates formed using a mixture of high degree of protein hydrolysis and high degree of starch hydrolysis, MdP-HiS: Conjugates formed using a mixture of medium degree of protein hydrolysis and high degree of starch hydrolysis and LwP-HiS: Conjugates formed using a mixture of low degree of protein hydrolysis and high degree of starch hydrolysis.

5.4.6.2 Quenching of aromatic amino acid residues

The endogenous fluorescence of proteins arises from amino acids like tryptophan and tyrosine, which emit fluorescence upon excitation (Qiu *et al.*, 2017). This fluorescence can be a key indicator for characterizing the early stages of the Maillard Reaction. When excited at 295 nm, the protein-enriched fraction (PPEF) displayed a maximum emission of 8366.67 CPS at 339 nm. All conjugates, including the control, exhibited lower CPS values compared to the PPEF. Similar findings were reported by Yang *et al.* (2022) who observed decreased intensity in all conjugates compared to raw gliadin proteins. Among the hydrolyzed conjugates, the HiP-MdS conjugates showed the highest intensity, approximately 7000 CPS, suggesting a lesser degree of covalent coupling compared to the other conjugates. These results are consistent with the ImageJ densitometry analysis, where a lower percentage intensity (8.61 %) was recorded for HiP-MdS conjugates (Table 5.1) relative to the other hydrolyzed conjugates. In hydrolyzed conjugates, fluorescence quenching and the shift in maximum emission wavelength can be attributed to changes in the tryptophan groups within the pea proteins (Shen *et al.*, 2012). It is believed that tryptophan residues in the conjugates are surrounded by starch/dextrin molecules, leading to a more compact tertiary structure in the starch-conjugated proteins compared to native pea proteins, which shields the tryptophan residues on the pea proteins and results in a weaker signal (Liu *et al.*, 2012). A reduction in fluorescence intensity is typically observed due to the quenching of aromatic amino acids by other species. Therefore, it can be inferred that the dextrins in the samples interacted with the aromatic amino acids of the hydrolyzed proteins through coupling, leading to protein-polysaccharide conjugation and a consequent decrease in fluorescence intensity (Yang *et al.*, 2022). While studying rice protein-*Arthrobacter* exopolysaccharide conjugates, Zhao *et al.* (2021) scanned the excitation from 300 nm to 400 nm and the emission was scanned from 370 nm to 570 nm. Sun *et al.* (2023) used an excitation of 295 nm and emission ranged from 375 nm to 550 nm for analyzing the intrinsic fluorescence spectra of soybean hydrolysate-glucose/fructose/galactose conjugates. The intrinsic fluorescence spectra of glycosylated soybean proteins were also studied in different research (Wang *et al*., 2020). In all these studies, a decrease in fluorescent intensity was recorded which reflected protein-polysaccharide conjugation.

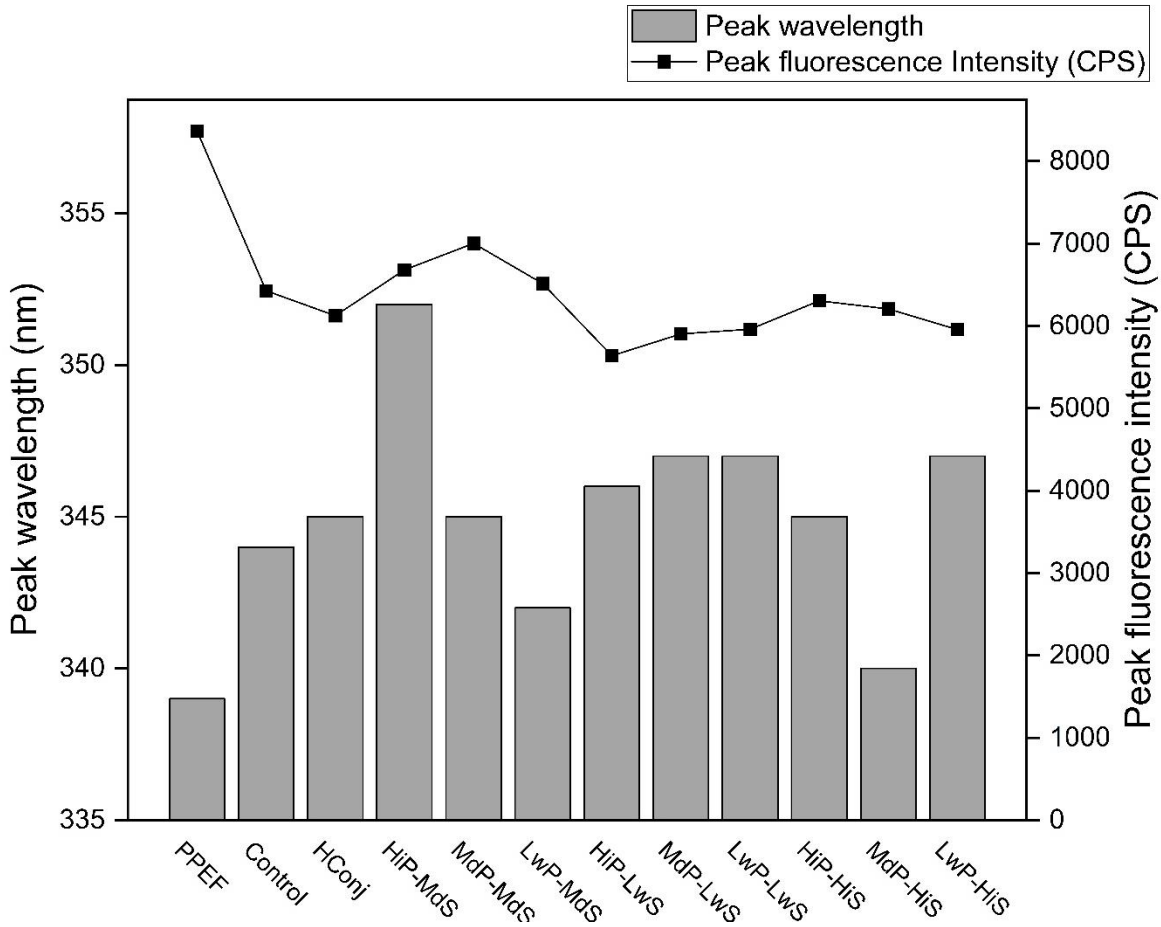

Figure 5.5. Fluorescent intensity spectrum of pea protein enriched flour (PPEF), control, heated conjugates (Hconj) and hydrolyzed conjugates by excitation at 295nm.

Control: No heat or enzyme treatment. Hconj: Heated raw PPEF and PSEF mixtures without any enzyme treatment. HiP-MdS: Conjugates formed using a mixture of high degree of protein hydrolysis and medium degree of starch hydrolysis, MdP-MdS: Conjugates formed using a mixture of medium degree of protein hydrolysis and medium degree of starch hydrolysis, LwP-MdS: Conjugates formed using a mixture of low degree of protein hydrolysis and medium degree of starch hydrolysis, HiP-LwS: Conjugates formed using a mixture of high degree of protein hydrolysis and low degree of starch hydrolysis, MdP-LwS: Conjugates formed using a mixture of medium degree of protein hydrolysis and low degree of starch hydrolysis, LwP-LwS: Conjugates formed using a mixture of low degree of protein hydrolysis and low degree of starch hydrolysis, HiP-HiS: Conjugates formed using a mixture of high degree of protein hydrolysis and high degree of starch hydrolysis, MdP-HiS: Conjugates formed using a mixture of medium degree of protein hydrolysis and high degree of starch hydrolysis and LwP-HiS: Conjugates formed using a mixture of low degree of protein hydrolysis and high degree of starch hydrolysis.

5.4.7 Surface properties analysis- surface charge

The surface charge of the control, heated and hydrolyzed conjugates were analyzed at pH 4, 7 and 10. One-way ANOVA followed by Tukey mean comparison test showed that there were significant differences ($p < 0.05$) between the surface charge of the conjugates at pH 4, 7 and 10 (Table 5.1). The zP of the controls and conjugates at pH 4 was significantly higher than that at pH 7 and 10 with the zP at the latter two pH values being highly negative. This can be attributed to the deprotonated carboxyl groups (COO^-) on the protein molecules of the conjugates that behaves as a buffer to compensate the increased amount of proton upon pH drop (Zha *et al.*, 2019b). Similar observations have also been made in Chapter III while studying the surface charge of pea proteins with the carbohydrates available in the fine fraction of air classified pea flours. Even between the same pH range, there were significant differences between the different conjugates under study. At pH 4, it was observed that the zP of the Hconj (8.4 mV ± 0.3 mV) was significantly higher than the other conjugates (0.8 ± 0.3 to 8.4 ± 0.3 mV). Among the hydrolyzed conjugates, LwP-MdS conjugates reported the highest surface charge at pH 4 (5.7 ± 0.2 mV) whereas HiP-LwS conjugates had significantly lower zP (0.8 ± 0.3 mV) as compared to the other conjugates. On the contrary, at pH 7, the heated conjugates showed the lowest surface charge (-19.5 ± 0.6 mV) whereas the controls exhibited the highest zP (-26.6 ± 0.9 mV). Among the surface charge of the conjugates studied at pH 7, there were significant differences ($p < 0.05$). Maillard reaction is believed to impact the charge density on the protein and the effect is specific to the sugar/polysaccharide binding to the protein molecule (Wang *et al.*, 2018). Since amylase hydrolysis resulted in the release of dextrins having a wide array of DE (Table 5.1), that resulted in the formation of a diverse range of MRPs having different charge densities. Similar changes in the zeta potential for soybean protein isolates Maillard conjugated with xylose/fructose contrary to raw soybean protein isolates has been reported elsewhere (Wang *et al.*, 2018). Contrary to zP at pH 4 and pH 7, the zP of the conjugates at pH 7 and 10 were not significantly different. MdP-MdS conjugates reported the highest zP (31.4 ± 2.7 mV). Proteins usually carry a positive charge at a pH below their isoelectric point (p*I*) and a negative charge above it (Lam *et al.*, 2017). The isoelectric point of pea proteins is about 4.3 and hence the surface charge of the conjugates were positive at pH 4 (Doan *et al.*, 2019) and negative at pH 7 and 10. The charge of a protein is a result of different intrinsic factors like the amino acid content, shape, size, and conformation of proteins, and extrinsic factors, such as solvent conditions (ionic strength and temperature), mixing time, and

protein concentration (Avramenko *et al.*, 2013). Hence the variation of the zP among the conjugates must be a result of changes in the intrinsic parameters. Enzymatic hydrolysis cleaves the proteins at different amino acids and as a result exposes buried amino acids from the core of the proteins (Mookerjee *et al.,* 2023). As a result, different amino acids having different functional groups (each of which ionizes differently in solution) are exposed leading to differential surface charge among the conjugates studied. Moreover, from Figure 5.3, the presence of bulky starch granules were noticed in association with the protein bodies as well as free starch granules. The steric effect of these bulky starch granules can also influence the surface charge by shielding charges on the protein bodies which leads to differences in the zP of the conjugates (Mookerjee *et al.*, 2023).

5.4.8 Functional properties

5.4.8.1 Solubility

5.4.8.1.1 Protein solubility

A comparative analysis of the protein solubility between the control and hydrolyzed conjugates has been reported in Figure 5.6. The control samples exhibited the highest solubility (55.2% ± 0.3%) among the samples tested including the conjugates. Similar findings were reported by Zha and colleagues, who observed a decrease in solubility for pea protein isolate-gum Arabic conjugates following extended incubation (Zha *et al.*, 2019b). A similar decrease in solubility was noted for egg-white pectin conjugates compared to raw egg white proteins, which was attributed to the formation of high molecular weight compounds (Al-Hakkak *et al.*, 2010). Among the hydrolyzed conjugates, the MdP-MdS conjugates displayed the highest protein solubility (46.8% ± 2%). The solubility of the other conjugates was not significantly different ($p < 0.05$), ranging from 31.6% ± 3.6% to 36.9% ± 6.0%.

5.4.8.1.2 Starch solubility

The starch solubility of the control (7.9% ± 0.1%) and hydrolyzed conjugates (8.8% ± 0.0%) was the lowest, while all the hydrolyzed conjugates exhibited significantly higher solubility (Figure 5.6). The degree of interaction between the crystalline and amorphous regions of starch granules influences how starch molecules interact with water, *i.e.*, solubility (Guo *et al.*, 2015). Sujka *et al.* (2013) explained that water molecules penetrating the interior of starch granules are more likely to interact with starch molecules due to increased exposure of hydrogen bonds in the

crystalline region, which enhances swelling power and thus impacts solubility. Improvement of solubility is also observed with mechanical damages to amorphous region (Zheng *et al.*, 2013). SEM imaging (Figure 5.3) reveals that the controls and heated conjugates mostly contained intact starch granules with minor surface deformations (Figure 5.3C). In contrast, the starch granules in the hydrolyzed conjugates exhibited surface damage due to amylase treatments, resulting in the formation of holes and the leaching of amylose chains (Figure 5.3 E-M), which likely enhanced hydrogen bonding with water. Additionally, enzymatic hydrolysis released soluble sugar molecules, which further enhanced solubility. Among the conjugates, the LwP-MdS conjugates demonstrated the highest starch solubility (27.4% ± 0.6%).

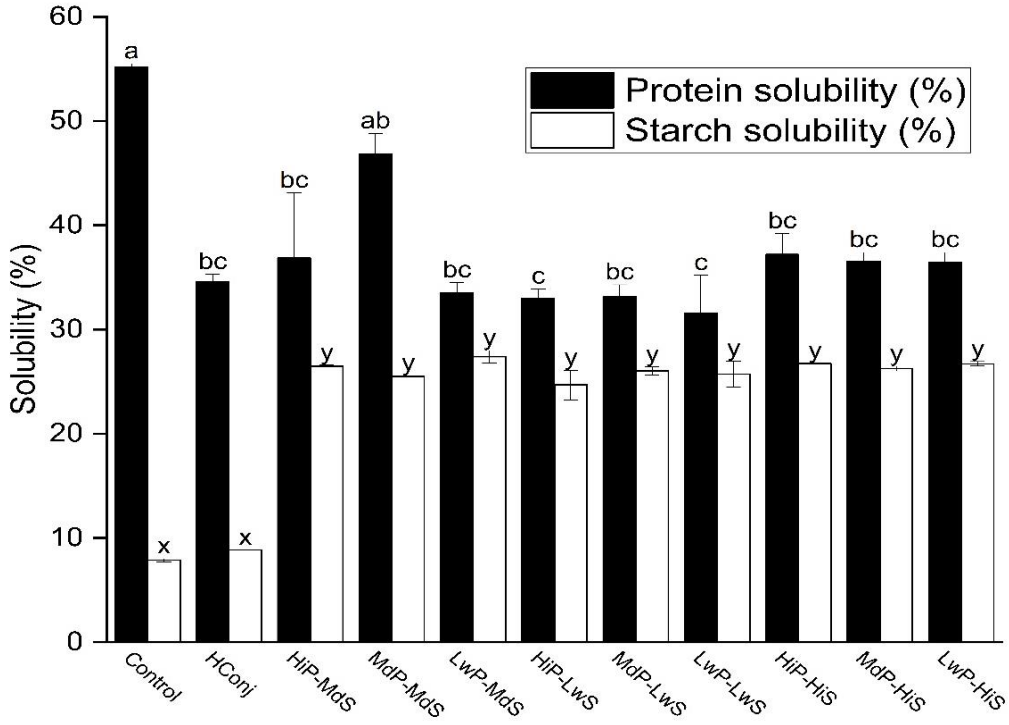

Figure 5.6. Protein and starch solubility of control, heated and hydrolyzed conjugates at pH 7

Control: No heat or enzyme treatment. Hconj: Heated raw PPEF and PSEF mixtures without any enzyme treatment. HiP-MdS: Conjugates formed using a mixture of high degree of protein hydrolysis and medium degree of starch hydrolysis, MdP-MdS: Conjugates formed using a mixture of medium degree of protein hydrolysis and medium degree of starch hydrolysis, LwP-MdS: Conjugates formed using a mixture of low degree of protein hydrolysis and medium degree of starch hydrolysis, HiP-LwS: Conjugates formed using a mixture of high degree of protein hydrolysis and low degree of starch hydrolysis, MdP-LwS: Conjugates formed using a mixture of medium degree of protein hydrolysis and low degree of starch hydrolysis, LwP-LwS: Conjugates formed using a mixture of low degree of protein hydrolysis and low degree of starch hydrolysis, HiP-HiS: Conjugates formed using a mixture of high degree of protein hydrolysis and high degree of starch hydrolysis, MdP-HiS: Conjugates formed using a mixture of medium degree of protein hydrolysis and high degree of starch hydrolysis and LwP-HiS: Conjugates formed using a mixture of low degree of protein hydrolysis and high degree of starch hydrolysis.

5.4.8.2 Foaming (foam capacity and foam stability)

The foam capacity (FC) and foam stability (FS) of the control, heated and hydrolyzed conjugates were analyzed at pH 4, 7 and 10. Two-way ANOVA followed by Tukey mean comparison test was performed to analyze the statistical significance of the results with pH and sample group being the two factors. The FC of all hydrolyzed conjugates at all the pH values were reported to be significantly higher than the FC of the controls and Hconj (Figure 5.7). Moreover, the FC at pH 4 was observed to be higher than the FC at pH 7 and 10 with MdP-MdS conjugates showing the highest FC (241.1% ± 8.1%) at pH 4 among all the conjugates. At pH 7, HiP-HiS conjugates exhibited the maximum FC of 216.1 %, whereas at pH 10, HiP-MdS conjugates recorded the maximum FC (223.3 %). Among all the conjugates studied, the control samples recorded the lowest FC at pH 7 (146.1 %). HiP-MdS conjugates exhibited the highest FC at both pH 10 (225.6% ± 15.6%) whereas HiP-HiS conjugates displayed the maximum FC at pH 7 (223.3% ± 0%).

The foaming properties of conjugates derived from enzymatically modified pea flour fine fraction through Maillard-induced conjugation was investigated in Chapter III. The FC of all conjugates was consistently higher than that of raw PPEF at pH 7 and 10, with significant variations at pH 4 depending on the specific enzyme treatment. Zhao *et al.* (2021) found that the foaming capacity of rice protein conjugates improved especially at pH levels below 5.5 and above 10.0, with conjugates' foaming properties doubling at pH 6.5. In different research, the foaming properties of peanut protein isolate (PnPI)-dextran conjugates were investigated (Liu *et al.*, 2012). The FC of dextran-conjugated PnPI showed significant improvements compared to untreated PnPI. The authors attributed this enhancement to the higher solubility of dextran-conjugated proteins, which allowed for faster transfer to the air-water interface, thereby improving FC (Liu *et al.*, 2012).

The FS of the conjugates did not show any significant differences ($p < 0.05$) from each other at the three pH values (4,7 and 10) under analysis. Although the controls recorded the highest FS at pH 4 (80.7 %), it was not significantly greater than the other conjugates. The Hconj samples recorded the highest FS at pH 10 (74.9 %). At pH 7, HiP-MdS conjugates revealed the highest FS of 81.1 % among all the conjugates. Contrary to previous research by Konieczny *et al.* (2020a) or Goertzen *et al.* (2021a), the FS of the conjugates at pH 4 in the present study had no significant differences when compared to the FS at pH 7 and 10. The lowest FS was recorded for HiP-LwS conjugates at pH 7.

Similar observations have been made in the first and second studies where it was revealed that the FS of trypsin-treated pea protein conjugates was significantly higher than that of papain-treated conjugates across all pH levels, with trypsin controls showing the highest FS values at pH 4 (76.9%) (Chapter III). Zha *et al.* (2019) reported that the FS of pea protein dextran conjugates increased by about 115 % after 7 days of reaction time relative to raw PnPI. Rice protein-Arthrobacter exopolysaccharide conjugates displayed improved foaming stability, indicating their potential for application in foamy food products (Zhao *et al.*, 2021).

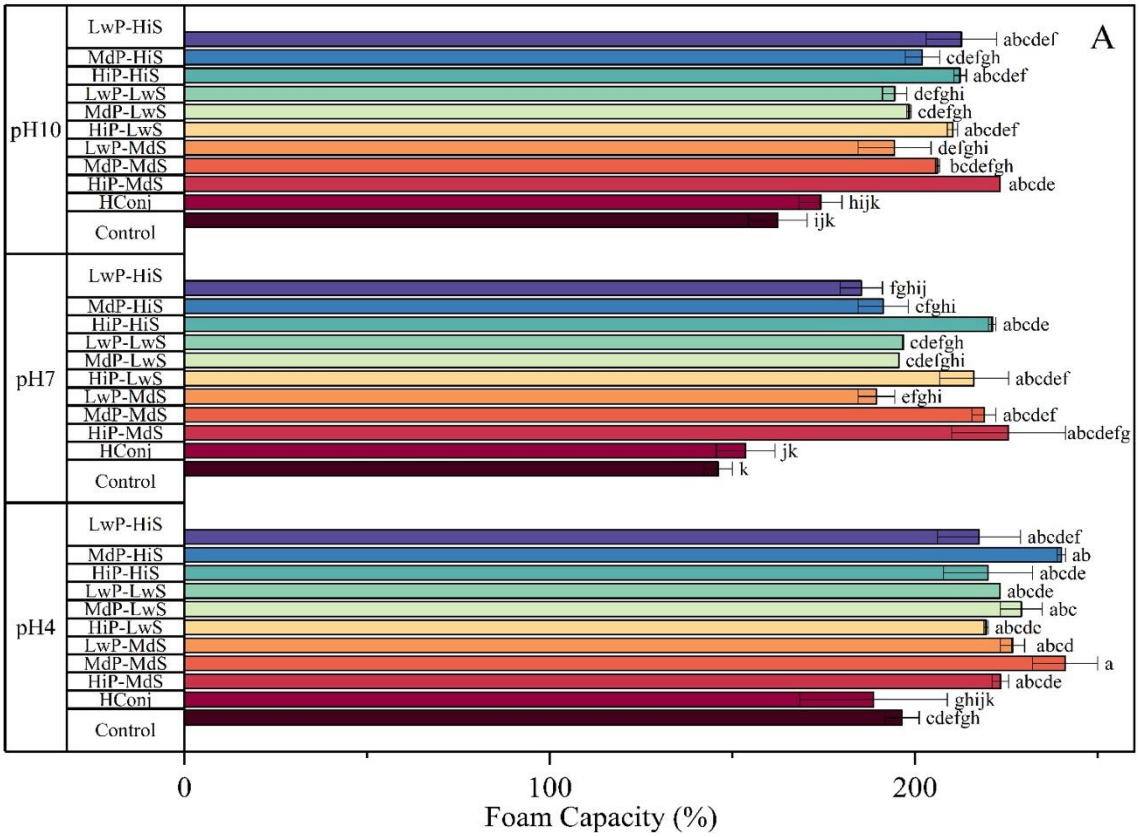
A
pH10
LwP-HiS
MdP-HiS
HiP-HiS
LwP-LwS
MdP-LwS
HiP-LwS
LwP-MdS
MdP-MdS
HiP-MdS
HConj
Control
abcdef
cdefgh
abcdef
defghi
cdefgh
abcdef
defghi
bcdefgh
abcde
hijk
ijk
pH7
fghij
efghi
abcde
cdefgh
cdefghi
abcdef
efghi
abcdef
abcdefg
jk
k
pH4
abcdef
ab
abcde
abcde
abc
abcde
abcd
a
abcde
ghijk
cdefgh
0
100
200
Foam Capacity (%)

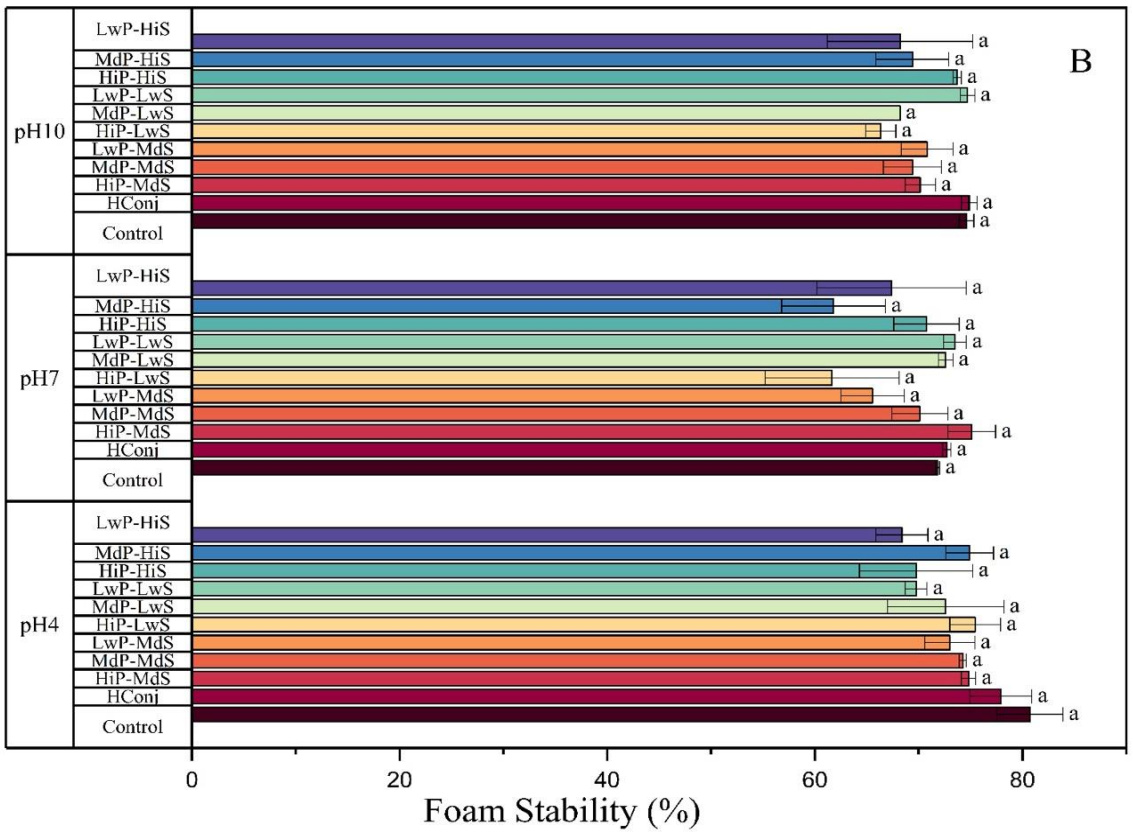
B
pH10
LwP-HiS
MdP-HiS
HiP-HiS
LwP-LwS
MdP-LwS
HiP-LwS
LwP-MdS
MdP-MdS
HiP-MdS
HConj
Control
a
pH7
pH4
0
20
40
60
80
Foam Stability (%)

Figure 5.7. (A) Foam capacity and (B) foam stability (%) of control, heated and hydrolyzed conjugates at pH 4, 7 and 10.

Control: No heat or enzyme treatment. Hconj: Heated raw PPEF and PSEF mixtures without any enzyme treatment. HiP-MdS: Conjugates formed using a mixture of high degree of protein hydrolysis and medium degree of starch hydrolysis, MdP-MdS: Conjugates formed using a mixture of medium degree of protein hydrolysis and medium degree of starch hydrolysis, LwP-MdS: Conjugates formed using a mixture of low degree of protein hydrolysis and medium degree of starch hydrolysis, HiP-LwS: Conjugates formed using a mixture of high degree of protein hydrolysis and low degree of starch hydrolysis, MdP-LwS: Conjugates formed using a mixture of medium degree of protein hydrolysis and low degree of starch hydrolysis, LwP-LwS: Conjugates formed using a mixture of low degree of protein hydrolysis and low degree of starch hydrolysis, HiP-HiS: Conjugates formed using a mixture of high degree of protein hydrolysis and high degree of starch hydrolysis, MdP-HiS: Conjugates formed using a mixture of medium degree of protein hydrolysis and high degree of starch hydrolysis and LwP-HiS: Conjugates formed using a mixture of low degree of protein hydrolysis and high degree of starch hydrolysis.

5.4.8.3 Emulsifying properties (emulsion activity index and emulsion stability index)

The emulsifying properties of the hydrolyzed control and unhydrolyzed samples were analyzed at pH 4, 7 and 10. A two-way ANOVA followed by Tukey mean comparison test was utilized to analyze significant differences at $p < 0.05$ with pH and conjugate as variable factors. The emulsion activity index (EAI) of the controls, unhydrolyzed conjugates and the hydrolyzed conjugates showed some significant differences. The EAI of all the samples were observed to be the highest at pH 10 (29.8 to 36.0 m^2/g) followed by EAI at pH 7 (25.4 to 30.7 m^2/g) and pH 4 (4.5 to 23.0 m^2/g). This can be correlated to the zP data (Table 5.1) which also shows that the surface charge of the conjugates are highly negative at pH 7 and 10 indicating higher solubility owing to electrostatic repulsive forces. As a result, the conjugates remain in solution and exhibit enhanced functional properties. Among the different conjugate and pH levels studied, LwP-MdS conjugates showed the highest EAI at pH 4 ($23.0 \pm 1.4 m^2/g$) and pH 10 ($36.0 \pm 1.0 m^2/g$), whereas MdP-LwS conjugates had the highest EAI at pH 7 ($30.7 \pm 0.3 m^2/g$). The EAI is a measure of the interfacial area between the oil and water droplets that can be coated by a gram of emulsifier and is dependent on the rate at which the emulsifier can diffuse through the solution and adsorb onto the oil water interface. This is again governed by the size of the conjugate, its spatial orientation as well as the distribution of hydrophobic and hydrophilic moieties on its surface. The above two conjugates possibly had one or more of the properties as a result of which they showed higher EAI than the other conjugates. The EAI of the hydrolyzed conjugates at pH 7 were not significantly different from each other ($p < 0.05$). The EAI of most of the conjugates were not significantly different at pH 7 and 10. However, significant differences were observed between the conjugates at pH 4 and pH 10. The lowest EAI was recorded for Hconj at pH 4 (4.5 m^2/g).

The difference in emulsion stability index (ESI) of the controls and conjugates at all three pH values was not statistically significant ($p < 0.05$). The highest ESI was observed for MdP-MdS conjugates (13.9 ± 0.1 min) followed by LwP-HiS (13.6 ± 0.1 min) at pH 4. Contrary to previous research by Konieczny *et al.* (2020a) and Goertzen *et al.* (2021a), the EAI at pH 4 were also similar to those obtained at pH 7 and 10 which also correlated with the FC data which showed that the conjugates at pH 4 had comparable FC to the conjugates at pH 7 and 10. The highest ESI at both pH 7 and pH 10 were recorded for HiP-MdS conjugates as 13.5 and 13.2 min respectively.

Zha and colleagues investigated the emulsification properties of pea protein concentrate-gum Arabic (PPC-GA) conjugates (Zha *et al.*, 2019). It was reported that the conjugates

significantly improved the physical stability of corn oil-in-water emulsions under varying pH conditions. In a separate research, Zhao and colleagues reported that rice protein-*Arthrobacter* exopolysaccharide conjugates displayed improved emulsifying ability across various pH levels, with the emulsifying activity and stability significantly higher than untreated rice protein, particularly at pH levels between 4.0 and 10 (Zhao *et al.*, 2021). Mu *et al.* (2011) noticed a 50 % increase in the EAI for the SPI-AG conjugates as compared to the native SPI at pH 7.5, whereas the increase at pH 4.5 was over 100%. The emulsification properties of enzymatically hydrolyzed pea protein conjugated with the carbohydrate fraction through the Maillard reaction have also been studied in Chapter III. The results indicated that all conjugates exhibited higher EAI than the raw PPEF at all tested pH levels. However, Tryp conjugates exhibited variable ESI at pH 7 and 10, whereas Pap conjugates consistently outperformed raw PPEF across all pH levels.

Table 5.3. Emulsion activity index (EAI), emulsion stability index, water holding capacity and oil holding capacity of control, unhydrolyzed and hydrolyzed conjugates

	Emulsion Activity Index (m^2/g)			Emulsion Stability Index (ESI)			WHC	OHC
Samples	**pH 4**	**pH 7**	**pH 10**	**pH 4**	**pH 7**	**pH 10**		
Controls	17.3 ± 0.2^{efgh}	26.9 ± 1.6^{abcdef}	34.0 ± 1.2^{a}	12.7 ± 0.2^{b}	12.6 ± 0.2^{b}	12.3 ± 0.2^{b}	1.9 ± 0.0^{ab}	1.0 ± 0.1^{bc}
Hconj	4.5 ± 0.0^{h}	25.4 ± 0.3^{abcdef}	29.8 ± 1.0^{abcd}	0^{a}	12.7 ± 0.2^{b}	12.7 ± 0.2^{b}	2.1 ± 0.1^{a}	1.0 ± 0.0^{bc}
HiP-MdS	19.6 ± 0.7^{defgh}	25.8 ± 0.2^{abcdefg}	31.1 ± 0.6^{abcd}	12.3 ± 0.4^{b}	13.5 ± 0.2^{b}	13.2 ± 0.2^{b}	1.2 ± 0.0^{c}	1.1 ± 0.0^{bc}
MdP-MdS	13.7 ± 0.6^{fgh}	28.4 ± 0.3^{abcdef}	34.0 ± 1.3^{abcd}	13.9 ± 0.1^{b}	12.7 ± 0.1^{b}	12.5 ± 0.1^{b}	1.2 ± 0.1^{bc}	1.3 ± 0.1^{ab}
LwP-MdS	16.2 ± 1.2^{gh}	29.9 ± 0.2^{abcdefg}	33.9 ± 1.4^{abcd}	12.9 ± 0.4^{b}	12.5 ± 0.1^{b}	12.5 ± 0.1^{b}	0.9 ± 0.1^{c}	1.5 ± 0.1^{a}
HiP-LwS	16.6 ± 0.8^{bcdefg}	28.8 ± 0.6^{abcde}	29.5 ± 1.2^{abc}	12.8 ± 0.5^{b}	13.1 ± 0.0^{b}	13.0 ± 0.2^{b}	1.2 ± 0.1^{c}	1.3 ± 0.1^{abc}
MdP-LwS	18.7 ± 0.4^{cdefg}	30.7 ± 0.3^{abcde}	33.4 ± 0.5^{abcd}	12.6 ± 0.1^{b}	12.7 ± 0.1^{b}	13.0 ± 0.1^{b}	1.2 ± 0.1^{bc}	0.9 ± 0.0^{c}
LwP-LwS	23.0 ± 1.4^{defgh}	30.3 ± 0.7^{abcde}	36.0 ± 1.0^{ab}	12.0 ± 0.3^{b}	12.5 ± 0.1^{b}	12.7 ± 0.1^{b}	1.1 ± 0.1^{c}	1.1 ± 0.1^{bc}
HiP-HiS	21.7 ± 0.6^{abcdefg}	26.9 ± 0.5^{abcdef}	34.9 ± 1.4^{abc}	12.0 ± 0.1^{b}	13.0 ± 0.2^{b}	13.1 ± 0.2^{b}	1.4 ± 0.2^{bc}	1.0 ± 0.0^{bc}
MdP-HiS	20.1 ± 1.0^{bcdefg}	30.4 ± 0.6^{abcde}	33.6 ± 1.2^{abcd}	12.5 ± 0.1^{b}	12.7 ± 0.1^{b}	12.8 ± 0.2^{b}	1.1 ± 0.1^{c}	1.0 ± 0.1^{bc}
LwP-HiS	15.4 ± 0.5^{efgh}	28.3 ± 0.6^{abcdef}	33.4 ± 1.1^{abcd}	13.6 ± 0.1^{b}	12.5 ± 0.1^{b}	12.8 ± 0.2^{b}	1.1 ± 0.2^{c}	1.0 ± 0.0^{bc}

Control: No heat or enzyme treatment. Hconj: Heated raw PPEF and PSEF mixtures without any enzyme treatment. HiP-MdS: Conjugates formed using a mixture of high degree of protein hydrolysis and medium degree of starch hydrolysis, MdP-MdS: Conjugates formed using a mixture of medium degree of protein hydrolysis and medium degree of starch hydrolysis, LwP-MdS: Conjugates formed using a mixture of low degree of protein hydrolysis and medium degree of starch hydrolysis, HiP-LwS: Conjugates formed using a mixture of high degree of protein hydrolysis and low degree of starch hydrolysis, MdP-LwS: Conjugates formed using a mixture of medium degree of protein hydrolysis and low degree of starch hydrolysis, LwP-LwS: Conjugates formed using a mixture of low degree of protein hydrolysis and low degree of starch hydrolysis, HiP-HiS: Conjugates formed using a mixture of high degree of protein hydrolysis and high degree of starch hydrolysis, MdP-HiS: Conjugates formed using a mixture of medium degree of protein hydrolysis and high degree of starch hydrolysis and LwP-HiS: Conjugates formed using a mixture of low degree of protein hydrolysis and high degree of starch hydrolysis.

5.4.8.4 Water holding capacity and oil holding capacity

The water and oil holding capacities of the controls and conjugates were studied at neutral pH. One way ANOVA followed by Tukey mean comparison test showed significant differences in the WHC and OHC of the conjugates. The WHC of the heated conjugates (2.1 g/g) was significantly higher ($p < .05$) than the hydrolyzed conjugates. The WHC of the conjugates followed the controls (1.8 g/g). The WHC is related to the intrinsic composition of the proteins and its ability to form hydrogen bonding with water. Figure 5.1 reveals that the extent of Amadori compound formation for Hconj is quite high and this might result in higher hydrogen bond formation with the water molecules owing to an increase in the number of hydroxy groups (of the polysaccharide fraction). It has been previously stated that highly charged protein molecules tend to hold more water through electrostatic forces of attraction (Stone *et al.,* 2015). This must be a cause for the increased WHC of the controls that carry an increased surface charge (-26.6 ± 0.9 mV) at pH 7 (Table 5.1). Thus, although there was no protein-starch conjugation, these controls revealed higher WHC than the other conjugates.

One-way ANOVA revealed significant differences between the OHC of conjugates. LwP-MdS conjugates showed the highest OHC (1.5 g/g) followed by the MdP-MdS conjugates (1.3 g/g). The OHC of the other conjugates were not significantly different with the lowest OHC being exhibited by MdP-LwS conjugates (0.9 g/g). Protein hydrolysis unravels the protein structure and exposes the buried hydrophobic groups from the core of the proteins (Mookerjee *et al.*, 2023). Owing to their non-polar nature, these groups interact with fat and bind them via hydrophobic interactions (Lam *et al.*, 2017; McClements, 2015). Low and medium degrees of protein hydrolysis unraveled the protein structure and resulted in the exposure of increased number of hydrophobic groups/patches as compared to the other conjugates as a result of which they could better orient and bind the oils (Goertzen *et al.*, 2021a; Konieczny *et al.*, 2020a).

5.5 Discussion

The primary objective of this study was to investigate how the addition of hydrolyzed starch influences the functional and structural properties of pea proteins. Both protein and starch were hydrolyzed at a variety of degrees using protease and amylase, respectively, and the resulting hydrolysates were heat-treated to form conjugates. The structure of protein-polysaccharide conjugates has been extensively in literature to better understand the various associations within these complexes. The microstructure of pea protein-gum Arabic conjugates obtained using a controlled Maillard reaction have been observed by using Scanning Electron microscopy (SEM) (Li *et al.*, 2016; Yuan *et al.*, 2024). The secondary structure can be further validated quantitatively through Fourier transform infrared (FTIR) spectroscopy by examining the formed functional groups (Chen *et al.*, 2019; Habinshuti *et al.*, 2021). The confirmational changes can also be analyzed by understanding the fluorescence spectra of the conjugates (Qiu *et al.*, 2017; Shen *et al.*, 2021). Owing to the differences in molecular weights between proteins and polysaccharides, along with the variability in functional groups, the food industry develops various processed foods with enhanced functional properties by combining proteins and polysaccharides (Cassiani *et al.*, 2013). Spectrograph of Amadori products (Figure 5.1) and size analyses using SDS-PAGE gels (Figure 5.2) and HP-SEC (Table 5.2) confirmed the formation of protein hydrolysates and high-molecular-weight protein-starch conjugates. SEM micrographs revealed a range of compounds, such as protein-protein aggregates, protein-starch and protein-carbohydrate conjugates, damaged starch granules, non-starch polysaccharides, and intact protein bodies (Figure 5.3). FTIR and fluorescence spectroscopy further supported the microstructure and molecular weight data, indicating the formation of new covalent interactions, as shown by the peaks in the graphs (Figures 4 and 5). The functional properties observed in this study could be a result of interactions between these macromolecular species and solvent molecules as discussed by several other groups (de Oliveira *et al.*, 2016; Kutzli *et al.*, 2021a; Wang *et al.*, 2018).

The controls were prepared by simply mixing protein and starch solutions, followed by spray drying. The high solubility of the control samples is likely due to the absence of a heat treatment step, which allowed the proteins to remain intact and thus enhanced their solubility. Heat treatment leads to partial protein denaturation, as evidenced by SEM imaging (Figure 5.3). The aggregation of denatured protein bodies, combined with the bulky nature of starch granules, likely reduced protein-water interactions, resulting in slightly decreased solubility for the conjugates.

The decreased solubility of Maillard Reaction products (MRPs) is often linked to the formation of final stages of MRPs, although this is contradicted by the Abs_{304nm} and Abs_{420nm} data (Figure 5.1A) which revealed that the formation of MRPs mostly remained at the initial stage of Maillard Reaction, *i.e.*, Amadori products (Zhong *et al.*, 2019). Oliver suggested that disulfide bonding and isopeptide crosslinking in proteins also affect the solubility of conjugates, emphasizing the importance of protein biochemistry and the molecular structure and chemistry of the reacting sugars in determining protein solubility (Oliver *et al.*, 2006). Enzymatic hydrolysis generated various polypeptides, as demonstrated in the SDS-PAGE gel (Figure 5.2A). These polypeptides exhibited different degrees of conjugation with dextrins of varying molecular masses, resulting in differing affinities for water and slight variations in solubility. Consequently, even though the conjugates displayed highly negative zP values, their solubility was not directly proportional to surface charge and was influenced by the presence of starch granules or other non-starch polysaccharides.

Foam capacity (FC) refers to a protein's ability to trap air within a continuous liquid or semi-solid phase. Protein molecules migrate to the air-water interface, where they unfold, orient, and concentrate to form a thick, viscoelastic film around gas bubbles (Mookerjee *et al.*, 2023). On the other hand, the emulsion activity index (EAI) provides a measure of the interfacial area between the oil droplets and water that can be coated by one gram of an emulsifier (Lam *et al.*, 2018). Both FC and EAI reflect the surface activity of proteins, which depends on their solubility, size, and molecular flexibility. When bulky starch molecules conjugate with proteins, they shield the electrical double layer and increase steric repulsion between molecular species (Mulcahy *et al.*, 2016; Wang *et al.*, 2012). Unlike hydrolyzed proteins, these conjugates do not aggregate or precipitate at acidic pH, leading to enhanced foam capacity for all hydrolyzed conjugates, particularly MdP-MdS, MdP-LwS, LwP-MdS, LwP-LwS, and HiP-LwS at pH 4 (Figure 5.7). Similarly, improved emulsion activity was observed for HiP-HiS, HiP-LwS, MdP-HiS, and HiP-MdS conjugates at pH 4 (Table 5.3). Enzymatic cleavage produces short-chain polypeptides (Figure 5.2A), and when complemented by starch conjugation, it likely results in conjugates with optimal size and molecular flexibility (Lam *et al.*, 2018). The formation of new molecular species is also evident in FTIR-ATR results (Figure 5.4). Consequently, it can be hypothesized that most conjugate mixtures at pH 7 and 10, such as HiP-MdS, HiP-LwS, HiP-HiS, and LwP-HiS, were able to migrate through the solution and adsorbed onto the air/water interface, showing improved

FC. SEM micrographs indicated protein-starch conjugation, suggesting increased amphiphilicity of the formed molecular species. High amphiphilicity, along with improved solubility, allowed for rapid surface adsorption of the conjugate species and hydrolyzed protein bodies at the oil-water interface, with hydrophobic groups facing the oil phase and hydrophilic groups facing the water phase, resulting in enhanced EAI of the heated and hydrolyzed conjugates at pH 7 and 10 (Table 5.3) (Konieczny *et al.*, 2020a; Mokni Ghribi *et al.*, 2015; Zha *et al.*, 2020). The significantly higher EAI observed for the control samples can be attributed to their high protein solubility of 55.2%, which led to rapid diffusion and effective surface stabilization of the emulsion droplets formed (Avramenko *et al.*, 2013).

Both the foam stability (FS) and emulsion stability index (ESI) of the conjugates showed no significant differences among pH 4, 7 and 10. Pea proteins are known to aggregate at acidic pH levels, particularly near their isoelectric point (Konieczny *et al.*, 2020a). Despite this tendency, the higher foam and emulsion stability observed at pH 4 should be attributed to proteins drawing closer together without aggregating, due to steric repulsion from carbohydrates. The balance between electrostatic attraction and steric repulsion likely stabilized the viscoelastic layer of the conjugates at the interface, resulting in enhanced foam and emulsion stability (Mookerjee *et al.*, 2023; Mulcahy *et al.*, 2016).

At neutral pH (pH 7), the starch solubility of the conjugate mixtures was lower than that of the proteins (Figure 5.6), and SEM micrographs revealed the presence of damaged yet intact starch granules (Figure 5.3). This suggests that the starch was not fully solubilized by the water molecules and instead existed as a dispersion, adding an additional layer to the proteins and further increasing their viscosity. This contributed to improved emulsion stability in most of the hydrolyzed conjugates and enhanced foam stability in HiP-MdS, LwP-LwS, HiP-HiS, and other conjugates at pH 7 and 10.

The correlation between the FC and FS data suggests that the conjugates not only diffused and oriented at the interface but also effectively stabilized the foams over an extended period. The EAI and ESI data showed a direct relationship at pH 7 and 10. However, at pH 4, while the EAI was lower, the ESI remained high, likely due to the presence of heavier starch granules that added an extra viscous layer, thereby stabilizing the foams (McClements, 2015).

The high water-holding capacity (WHC) observed in the heated conjugates is likely due to their conjugation with intact hydrophilic starch granules, which increased the number of hydroxy

groups in the system. As shown in Figure 5.6, the starch solubility of the heated conjugates was lower than that of the hydrolyzed conjugates, indicating that the hydrolyzed dextrins were mostly solubilized by water molecules. Since no enzymatic pretreatments were applied to the heated conjugates, intact starch granules likely remained dispersed in the solution, increasing their affinity for water molecules without being fully solubilized. This water-binding property of starch through electrostatic forces and hydrogen bonding likely contributed to the increased WHC of the heated conjugates compared to the hydrolyzed ones (Chapter III). The high oil-holding capacity of the LwP-MdS conjugates can be attributed to low trypsin activity, which may have resulted in optimal cleavage of protein molecules and exposure of hydrophobic amino acids, allowing for better interaction and binding with oils (Goertzen *et al.*, 2021a). Figure 5.5 also shows lower intensity for the LwP-MdS conjugates, indicating less tryptophan quenching, which would enable more hydrophobic interactions with the oil droplets.

Literature suggests that extensive proteolysis typically leads to a loss of protein structure, resulting in a marked reduction in functional properties (Konieczny *et al.*, 2020a). However, this research demonstrated that high degrees of proteolysis, when combined with starch conjugation, enhanced the techno functionality of proteins. Conjugates with a high degree of proteolysis (HiP-LwS, HiP-MdS, HiP-HiS) showed improved foaming capacities at pH 7 and 10, along with enhanced foam stability across all tested pH values. Additionally, HiP-HiS and HiP-LwS exhibited the highest emulsification activity at pH 4 and pH 7, respectively, although no significant differences were observed between highly proteolyzed and other samples ($p < 0.05$). Notably, HiP-HiS also demonstrated the greatest water-holding capacity (WHC) among all hydrolyzed conjugates.

A closer analysis of Figure 5.2A reveals the formation of more low molecular weight peptides, suggesting the creation of shorter, more flexible conjugates that diffuse more efficiently through the solution and reorient at the air-water and oil-water interfaces, enhancing both foaming capacity and emulsification activity (Mookerjee *et al.*, 2023). Furthermore, absorbance data at 304 nm (Figure 1) indicates significantly higher values for HiP-MdS conjugates, with HiP-HiS and HiP-LwS also showing elevated absorbance at this wavelength. This is corroborated by SEM images (Figure 5.3: Images E, H, and K), which illustrate increased conjugation in highly proteolyzed samples. The greater degree of conjugation enhanced the amphiphilic properties of

these conjugates, contributing to their improved surface activity leading to enhanced FS and ESI (Chapter III).

5.6 Conclusion

This research highlights the significant impact of structural modifications on the functional properties of pea protein-starch conjugates, demonstrating how enzymatic hydrolysis and heat induced Maillard conjugation can be effectively utilized to enhance these biopolymers' functionality. The study found that enzymatic hydrolysis, followed by heat treatment, produced conjugates with markedly improved starch solubility, foaming and emulsification properties, and water-holding and oil-holding capacities. These improvements are attributed to the structural changes induced by the conjugation process, including the formation of protein-starch conjugates, protein-protein aggregates, and the interaction between hydrophilic starch granules and protein molecules. Of notable mention were the conjugates having high degrees of proteolysis which showed improved foaming and emulsification properties at all the three pH values which indicated that although high degrees of protein hydrolysis deteriorate the protein structure, complexed with starch and other polysaccharides they can show improved functionality.

The practical implications are substantial, particularly for developing food products that demand improved solubility, emulsification, and stabilization. The superior functional properties of these conjugates make them suitable for use in low-fat and high-protein formulations where texture, moisture, and stability are critical. Additionally, employing starch-rich byproducts from air classification to create these functional ingredients offers a sustainable approach to utilizing potentially wasted materials, promoting more efficient, cost-effective, and eco-friendly food production practices. Their enhanced solubility can be applied in the production of plant-based protein shakes to achieve the desired mouthfeel. Improved foaming capacity at pH 4 suggests their potential as foaming agents in beverages like lattes, cappuccinos, and fruit-based drinks such as smoothies. The increased emulsification stability at pH 4 could be beneficial in applications such as salad dressings, creamy spreads, and mayonnaise. Additionally, their improved oil-holding capacity makes them suitable for fat replacement in reduced-fat foods, providing similar sensory qualities to high-fat alternatives, and for enhancing texture in meat substitutes and vegetarian patties. Finally, the enhanced water-holding capacity can be utilized to develop high-fiber snacks, like granola bars, promoting better digestive health.

Future research should focus on further exploring the application of these pea protein-starch conjugates in various food systems, especially under conditions that may impact protein functionality (like acidic pH ranges). Additionally, optimizing the hydrolysis and conjugation processes could tailor these conjugates' functionality for specific applications, such as in gluten-free products, dairy alternatives, and plant-based meat substitutes. Refining these processes may lead to the development of highly specialized ingredients, such as plant-based foaming agents, emulsifiers, and binding agents, meeting the growing demand for functional and sustainable food products in the global market.

CHAPTER VI

6 General Discussion, Overall Conclusion, And Future Studies

6.1 General discussion

The primary objective of this project was to enhance the amphiphilicity of proteins by introducing hydrophilic groups onto their surfaces. It was hypothesized that this increased amphiphilicity would improve the proteins' functional properties. To achieve this, a natural approach, *i.e.*, heat-induced Maillard reaction conjugation was employed. This method is widely used as a glycation method, believed to avoid toxic byproducts. Additionally, by minimizing the use of exogenous additives and by utilizing low-value byproduct streams like the starch enriched fraction, it was aimed to make the process more sustainable. This study provides insights into how heat-induced conjugation with carbohydrate or starch fractions can significantly enhance the techno-functional properties of hydrolyzed pea proteins without relying on costly processing aids. Plant proteins typically exhibit low solubility at acidic pH due to their isoelectric points being in the acidic range. This leads to low stability of plant proteins in techno-functional applications. This thesis research, conducted across three studies, has demonstrated that protein-carbohydrate and protein-starch conjugates exhibit improved stability under varying pH conditions and show enhanced functional properties, such as foaming and emulsification. Understanding the necessary conditions for formulating these ingredients is crucial for scaling up the process for industrial production. This thesis research has also elucidated the extent to which different process parameters can be controlled to optimize conjugate formation and functional property enhancement. Additionally, the incorporation of more legume-based materials into the food and feed industries could boost their popularity and serve as a foundation for reducing reliance on animal-based products in the functional food sector. The first study (Chapter III) focused on developing protein-carbohydrate conjugates using hydrolyzed pea proteins derived from the fine fraction of air-classified pea flours and the starch present in this fraction.

Two proteases, trypsin and papain, were used to hydrolyze the protein fraction to achieve low and medium degrees of hydrolysis. These hydrolysates were then heat-treated to form conjugates with carbohydrates and residual cell wall materials from the fine fraction of the air classification process. Results revealed that the conjugation degree (CD) was notably higher in the papain treated conjugates which indicated a more extensive Maillard reaction compared to the trypsin-treated samples. Absorbance at 304 nm, indicative of Amadori compound formation, was significantly greater in the conjugated samples than in untreated pea protein-enriched flour (PPEF), confirming successful conjugation. The protein content in the conjugates was obtained to be less than the control samples reflecting the formation of covalent bonds between the α-amino groups of proteins and the hydroxyl groups of carbohydrates during the Maillard reaction. The SDS-PAGE stained using Fuchsin sulfite also showed a pink smear further proving the formation of protein-carbohydrate conjugates which in turn showed a positive correlation with the functional properties. Increased negative zeta potential at neutral and alkaline pH levels indicates better solubility due to enhanced electrostatic repulsion. Trypsin treated conjugates showed significant improvement in both foam capacity and emulsion stability at pH 4 over untreated sample. On the other hand, foam stability was the highest in heated trypsin controls at pH 4, reflecting enhanced stability at acidic pH. The emulsion activity index (EAI) was higher for hydrolyzed protein-carbohydrate conjugates at pH 4 than at pH 7, suggesting better emulsion formation under acidic conditions. Water-holding capacity (WHC) of both the controls and treated conjugates and oil-holding capacity (OHC) in the control were significantly improved. The study effectively demonstrated that enzymatic proteolysis followed by Maillard-induced conjugation significantly improves the functional properties of pea protein-enriched flour. The improved foaming capacity and emulsion stability at pH 4 suggest their suitability for acidic food products such as processed drinks and salad dressings. The notable increases in WHC and OHC make these conjugates ideal for applications requiring moisture retention and fat binding, such as in low-fat formulations. Moreover, utilizing naturally occurring carbohydrates in the pea flour, rather than external additives, will reduce production costs and heat treatment as a processing parameter support clean-label trends as envisioned, offering a sustainable solution for the food industry. Overall, the findings highlight the potential of enzymatically modified pea proteins with low and medium degrees of hydrolysis as versatile, functional ingredients, particularly for applications requiring enhanced solubility, emulsion stability, water hydration and oil binding.

Proteins with high degrees of hydrolysis are typically considered to exhibit poor techno-functional properties. This is due to the complete unraveling of the protein structure, resulting in the formation of short peptides that diminish functionality. As the first study showed significant improvements in techno-functionality, the second study hypothesized that conjugating extensively hydrolyzed proteins with the residual carbohydrate fraction of the coarse fraction will lead to the formation of protein-carbohydrate conjugates which combined with the protein-protein aggregates in the conjugate mixtures could enhance the stability of these conjugate mixtures and potentially achieve functionality comparable to, or better than, that of native proteins. The second study aimed to evaluate the effect of carbohydrate conjugation on proteins with high degrees of hydrolysis (greater than 15%) on their functional properties. As in the first study, both trypsin and papain were used, with varying ratios to produce hydrolysates with different degrees of hydrolysis. The initial starch concentration, *i.e*., added starch rich flour, was set at less than 3%, limiting the dextrose equivalent to lesser than 1%. Trypsin-treated samples demonstrated a higher degree of hydrolysis, compared to papain-treated samples. This extensive hydrolysis resulted in increased exposure of α-amino groups, facilitating improved conjugation with carbohydrates. This is also confirmed by higher absorbance at 304 nm, indicating a greater formation of early Maillard reaction products for the trypsin conjugates. Microstructure analysis also showed the presence of homogenous starch matrix along with protein-starch conjugates, the combined effects of which are believed to improve functionality. Increased Amadori formation was thought to improve the amphiphilicity thereby resulting in enhanced functional properties which was also shown in the study. Highly negative zeta potential (zP) values of the conjugates indicated improved solubility and reduced aggregation. The foam capacity (FC) and foam stability (FS) of trypsin-treated conjugates were significantly higher than those of untreated PPEF which can be attributed to increased ARP formation. Similarly, the Emulsion Activity Index (EAI) and Emulsion Stability (ES) were significantly improved in trypsin-treated conjugates. Water-holding capacity (WHC) of trypsin-treated conjugates and oil-holding capacity (OHC) of the trypsin controls demonstrated significant improvement. This study also underscores the effectiveness of combining enzymatic hydrolysis with Maillard-induced conjugation to enhance the functional properties of pea protein-enriched flour. Owing to the improvement in different functional properties, these conjugates can also be suitable for applications in food products that require enhanced foaming, moisture retention, and emulsification. The higher degrees of hydrolysis achieved with trypsin facilitated better

carbohydrate conjugation, leading to significant functional enhancements. These findings suggest that enzymatically modified pea protein conjugates having high degrees of proteolysis also have strong potential as versatile functional ingredients in the food industry, aligning with the increasing demand for plant-based and sustainable food products.

In the first two studies, the residual carbohydrate fraction present in the fine fraction of air-classified pea flour was used for conjugation reactions. To explore whether the functional properties could be further enhanced with additional starch presence, the low-value byproduct from air classification, the starch-rich coarse fraction, was separately hydrolyzed to achieve different degrees of dextrose equivalent in the third study. This hydrolyzed starch was then Maillard-conjugated with the hydrolyzed protein fraction to create conjugates with varying degrees of protein and starch hydrolysis. A comprehensive analysis of the microstructure, molecular weight distribution, and functional groups was carried out to understand the nature and complexity of the compounds produced.

In this study, three different enzyme-to-substrate (E/S) ratios were employed to achieve varying degrees of hydrolysis (DH) for both protein and starch. The protein DH ranged from low to high (>20%), while starch dextrose equivalent (DE) varied from low to high. Higher E/S ratios and extended reaction times significantly increased DH and DE, consistent with trends observed in previous studies. Absorbance measurements at 304 nm and 420 nm, similar to the first and second studies, indicated the formation of early and intermediate Maillard reaction products, respectively. The absorbance at 420 nm was notably lower, suggesting limited progression to advanced Maillard products due to the brief heat treatment. High-Pressure Size Exclusion Chromatography (HP-SEC) revealed that hydrolyzed conjugates had higher molecular weight peaks. Scanning Electron Microscopy (SEM) revealed structural changes resulting from enzymatic hydrolysis and conjugation. These structural changes like roughness and structural deformations in starch granules, along with the clustering of protein bodies, suggest that conjugation led to stronger associations between protein and starch, enhancing functional properties. Fourier Transform Infrared Spectroscopy (FTIR) revealed changes in the functional groups in the conjugates. In conjugates, the intensity of the characteristic amide and saccharide peaks decreased, disappearance of some old peaks and appearance of new peaks were identified, indicating protein structure was altered during enzymatic hydrolysis and suggesting the formation of new covalent bonds between protein amino acids and starch hydroxyl groups as a result of heat treatment. All

these changes likely contributed to the improved functional properties, such as increased foaming and emulsification properties which was reflected in the third study. Negative zP was an indication of higher solubility which corroborated with the protein solubility results. In terms of solubility, the control samples exhibited the highest solubility while other conjugates exhibited moderate solubility. The medium hydrolyzed conjugates displayed the highest foaming capacity at pH 4, whereas foam stability at pH 7 was recorded to be the highest. The highest emulsion activity and stability indices were recorded at pH 4 and pH 10 respectively. Heated conjugates displayed the highest water-holding capacity, showing a significant increase compared to other conjugates. Proteolyzed conjugate having low DH exhibited the highest oil-holding capacity showing a significant increase over the lowest-performing conjugates. This third study demonstrated that a combination of enzymatic proteolysis and amylolysis followed by Maillard-induced conjugation significantly enhances the functional properties of pea protein-enriched flour conjugated with starch enriched flour.

Overall, this study highlights the potential of enzyme-modified pea protein-starch conjugates as functional ingredients in food products, offering enhanced stability, solubility, and textural properties. The microstructural and molecular changes observed through SEM and FTIR provide a deeper understanding of how these modifications contribute to the improved functionality of the conjugates.

Across the three research studies conducted, various conjugates with differing degrees of protein hydrolysis and dextrose equivalents were developed, each demonstrating enhancements in specific functional properties. It is challenging to single out one conjugate as the best, as their utility varies depending on the intended application. Even conjugates that did not show significant improvements or exhibited reduced functionality may still hold value, given that some food products require lower functional properties. For instance, while latte and cappuccinos demand high foam stability, carbonated beverages benefit from a thin layer of foam that quickly dissipates, indicating low foaming capacity. Similarly, mayonnaise and salad dressings require highly stable emulsions, whereas flavored yogurt, typically consumed within a few weeks of production, can afford lower emulsion stability. Low-fat products might require ingredients with minimal oil-holding capacity, whereas burger patties that aim to replicate the juiciness of beef may need high oil-holding properties.

While a comprehensive cost analysis of the process has not yet been conducted, an estimate based on the market value of the raw materials suggests that the final products will be relatively inexpensive. Pea protein-enriched fractions are currently priced at approximately $3/kg, while starch-enriched fractions cost about $2/kg. With the average cost of electricity in Canada being $0.15/kWh, producing around 1.6 kg of heated conjugates without enzymatic treatment would cost roughly $6, including raw material expenses and the electricity required for heating on a hot plate and spray drying (assuming an efficiency of ~80%). An 890 mL bottle of Great Value mayonnaise contains approximately 3.5 g of lecithin as an emulsifier. If our conjugates were used to fully replace the lecithin, the cost of the conjugates would amount to just $0.02 per bottle of mayonnaise (890 mL). Alternatively, if hydrolyzed conjugates were utilized, the price would increase slightly to account for the cost of enzymes and the conditions required to maintain enzymatic activity. However, this increase would remain minimal, ensuring the product is still cost-effective. If the conjugates were used directly in solution form as partial ingredients, the overall cost would be further reduced by eliminating the expense of spray drying.

Table 6.1 summarized a potential applications of the best conjugates based on their functional properties. This categorization provides a practical guide for selecting the most suitable conjugates from the research based on specific functional requirements, aligning them with various food product applications. It is important to note that no prototype products have been formulated; this categorization is based solely on the functional properties evaluated in the research, tailored to fit optimal applications as suggested by specific property applications discussed in literature.

Table 6.1: Probable industrial applications of specific conjugates obtained from Chapters III, IV and V based on existing literature

Conjugate	Components	Use	Application	Functional property	Rationale
MdP-MdS	Hydrolyzed protein & hydrolyzed starch	Ingredient	Supplements	Foaming, solubility	Moderate foaming capacity And improved solubility indicating quick dissolution
Pap9.1	Hydrolyzed Protein				
Tryp0	Untreated proteins	Ingredient	Coffee, Wheat beer, Craft beer, Draught beer	Foaming	Improved foam stability creating a smooth creamy mouthfeel
Hconj	Heated proteins				
MdP-HiS	Hydrolyzed protein & hydrolyzed starch				
Tryp9.9 P14.8	Hydrolyzed protein				
HiP-MdS	Hydrolyzed protein & Hydrolyzed starch	Ingredient	Soft drinks/energy drinks	Foaming	High foam capacity, low foam stability indicating rapid foam formation
Pap8.1	Hydrolyzed protein				
T19.A	Hydrolyzed protein				
MdP-MdS	Hydrolyzed protein & hydrolyzed starch	Ingredient	Lager/pilsner	Foaming	High foam capacity, moderate foam stability indicating quick foam dissipation
Pap10.2	Hydrolyzed protein				
Tryp2.5 Tryp9.9 Pap5.2	Hydrolyzed protein	Ingredient	Salad dressing	Emulsification	Enhanced emulsion stability
HiP-MdS	Hydrolyzed protein & hydrolyzed starch				

Tryp0 Pap0 MdP-MdS	Untreated proteins Hydrolyzed protein & hydrolyzed starch	Ingredient	Mayonnaise	Emulsification. Solubility	Enhanced emulsion stability, improved solubility
MdP-MdS	Hydrolyzed protein & hydrolyzed starch	Partial food	Flavoured yogurt	Emulsification, solubility	Moderate emulsion stability, improved solubility
T17.7A HiP-MdS	Hydrolyzed protein Hydrolyzed protein & hydrolyzed starch	Partial food/ ingredient	Spreads	Emulsification	Improved emulsification creating smooth texture
Tryp10.8 P15.6 HiP-MdS	Hydrolyzed protein Hydrolyzed protein Hydrolyzed protein & hydrolyzed starch	Ingredient	Reduced fat foods	Oil holding	Increased oil holding mimicking mouthfeel
Tryp0 T17.7 LwP-MdS	Untreated proteins Hydrolyzed protein Hydrolyzed protein & hydrolyzed starch	Ingredient	Vegan sausages/patties	Oil holding	Ability to bind oil and improve juiciness
Tryp0 T25.9 HiP-HiS	Untreated proteins Hydrolyzed protein Hydrolyzed protein & hydrolyzed starch	Ingredient	Energy bars	Water holding	Ability to bind water effectively
Tryp0 Hconj Pap5.2	Untreated proteins Heated proteins Hydrolyzed protein	Ingredient	Baked goods	Water holding	Improved water binding ability

6.2 Overall conclusions

Three research studies in this thesis pursued a range of objectives, each aimed at advancing the understanding of how to enhance the functional properties of pea protein-enriched flour. Initially, the focus was on determining whether protein hydrolysis followed by heat-induced conjugation could improve the functional properties of proteins at various degrees of hydrolysis, without the addition of exogenous starch. Subsequently, the studies explored the impact of high DH of proteins and low pH on the functional properties of these conjugates. The third study then examined whether the inclusion of hydrolyzed external starch and its conjugation with the protein fraction could further enhance functionality. Finally, the research sought to investigate the nature of the compounds formed during the Maillard reaction, particularly how these macromolecules interact within the system, providing deeper insights into their functional properties. Collectively, these three studies underscore the transformative potential of enzymatic modification and Maillard-induced conjugation in improving the functional properties of pea protein-enriched flour. Each study highlights different aspects of how these processes influence the structural, molecular, and functional characteristics of pea proteins, thereby enhancing their suitability for a wide array of food applications. Scanning electron microscopy (SEM) employed revealed significant microstructural changes in the protein-starch conjugates resulting from enzymatic hydrolysis and Maillard conjugation. These changes, including increased surface roughness and clustering of protein bodies, likely contribute to the improved functional properties by fostering stronger interactions between proteins and starches. High-pressure size exclusion chromatography (HP-SEC) and SDS-PAGE analyses demonstrated that the Maillard reaction resulted in the formation of higher molecular weight conjugates, confirming successful protein-starch conjugation. These higher molecular weight species are likely responsible for the enhanced functionality observed in the conjugates. Fourier transform infrared spectroscopy (FTIR) provided further evidence, showing new covalent bonds forming between protein and starch molecules, as indicated by shifts in amide peaks and the disappearance of saccharide peaks. These structural modifications confirm the successful integration of proteins and starches into more complex, functional biopolymers. Although there were some reductions in solubility following hydrolysis and conjugation, the overall functionality of the proteins was significantly enhanced. The conjugates maintained sufficient solubility to be effective in various food systems, particularly those requiring moderate solubility. The studies consistently demonstrated that enzymatic modification and Maillard

conjugation significantly improved the foaming capacity, foam stability, emulsion activity index (EAI), and emulsion stability index (ESI) of pea proteins. These enhancements make the conjugates particularly suitable for applications such as whipped toppings, emulsified sauces, and plant-based dairy alternatives. The improved water-holding capacity (WHC) and oil-holding capacity (OHC) observed across the studies suggest that these modified proteins are well-suited for products where moisture retention and fat-binding are critical, such as in low-fat or plant-based meat formulations.

Together, these three research studies provide a comprehensive understanding of how enzymatic modification and Maillard-induced conjugation can be leveraged to significantly enhance the functionality of pea protein-enriched flour. The findings not only advance the scientific knowledge of protein-carbohydrate interactions but also offer valuable insights into the development of new, highly functional food ingredients. This body of work paves the way for future research to further optimize these processes, ultimately leading to the creation of innovative, sustainable, and functional food products that meet the growing demand for plant-based and allergen-free alternatives in the global market. The use of naturally occurring carbohydrates from pea starch in the conjugation process, as explored in the first two research studies, also aligns with clean-label and sustainable food trends, providing cost-effective and eco-friendly solutions for the industry.

6.3 Future studies and prospects

This study conducted a comprehensive analysis of the enhancement in functional properties using two different proteases, i.e., trypsin (animal derived) and papain (plant derived) and α-amylase (microbial source). Both native starch and an external starch source were employed to assess the impact of their conjugation on the techno-functional properties of the resulting conjugates. Additionally, an in-depth analysis of the structural and functional properties of the conjugates was performed, with the most effective conjugates identified through lab-scale experiments.

For future research, a key focus will be on developing a similar process to produce the desired conjugates on an industrial scale. Among the conjugates studied, the most cost-effective process was observed during the production of the conjugates without any enzymatic treatments and hence they can be the first samples considered for scale-up. These untreated conjugates

demonstrated enhanced foaming, emulsification, and oil-holding properties. Since no enzyme was used in their production, scaling up the control samples could reduce enzyme-related costs, making the process more economically viable and potentially lowering the cost of the final products. Conducting a detailed lab-scale cost analysis of each procedure—from raw material and processing costs to energy consumption—can provide insights into the feasibility of scaling up the production of these lab-scale conjugates to a pilot scale, with the potential for commercialization in the food industry.

Color is a crucial attribute of food ingredients, as it significantly influences the visual appeal of food products. The Maillard reaction leads to the formation of colored pigments that may negatively affect this visual appeal (Kutzli *et al*., 2021). Therefore, it is essential to assess the color profile of these ingredients prior to their incorporation into food products. In the future, the *L**, *a**, and *b** values can be analyzed using a Hunter Lab colorimeter to evaluate their color characteristics.

While most functional properties were influenced by the interfacial characteristics of the conjugate mixtures, these specific interfacial properties were not examined in this study. Investigating interfacial properties of protein-dextrin conjugates—such as surface tension, interfacial tension, interfacial dynamics, and interfacial rheology—could provide deeper insights into their interactions with various solvents and food matrices and represents a promising area for future research.

While the degree of protease hydrolysis did influence the functional properties, there were no significant differences observed between the various combinations of protein and starch hydrolysis levels studied. Therefore, it would be worthwhile to explore different ratios of protein from the fine fraction and starches from the coarse fraction to formulate the conjugate mixtures. A specific protein-to-starch ratio might significantly enhance the functional properties of the conjugates. Conjugate preparation using different protein to polysaccharide ratios have been reported extensively in the literature (Kutzli *et al.*, 2021; Niu *et al.*, 2011; Pirestani *et al.*, 2017; Yang *et al.*, 2022; Zhang *et al.*, 2022).

Various researchers have experimented with different Maillard reaction conditions. In this thesis experiments, the mixtures were heated at 90°C for 30 minutes. Adjusting the reaction conditions—such as lowering the temperature and/or extending the reaction time—could potentially increase covalent crosslinking, leading to the formation of more conjugates and thereby

enhancing functionality (Kutzli *et al.*, 2020). However, it is crucial to carefully monitor the heating temperature and duration, as prolonged exposure to high temperatures can lead to the formation of advanced Maillard reaction products. These advanced products are often undesirable, as they can negatively impact the sensory properties of food and are implicated in the pathogenesis of chronic diseases (de Oliveira *et al.*, 2016).

The Maillard reaction generates a wide array of compounds during its initial stages, including various aminoketoses, N-ketosylamines, aminodeoxyaldoses, furfural, hydroxymethylfurfural, acetol, pyruvaldehyde, and diacetyl. As the reaction progresses, these early-stage compounds undergo complex processes such as cyclization, dehydration, retroaldolization, enolization, oxidation, fragmentation, rearrangement, isomerization, and further condensation, resulting in the formation of numerous poorly characterized compounds (Kutzli *et al.*, 2021). Many of these compounds contribute to specific sensory attributes, such as aroma and flavor, when present in food ingredients. Future research could involve in-depth analysis of these compounds using headspace GC-MS to better understand the sensory properties associated with each compound (Kryachko *et al.*, 2020; Zha *et al.*, 2019). This would aid in the formulation of food products with desired aromas while minimizing undesirable off-flavors in processed foods.

While the initial stages of the Maillard reaction are responsible for producing desirable aromas and flavors, the advanced stages of this reaction can result in the formation of acrylamide, an undesirable byproduct. Acrylamide is known for its neurotoxic effects at high doses and has been classified as a probable human carcinogen. To mitigate potential health risks associated with these conjugates, it would be essential to quantify acrylamide levels in the conjugate solutions. Analytical techniques such as high-performance liquid chromatography-mass spectrometry (HPLC-MS), gas chromatography-mass spectrometry (GC-MS), or enzyme-linked immunosorbent assay (ELISA) can be employed to achieve accurate and reliable detection.

The future prospects of this research also hold great potential for further enhancing the functional properties of protein-starch conjugates and expanding their industrial applications. By refining production processes and optimizing reaction conditions, these advancements could lead to the development of innovative food ingredients with improved functionality. Continued research in this area will contribute to creating more sustainable, cost-effective, and versatile food products, addressing the evolving needs of both the industry and consumers.

CHAPTER VII

7 References

AACC International (2000). *Approved methods of the AACC International:* Method 22-40.01 (10th ed.) St. Paul, MN, USA: American Association of Cereal Chemists.

Abd El-Salam, M. H., El-Shibiny, S., & Salem, A. (2009). Factors affecting the functional properties of whey protein products: A review. *Food Reviews International*, *25*(3), 251–270. https://doi.org/10.1080/87559120902956224

Achouri, A., Zhang, W., & Shiying, X. (1998). Enzymatic hydrolysis of soy protein isolate and effect of succinylation on the functional properties of resulting protein hydrolysates. *Food Research International*, *31*(9), 617–623. https://doi.org/10.1016/S0963-9969(98)00104-5

Adal, E., Sadeghpour, A., Connell, S., Rappolt, M., Ibanoglu, E., & Sarkar, A. (2017). Heteroprotein Complex Formation of Bovine Lactoferrin and Pea Protein Isolate: A Multiscale Structural Analysis. *Biomacromolecules*, *18*(2), 625–635. https://doi.org/10.1021/acs.biomac.6b01857

Adebiyi, A. P., & Aluko, R. E. (2011). Functional properties of protein fractions obtained from commercial yellow field pea (Pisum sativum L.) seed protein isolate. *Food Chemistry*, *128*(4), 902–908. https://doi.org/10.1016/j.foodchem.2011.03.116

Adler-Nissen, J. (1979). Determination of the Degree of Hydrolysis of Food Protein Hydrolysates by Trinitrobenzenesulfonic Acid. *Journal of Agricultural and Food Chemistry*, *27*(6), 1256–1262. https://doi.org/10.1021/jf60226a042

Adler-Nissen, J. (1986). *Enzymic Hydrolysis of Food Protein* (Vols. 132–68). Elsevier Applied Science Publishers. London, United Kingdom.

Aguilera, J. M. (2005). Why food micro structure? *Journal of Food Engineering*, *67*(1–2), 3–11. https://doi.org/10.1016/j.jfoodeng.2004.05.050

Ahmed, J., & Auras, R. (2011). Effect of acid hydrolysis on rheological and thermal characteristics of lentil starch slurry. *LWT - Food Science and Technology*, *44*(4), 976–983. https://doi.org/10.1016/j.lwt.2010.08.007

Ahmad Nadzri, F. N., Tawalbeh, D., & Sarbon, N. M. (2021). Physicochemical properties and antioxidant activity of enzymatic hydrolysed chickpea (Cicer arietinum L.) protein as influenced by alcalase and papain enzyme. *Biocatalysis and Agricultural Biotechnology, 36*, 102131. https://doi.org/10.1016/j.bcab.2021.102131

Akharume, F., Santra, D., & Adedeji, A. (2020). Physicochemical and functional properties of proso millet storage protein fractions. *Food Hydrocolloids, 108*, 105497. https://doi.org/10.1016/j.foodhyd.2019.105497

Alajaji, S. A., & El-Adawy, T. A. (2006). Nutritional composition of chickpea (Cicer arietinum L.) as affected by microwave cooking and other traditional cooking methods. *Journal of Food Composition and Analysis*, *19*(8), 806–812. https://doi.org/10.1016/j.jfca.2006.03.015

Aluko, R. E., & Monu, E. (2003). Functional and bioactive properties of quinoa seed protein hydrolysates. *Journal of Food Science*, *68*(4), 1254–1258. https://doi.org/10.1111/j.1365-2621.2003.tb09635.x

Alzagtat, A. A., & Alli, I. (2002). Protein-lipid interactions in food systems: A review. *International Journal of Food Sciences and Nutrition, 53(3)*, 249–260. https://doi.org/10.1080/09637480220132850

Ames, J. M. (1992). The Maillard Reaction. In B. J. F. Hudson (Ed.), *Biochemistry of Food Proteins* (1st ed., pp. 99–153). Springer New York.

Amri, E., & Mamboya, F. (2012). Papain, a plant enzyme of biological importance: A review. *American Journal of Biochemistry and Biotechnology, 8(2)*, 99–104. https://doi.org/10.3844/ajbbsp.2012.99.104

Andlinger, D. J., & Kulozik, U. (2022). Protein-protein interactions explain the temperature-dependent viscoelastic changes occurring in colloidal protein gels. *Soft Matter*,19(6), 1144-1151. https://doi.org/10.1039/d2sm01092e

AOAC. (2005). Official methods of analysis (16th ed.) Washington D.C. Association of Official

Analytical Chemists.Arena, S., Renzone, G., D'Ambrosio, C., Salzano, A. M., & Scaloni, A. (2017). Dairy products and the Maillard reaction: A promising future for extensive food

characterization by integrated proteomics studies. *Food Chemistry*, *219*, 477–489. https://doi.org/10.1016/j.foodchem.2016.09.165

Arif, M., & Pauls, K. P. (2018). Properties of plant proteins. In *Plant Bioproducts* (pp. 121–142). Springer New York. https://doi.org/10.1007/978-1-4939-8616-3_8

Avramenko, N. A., Low, N. H., & Nickerson, M. T. (2013). The effects of limited enzymatic hydrolysis on the physicochemical and emulsifying properties of a lentil protein isolate. *Food Research International*, *51*(1), 162–169. https://doi.org/10.1016/j.foodres.2012.11.020

Baks, T., Bruins, M. E., Matser, A. M., Janssen, A. E. M., & Boom, R. M. (2008). Effect of gelatinization and hydrolysis conditions on the selectivity of starch hydrolysis with α-amylase from *Bacillus licheniformis*. *Journal of Agricultural and Food Chemistry,* 56(2), 488–495. https://doi.org/10.1021/jf072217j

Baks, T., Kappen, F. H. J., Janssen, A. E. M., & Boom, R. M. (2008). Towards an optimal process for gelatinisation and hydrolysis of highly concentrated starch-water mixtures with alpha-amylase from B. licheniformis. *Journal of Cereal Science*, *47*(2), 214–225. https://doi.org/10.1016/j.jcs.2007.03.011

Bandyopadhyay, K., Misra, G., & Ghosh, S. (2008). Preparation and Characterization of Protein Hydrolysates from Indian Defatted Rice Bran Meal. *Journal of Oleo Science*, *57*(1), 47–52. https://doi.org/10.5650/jos.57.47

Barac, M., Cabrilo, S., Pesic, M., Stanojevic, S., Zilic, S., Macej, O., & Ristic, N. (2010). Profile and functional properties of seed proteins from six pea (Pisum sativum) genotypes. *International Journal of Molecular Sciences*, *11*(12), 4973–4990. https://doi.org/10.3390/ijms11124973

Boye, J., Zare, F., & Pletch, A. (2010). Pulse proteins: Processing, characterization, functional properties and applications in food and feed. *Food Research International*, *43*(2), 414–431. https://doi.org/10.1016/j.foodres.2009.09.003

Biladeris, C. G., & D. R., G. (1979). A Comparison of the Enzymatic Hydrolysis of Smooth Pea Starch to that of Corn and Wheat. *Canadian Institute of Food Science and Technology Journal*, *12*(3), 131–134. https://doi.org/10.1016/s0315-5463(79)73099-9

Çabuk, B., Nosworthy, M. G., Stone, A. K., Korber, D. R., Tanaka, T., House, J. D., & Nickerson, M. T. (2018). Effect of fermentation on the protein digestibility and levels of non-nutritive

compounds of pea protein concentrate. *Food Technology and Biotechnology*, *56*(2), 257–264. https://doi.org/10.17113/ftb.56.02.18.5450

Capozzi, F., Magkos, F., Fava, F., Milani, G. P., Agostoni, C., Astrup, A., & Saguy, I. S. (2021). A multidisciplinary perspective of ultra-processed foods and associated food processing technologies: A view of the sustainable road ahead. *Nutrients*, *13*(11). https://doi.org/10.3390/nu13113948

Carbone, J. W., & Pasiakos, S. M. (2019). Dietary protein and muscle mass: Translating science to application and health benefit. *Nutrients*, *11*(5), 1–13. https://doi.org/10.3390/nu11051136

Cassiani, D. M., Yamul, D. K., Conforti, P. A., Pérez, V. A., & Lupano, C. E. (2013). Structure and Functionality of Whey Protein Concentrate-Based Products with Different Water Contents. *Food and Bioprocess Technology*, *6*(1), 217–227. https://doi.org/10.1007/s11947-011-0680-x

Chao, D., & Aluko, R. E. (2018). Modification of the structural, emulsifying, and foaming properties of an isolated pea protein by thermal pretreatment. *CYTA - Journal of Food*, *16*(1), 357–366. https://doi.org/10.1080/19476337.2017.1406536

Chatterjee, N., & Walker, G. C. (2017). Mechanisms of DNA damage, repair, and mutagenesis. *Environmental and Molecular Mutagenesis*, *58*(5), 235–263. https://doi.org/10.1002/em.22087

Cheetangdee, N., & Fukada, K. (2014). Emulsifying activity of bovine β-lactoglobulin conjugated with hexoses through the Maillard reaction. *Colloids and Surfaces A: Physicochemical and Engineering Aspects, 450(1)*, 148–155. https://doi.org/10.1016/j.colsurfa.2014.03.026

Cheison, S. C., Zhang, S. B., Wang, Z., & Xu, S. Y. (2009). Comparison of a modified spectrophotometric and the pH-stat methods for determination of the degree of hydrolysis of whey proteins hydrolysed in a tangential-flow filter membrane reactor. *Food Research International*, *42*(1), 91–97. https://doi.org/10.1016/j.foodres.2008.09.003

Chen, Y., Chen, X., Guo, T. L., & Zhou, P. (2015). Improving the thermostability of β-lactoglobulin via glycation: The effect of sugar structures. In *Food Research International* 69(1), 106–113. https://doi.org/10.1016/j.foodres.2014.12.017

Chiu, T., Chen, M., & Chang, H. (2009). Comparisons of emulsifying properties of Maillard reaction products conjugated by green, red seaweeds and various commercial proteins. *Food Hydrocolloids, 23(8)*, 2270–2277. https://doi.org/10.1016/j.foodhyd.2009.06.003

Cleaves, H. J. (2022). Isoelectric point. In Muriel Gargaud, Ricardo Amils, José Cernicharo Quintanilla, Henderson James (Jim) Cleaves, William M. Irvine, Daniele L. Pinti, Michel Viso (Eds.) , *Encyclopedia of astrobiology* (1st ed., pp 1853) Springer. Berlin, Germany. https://doi.org/10.1007/978-3-642-11274-4

Cui, H., Yu, J., Xia, S., Duhoranimana, E., Huang, Q., & Zhang, X. (2019). Improved controlled flavor formation during heat-treatment with a stable Maillard reaction intermediate derived from xylose-phenylalanine. *Food Chemistry, 271*, 47–53. https://doi.org/10.1016/j.foodchem.2018.07.161

Damodaran, S. (2008). Amino Acids, Peptides, and Proteins. In S. Damodaran, K. L. Parkin, & O. R. Fennema (Eds.), *Fennema's Food Chemistry* (4th ed.). CRC Press. Boca Raton, FL, United States.

De Kruif, C. G., Weinbreck, F., & De Vries, R. (2004). Complex coacervation of proteins and anionic polysaccharides. *Current Opinion in Colloid and Interface Science*, *9*(5), 340–349. https://doi.org/10.1016/j.cocis.2004.09.006

de Oliveira, F. C., Coimbra, J. S. dos R., de Oliveira, E. B., Zuñiga, A. D. G., & Rojas, E. E. G. (2016). Food Protein-polysaccharide Conjugates Obtained via the Maillard Reaction: A Review. *Critical Reviews in Food Science and Nutrition*, *56*(7), 1108–1125. https://doi.org/10.1080/10408398.2012.755669

Dickinson, E. (2010). Flocculation of protein-stabilized oil-in-water emulsions. *Colloids and Surfaces B: Biointerfaces, 81(1)*, 130–140. https://doi.org/10.1016/j.colsurfb.2010.06.033

Dickinson, E., & Euston, S. R. (1991). Stability of food emulsions containing both protein and polysaccharides. In E. Dickinson (Ed.), *Food Polymers, Gels and Colloids* (pp. 132–146). Royal Society of Chemistry. Cambridge, United Kingdom.

Dıblan, S., Kadiroğlu, P., & Aydemir, L. Y. (2018). FT-IR spectroscopy characterization and chemometric evaluation of legumes extracted with different solvents. *Food and Health*, 4 (2), 80–88. https://doi.org/10.3153/fh18008

Doan, C. D., & Ghosh, S. (2019). Formation and stability of pea protein nanoparticles using ethanol-induced desolvation. *Nanomaterials, 9(7)*. https://doi.org/10.3390/nano9070949

Dzwolak, W., & Ziajka, S. (1999). Enzymatic Hydrolysis of Milk Proteins Under Alkaline and Acidic Conditions. *Journal of Food Science*, *64*(3), 393–395. https://doi.org/10.1111/j.1365-2621.1999.tb15049.x

Eckert, E., Han, J., Swallow, K., Tian, Z., Jarpa-Parra, M., & Chen, L. (2019). Effects of enzymatic hydrolysis and ultrafiltration on physicochemical and functional properties of faba bean protein. *Cereal Chemistry*, *96*(4), 725–741. https://doi.org/10.1002/cche.10169

Edwards, C. H., Maillot, M., Parker, R., & Warren, F. J. (2018). A comparison of the kinetics of in vitro starch digestion in smooth and wrinkled peas by porcine pancreatic alpha-amylase. *Food Chemistry*, *244*, 386–393. https://doi.org/10.1016/j.foodchem.2017.10.042

Elgendy, A. (2016). A literature review on trypsin enzyme by: Ahmed Sedeek Elgendy and Mahmoud Khatib Abdelrasool. Retrieved from https://www.researchgate.net/publication/289376015_A_Literature_Review_on_Trypsin_Enzyme on 13th November, 202.

Eyraud, V., Karaki, L., Rahioui, I., Sivignon, C., Da Silva, P., Rahbé, Y., Royer, C., & Gressent, F. (2013). Expression and biological activity of the cystine knot bioinsecticide PA1b (Pea Albumin 1 subunit b). *PLoS ONE*, *8*(12), 81619. https://doi.org/10.1371/journal.pone.0081619

Fan, R., Zhang, T., Tai, K., & Yuan, F. (2020). Surface properties and adsorption of lactoferrin-xanthan complex in the oil-water interface. *Journal of Dispersion Science and Technology*, *41*(7), 1037–1044. https://doi.org/10.1080/01932691.2019.1614041

FAO. (2013). The state of food insecurity in the world: the multiple dimensions of food security.

Retrieved from: http://www.fao.org/docrep/018/i3434e/i3434e.pdf.

Fechner, A., Knoth, A., Scherze, I., & Muschiolik, G. (2007). Stability and release properties of double-emulsions stabilised by caseinate-dextran conjugates. *Food Hydrocolloids*, *21*(5–6), 943–952. https://doi.org/10.1016/j.foodhyd.2006.10.021

Friedman, M. (1996). Food Browning and Its Prevention: An Overview. *Journal of Agriculture and Food Chemistry*, *4*(3), 632–653. https://doi.org/10.1021/jf950394r

Garcia-Amezquita, L. E., Martinez-Alvarenga, M. S., Olivas, G. I., Zamudio-Flores, P. B., Acosta-Muñiz, C. H., & Sepulveda, D. R. (2014). Effect of Maillard reaction conditions on the degree of glycation and functional properties of whey protein isolate-maltodextrin conjugates. *Food Hydrocolloids, 38*, 110–118. https://doi.org/10.1016/j.foodhyd.2013.11.006

García Arteaga, V., Apéstegui Guardia, M., Muranyi, I., Eisner, P., & Schweiggert-Weisz, U. (2020). Effect of enzymatic hydrolysis on molecular weight distribution, techno-functional

properties and sensory perception of pea protein isolates. *Innovative Food Science and Emerging Technologies, 65*, 102449. https://doi.org/10.1016/j.ifset.2020.102449

Goertzen, A. D., Nickerson, M. T., & Tanaka, T. (2021a). The improvement of the functional properties of a chickpea protein isolate through proteolysis with three proteases. *Cereal Chemistry*, *98*(3), 439–449. https://doi.org/10.1002/cche.10383

Goertzen, A. D., House, J. D., Nickerson, M. T., & Tanaka, T. (2021b). The impact of enzymatic hydrolysis using three enzymes on the nutritional properties of a chickpea protein isolate. *Cereal Chemistry*, *98*(2), 275–284. https://doi.org/10.1002/cche.10361

Goldstein, J., Newbury, D., Joy, D., Lyman, P., Echlin, E., Lifshin, L., Sawyer, L., & Michael, J. (2003). Scanning Electron Microscopy and X-Ray Microanalysis. *Microscopy and Microanalysis*, *9*(5), 484–484. https://doi.org/10.1017/s1431927603030617

Gorissen, S. H. M., Crombag, J. J. R., Senden, J. M. G., Waterval, W. A. H., Bierau, J., Verdijk, L. B., & van Loon, L. J. C. (2018). Protein content and amino acid composition of commercially available plant-based protein isolates. *Amino Acids*, *50*(12), 1685–1695. https://doi.org/10.1007/s00726-018-2640-5

Grossi, G., Goglio, P., Vitali, A., & Williams, A. G. (2019). Livestock and climate change: Impact of livestock on climate and mitigation strategies. *Animal Frontiers*, *9*(1), 69–76. https://doi.org/10.1093/af/vfy034

Guleria, S., Dua, S., & Chongtham, N. (2009). Analysis of variability in different genotypes of pea (Pisum sativum L.) on the basis of protein markers. *Legume Research*, *32*(4), 265–269.

Habinshuti, I., Mu, T. H., & Zhang, M. (2021). Structural, antioxidant, aroma, and sensory characteristics of Maillard reaction products from sweet potato protein hydrolysates as influenced by different ultrasound-assisted enzymatic treatments. *Food Chemistry*, *361*, 1-12. https://doi.org/10.1016/j.foodchem.2021.130090

Hadidi, M., Khaksar, F. B., Pagan, J., & Ibarz, A. (2020). Application of Ultrasound-Ultrafiltration-Assisted alkaline isoelectric precipitation (UUAAIP) technique for producing alfalfa protein isolate for human consumption: Optimization, comparison, physicochemical, and functional properties. *Food Research International*, *130*, 1-10. https://doi.org/10.1016/j.foodres.2019.108907

Hall, G. M. (Ed.). (1996). *Methods of testing protein functionality* (1st ed.). Springer New York NY, USA.

Haslaniza, H., Maskat, M. Y., Wan Aida, W. M., & Mamot, S. (2010). The effects of enzyme concentration, temperature and incubation time on nitrogen content and degree of hydrolysis of protein precipitate from cockle (Anadara granosa) meat wash water. *International Food Research Journal, 17*, 147–152.

Herrero, M., Gerber, P., Vellinga, T., Garnett, T., Leip, A., Opio, C., & McAllister, T. A. (2011). Livestock and greenhouse gas emissions: The importance of getting the numbers right. *Animal Feed Science and Technology, 166*, 779–782. https://doi.org/10.1016/j.anifeedsci.2011.04.083

Hertzler, S. R., Lieblein-Boff, J. C., Weiler, M., & Allgeier, C. (2020). Plant proteins: Assessing their nutritional quality and effects on health and physical function. *Nutrients*, *12*(12), 1–27. https://doi.org/10.3390/nu12123704

Higgins, T. J. V., Chandler, P. M., Randall, P. J., Spencer, D., Beach, L. R., Blagrove, R. J., Kortt, A. A., & Inglis, A. S. (1986). Gene structure, protein structure, and regulation of the synthesis of a sulfur-rich protein in pea seeds. *Journal of Biological Chemistry*, *261*(24), 11124–11130. https://doi.org/10.1016/S0021-9258(18)67357-0

Hiller, B., & Lorenzen, P. C. (2010). Functional properties of milk proteins as affected by Maillard reaction-induced oligomerisation. *Food Research International, 43(4)*, 1155–1166. https://doi.org/10.1016/j.foodres.2010.02.006

Hizukuri, S. (1985). Relationship between the distribution of the chain length of amylopectin and the crystalline structure of starch granules. *Carbohydrate Research*, *145*, 295–306. https://doi.org/10.1016/S0008-6215(00)90461-0

Hizukuri, S., Takeda, Y., Maruta, N., & Juliano, B. O. (1989). Molecular structures of rice starch. *Carbohydrate Research*, *189*, 227–235. https://doi.org/10.1016/0008-6215(89)84099-6

Hizukuri, S., Takeda, Y., Yasuda, M., & Suzuki, A. (1981). Multibranched nature of amylose and action of debranching enzymes. *Carbohydrate Research*, *94*, 205–213. https://doi.org/10.1016/S0008-6215(00)80718-1

Hodge, J. E. (1953). Dehydrated foods, Chemistry of Browning Reactions in Model Systems. *Journal of Agricultural and Food Chemistry*, *1*(15), 928–943. https://doi.org/10.1021/jf60015a004

Jacobsen, C. F., Léonis, J., Linderstrøm-Lang, K., & Ottesen, M. (1957). The pH-Stat and Its Use in Biochemistry. *Methods of Biochemical Analysis*, 4, 171–210. doi: 10.1002/9780470110201.ch5.

Jamdar, S. N., Rajalakshmi, V., Pednekar, M. D., Juan, F., Yardi, V., & Sharma, A. (2010). Influence of degree of hydrolysis on functional properties, antioxidant activity and ACE inhibitory activity of peanut protein hydrolysate. *Food Chemistry*, *121*(1), 178–184. https://doi.org/10.1016/j.foodchem.2009.12.027

Jia, R., Zhang, M., Yang, T., Ma, M., Sun, Q., & Li, M. (2022). Evolution of the morphological, structural, and molecular properties of gluten protein in dough with different hydration levels during mixing. *Food Chemistry: X*, *15*, 1-15. https://doi.org/10.1016/j.fochx.2022.100448

Jiménez-Castaño, L., Villamiel, M., & López-Fandiño, R. (2007). Glycosylation of individual whey proteins by Maillard reaction using dextran of different molecular mass. *Food Hydrocolloids, 21(3)*, 433–443. https://doi.org/10.1016/j.foodhyd.2006.05.006

Joshi, M., Aldred, P., McKnight, S., Panozzo, J. F., Kasapis, S., Adhikari, R., & Adhikari, B. (2013). Physicochemical and functional characteristics of lentil starch. *Carbohydrate Polymers*, *92*(2), 1484–1496. https://doi.org/10.1016/j.carbpol.2012.10.035

Kasran, M., Cui, S. W., & Goff, H. D. (2013). Covalent attachment of fenugreek gum to soy whey protein isolate through natural Maillard reaction for improved emulsion stability. *Food Hydrocolloids*, *30*(2), 552–558. https://doi.org/10.1016/j.foodhyd.2012.08.004

Kasran, M., Cui, S. W., & Goff, H. D. (2013). Emulsifying properties of soy whey protein isolate-fenugreek gum conjugates in oil-in-water emulsion model system. *Food Hydrocolloids, 30(2)*, 691–697. https://doi.org/10.1016/j.foodhyd.2012.09.002

Kato, A. (2000). Maillard-type protein-polysaccharide conjugates. *Developments in Food Science, 41*, 385-395. https://doi.org/10.1016/S0167-4501(00)80017-5

Kharbach, M., Alaoui Mansouri, M., Taabouz, M., & Yu, H. (2023). Current Application of Advancing Spectroscopy Techniques in Food Analysis: Data Handling with Chemometric Approaches. *Foods*, 12(14), 1-46. https://doi.org/10.3390/foods12142753

Kinsella, J. E. (1981). Functional properties of proteins: Possible relationships between structure and function in foams. *Food Chemistry*, 7(4), 273-288. https://doi.org/10.1016/0308-8146(81)90033-9

Kobayashi, S., Schwartz, S. J., & Lineback, D. R. (1986). Comparison of the structure of amylopectin from different wheat varieties. *Cereal Chemistry*, 63(2), 71–74.

Koga, D., Kusumi, S., Shibata, M., & Watanabe, T. (2021). Applications of Scanning Electron Microscopy Using Secondary and Backscattered Electron Signals in Neural Structure. *Frontiers in Neuroanatomy*, *15*. https://doi.org/10.3389/fnana.2021.759804

Konieczny, D., Stone, A. K., Korber, D. R., Nickerson, M. T., & Tanaka, T. (2020). Physicochemical properties of enzymatically modified pea protein-enriched flour treated by different enzymes to varying levels of hydrolysis. *Cereal Chemistry*, *97*(2), 326–338. https://doi.org/10.1002/cche.10248

Konieczny, D., Stone, A. K., Nosworthy, M. G., House, J. D., Korber, D. R., Nickerson, M. T., & Tanaka, T. (2020). Nutritional properties of pea protein-enriched flour treated with different proteases to varying degrees of hydrolysis. *Cereal Chemistry*, *97*(2), 429–440. https://doi.org/10.1002/cche.10258

Kopjar, M., Buljeta, I., Jelić, I., Kelemen, V., Šimunović, J., & Pichler, A. (2021). Encapsulation of cinnamic acid on plant-based proteins: Evaluation by HPLC, DSC and FTIR-ATR. *Plants*, *10*(10) 1-10. https://doi.org/10.3390/plants10102158

Kryachko, Y., Batbayar, B., Tanaka, T., Nickerson, M. T., & Korber, D. R. (2020). Production of glycerol by Lactobacillus plantarum NRRL B-4496 and formation of hexamine during fermentation of pea protein enriched flour. *Journal of Biotechnology*, *323*, 331–340. https://doi.org/10.1016/j.jbiotec.2020.09.009

Kumar, A., Nayak, R., Purohit, S. R., & Rao, P. S. (2021). Impact of UV-C irradiation on solubility of Osborne protein fractions in wheat flour. *Food Hydrocolloids*, *110,* 10845. https://doi.org/10.1016/j.foodhyd.2020.105845

Kumanyika, S., Afshin, A., Arimond, M., Lawrence, M., McNaughton, S. A., & Nishida, C. (2020). Approaches to defining healthy diets: A background paper for the international expert consultation on sustainable healthy diets. *Food and Nutrition Bulletin, 41(2)*, 7–30. https://doi.org/10.1177/0379572120973111

Kumitch, H. M., Stone, A. K., Nickerson, M. T., Korber, D. R., & Tanaka, T. (2020). Effect of fermentation time on the physicochemical and functional properties of pea protein-enriched flour fermented by Aspergillus oryzae and Aspergillus niger. *Cereal Chemistry*, *97*(2), 416–428. https://doi.org/10.1002/cche.10257

Kutzli, I., Griener, D., Gibis, M., Schmid, C., Dawid, C., Baier, S. K., Hofmann, T., & Weiss, J. (2020). Influence of Maillard reaction conditions on the formation and solubility of pea protein isolate-maltodextrin conjugates in electrospun fibers. *Food Hydrocolloids*, 101, 1-8. https://doi.org/10.1016/j.foodhyd.2019.105535

Kutzli, I., Weiss, J., & Gibis, M. (2021). Glycation of plant proteins via maillard reaction: Reaction chemistry, technofunctional properties, and potential food application. *Foods*, 10 (2), 1-40. https://doi.org/10.3390/foods10020376

Laemmli. (1970). Glycine-SDS-PAGE for separation of proteins. *Nature*, *227*, 680–685.

Lafarga, T., Álvarez, C., Villaró, S., Bobo, G., & Aguiló-Aguayo, I. (2020). Potential of pulse-derived proteins for developing novel vegan edible foams and emulsions. *International Journal of Food Science and Technology, 55(2)*, 475–481. https://doi.org/10.1111/ijfs.14286

Lam, A. C. Y., Warkentin, T. D., Tyler, R. T., & Nickerson, M. T. (2017). Physicochemical and functional properties of protein isolates obtained from several pea cultivars. *Cereal Chemistry, 94(1)*, 89–97. https://doi.org/10.1094/CCHEM-04-16-0097-FI

Lam, A. C. Y., Can Karaca, A., Tyler, R. T., & Nickerson, M. T. (2018). Pea protein isolates: Structure, extraction, and functionality. *Food Reviews International*, *34*(2), 126–147. https://doi.org/10.1080/87559129.2016.1242135

Leite, J. A. S., Montoya, C. A., Loveday, S. M., Maes, E., Mullaney, J. A., McNabb, W. C., & Roy, N. C. (2021). Heat-treatments affect protease activities and peptide profiles of ruminants' milk. *Frontiers in Nutrition, 8*, 1–10. https://doi.org/10.3389/fnut.2021.626475

Li, L., Yuan, T. Z., Setia, R., Raja, R. B., Zhang, B., & Ai, Y. (2019). Characteristics of pea, lentil and faba bean starches isolated from air-classified flours in comparison with commercial starches. *Food Chemistry*, *276*, 599–607. https://doi.org/10.1016/j.foodchem.2018.10.064

Li, S., Jiang, Z., Wang, F., Wu, J., Liu, Y., & Li, X. (2020). Characterization of rice glutelin fibrils and their effect on in vitro rice starch digestibility. *Food Hydrocolloids*, *106*, 105918. https://doi.org/10.1016/j.foodhyd.2020.105918

Li, W., Zhao, H., He, Z., Zeng, M., Qin, F., & Chen, J. (2016). Modification of soy protein hydrolysates by Maillard reaction: Effects of carbohydrate chain length on structural and interfacial properties. *Colloids and Surfaces B: Biointerfaces, 138*, 70–77. https://doi.org/10.1016/j.colsurfb.2015.11.038

Li, Y., Zhong, F., Ji, W., Yokoyama, W., Shoemaker, C. F., Zhu, S., & Xia, W. (2013). Functional properties of Maillard reaction products of rice protein hydrolysates with mono-, oligo- and polysaccharides. *Food Hydrocolloids*, *30*(1), 53–60. https://doi.org/10.1016/j.foodhyd.2012.04.013

Liu, J., Ru, Q., & Ding, Y. (2012). Glycation a promising method for food protein modification: Physicochemical properties and structure, a review. *Food Research International, 49(1)*, 170–183. https://doi.org/10.1016/j.foodres.2012.07.034

Liu, S., Yuan, T. Z., Wang, X., Reimer, M., Isaak, C., & Ai, Y. (2019). Behaviors of starches evaluated at high heating temperatures using a new model of Rapid Visco Analyzer – RVA 4800. *Food Hydrocolloids*, *94*, 217–228. https://doi.org/10.1016/j.foodhyd.2019.03.015

Liu, Y., Zhao, G., Zhao, M., Ren, J., & Yang, B. (2012). Improvement of functional properties of peanut protein isolate by conjugation with dextran through Maillard reaction. *Food Chemistry*, *131*(3), 901–906. https://doi.org/10.1016/j.foodchem.2011.09.074

Lu, Z. X., He, J. F., Zhang, Y. C., & Bing, D. J. (2019). Composition, physicochemical properties of pea protein and its application in functional foods. *Critical Reviews in Food Science and Nutrition*, *60(15)*, 2593-2605.https://doi.org/10.1080/10408398.2019.1651248

Ma, M., Wang, Y., Wang, M., Jane, J. lin, & Du, S. kui. (2017). Physicochemical properties and in vitro digestibility of legume starches. *Food Hydrocolloids*, *63*, 249–255. https://doi.org/10.1016/j.foodhyd.2016.09.004

Maitena, U., Katayama, S., Sato, R., & Saeki, H. (2004). Improved solubility and stability of carp myosin by conjugation with alginate oligosaccharide. *Fisheries Science*, *70*(5), 896–902. https://doi.org/10.1111/j.1444-2906.2004.00884.x

Malik, M. A., Sharma, H. K., & Saini, C. S. (2017). High intensity ultrasound treatment of protein isolate extracted from dephenolized sunflower meal: Effect on physicochemical and functional properties. *Ultrasonics Sonochemistry*, *39*, 511–519. https://doi.org/10.1016/j.ultsonch.2017.05.026

Manelius, R., Qin, Z., Åvall, A. K., Andtfolk, H., & Bertoft, E. (1997). The mode of action on granular wheat starch by bacterial α-amylase. *Starch/Staerke*, *49*(4), 142–147. https://doi.org/10.1002/star.19970490405

Martins, S. I. F. S., Jongen, W. M. F., & Van Boekel, M. A. J. S. (2001). A review of Maillard reaction in food and implications to kinetic modelling. *Trends in Food Science and Technology*, *11(9-10)*, 364–373. https://doi.org/10.1016/S0924-2244(01)00022-X

McClements, J. (2015). *Food Emulsions Principles, Practices, And Techniques*, In *Boca Raton: CRC Press*. Boca Raton, FL, USA, https://doi.org/10.1201/b18868

Mekonnen, M. M., & Hoekstra, A. Y. (2012). A global assessment of the water footprint of farm animal products. *Ecosystems, 15(3)*, 401–415. https://doi.org/10.1007/s10021-011-9517-8

Mertens, C., Dehon, L., Bourgeois, A., Verhaeghe-Cartrysse, C., & Blecker, C. (2012). Agronomical factors influencing the legumin/vicilin ratio in pea (Pisum sativum L.) seeds. *Journal of the Science of Food and Agriculture*, *92*(8), 1591–1596. https://doi.org/10.1002/jsfa.4738

Mir, N. A., Riar, C. S., & Singh, S. (2019). Physicochemical, molecular and thermal properties of high-intensity ultrasound (HIUS) treated protein isolates from album (Chenopodium album) seed. *Food Hydrocolloids*, *96*, 433–441. https://doi.org/10.1016/j.foodhyd.2019.05.052

Mir, N. A., Riar, C. S., & Singh, S. (2020). Structural modification in album (Chenopodium album) protein isolates due to controlled thermal modification and its relationship with protein digestibility and functionality. *Food Hydrocolloids*, *103,* 105708. https://doi.org/10.1016/j.foodhyd.2020.105708

Mokni Ghribi, A., Maklouf Gafsi, I., Sila, A., Blecker, C., Danthine, S., Attia, H., Bougatef, A., & Besbes, S. (2015). Effects of enzymatic hydrolysis on conformational and functional properties of chickpea protein isolate. *Food Chemistry*, *187*, 322–330. https://doi.org/10.1016/j.foodchem.2015.04.109

Möller, A. C., van der Padt, A., & van der Goot, A. J. (2021). From raw material to mildly refined ingredient – Linking structure to composition to understand fractionation processes. *Journal of Food Engineering*, *291,* 110321. https://doi.org/10.1016/j.jfoodeng.2020.110321

Mookerjee, A., & Tanaka, T. (2023). Influence of enzymatic treatments on legume proteins for improved functional and nutritional properties: expansion of legume protein utilization as food ingredients. *Current Opinion in Food Science,* 49, 1-10. https://doi.org/10.1016/j.cofs.2022.100974

Mulcahy, E. M., Mulvihill, D. M., & O'Mahony, J. A. (2016). Physicochemical properties of whey protein conjugated with starch hydrolysis products of different dextrose equivalent values. *International Dairy Journal*, *53*, 20–28. https://doi.org/10.1016/j.idairyj.2015.09.009

Mune Mune, M. A., & Minka, S. R. (2017). Antinutritional factors in vegetable protein isolates: A review. *Food Research International, 96*, 96–102. https://doi.org/10.1016/j.foodres.2017.03.012

Naik, M. D. (2012). Protein and polysaccharide interactions and functionality in food systems. *Food Hydrocolloids: Principles, Techniques, and Applications*, *48*, 18-27. https://doi.org/10.1016/j.cocis.2020.03.002

Nesterenko, A., Alric, I., Violleau, F., Silvestre, F., & Durrieu, V. (2014). The effect of vegetable protein modifications on the microencapsulation process. *Food Hydrocolloids*, *41*, 95–102. https://doi.org/10.1016/j.foodhyd.2014.03.017

Nikbakht Nasrabadi, M., Sedaghat Doost, A., & Mezzenga, R. (2021). Modification approaches of plant-based proteins to improve their techno-functionality and use in food products. *Food Hydrocolloids*, *118*, 106789. https://doi.org/10.1016/j.foodhyd.2021.106789

Niu, L. Y., Jiang, S. T., Pan, L. J., & Zhai, Y. S. (2011). Characteristics and functional properties of wheat germ protein glycated with saccharides through Maillard reaction. *International Journal of Food Science and Technology*, *46*(10), 2197–2203. https://doi.org/10.1111/j.1365-2621.2011.02737.x

Nosworthy, M. G., Medina, G., Franczyk, A. J., Neufeld, J., Appah, P., Utioh, A., Frohlich, P., & House, J. D. (2018). Effect of processing on the in vitro and in vivo protein quality of red and green lentils (Lens culinaris). *Food Chemistry*, *240,* 588–593. https://doi.org/10.1016/j.foodchem.2017.07.129

Nunes, C. A. (2014). Vibrational spectroscopy and chemometrics to assess authenticity, adulteration and intrinsic quality parameters of edible oils and fats. *Food Research International* 60, 255–261. Elsevier Ltd. https://doi.org/10.1016/j.foodres.2013.08.041

Núñez, O., & Lucci, P. (2020). Application of liquid chromatography in food analysis. *Foods*, *9(9)*, 1277.https://doi.org/10.3390/foods9091277

Nwachukwu, I. D., & Aluko, R. E. (2021). Food protein structures, functionality and product development. In C. Udenigwe (Ed.), *Food Chemistry, Function and Analysis* (Issue 27,

Chapter 1). The Royal Society of Chemistry, Cambridge, United Kingdom. https://doi.org/10.1039/9781839163425-00001

Oates, C. G. (1997). Towards an understanding of starch granule structure and hydrolysis. *Trends in Food Science and Technology*, *8(11)*, 375–382. https://doi.org/10.1016/S0924-2244(97)01090-X

Oguntoyinbo, F. A. (2014). Effects of heat-moisture treatment and retrogradation on the pasting and functional properties of starches from selected improved cassava (Manihot esculenta) varieties. *International Journal of Biological Macromolecules, 66*, 245–252. https://doi.org/10.1016/j.ijbiomac.2014.02.020

O'Kane, F. E., Happe, R. P., Vereijken, J. M., Gruppen, H., & Van Boekel, M. A. J. S. (2004). Characterization of Pea Vicilin. 2. Consequences of Compositional Heterogeneity on Heat-Induced Gelation Behavior. *Journal of Agricultural and Food Chemistry*, *52(10)*, 3149–3154. https://doi.org/10.1021/jf035105a

Panghal A, Khatkar BS, S. U. (2006). Cereal proteins and their role in food industry. *Indian Food Industry*, *25*(5), 58.

Panyam, Dinakar and Kilara, A. (1996). Enhancing the functionality of food proteins by enzymatic modification Dinakar Panyam and Arun Kilara I. *Trends in Food Science and Technology*, *7(4)*, 120–125. https://doi.org/10.1016/0924-2244(96)10012-1

Paraman, I., Wagner, M. E., & Rizvi, S. S. H. (2012). Micronutrient and protein-fortified whole grain puffed rice made by supercritical fluid extrusion. *Journal of Agricultural and Food Chemistry*, *60*(44), 11188–11194. https://doi.org/10.1021/jf3034804

Parolia, S., Maley, J., Sammynaiken, R., Green, R., Nickerson, M., & Ghosh, S. (2022). Structure – Functionality of lentil protein-polyphenol conjugates. *Food Chemistry*, *367,* 130603. https://doi.org/10.1016/j.foodchem.2021.130603

Pearce, K. N., & Kinsella, J. E. (1978). Emulsifying Properties of Proteins: Evaluation of a Turbidimetric Technique. *Journal of Agricultural and Food Chemistry*, *26*(3), 716–723. https://doi.org/10.1021/jf60217a041

Pelgrom, P. J. M., Vissers, A. M., Boom, R. M., & Schutyser, M. A. I. (2013). Dry fractionation for production of functional pea protein concentrates. *Food Research International*, *53*(1), 232–239. https://doi.org/10.1016/j.foodres.2013.05.004

Pelgrom, P. J. M., Wang, J., Boom, R. M., & Schutyser, M. A. I. (2015). Pre- and post-treatment enhance the protein enrichment from milling and air classification of legumes. *Journal of Food Engineering*, *155*, 53–61. https://doi.org/10.1016/j.jfoodeng.2015.01.005

Periago, M. J., Ma, " ", Vidal, L., Ros, G., Rinc6n, F., Martinez, C., Lbpez, G., Rodrigo, J., & Martinez, I. (1998). Influence of enzymatic treatment on the nutritional and functional properties of pea flour. *Food Chemistry*, *63*(1), 71–78.

Petruzzello, M. (2023, June 29). *list of plants in the family Fabaceae*. *Encyclopedia Britannica*. https://www.britannica.com/topic/list-of-plants-in-the-family-Fabaceae-2021803 Phillips, L. G., Schulman, W., & Kinsella, J. E. (1990). pH and Heat Treatment Effects on Foaming of Whey Protein isolate. *Journal of Food Science*, *55(4)*, 1116–1119. https://doi.org/10.1111/j.1365-2621.1990.tb01612.x

Pirestani, S., Nasirpour, A., Keramat, J., & Desobry, S. (2017). Preparation of chemically modified canola protein isolate with gum Arabic by means of Maillard reaction under wet-heating conditions. *Carbohydrate Polymers*, *155*, 201–207. https://doi.org/10.1016/j.carbpol.2016.08.054

Plaza, M., Dambekodi, P. C., Syed, Z., & Dexter, J. E. (2020). Air classification: An alternative to wet fractionation for producing pulse protein concentrates. *Journal of Food Engineering, 274*, 109835. https://doi.org/10.1016/j.jfoodeng.2019.109835

Pownall, T. L., Udenigwe, C. C., & Aluko, R. E. (2010). Amino acid composition and antioxidant properties of pea seed (Pisum sativum L.) Enzymatic protein hydrolysate fractions. *Journal of Agricultural and Food Chemistry*, *58*(8), 4712–4718. https://doi.org/10.1021/jf904456r

Radotić, K., Stanković, M., Bartolić, D., & Natić, M. (2023). Intrinsic Fluorescence Markers for Food Characteristics, Shelf Life, and Safety Estimation: Advanced Analytical Approach. *Foods, 12(16)*, 3023. https://doi.org/10.3390/foods12163023

Raghunathan, R., Hoover, R., Waduge, R., Liu, Q., & Warkentin, T. D. (2017). Impact of molecular structure on the physicochemical properties of starches isolated from different field pea (Pisum sativum L.) cultivars grown in Saskatchewan, Canada. *Food Chemistry*, *221*, 1514–1521. https://doi.org/10.1016/j.foodchem.2016.10.142

Rahimi, F., Chatzimichail, S., Saifuddin, A., Surman, A. J., Taylor-Robinson, S. D., & Salehi-Reyhani, A. (2020). A Review of Portable High-Performance Liquid Chromatography: the

Future of the Field? *Chromatographia*, *83(10)*, 1165–1195. Springer. https://doi.org/10.1007/s10337-020-03944-6

Ramos, O. S., & Malcata, F. X. (2011). Food-grade enzymes. In M. Moo-Young (Ed.), *Comprehensive biotechnology* (2nd ed., Vol. 3, pp. 555–569). Academic Press, Oxford, United Kingdom. https://doi.org/10.1016/B978-0-08-088504-9.00213-0

Ratnayake, W. S., Hoover, R., & Warkentin, T. (2002). Pea starch: Composition, structure and properties - A review. *Starch*, *54(6)*, 217–234. https://doi.org/10.1002/1521-379X(200206)54:6<217::AID-STAR217>3.0.CO;2-R

Rebello, C. J., Greenway, F. L., & Finley, J. W. (2014). Whole grains and pulses: A comparison of the nutritional and health benefits. *Journal of Agricultural and Food Chemistry,* 62(29) 7029–7049. American Chemical Society. https://doi.org/10.1021/jf500932z

Reinkensmeier, A., Bußler, S., Schlüter, O., Rohn, S., & Rawel, H. M. (2015). Characterization of individual proteins in pea protein isolates and air classified samples. *Food Research International*, *76*(P1), 160–167. https://doi.org/10.1016/j.foodres.2015.05.009

Rempel, C., Geng, X., & Zhang, Y. (2019). Industrial scale preparation of pea flour fractions with enhanced nutritive composition by dry fractionation. *Food Chemistry*, *276*, 119–128. https://doi.org/10.1016/j.foodchem.2018.10.003

Ren, Y., Setia, R., Warkentin, T. D., & Ai, Y. (2021). Functionality and starch digestibility of wrinkled and round pea flours of two different particle sizes. *Food Chemistry*, *336*, 127711. https://doi.org/10.1016/j.foodchem.2020.127711

Ren, Y., Yuan, T. Z., Chigwedere, C. M., & Ai, Y. (2021). A current review of structure, functional properties, and industrial applications of pulse starches for value-added utilization. *Comprehensive Reviews in Food Science and Food Safety*, *20*(3), 3061–3092. https://doi.org/10.1111/1541-4337.12735

Robinson, P. K. (2015). Enzymes: principles and biotechnological applications. *Essays in Biochemistry*, *59*, 1–41. https://doi.org/10.1042/BSE0590001

Rocha, T. de S., Carneiro, A. P. de A., & Franco, C. M. L. (2010). Effect of enzymatic hydrolysis on some physicochemical properties of root and tuber granular starches. *Ciência e Tecnologia de Alimentos*, *30*(2), 544–551. https://doi.org/10.1590/s0101-20612010000200039

Roth, M., & Hampay, A. (1973). Column chromatography of amino acids with fluorescence detection. *Journal of Chromatography*, *83*, 353–356. doi: 10.1016/s0021-9673(00)97051-1

Rubio, L. A., Pérez, A., Ruiz, R., Guzmán, M. Á., Aranda-Olmedo, I., & Clemente, A. (2014). Characterization of pea (Pisum sativum) seed protein fractions. *Journal of the Science of Food and Agriculture*, *94*(2), 280–287. https://doi.org/10.1002/jsfa.6250

Rutherfurd, S. M. (2010). Methodology for Determining Degree of Hydrolysis of Proteins in Hydrolysates: A Review. *Journal of AOAC International*, *93*(5), 1515–1522. https://academic.oup.com/jaoac/article/93/5/1515/5655787

Saldanha do Carmo, C., Silventoinen, P., Nordgård, C. T., Poudroux, C., Dessev, T., Zobel, H., Holtekjølen, A. K., Draget, K. I., Holopainen-Mantila, U., Knutsen, S. H., & Sahlstrøm, S. (2020). Is dehulling of peas and faba beans necessary prior to dry fractionation for the production of protein- and starch-rich fractions? Impact on physical properties, chemical composition and techno-functional properties. *Journal of Food Engineering*, *278*, 109937. https://doi.org/10.1016/j.jfoodeng.2020.109937

Sánchez-Reséndiz, A., Rodríguez-Barrientos, S., Rodríguez-Rodríguez, J., Barba-Dávila, B., Serna-Saldívar, S. O., & Chuck-Hernández, C. (2018). Phosphoesterification of soybean and peanut proteins with sodium trimetaphosphate (STMP): Changes in structure to improve functionality for food applications. *Food Chemistry*, *260*, 299–305. https://doi.org/10.1016/j.foodchem.2018.04.009

Sauceau, M., Fages, J., Common, A., Nikitine, C., & Rodier, E. (2011). New challenges in polymer foaming: A review of extrusion processes assisted by supercritical carbon dioxide. *Progress in Polymer Science*, *36*(6), 749–766. https://doi.org/10.1016/j.progpolymsci.2010.12.004

Schneider, A. V. C. (2002). Overview of the market and consumption of puises in Europe. *British Journal of Nutrition*, *88*(S3), 243–250. https://doi.org/10.1079/bjn2002713

Sebii, H., Karra, S., Bchir, B., Nhouchi, Z., Ghribi, A. M., Karoui, R., Blecker, C., & Besbes, S. (2021). Effect of succinylation on the secondary structures, surface, and thermal properties of date palm pollen protein concentrate. *Journal of Food Science and Technology*, *58*(2), 632–640. https://doi.org/10.1007/s13197-020-04577-1

Sedaghat Doost, A., Nikbakht Nasrabadi, M., Goli, S. A. H., van Troys, M., Dubruel, P., De Neve, N., & Van der Meeren, P. (2020). Maillard conjugation of whey protein isolate with water-

soluble fraction of almond gum or flaxseed mucilage by dry heat treatment. *Food Research International*, *128*, 108779. https://doi.org/10.1016/j.foodres.2019.108779

Sedaghat Doost, A., Nikbakht Nasrabadi, M., Kassozi, V., Nakisozi, H., & Van der Meeren, P. (2020). Recent advances in food colloidal delivery systems for essential oils and their main components. *Trends in Food Science and Technology*, 99, 474–486. https://doi.org/10.1016/j.tifs.2020.03.037

Shah, N. N., K.V., U., & Singhal, R. S. (2019). Hydrophobically modified pea proteins: Synthesis, characterization and evaluation as emulsifiers in eggless cake. *Journal of Food Engineering*, *255*, 15–23. https://doi.org/10.1016/j.jfoodeng.2019.03.005

Sharma, V., & Bhardwaj, A. (2019). Scanning electron microscopy (SEM) in food quality evaluation. In J. Zhong & X. Wang (Eds.), *Evaluation technologies for food quality* (pp. 743–761). Woodhead Publishing. Cambridge, United Kingdom.

Shen, Y., & Li, Y. (2021). Acylation modification and/or guar gum conjugation enhanced functional properties of pea protein isolate. *Food Hydrocolloids*, *117,* 106686. https://doi.org/10.1016/j.foodhyd.2021.106686

Shewry, P. R., Napier, J. A., & Tatham, A. S. (1995). Seed Storage Proteins: Structures and Biosynthesis. *Special Review Issue on Plant Biochemistry*, *7(7)*, 945-956. https://doi.org/10.1105/tpc.7.7.945

Sim, S. Y. J., Srv, A., Chiang, J. H., & Henry, C. J. (2021). Plant proteins for future foods: A roadmap. *Foods*, *10(8)*, 1–31. https://doi.org/10.3390/foods10081967

Statistics Canada. (2014). *Pulses in Canada* (by E. Bekkering). Canadian Agriculture at a Glance, 96, 1–12. https://www150.statcan.gc.ca/n1/en/pub/96-325-x/2014001/article/14102-eng.pdf

Stone, A. K., Avarmenko, N. A., Warkentin, T. D., & Nickerson, M. T. (2015). Functional properties of protein isolates from different pea cultivars. *Food Science and Biotechnology*, *24(3)*, 827–833. https://doi.org/10.1007/s10068-015-0107-y

Stone, A. K., Karalash, A., Tyler, R. T., Warkentin, T. D., & Nickerson, M. T. (2015). Functional attributes of pea protein isolates prepared using different extraction methods and cultivars. *Food Research International*, *76(1)*, 31–38. https://doi.org/10.1016/j.foodres.2014.11.017

Sun, L., Wang, D., Huang, Z., Elfalleh, W., Qin, L., & Yu, D. (2023). Structure and flavor characteristics of Maillard reaction products derived from soybean meal hydrolysates-reducing sugars. *LWT*, *185,* 115097. https://doi.org/10.1016/j.lwt.2023.115097

Takeda, Y., Hizukuri, S., Takeda, C., & Suzuki, A. (1987). Structures of branched molecules of amyloses of various origins and molar fractions of branched and unbranched molecules. *Carbohydrate Research*, *165(1)*, 139–145. https://doi.org/10.1016/0008-6215(87)80089-7

Tavano, O. L. (2013). Protein hydrolysis using proteases: An important tool for food biotechnology. *Journal of Molecular Catalysis B: Enzymatic*, *90*, 1–11. https://doi.org/10.1016/j.molcatb.2013.01.011

Tian, X., & Yu, D. (2019). Pea protein hydrolysates produced by Alcalase: Antioxidant activity, peptide characterization and the effect of enzymatic hydrolysis on functional properties. *LWT, 115*, 108412. https://doi.org/10.1016/j.lwt.2019.108412

Tömösközi, S., Lásztity, R., Haraszi, R., & Baticz, O. (2001). Isolation and study of the functional properties of pea proteins. *Nahrung - Food*, *45(6)*, 399–401. https://doi.org/10.1002/1521-3803(20011001)45:6<399::AID-FOOD399>3.0.CO;2-0

Tosh, S., Farnworth, E., Brummer, Y., Duncan, A., Wright, A., Boye, J., Marcotte, M., & Benali, M. (2013). Nutritional Profile and Carbohydrate Characterization of Spray-Dried Lentil, Pea and Chickpea Ingredients. *Foods*, *2*(3), 338–349. https://doi.org/10.3390/foods2030338

Turgeon, S. L., Schmitt, C., & Sanchez, C. (2007). Protein-polysaccharide complexes and coacervates. *Current Opinion in Colloid and Interface Science*, *12(4–5)*, 166–178. https://doi.org/10.1016/j.cocis.2007.07.007

Tzitzikas, E. N., Vincken, J. P., De Groot, J., Gruppen, H., & Visser, R. G. F. (2006). Genetic variation in pea seed globulin composition. *Journal of Agricultural and Food Chemistry*, *54(2)*, 425–433. https://doi.org/10.1021/jf0519008

Varghese, K. S., Pandey, M. C., Radhakrishna, K., & Bawa, A. S. (2014). Technology, applications and modelling of ohmic heating: a review. *Journal of Food Science and Technology*, *51(10)*, 2304–2317. https://doi.org/10.1007/s13197-012-0710-3

Wang, H. Y., Qian, H., & Yao, W. R. (2011). Melanoidins produced by the Maillard reaction: Structure and biological activity. *Food Chemistry*, *128(3)*, 573–584. https://doi.org/10.1016/j.foodchem.2011.03.075

Wang, L. H., Sun, X., Huang, G. Q., & Xiao, J. X. (2018). Conjugation of soybean protein isolate with xylose/fructose through wet-heating Maillard reaction. *Journal of Food Measurement and Characterization*, *12*(4), 2718–2724. https://doi.org/10.1007/s11694-018-9889-y

Wang, L., & Shah, B. R. (2020). Improving the foaming properties of soy protein by Maillard reaction with xylose. *Food Hydrocolloids, 100*, 105401. https://doi.org/10.1016/j.foodhyd.2019.105401

Wang, N., Warkentin, T. D., Vandenberg, B., & Bing, D. J. (2014). Physicochemical properties of starches from various pea and lentil varieties, and characteristics of their noodles prepared by high temperature extrusion. *Food Research International*, *55*, 119–127. https://doi.org/10.1016/j.foodres.2013.10.043

Wang, Q., & Ismail, B. (2012). Effect of Maillard-induced glycosylation on the nutritional quality, solubility, thermal stability and molecular configuration of whey proteins. *International Dairy Journal*, *25*(2), 112–122. https://doi.org/10.1016/j.idairyj.2012.02.009

Wang, Q., Liu, J., & Zhu, H. (2018). Genetic and molecular mechanisms underlying symbiotic specificity in legume-rhizobium interactions. *Frontiers in Plant Science, 9(9)*, 313. https://doi.org/10.3389/fpls.2018.00313

Wang, Y., Zhang, A., Wang, Y., Wang, X., Xu, N., & Jiang, L. (2020). Effects of irradiation on the structure and properties of glycosylated soybean proteins. *Food and Function*, *11*(2), 1635–1646. https://doi.org/10.1039/c9fo01879d

Wang, Y., & Sheng, H. (2020). Enzyme-catalyzed cross-linking of soy proteins: A review of principles and applications. *Trends in Food Science & Technology, 108*, 233–245. https://doi.org/10.1016/j.tifs.2020.12.008

Wierenga, P. A., & Gruppen, H. (2010). New views on foams from protein solutions. *Current Opinion in Colloid and Interface Science*, 15(5), 365–373. https://doi.org/10.1016/j.cocis.2010.05.017

Wood, J. A., & Malcolmson, L. J. (2020). Pulse milling technologies. In B. K. Tiwari, A. Gowen, & B. McKenna (Eds.), *Pulse foods: Processing, quality and nutraceutical applications* (2nd ed., pp. 213–263). Academic Press. London, United Kingdom. https://doi.org/10.1016/B978-0-12-818184-3.00010-6

Xing, Q., Dekker, S., Kyriakopoulou, K., Boom, R. M., Smid, E. J., & Schutyser, M. A. I. (2020). Enhanced nutritional value of chickpea protein concentrate by dry separation and solid-state fermentation. *Innovative Food Science and Emerging Technologies*, *59,* 102269. https://doi.org/10.1016/j.ifset.2019.102269

Yang, W., Wang, Q., Chen, Y., Lei, L., Lei, X., Zhao, J., Zhang, Y., & Ming, J. (2022). Changes in the structural and physicochemical properties of wheat gliadin and maize amylopectin conjugates induced by dry-heating. *Journal of Food Science*, *87(8)*, 3459–3471. https://doi.org/10.1111/1750-3841.16252

Yin, S. W., Tang, C. H., Cao, J. S., Hu, E. K., Wen, Q. B., & Yang, X. Q. (2008). Effects of limited enzymatic hydrolysis with trypsin on the functional properties of hemp (Cannabis sativa L.) protein isolate. *Food Chemistry*, *106(3)*, 1004–1013. https://doi.org/10.1016/j.foodchem.2007.07.030

Yuan, M., Cao, Y., Zheng, H., Chen, K., Lu, Y., Wang, J., Zhu, L., Chen, M., Cai, Z., & Shen, Y. (2024). Structural and functional properties of Maillard-reacted casein phosphopeptides with different carbohydrates. *Food Science and Biotechnology*, *33*(7), 1603–1614. https://doi.org/10.1007/s10068-023-01463-2

Zacharius, R. M., Zell, T. E., Morrison, J. H., & Woodlock, J. J. (1969). Glycoprotein staining following electrophoresis on acrylamide gels. *Analytical Biochemistry*, *30*(1), 148–152. https://doi.org/10.1016/0003-2697(69)90383-2

Zha, F., Dong, S., Rao, J., & Chen, B. (2019a). Pea protein isolate-gum Arabic Maillard conjugates improves physical and oxidative stability of oil-in-water emulsions. *Food Chemistry*, *285*, 130–138. https://doi.org/10.1016/j.foodchem.2019.01.151

Zha, F., Dong, S., Rao, J., & Chen, B. (2019b). The structural modification of pea protein concentrate with gum Arabic by controlled Maillard reaction enhances its functional properties and flavor attributes. *Food Hydrocolloids*, *92*, 30–40. https://doi.org/10.1016/j.foodhyd.2019.01.046

Zha, F., Yang, Z., Rao, J., & Chen, B. (2019). Gum Arabic-Mediated Synthesis of Glyco-pea Protein Hydrolysate via Maillard Reaction Improves Solubility, Flavor Profile, and Functionality of Plant Protein. *Journal of Agricultural and Food Chemistry*, *67*(36), 10195–10206. https://doi.org/10.1021/acs.jafc.9b04099

Zha, F., Yang, Z., Rao, J., & Chen, B. (2020). Conjugation of Pea Protein Isolate via Maillard-Driven Chemistry with Saccharide of Diverse Molecular Mass: Molecular Interactions Leading to Aggregation or Glycation. *Journal of Agricultural and Food Chemistry*, *68*(37), 10157–10166. https://doi.org/10.1021/acs.jafc.0c04281

Zhang, M., Yue, W., & Zheng, Z. (2019). Interfacial behavior and emulsion stability of Maillard conjugates from ovalbumin-dextran. *Food Hydrocolloids, 89*, 293–300. https://doi.org/10.1016/j.foodhyd.2018.10.022

Zhang, Z., Wang, B., & Adhikari, B. (2022). Maillard reaction between pea protein isolate and maltodextrin via wet-heating route for emulsion stabilisation. *Future Foods*, *6,* 100193. https://doi.org/10.1016/j.fufo.2022.100193

Zhao, S., Huang, Y., McClements, D. J., Liu, X., Wang, P., & Liu, F. (2022). Improving pea protein functionality by combining high-pressure homogenization with an ultrasound-assisted Maillard reaction. *Food Hydrocolloids*, *126*, 107441. https://doi.org/10.1016/j.foodhyd.2021.107441

Zhao, Y., Ye, S., Wan, H., Zhang, X., & Sun, M. (2021). Characterization and functional properties of conjugates of rice protein with exopolysaccharides from *Arthrobacter* ps-5 by Maillard reaction. *Food Science and Nutrition*, *9*(9), 4745–4757. https://doi.org/10.1002/fsn3.2336

Zhong, L., Ma, N., Wu, Y., Zhao, L., Ma, G., Pei, F., & Hu, Q. (2019). Characterization and functional evaluation of oat protein isolate-Pleurotus ostreatus β-glucan conjugates formed via Maillard reaction. *Food Hydrocolloids*, *87*, 459–469. https://doi.org/10.1016/j.foodhyd.2018.08.034

Zhou, M., Hu, X., Yu, D., & Sun, J. (2018). Effect of hydrolysis degree on the functionalities of Maillard reaction products from whey protein hydrolysates. *Food Chemistry, 268*, 305–310. https://doi.org/10.1016/j.foodchem.2018.06.129

Zhou, Y., Hoover, R., & Liu, Q. (2004). Relationship between α-amylase degradation and the structure and physicochemical properties of legume starches. *Carbohydrate Polymers*, *57*(3), 299–317. https://doi.org/10.1016/j.carbpol.2004.05.010

Zhu, A.-p., Yuan, L.-h., Chen, T., Wu, H., & Zhao, F. (2007). Interactions between N-succinyl-chitosan and bovine serum albumin. *Carbohydrate Polymers*, *69*(2), 363–370. https://doi.org/10.1016/j.carbpol.2006.11.023

Zhu, D. A. N., Damodaran, S., & Lucey, J. A. (2010). Physicochemical and emulsifying properties of whey protein isolate (WPI)-dextran conjugates produced in aqueous solution. *Journal of Agricultural and Food Chemistry*, *58*(5), 2988–2994. https://doi.org/10.1021/jf903643p